REFORMING OF ACETONE-BUTANOL-ETHANOL MIXTURE FOR H_2 PRODUCTION: THERMODYNAMIC AND EXERGY ANALYSIS

Ph.D. THESIS

by

BRAJESH KUMAR

DEPARTMENT OF CHEMICAL ENGINEERING
INDIAN INSTITUTE OF TECHNOLOGY ROORKEE
ROORKEE-247667 (INDIA)
JUNE, 2018

REFORMING OF ACETONE-BUTANOL-ETHANOL MIXTURE FOR H_2 PRODUCTION: THERMODYNAMIC AND EXERGY ANALYSIS

A THESIS

Submitted in partial fulfilment of the requirements for the award of the degree

of

DOCTOR OF PHILOSOPHY

in

CHEMICAL ENGINEERING

by

BRAJESH KUMAR

DEPARTMENT OF CHEMICAL ENGINEERING
INDIAN INSTITUTE OF TECHNOLOGY ROORKEE
ROORKEE-247667 (INDIA)
JUNE, 2018

INDIAN INSTITUTE OF TECHNOLOGY ROORKEE
ROORKEE

CANDIDATE'S DECLARATION

I hereby certify that the work which is being presented in the thesis entitled **"REFORMING OF ACETONE-BUTANOL-ETHANOL MIXTURE FOR H_2 PRODUCTION: THERMODYNAMIC AND EXERGY ANALYSIS"** in partial fulfilment of the requirements for the award of the Degree of Doctor of Philosophy and submitted in the Department of Chemical Engineering of the Indian Institute of Technology Roorkee, Roorkee is an authentic record of my own work carried out during a period from January, 2013 to June, 2018 under the supervision of Dr. Shishir Sinha, Professor& Head, and Late Dr. (Mrs.) Shashi, Professor, Department of Chemical Engineering, Indian Institute of Technology Roorkee, Roorkee. The matter presented in this thesis has not been submitted by me for the award of any other degree of this or any other Institution.

(BRAJESH KUMAR)

This is to certify that the above statement made by the candidate is correct to the best of my knowledge.

(Shishir Sinha)
Supervisor

Date: June, 2018

ABSTRACT

Recently, the gap between demand and supply of energy has been increased due to exorbitant consumption of non renewable energy sources all over the world. These energy sources are finite in quantity and release harmful contaminated gaseous emissions in the environment which also affect the health of all living creatures. To overcome these concerns, numerous efforts by multitudinous researchers for the advancement of novel and sustainable economical energy source are being made in the form of a great substitution as biorenewable source to ensure energy security with high efficiency. In past decades, H_2 from biomass derived energy sources as feedstock is getting much attention for fuel cell operation to generate electricity. H_2 can be produced by many processes viz. thermochemical water splitting, pyrolysis, coal gasification, hydrocarbon reforming, etc. Biorenewable energy sources or biofuels (methanol, butanol, ethanol, propane, glycerol, biogas, etc.) can be obtained as primary energy sources for the production of H_2 as clean energy fuel by using fermentation of various feedstocks such as lignocellulosic biomass materials (sugarbeets, wheat, sugarcane, corncob, agricultural wastes, cornstalk, barley straw, switch grass, etc.), aqueous phase liquids of biomass pyrolysis, and micro-algae. For fermentation, *Clostridium* strain, is the most popular strain, and is thus used to ferment a variety of substrates (glucose, sucrose, xylose, lactose, and starch) and ligno-cellulosic biomass materials to obtain ABE (acetone-butanol-ethanol) mixture.

ABE mixture contains 60 wt% water and remaining 40 wt% is ABE (Acetone:Butanol:Ethanol = 3:6:1) mixture in terms of mass ratio. Many separation techniques are used to recover butanol, acetone, and ethanol from fermentation broth such as distillation, adsorption, liquid-liquid extraction, reverse-osmosis, thermopervaporation, gas stripping etc. Amongst them, distillation is very popular and well-established unit operation, and therefore, was used by many chemical process plants to separate the components from this mixture. Generally, four components are separated by a series of four distillation columns. The first column is used to remove approximately 99.5 wt% acetone at operating pressure of 0.7 atm. Due to complex nature, butanol and ethanol obtained from ABE form azeotropes with water. Therefore, the other columns recover the rest butanol, ethanol, and water from the mixture which need high investment cost, and high operating cost because of high energy requirement. This high cost is the challenge for the researchers to innovate an optimum and economic alternate way. As an alternative, use of butanol-ethanol mixture, and acetone-butanol-ethanol mixture as obtained can be the better options. To the best of our knowledge, studies on the reforming of ABE mixture has not yet been done, and thus no information is available in the literature.

Thus, the present study is focused on the utilization of these mixtures as biorenewable energy sources for the production of hydrogen to achieve the economic and environmental benefits. Steam reforming, dry reforming, oxidative steam reforming or autothermal reforming, etc. are several fuel processing technologies for the conversion of biorenewable sources to hydrogen. Among these, steam reforming has been chosen for the present study because it provides higher percentage of hydrogen as compared to other processes.

Objectives of present research work are formulated as given below: Thermodynamic and Exergy Analysis of following biomass fermentation based Biofuels for efficient, environmental friendly and economic production of H_2 by steam reforming:

(i) Acetone, butanol, and ethanol as individual fuels,

(ii) Butanol-ethanol (B–E) mixture as a fuel

For this biofuel, oxidative steam reforming has also been studied.

(iii) Acetone-butanol-ethanol-water mixture as a fuel

Lastly, the comparative evaluation of these fuels has been done with respect to several parameters namely, yield of H_2 , process conditions, carbon formation, steam to fuel molar ratio, thermal and exergy efficiencies, etc.

First, steam reforming of acetone, butanol, and ethanol individually has been performed for the sake of completeness and comparison. Thereafter, the butanol-ethanol (B–E) mixture with water, is studied as a renewable biofuel for the production of clean energy carrier hydrogen by steam reforming process (SRB–E). The butanol–ethanol water mixture (BE mixture) contains 8.66 mole of butanol, 2.32 mole of ethanol and 89.02 mole of water. If butanol and ethanol mixture is considered as a renewable biofuel, then it consists of 78.87 mol% butanol and 21.13 mol% ethanol or in this renewable fuel butanol and ethanol are approximately in 80:20 ratio on molar basis. Likewise, water is about 8 times this renewable fuel on molar basis. The thermodynamic analysis of steam Reforming of B–E mixture is carried out by Gibbs free energy minimization method. The thermal and exergy efficiencies for the process are investigated to exploit the potential of B–E mixture for hydrogen production. For performance evaluation, the variational trends of moles of products (H_2, CO, CO_2, CH_4, and carbon) are studied at equilibrium as a function of temperature (573–1473 K), pressure (1–10 atm), steam/fuel molar feed ratio (0–12) for composition of B–E mixture (50 to 90% B). For mixture (90% B), the maximum production of H_2 (9.56 mol per mol of fuel) is achieved at 973 K temperature, 1 atm

pressure, molar feed ratio of 12. Methane and carbon formation are negligible at high temperature (> 873 K) and molar feed ratio (> 5) for all B–E compositions. Energy required per mol of H_2 is 50.77 kJ/mol for mixture (90% B) and is lower than that for steam reforming of butanol. The thermal efficiency is 70.07%, close to maximum for mixture (90% B), which is higher than butanol (69.89%), and ethanol (68.49%). For 90%B mixture, exergy efficiency (48.58%) is also comparable with that of butanol (48.69%) and ethanol (46.15%). This study proposes direct use of B-E mixture as a renewable fuel for H_2 production.

Further, the mixture of acetone-butanol-ethanol-water contains 5.24mol of acetone, 8.21 mol of butanol, 2.20 mol of ethanol, and 84.35 mol of water, respectively. In this biorenewable fuel; acetone, butanol, and ethanol are present approximately in the molar ratio of 33:52:15. A thermodynamic equilibrium analysis on steam reforming of this mixture has been performed to produce H_2 by Gibbs free energy minimization method. The effect of process variables such as temperature (573-1473K), pressure (1-10atm), and steam/fuel molar feed ratio (F_{ABE}=5.5-12) have been investigated on equilibrium compositions of products, H_2, CO, CO_2, CH_4 and solid carbon. The best suitable conditions for maximization of desired product H_2, suppression of CH_4, and inhibition of solid carbon are 973 K, 1 atm, steam/fuel molar feed ratio=12. Under these conditions, the maximum molar production of hydrogen is 8.35 with negligible formation of carbon and methane. Furthermore, the energy requirement per mol of H_2 (48.96 kJ), thermal efficiency (69.13%), exergy efficiency (55.09%), exergy destruction (85.36 kJ/mol), and generated entropy (0.286 kJ/mol.K) have been achieved at same operating conditions.

Generally, steam reforming (SR) is the most widely used for the production of hydrogen as it provides high yield of H_2. However, SR processes are highly endothermic and so it is operated at relatively high temperature. Consequently, a large amount of heat from the external source is required to drive the process. High energy requirement directly influences the production cost. Another drawback is that the SR process suffers from severe catalytic deactivation due to the formation of carbon during the reaction which also lowers the H_2 production efficiency. The problem of carbon formation can be analyzed in either of the two ways- one by introducing oxidant like O_2 to the feed and other by developing coke resistant catalysts. The addition of O_2 to the feed of SR process results in the oxidation of hydrocarbon fuel which is an exothermic process. This process does not require an external heat source and results in negligible carbon formation but at the expense of low hydrogen yield. Therefore, in order to reduce the external energy consumption and to achieve energy self sufficient system, oxidative steam reforming of butanol-ethanol mixture as fuel has also been explored in the present work to produce H_2 by

using Gibbs free energy minimization method. The effects of pressure (1-10 atm), temperature (573-1473 K), steam/fuel molar feed ratio (f_{O1}= 9 and 12), O_2/fuel molar feed ratio (f_{O2}=0-3), and B-E mixture compositions (50-90%B) on equilibrium compositions of H_2, CO, CO_2, CH_4, and carbon are performed. The maximum H_2 yield (65.46% for f_{O2}=0, and 58% for f_{O2}=0.75) has been achieved at f_{O1}=9, 90% B mixture, 1 atm, and 973 K. The yields of CO, CO_2, and CH_4 with respect to maximum H_2 are 53.39%, 44.38%, and 2.23% for f_{O2}=0, and 45.68%, 53.27%, and 1.05% for f_{O2}=0.75, respectively. Energy required per mol of H_2, thermal and exergy efficiencies for the process are also evaluated.

The results of steam reforming and oxidative steam reforming of butanol-ethanol mixture in terms of maximum hydrogen production have been compared. It is found that the overall performance of oxidative steam reforming is less than that of steam reforming of butanol-ethanol mixture. The production of hydrogen and thermal efficiency of reformer are found less in oxidative steam reforming of B-E mixture (OSRB-E) as compared to its steam reforming.

Further, the evaluation of various fuels such as methanol, glycerol, acetone, butanol, ethanol, butanol-ethanol mixture, acetone-butanol-ethanol mixture has been considered for comparison. It is our view that SR-ABE process is efficient, economical and environment friendly, and utilizes water rich ABE mixture as a renewable fuel for H_2 production. The process utilizes ABE mixture as produced during fermentation and avoids the use of costly processing in the train of separation units.

ACKNOWLEDGEMENT

I would like to express my deep and sincere gratitude to my supervisors Late Dr. (Mrs.) Shashi, Professor, Department of Chemical Engineering, and Dr. Shishir Sinha, Professor & Head, Department of Chemical Engineering, Indian Institute of Technology Roorkee, for their blessings, patient guidance, enthusiastic encouragement and useful critiques for this thesis work. This thesis would not have been possible without their constant inspiration and motivation.

I take this golden opportunity to express my heartfelt and deepest sense of gratitude to Dr. Surendra Kumar, Former Professor, Department of Chemical Engineering, Indian Institute of Technology Roorkee, who helped me to complete my Ph.D. thesis. His guidance and unsurpassed knowledge encouraged me all the time of research and writing of this thesis. His constant guidance, cooperation and support have always kept me going ahead. I owe a lot of gratitude to him for always being there for me and I feel privileged to be associated with a person like him during my doctoral studies.

A special thanks to my family. I am obliged to my parents for everything they did for me, their greatest support, motivation and trust in me, which helped me aim higher from time to time. I would also like to thank my brothers Pramesh Kumar and Sachin Kumar, my best friend Bachendra Pal Singh for being a constant source of inspiration and support for all possible help throughout my doctoral studies.

I would like to say thanks to my friends and colleagues, Mr. Naveen Kumar, Dr. Deepak Kumar, Dr. Litan Kumar, Prashant, Bhupendra, Aniruddha, Lovjeet, Jawed, Kantilal, whose communication and mental support, through from near and far places, have been great source of inspiration. I would also like to acknowledge the support and cooperation of all the staff of Reaction Engineering Laboratory especially Mange Ram.

I offer my regards and blessings to all of those who supported me in any respect during the completion of this thesis.

JUNE, 2018 **(Brajesh Kumar)**

RESEARCH PUBLICATIONS FROM THESIS

- **INTERNATIONAL JOURNALS**

1. **Brajesh Kumar**, Shashi Kumar, Shishir Sinha, Surendra Kumar, **2018**. Utilization of acetone-butanol-ethanol-water mixture obtained from biomass fermentation as renewable feedstock for hydrogen production via steam reforming: Thermodynamic and energy analyses. **Bioresource Technology**; 261:385–393.
2. **Brajesh Kumar**, Shashi Kumar, Surendra Kumar, **2018**. Thermodynamic analysis of H_2 production by oxidative steam reforming of butanol-ethanol water mixture recovered from Acetone:Butanol:Ethanol fermentation. **International Journal of Hydrogen Energy**; 43:6491-6503.
3. **Brajesh Kumar**, Shashi Kumar and Surendra Kumar, **2018**. Butanol reforming: an overview on recent developments and future aspects. **Reviews in Chemical Engineering**; 34(1):1–19.
4. **Brajesh Kumar**, Shashi Kumar, Surendra Kumar, **2017**. Thermodynamic and energy analysis of renewable butanol–ethanol fuel reforming for the production of hydrogen. **Journal of Environmental Chemical Engineering**; 5:5876–5890.

- **BOOK CHAPTER**

1. **Brajesh Kumar,** Shashi Kumar, and Surendra Kumar, Methane production by butanol decomposition: thermodynamic analysis. Chapter 10, Chemical and Bioprocess Engineering: Trends and developments, Apple Academic Press and CRC Press (Taylor and Francis Group), 2015.

- **INTERNATIONAL CONFERENCE**

1. **Brajesh Kumar**, Shashi Kumar, Thermal efficiency analysis of butanol steam reforming for hydrogen production, CHEMCON-2014 (IICHE), 27-30 December 2014, Chandigarh, India.

CONTENTS

	Page No.
ABSTRACT	i-iv
ACKNOEDGEMENT	v
RESEARCH PUBLICATIONS FROM THESIS	vii
CONTENT	ix-xii
LIST OF FIGURES	xiii-xv
LIST OF TABLES	xvii-xviii
NOMANCLATURE	xix-xxiv
CHAPTER I INTRODUCTION	**1-16**
1.1 GENERAL	**1**
1.2 REFORMING PROCESSES	**8**
1.2.1 Steam reforming (SR)	**9**
1.2.2 Dry reforming (DR)	**9**
1.2.3 Partial oxidation (POX)	**9**
1.2.4 Autothermal reforming (ATR) or Oxidative steam reforming (OSR)	**10**
1.2.5 Aqueous phase reforming (APR)	**11**
1.2.6 Supercritical water reforming (SCWR)	**11**
1.3 SELECTION OF REFORMING PROCESSES OF PRESENT WORK	**12**
1.4 OBJECTIVES OF THIS RESEARCH WORK	**15**
1.5 ORGANIZATION OF THESIS	**15**
CHAPTER II LITERATURE REVIEW	**17-55**
2.1 INTRODUCTION	**17**
2.2 ACETONE REFORMING	**17**
2.2.1 Steam reforming of acetone	**17**
2.3 BUTANOL REFORMING TECHNOLOGIES	**22**
2.3.1 Steam reforming (SR) of butanol	**22**
2.3.2 Dry reforming (DR) of butanol	**27**
2.3.3 Partial oxidation (POX) of butanol	**27**
2.3.4 Autothermal reforming (ATR) of butanol or Oxidative steam reforming (OSR) of butanol	**31**

2.3.5 Aqueous phase reforming (APR) of butanol **33**
2.3.6 Supercritical water reforming (SCWR) of butanol **35**
2.4 ETHANOL REFORMING **41**
2.4.1 Steam reforming of ethanol **41**
2.4.2 Dry reforming of ethanol **44**
2.4.3 Aqueous phase reforming of ethanol **45**
2.4.4 Oxidative steam reforming of ethanol **46**
2.4.5 Partial oxidation of ethanol **47**
2.4.6 Supercritical water reforming of ethanol **47**
2.5 REFORMING OF MIXTURES **53**
2.6 REFORMING OF OTHER OXYGENATED COMPONENTS TO PRODUCE HYDROGEN **53**
2.7 MOTIVATION FOR THE PRESENT STUDY **55**

CHAPTER III METHODOLOGY **57-67**
3.1 INTRODUCTION **57**
3.2 THERMODYNAMIC EQUILIBRIUM ANALYSIS **57**
3.3 THERMAL EFFICIENCY **61**
3.4 EXERGY EFFICIENCY **63**
3.5 SOLUTION PROCEDURE **65**
3.6 CONCLUDING REMARKS **67**

CHAPTER IV STEAM REFORMING OF BUTANOL-ETHANOL MIXTURE **69-96**
4.1 INTRODUCTION **69**
4.2 METHODOLGY **69**
4.3 STEAM REFORMING OF ACETONE **72**
4.3.1 Thermodynamic analysis **72**
4.3.2 Thermal Efficiency and exergy Efficiency **73**
4.4 STEAM REFORMING OF BUTANOL-ETHANOL MIXTURE **74**
4.4.1 Production of H_2 **78**
4.4.2 Production of CH_4 **81**
4.4.3 Production of CO and CO_2 **82**
4.4.4 Carbon formation **86**
4.4.5 Analysis of energy requirement **87**
4.4.6 Thermal efficiency **93**

4.4.7 Exergy efficiency **93**

4.4.8 Comparison of steam reforming of acetone, butanol, and ethanol **96**

4.5 CONCLUDING REMARKS **96**

CHAPTER V OXIDATIVE STEAM REFORMING OF BUTANOL-ETHANOL MIXTURE **97-118**

5.1 INTRODUCTION **97**

5.2 METHODOLOGY **97**

5.3 OXIDATIVE STEAM REFORMING OF BUTANOL-ETHANOL MIXTURE **100**

5.3.1 Effect of pressure **100**

5.3.2 Carbon formation **100**

5.3.3 Yield of H_2 **103**

5.3.4 Yield of CH_4 **108**

5.3.5 Yields of CO and CO_2 **109**

5.3.6 Energy requirement **111**

5.3.7 Thermal efficiency **113**

5.3.8 Exergy efficiency **115**

5.4 CONCLUDING REMARKS **118**

CHAPTER VI STEAM REFORMING OF ACEONE-BUTANOL-ETHANOL MIXTURE **119-136**

6.1 INTRODUCTION **119**

6.2 METHODOLOGY **119**

6.3 STEAM REFORMING OF ACETONE-BUTANOL-ETHANOL MIXTURE **121**

6.3.1 Effect of pressure **121**

6.3.2 Carbon formation **122**

6.3.3 Hydrogen production **125**

6.3.4 Methane production **127**

6.3.5 Carbon monoxide and carbon dioxide production **129**

6.3.6 Energy analysis and thermal efficiency of reformer **131**

6.3.7 Exergy analysis **134**

6.4 CONCLUDING REMARKS **136**

CHAPTER VII CONCLUSIONS AND RECOMMENDATIONS 137-140

7.1 CONCLUSIONS **137**

7.1.1 Steam reforming of acetone, butanol, and ethanol **137**

7.1.2 Steam reforming of butanol-ethanol mixture **138**

7.1.3 Oxidative steam reforming of butanol-ethanol mixture **139**

7.14 Steam reforming of acetone-butanol-ethanol mixture **140**

7.2 RECOMMENDATIONS FOR FUTURE WORK **140**

BIBLIOGRAPHY 141-160

APPENDIX A1 161-163

APPENDIX A2 165

LIST OF FIGURES

Figure No.	Caption	Page No.
Figure 1.1	Hydrogen production techniques at a glance [Holladay et al., 2009]	**5**
Figure 1.2	The process scheme for the production of acetone-butanol-ethanol mixture from various feedstocks	**6**
Figure 1.3	Various types of reforming processes with their operating conditions and possible products	**8**
Figure 1.4	Phase diagram and critical point. Reprinted with permission from Anger et al. 2011. Copyright Elsevier.	**11**
Figure 1.5	Operational regimes for SR, ATR, OSR and POX. Reprinted with permission from Rabenstein et al. 2008. Copyright Elsevier.	**12**
Figure 2.1	Coke formed and coke free zones in (A) SR, (B) POX, and (C) DR of butanol at different pressures. Reprinted with permission from Wang et al. 2010, 2011 and Wang 2011. Copyright Elsevier.	**29**
Figure 2.2	Possible reaction pathways for aqueous phase reforming of butanol. Reprinted with permission from Roy et al. 2011 and 2014. Copyright Elsevier.	**35**
Figure 4.1	Molar production of products in steam reforming of acetone at F_A=12 with respected to temperature	**73**
Figure 4.2	Effect of pressure on production of H_2 with (a) f_1 in SRB process at 973 K (b) $f_2$in SRE process at 873 K	**77**
Figure 4.3 (a) and (b)	Molar Production of H_2 and CH_4 as a function of temperature at molar feed ratio (a) f_1 (0-12) in SRB, and (b) f_2 (0-12) in SRE	**79**
Figure 4.3 (c) and (d)	Molar Production of H_2 and CH_4 as a function of temperature at molar feed ratio in SRB-E (c) f_3=12 for H_2, and (d) f_3=12 for CH_4	**80**

Figure 4.4 (a) and (b)	Molar production of CO and CO_2 as a function of temperature at molar feed ratio (a) f_1(0-12) in SRB (b) f_2(0-12) in SRE	**84**
Figure 4.4 (c) and (d)	Molar production of CO and CO_2 as a function of temperature at molar feed ratio in SRB-E (c) f_3=12 for CO, (d) f_3=12 for CO_2	**85**
Figure 4.5	Molar production of carbon as a function of temperature at molar feed ratio (a) f_1 (0-12) in SRB (b) f_2 (0-12) in SRE	**89**
Figure 4.6	Molar production of carbon as a function of temperature at molar feed ratio f_3 (0-12) in SRB-E with (a) 90% B (b) 80% B (c) 70% B (d) 60% B (e) 50% B	**90**
Figure 4.7	Energy requirement as a function of temperature at different f_1 values for SRB process	**91**
Figure 5.1	Effect of pressure on production of H_2 with (a) f_{O1}= 9 and (b) f_{O1}= 12 in OSRB-E process at 973K	**101**
Figure 5.2	Molar production of carbon as a function of temperature and steam to fuel molar feed ratio in (a) steam reforming of butanol and, (b) steam reforming of ethanol	**102**
Figure 5.3	Percent yields of H_2 (by using Eq. 5.3a) and CH_4 at various temperatures, molar O_2/fuel ratio (f_{O2}) and molar steam/fuel ratio (a) f_{O1}=9 (b) f_{O1}=12	**105**
Figure 5.4	Percent yields of H_2 (by using Eq. 5.3b) at various temperatures, molar O_2/fuel ratio (f_{O2}) and molar steam/fuel ratio (a) f_{O1}=9 (b) f_{O1}=12	**107**
Figure 5.5	Percent yields of CO and CO_2 at various temperatures, molar O_2/fuel ratio (f_{O2}) and molar steam/fuel ratio (a) f_{O1}=9 (b) f_{O1}=12	**110**
Figure 5.6	Energy requirement as a function of temperature at f_{O1} = 9 for SRB-E process	**112**
Figure 5.7	Thermal efficiency of SRB-E process with respect to temperature and O_2/ B-E mixture molar feed ratio (f_{O2})	**114**

Figure 5.8	Exergy efficiency of SRB-E process with respect to temperature and O_2/ B-E mixture molar feed ratio (f_{O2})	**116**
Figure 5.9	Effect of O_2/B-E mixture molar feed ratio (f_{O2}) and temperature on exergy destruction	**117**
Figure 6.1	(a) Molar production of H_2 as a function of steam/fuel molar feed ratio (F_{ABE}) at different pressures; (b) carbon formation and carbon-free zones at various temperatures and molar feed ratios of steam/fuel (F_{ABE}), 1 atm	**123**
Figure 6.2	Molar production of hydrogen with variation in temperature and molar feed ratio of steam/fuel (F_{ABE})	**125**
Figure 6.3	Molar production of methane with variation in temperature and molar feed ratio of steam/fuel (F_{ABE})	**128**
Figure 6.4 (a)	Molar Production of carbon monoxide with variation in temperature and molar feed ratio of steam/fuel (F_{ABE})	**129**
Figure 6.4 (b)	Molar Production of carbon dioxide with variation in temperature and molar feed ratio of steam/fuel (F_{ABE})	**130**
Figure 6.5 (a)	Energy requirement with variation in temperature at different molar feed ratio of steam/fuel (F_{ABE})	**132**
Figure 6.5 (b)	Thermal efficiency with variation in temperature at different molar feed ratio of steam/fuel (F_{ABE})	**133**
Figure 6.6	(a) Exergy efficiency, and (b) exergy destruction with variation in temperature at different molar feed ratio of steam/fuel (F_{ABE})	**135**

LIST OF TABLES

Table No.	Caption	Page No.
Table 1.1	Summary of various types of fuel cells [Carrette et al., 2001; Song, 2002]	**3**
Table 1.2	Physical and chemical properties of acetone, butanol and ethanol [Jin et al., 2011]	**7**
Table 1.3	Comparison of reforming technologies [Holladay et al., 2009; Kalamaras et al., 2013]	**10**
Table 2.1	Acetone reforming (Experimental and thermodynamic modeling studies)	**20-21**
Table 2.2	Butanol reforming (Experiment and thermodynamic modeling studies)	**37-40**
Table 2.3	Ethanol reforming (Experiment and thermodynamic modeling studies)	**49-52**
Table 4.1	Validation of simulation results with reported experimental and computational results	**71**
Table 4.2	Reaction network for steam reforming of acetone	**72**
Table 4.3	Molar production of H_2, thermal efficiency and exergy efficiency of SRA process at highest H_2 production conditions on the basis of 1 mol fuel in the feed	**74**
Table 4.4	Chemical reactions involved in SRB, SRE, and SRB-E processes	**76**
Table 4.5	Energy and component analysis in SRB, SRE, and SRB-E processes at molar feed ratio of 12	**92**
Table 4.6	Thermal efficiency and exergy efficiency of SRB, SRE, and SRB-E processes at highest H_2 production conditions on the basis of 1 mol fuel in the feed	**95**
Table 4.7	Comparison of SRA, SRB, and SRE	**96**

Table 5.1 Chemical reactions involved in OSRB-E process **99**

Table 5.2 Equilibrium yields (%) of products and energy evaluation for various B-E mixtures at f_{O1} =9, f_{O2}= 0 and 0.75, and temperature corresponding to maximum H_2 yield **104**

Table 5.3 Equilibrium yields (%) of products and energy evaluation for various B-E mixtures at f_{O1} =12, f_{O2}= 0 and 0.75, and temperature corresponding to maximum H_2 yield **106**

Table 6.1 Chemical reactions network for SR-ABE process **124**

Table 6.2 Operating conditions and corresponding results with respect to maximum hydrogen production for SRA, SRB, SRE, SRB-E, and SR-ABE processes and comparison with other oxygenated compounds reported in the literature **126**

NOMANCLATURE

CHAPTER I

Abbreviations

ABE	Acetone-Butanol-Ethanol
AFC	Alkaline Fuel Cell
APR	Aqueous Phase Reforming
DR	Dry Reforming
MCFC	Molten Carbonate Fuel Cell
MMTPA	Million Metric Tonne Per Annum
OSR/ATR	Oxidative Steam Reforming/Autothermal Reforming
PAFC	Phosphoric Acid Fuel Cell
PEMFC	Polymer Electrolyte Membrane Fuel Cell
SCWR	Supercritical Water Reforming
SOFC	Solid Oxide Fuel Cell
SR	Steam Reforming
POX	Partial Oxidation
CPOX	Catalytic Partial Oxidation

CHAPTER II

Abbreviations

ABE	Acetone-Butanol-Ethanol mixture
APR	Aqueous Phase Reforming
ATR	Autothermal Reforming
BET	Brunauer–Emmett–Teller
CSR	Conventional Steam Reforming
CAC	CO_2 Adsorption Calorimetry
CBR	Carbon Dioxide to Butanol Molar Feed Ratio
CHNS+O	Carbon Hydrogen Nitrogen Sulphur + Oxygen
COPROX	Carbon Monoxide Preferential Oxidation
CPOX	Catalytic Partial Oxidation
DR	Dry Reforming
DRIFTS	Diffuse Reflectance Infrared Fourier Transform Spectroscopy
FBR	Fixed Bed Reactor

FESEM	Field Emission Scanning Electron Microscope
FID	Flame Ionization Detector
FTIR	Fourier Transform Infrared Spectroscopy
GC	Gas Chromatograph
GHSV	Gas Hourly Space Velocity
LHSV	Liquid Hourly Space velocity
LDH	Layered Double Hydroxide
NR	Not Reported
OBR	Oxygen to Butanol Molar Feed Ratio
OSC	Oxygen Storage Capacity
OSR	Oxidative Steam Reforming
POX	Partial Oxidation
PEMFC	Polymer Electrolyte Exchange Membrane Fuel Cell
RS	Raman Spectra
SBR	Steam to Butanol Molar Feed Ratio
SCWR	Super Critical Water Reforming
SEM	Scanning Electron Microscopy
SESR	Sorption Enhanced Steam Reforming
SESRB	Sorption Enhanced Steam Reforming of Butanol
SR	Steam Reforming
TCD	Thermal Conductivity Detector
TGA	Thermogravimetric Analysis
TEM	Transmission Electron Microscopy
TPD	Temperature Programmed Desorption
TPO	Temperature Programmed Oxidation
TPR	Temperature Programmed Reduction
WBR	Water to Butanol Molar Feed Ratio
WGS	Water Gas Shift
XPS	X-ray Photoelectron Spectra
XRD	X-ray Diffraction
XRF	X-ray Fluorescence
XANES	X-ray Absorption Near Edge Structure

CHAPTER III

a_{ik}	Number of atoms of the k^{th} element presents in each molecule of chemical component i [–]
A_k	Total number of atoms of k^{th} element in the feed [–]
c_{p_i}	Heat capacity of component i [kJ/mol.K]
Ex_{chem}	Total chemical exergy [kJ/mol]
$Ex_{chem,i}$	Standard molar chemical exergy of pure component i in gas phase [kJ/mol]
Ex_{dest}	Exergy destruction [kJ/mol]
Ex_{mix}	Exergy of mixing [kJ/mol]
Ex_{phy}	Physical exergy [kJ/mol]
Ex_T	Total exergy [kJ/mol]
$(Ex_T)_{in}$	Total exergy of inlet stream [kJ/mol]
$(Ex_T)_{out}$	Total exergy of outlet stream [kJ/mol]
$\overline{f_i}$	Fugacity of component i [atm]
f_i^0	Standard fugacity of component i [atm]
F	Function defined by Eq. (3.6)
$G^0_{fC(s)}$	Standard GFE of formation of carbon [kJ/mol]
G^0_{fi}	Standard GFE of formation of component i [kJ/mol]
G_T	Total Gibbs free energy of the system [kJ]
ΔG_T	Change in Gibbs free energy [kJ]
$H^{in}_{T,i}$	Enthalpy of i^{th} component in the inlet stream [kJ/mol]
$H^{out}_{T,i}$	Enthalpy of i^{th} component in the outlet stream [kJ/mol]
H^{in}_T	Total enthalpy of inlet stream at temperature T [kJ/mol]
H^{out}_T	Total enthalpy of outlet stream at temperature T [kJ/mol]
$H_{298,i}$	Molar enthalpy of component i at a temperature of 298 K [kJ/mol]
ΔH_L	Latent heat of steam in the feed [= 40.69 kJ/mol]
ΔH	Change in enthalpy [kJ/mol]
k	Atomic element [–] or a particular atom (e. g. C, H, O)
$LHV_{butanol}$	Low heating value of butanol [= 2444.6 kJ/mol]

$LHV_{ethanol}$	Low heating value of ethanol [= 1240 kJ/mol]
LHV_{fuel}	Low heating value of feeding fuel [kJ/mol]
LHV_{H_2}	Low heating value of H_2 [= 241.82 kJ/mol]
M	Total number of atomic elements comprising the reacting system [–]
N	Total number of chemical components in the reacting system [–]
N_1	Number of chemical components present in inlet stream [–]
N_2	Number of chemical components present in outlet stream [–]
N_S	Number of chemical reaction components present in the stream [–]
$n_{butanol}^{in}$	Moles of butanol in inlet stream [mol]
n_C	Moles of carbon (graphite) in the system [mol]
$n_{ethanol}^{in}$	Moles of ethanol in inlet stream [mol]
$n_{H_2}^{out}$	Moles of hydrogen in outlet stream [mol]
n_i	Number of moles of component *i* [–]
n_i^{in}	Moles of component *i* in inlet stream [mol]
n_i^{out}	Moles of component *i* in outlet stream [mol]
n_{steam}^{in}	Moles of steam in inlet stream [mol]
n_T	Total number of moles of all components [–] ($n_T = \sum_{i=1}^{N} n_i$)
n_{fuel}^{in}	Moles of fuel at inlet
P	Pressure [atm]
P_0	Standard pressure [=1 atm]
Q_T	Net change in total enthalpies of inlet and outlet streams [kJ]
R	Universal gas constant [= 8.314 kJ/K.kmol]
S	Entropy [kJ/mol.K]
S_{gen}	Entropy generated [kJ/mol.K]
ΔS	Change in entropy [kJ/mol.K]
T	Temperature (K)
V	Volume [m^3]
y_i	Mole fraction of component *i* in the gaseous stream [–]

Greek Symbols

ϕ_i	Fugacity coefficient of component *i* [–]
μ_i	Chemical potential of the component *i* [kJ/mol]
η_{Ex}	Exergy efficiency [–]
λ_k	Lagrange multiplier for k^{th} element [–]
η_{th}	Thermal efficiency [–]

CHAPTER IV

f_1	Steam to butanol molar feed ratio [-]
f_2	Steam to ethanol molar feed ratio [-]
f_3	Steam to butanol-ethanol molar feed ratio [-]
F_A	Steam to acetone molar feed ratio [-]

Abbreviation

ABE	Acetone-Butanol-Ethanol
B–E	Butanol–Ethanol
GFE	Gibbs Free Energy
RWGS	Reverse Water Gas Shift Reaction
SR	Steam Reforming
SRA	Steam Reforming of Acetone
SRB	Steam Reforming of Butanol
SRB-E	Steam Reforming of Butanol-Ethanol Mixture
SRE	Steam Reforming of Ethanol
WGS	Water Gas Shift Reaction

CHAPTER V

f_{O1}	Steam to fuel molar feed ratio [-]
f_{O2}	Oxygen to fuel molar feed ratio [-]

Abbreviation

ABE	Acetone-Butanol-Ethanol
B–E	Butanol–Ethanol
GFE	Gibbs Free Energy
OSR	Oxidative steam reforming
OSRB–E	Oxidative Steam reforming of Butanol–Ethanol Mixture

RWGS	Reverse Water Gas Shift Reaction
SRB	Steam Reforming of Butanol
SRE	Steam Reforming of Ethanol
WGS	Water Gas Shift Reaction

CHAPTER VI

F_{ABE}	Steam to acetone molar feed ratio [-]

Abbreviation

ABE	Acetone-Butanol-Ethanol
GFE	Gibbs Free Energy
RWGS	Reverse Water Gas Shift Reaction
SR	Steam Reforming
SR-ABE	Steam Reforming of Acetone-Butanol–Ethanol Mixture
SRB	Steam Reforming of Butanol
SRB-E	Steam Reforming of Butanol-Ethanol Mixture
SRE	Steam Reforming of Ethanol
SRG	Steam Reforming of Glycerol
SRM	Steam Reforming of Methanol
WGS	Water Gas Shift Reaction

CHAPTER I

INTRODUCTION

1.1 GENERAL

From primeval period, human beings are consuming conventional sources which contain higher carbon content e.g., coal, petroleum reserve based fuels, and natural gas for energy generation. Especially, petroleum oil reserves are the major source of fuels for transportation all over the world [Nahar et al., 2010]. These non-renewable fuels are available in the limited amount on this terra and our dependence on these fuels is increasing day by day. The conventional sources of energy for fuel generation are diminishing in an extensive manner with the passage of time and emit higher percentage of pollutant gases in our environment which accelerate global warming and other harmful effects on human habitation [Luo et al., 2007]. Nowadays, there is a great concern pertaining to the depletion of conventional sources in response to the energy crisis, which is creating a huge difference between demand and supply of energy. In the last few decades, depletion of fossil fuels, emissions of pollutant gases, and the growing demand for energy generation have received increasing attention for searching new technologies and fuels which can provide high-efficiency energy use [Hartley et al., 2015]. In the era of consuming non-renewable sources, it is imperative to explore ways to produce more efficient, effective, and attractive nonconventional energy fuels in order to suppress the economic and environmental impacts associated with conventional fuel utilization [Seretis and Tsiakaras, 2015]. To achieve this goal, significant efforts of multitudinous researchers (both academic and industrial) are being focused worldwide on the development of various sustainable technologies to convert the renewable resources into valuable fuels and quality chemicals in recent years [Ortiz et al., 2011].

The demand of fuel cell is increasing day by day as leading power generating devices because of their higher energy efficient nature and less emissions of harmful or contaminated gases in the environment for the perpetual and profitable energy conversion as compared to other electricity generation systems. Fuel cell is an electrochemical device, responsible for the power generation due to electrochemical reaction between hydrogen and oxygen which is characterized by thermodynamic equilibrium potential to promote a variety of applications in our daily use. Fuel cell is also known as clean and green cell because it works without polluting the environment and provides energy 2-3 times more than combustion based conventional power plants. Normally, an existing power plant produces electricity with 33-

35% energy efficiency whereas fuel cell can generate power upto 60% and more energy efficiency using co-generation process [Roy et al., 2014]. Due to lack of a fine hydrogen infrastructure, the proper use of fuel cell in transport and the combined generation of heat and electricity is limited [Vaidya and Rodrigues, 2009]. Fuel cell devices can be portable in nature which is classified under 10 kg in terms of weight and less than 5 kW in terms of producing electricity. The devices are very beneficial in modern age for mobile phones, laptops, computers, inverters, etc. The summary of various types of fuel cellsusing hydrogen as fuel for electricity generation with muchvaluable and essential information (e.g., applications, reactions at anode and cathode, advantages and disadvantages, efficiency, etc.) are presented in Table 1.1. It is clear from this table that fuel cell can be used as a promising device to fulfill the future global energy expectations as an alternative to conventional systems [Methekaret al., 2007a and 2007b; Wen et al., 2008; Tyagi et al., 2015].

Hydrogen can be used as a potential feed for fuel cell applications due to its plenteous, attractive, and eco-friendly attributes [Methekaret al., 2010; Li et al., 2011]. It can also be considered as a significant contributor of present as well as future energy systems (e.g. Fuel cell) [Huang et al., 2015, Harju et al., 2016]. H_2 is the simplest and most abundant element present on the earth, which modulates easily with other chemical elements and exists as a part of various chemical compounds and water. It is also found in biomass constituting living organisms such as trees and animals. Due to this reason, H_2 is known as an energy source [Kalamaras and Efstathiou, 2013]. It is also utilized as a clean fuel for on-board vehicles powered by the fuel cell at specified operating regime because it contains higher energy content during combustion process [Roy et al., 2011]. H_2 is obtained by using different feedstocks such as coal, natural gas, nuclear and many other renewable energy sources. This vital factor makes H_2 as a promising fuel for energy security. The hydrogen has many applications as it can be used as by-product in various chemical industries to obtain cyclohexane, hydrocholric acid, methacylates, formic acid, polyurethane and also used in the manufacturing process of ammonia and methanol to synthesize other reagents such as formaldehyde, methyl terc-butyl ether, acetic acid and urea. Except these, the hydrocracking process in petrochemical refineries and hydrogenation in food industries are also dependent on hydrogen [Schwengber et al., 2016].

Table 1.1 Summary of various types of fuel cells [Carrette et al., 2001; Song, 2002]

Properties	PEMFC	AFC	PAFC	MCFC	SOFC
Operating Temperature (°C)	60-120	90-100	160-220	600-800	800-1000
Electrolyte	Polymer Membrane	Aqueous Solution of Alkaline	Molten Phosphoric Acid	Molten Alkaline Carbonate	O^{2-} containing ceramic oxide
Anode Reaction	$H_2 \rightarrow 2H^+ + 2e^-$	$2H_2 + 4OH^- \rightarrow 4H_2O + 4e^-$	$2H_2 \rightarrow 4H^+ + 4e^-$	$H_2 + CO_3^{2-} \rightarrow H_2O + CO_2 + 2e^-$	$H_2 + O^{2-} \rightarrow H_2O + 2e^-$
Cathode Reaction	$\frac{1}{2}O_2 + 2H^+ + 2e^- \rightarrow H_2O$	$O_2 + 2H_2O + 4e^- \rightarrow 4OH^-$	$O_2 + 4H^+ + 4e^- \rightarrow 2H_2O$	$\frac{1}{2}O_2 + CO_2 + 2e^- \rightarrow CO_3^{2-}$	$\frac{1}{2}O_2 + 2e^- \rightarrow O^{2-}$
Applications	• Backup Power • Portable Power • Transportation • Distributed Power	• Military • Space	• Electric Utility • Transportation • Distributed Generation	• Electric utility • Distributed Generation	• Electric utility • Auxiliary Power • Distributed Generation
Charge Carrier in the Electrolyte	H^+	OH^-	H^+	CO_3^{2-}	O^{2-}
Advantages	• Solid Electrolyte • Low Temperature • Quick Startup	• High Performance • Low cost components	• Up to 85% Efficiency in Cogeneration of Electricity and Heat	• High efficiency • Fuel flexibility • Can use a variety of products	• High efficiency • Fuel Flexibility • Solid Electrolyte • Quick Start-up
Disadvantages	• Expensive catalysts • Sensitive to fuel impurities	• Electrolyte management • Sensitive to CO_2 in fuel and air	• Start up time • Low current and power	• Long startup time • Low power density	• High temperature corrosion and breakdown of cell components • Long startup time
Efficiency (Cell)	50-70%	60-70%	55%	55%	60-65%
Efficiency (System)	30-50%	62%	40% Co-Gen (90%)	47%	55-60%

Additionally, hydrogen is also used in the manufacturing processes of plastics, pharmaceuticals, various quality and useful chemicals such as methanol, ethanol, butanol, glycerol, dimethyl ether, methane, biodiesel, etc. on a large scale [Frusteri et al., 2004; Mathew et al., 2005; Specchia et al., 2006; Cao et al., 2006; Zang et al., 2008]. Around 50 MMTPA of H_2 is produced worldwide [Deng et al., 2010, Sharma et al., 2015] in which 90-95% H_2 comes from fossil fuels while 5-10% H_2 is produced from other sources. It is noteworthy that the hydrogen plays an essential part in the field of low carbon transportation fuel production with the minimization of emissions of harmful gases from vehicles [Serdaroglu et al., 2015].The approximate value of global market for hydrogen is $420-500 billion yearly with a 20% annual growth rate [Naterer et al., 2008, Kalamaras and Efstathiou, 2013]. Moreover, Hydrogen is produced by using various non-reforming technologies namely electrolysis [Takata et al., 2007, Wang et al., 2014], biomass gasification [Norbeck et al. 1996, Janssen et al. 2004, Pettersson et al. 2006], photoelectrolysis [Licht, 2003; Demirbas, 2008], thermochemical water splitting [Funk, 2001; Steinfeld, 2005; Adhikari et al. 2008; Lin, 2013],ozone pretreatment [Wu et al., 2013a and 2013 b; Jibouri et al., 2018], and hydrocarbon reforming processes such as steam reforming, dry reforming, aqueous phase reforming, oxidative steam reforming/autothermal reforming, supercritical water reforming. Figure 1.1 depicts many possible processes for H_2 production.

Biorenewable energy sources or biofuels (methanol, butanol, ethanol, propane, glycerol, biogas, etc.) can be obtained as primary energy sources for the production of H_2 as clean energy fuel by using fermentation of various feedstocks such as lignocellulosic biomass materials (sugarbeets, wheat, sugarcane, corncob, agricultural wastes, cornstalk, barley straw, switch grass, etc.), aqueous phase liquids of biomass pyrolysis, micro-algae, and human faeces etc.[Takur et al., 2013; Timung et al., 2015; Onabanjo et al., 2016a and 2016b; Jurado et al., 2018]. During fermentation process, *Clostridium* strain, the most popular strain, which is used to ferment a large variety of substrates (glucose, sucrose, xylose, lactose, and starch) and ligno-cellulosic biomass materials to obtain ABE (acetone-butanol-ethanol) mixture [Qureshi and Blaschek, 2001; Cohce et al., 2011; Thakur et al., 2013; Mohan et al., 2015]. Figure 1.2 shows the process scheme for the production of ABE mixture from various feedstocks, and Table 1.2 summarizes the physical and chemical properties of acetone, butanol, and ethanol.

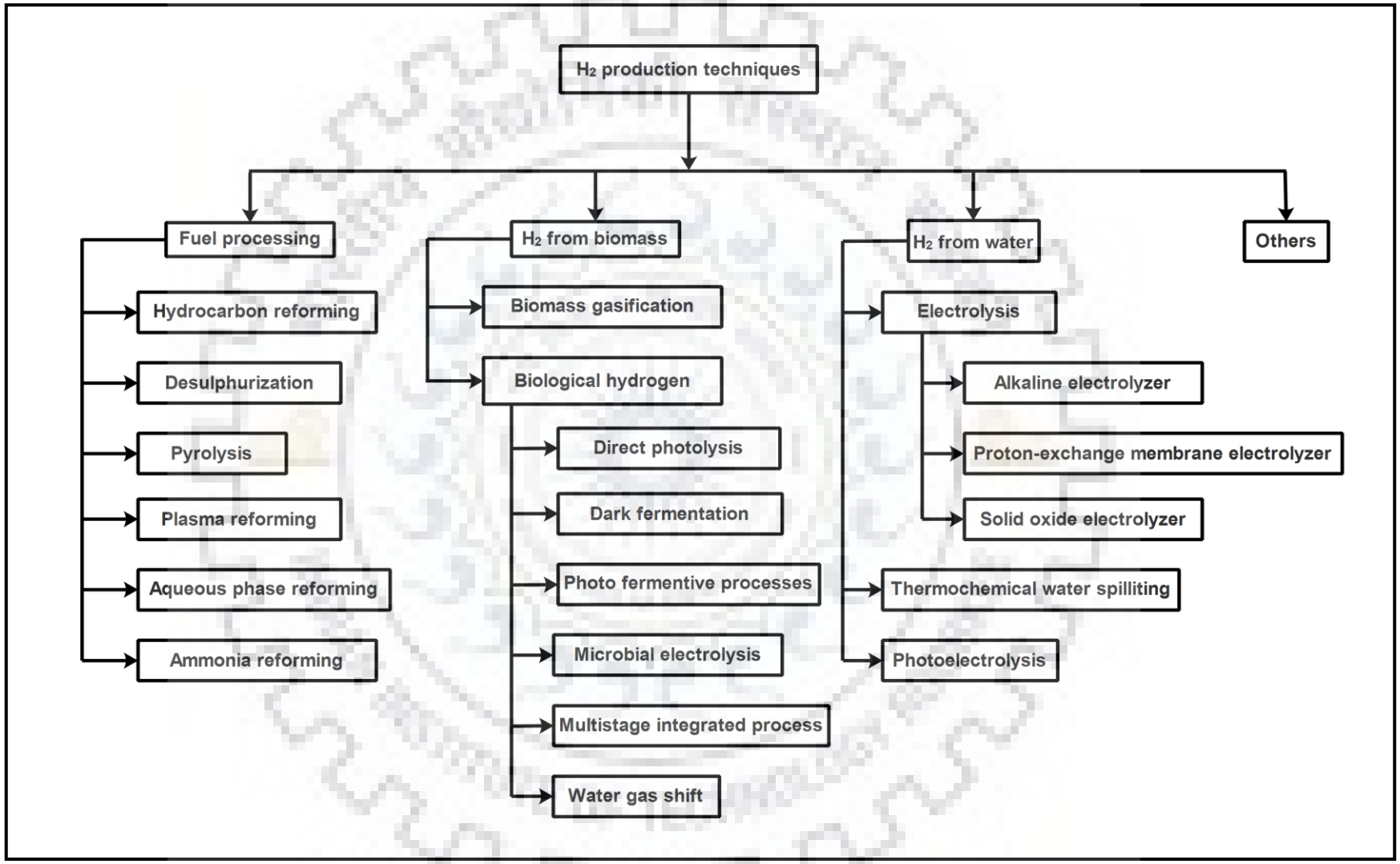

Figure 1.1 Hydrogen production techniques at a glance [Holladay et al., 2009]

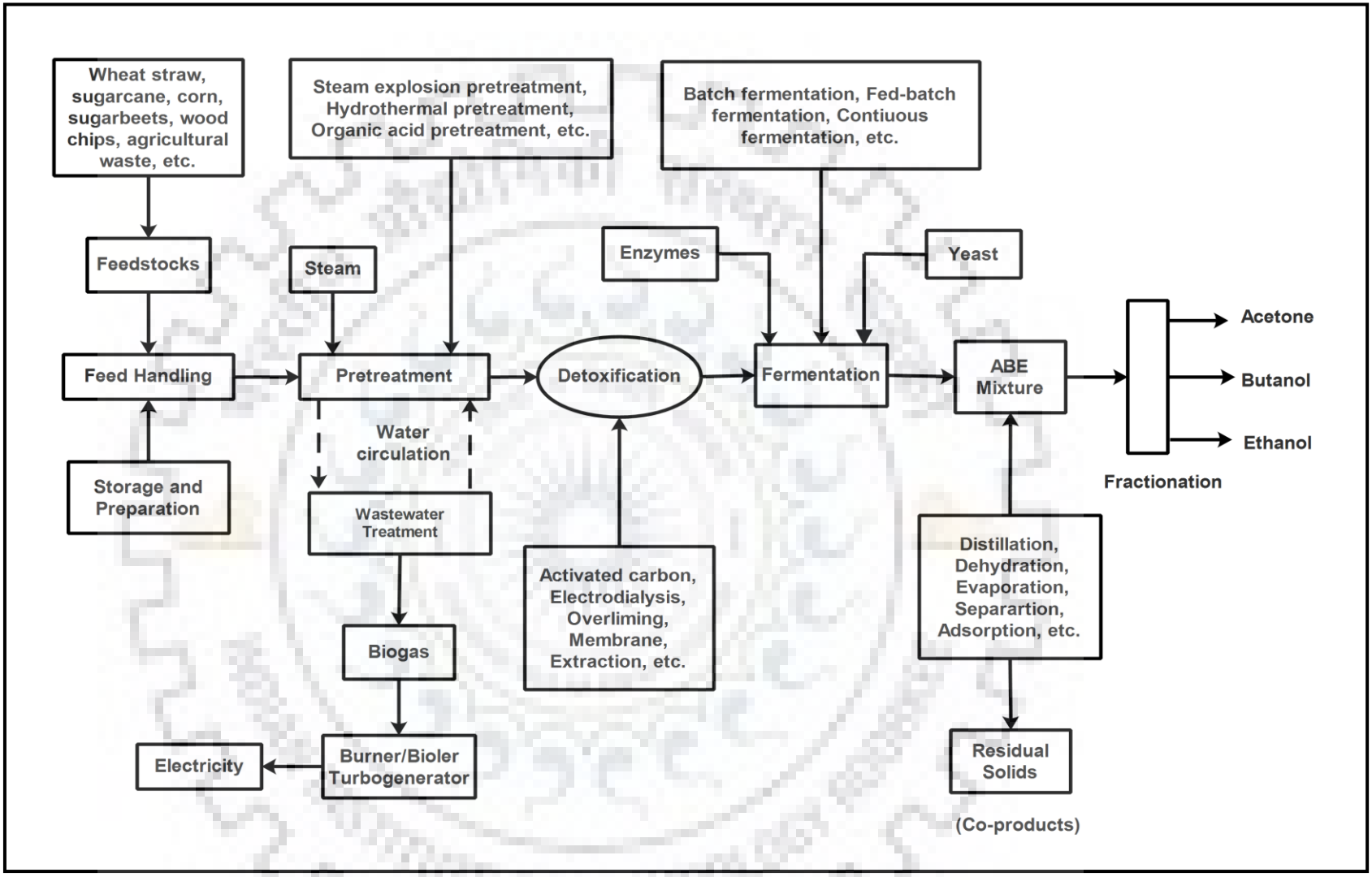

Figure 1.2 The process scheme for the production of acetone-butanol-ethanol mixture from various feedstocks

ABE mixture contains 60 wt% water-vapour and remaining 40 wt% is ABE (Acetone:butanol:ethanol = 3:6:1) mixture in terms of mass ratio [Jin et al., 2011; Cai et al., 2014]. The mixture of acetone-butanol-ethanol-water contains 5.24mol of acetone, 8.21mol of butanol, 2.20 mol of ethanol, and 84.35 mol of water, respectively. In this biorenewable fuel; acetone, butanol, and ethanol are present approximately in terms of molar ratio of 33:52:15.

Table 1.2 Physical and chemical properties of acetone, butanol and ethanol [Jin et al., 2011]

Properties	**Acetone**	**Butanol**	**Ethanol**
Chemical formula	C_3H_6O	C_4H_9OH	C_2H_5OH
Octane number	110	96	107
Cetane number	---	25	8
Appearance	Colourless Liquid	Refractive Liquid, Colourless	Colourless
Odor	Pungent and Floral	Harsh and Alcoholic	Alcoholic and Sweet
Density (at 293 K)	0.78 g/cm^3	0.81 g/cm^3	0.79 g/cm^3
Molar mass	58.08 g/mol	74.12 g/mol	46.07 g/mol
Melting point	178.5 K	183.3 K	158.8 K
Boiling point	329.20 K	390.8 K	351.6 K
Auto ignition temperature	738 K	616 K	606 K
Flash point	253 K	308 K	285.92 K
Lower heating value	29.6 MJ/kg	33.1 MJ/kg	26.8 MJ/kg
Acidity	19.2 pKa	16.10 pKa	15.9 pKa
Refractive index (at 293 K)	1.36	1.39	1.36
Vapour pressure (at 293 K)	24.73 kPa	0.53 kPa	7.58 kPa
Air-fuel ratio	9.54	11.2	9

1.2 REFORMING PROCESSES

The fuel processor or reformer plays an important role in the production of hydrogen from different sources to generate electricity through fuel cell system. In H_2 production via reforming processes, catalysts are essential to lower the activation energy, favouring the kinetics of chemical reactions. The catalysts are used in reforming processes to accelerate the chemical reaction. Carbon formation is an important issue in reforming processes. Then, the catalysts must be more productive, active and stable so that sintering or corrosion and coke formation can be avoided [Peela and Kunzru, 2011; Wanat et al., 2004]. For various types of reforming processes reported in the literature namely steam reforming, dry reforming, aqueous phase reforming, partial oxidation, oxidative steam reforming/autothermal reforming, and supercritical water reforming, operating conditions and possible products are given in Figure 1.3.

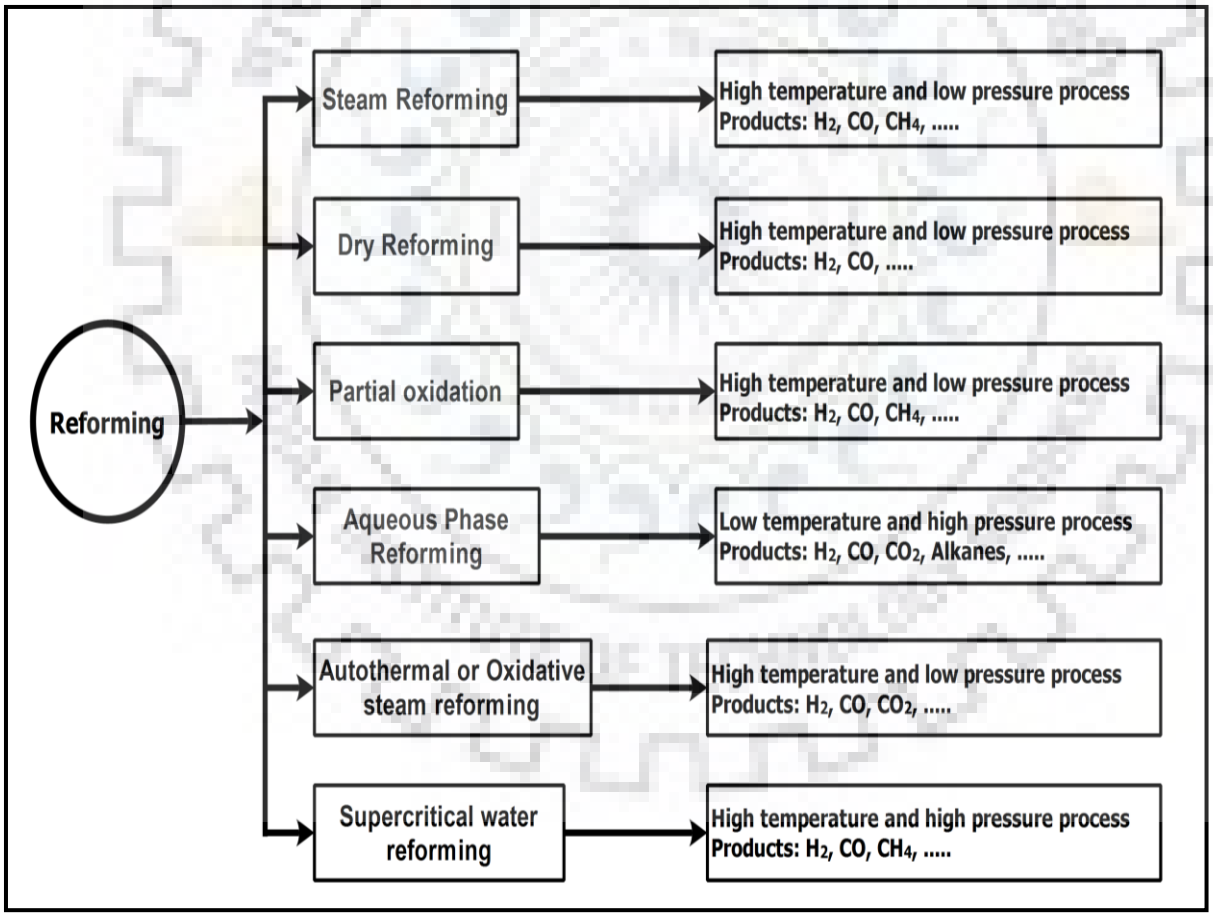

Figure 1.3 Various types of reforming processes with their operating conditions and possible products

A brief description of each aforementioned reforming process is given below.

1.2.1 Steam reforming (SR)

Steam reforming is the popular and promising technology used in many chemical industries because it fulfills the required criteria of industries and do not affect the scale of current industrial aspects of hydrogen fuel production [Ogden et al., 1999]. The most common raw materials for steam reforming are methane, methanol, ethanol, butanol, and other hydrogenated carbons. In this process, the raw materials react with steam or water vapour in the presence of an appropriate catalyst for the production of several products such as hydrogen, carbon monoxide, methane, carbon dioxide [Garcia and Laborde, 1991; Lwin et al., 2000; Onozaki et al., 2006]. Hydrogen is separated from water vapor simultaneously, which accelerates the yield of the steam reforming reaction system. Due to this reason, this is preferred over other reforming processes for higher hydrogen production in industries. This process demands sulfur free raw materials which reduce the chances of catalyst deactivation.

1.2.2 Dry reforming (DR)

Dry reforming is the reaction in which CO_2 reacts with raw materials such as methane, propane, and butanol, in presence of an appropriate catalyst without using steam in the main reaction. Due to the participation of CO_2 directly in the global reaction, this is also known as CO_2 reforming. Dry reforming process is highly endothermic in nature and produces H_2 and CO. H_2 can be produced through many pathways in CO_2 reforming reaction network.

1.2.3 Partial oxidation (POX)

Partial oxidation (POX termed as non-catalytic) and catalytic partial oxidation (CPOX) of oxygenated hydrocarbons have been investigated for the production of hydrogen as a fuel in automobile fuel cell and other commercial purposes [Hohn and Schmidt, 2001; Krummenacher et al. 2003]. Beside desulphurization, partial oxidation provides another advantage over steam reforming as fast start-up time due to exothermic nature of the oxidation reaction.

Table 1.3 exhibits merits, demerits, efficiency, and maturity of major processes such as SR, ATR, and APR and POX, respectively.

Table 1.3 Comparison of reforming technologies [Holladay et al., 2009; Kalamaras et al., 2013]

	Steam Reforming (SR)	**Autothermal Reforming (AR)**	**Aqueous phase Reforming (APR)**	**Partial Oxidation (PO)**
Merits	• Mostly used on industrial scale • O_2 not required for process • Best H_2/CO ratio for H_2 formation	• Required lower temperature to process than PO • Low methane slip	• Low temperature process • Vaporization not needed	• Reduced desulphurization • Fast Startup
Demerits	• Higher air emissions • Vaporization needed	• Required O_2 or air to process • Moderate industrial process	• High pressure process • Lower H_2 yield • High dependence on catalysts	• Low H_2/CO ratio Very high processing temp. • Process complexity • Soot Formation
Efficiency[a]	70-85%	60-75%	35-55%	60-75%
Maturity	Commercial	Near Term	Medium Term	Commercial

[a]Thermal efficiency (based on the higher heating values) is defined as the ratio of heat input to heat output of the system.

1.2.4 Autothermal reforming (ATR) or Oxidative steam reforming (OSR)

Autothermal reforming also known as oxidative steam reforming**,** is a major thermochemical reforming technology which combines steam reforming (endothermic in nature) and partial oxidation (exothermic in nature) reactions with minimal supply of external heat or energy for higher yield of hydrogen [Turco et al. 2004, Ni et al. 2007, Miletić et al. 2015]. In this reforming, the heat released during POX can fulfill the requirement of endothermic energy for steam reforming reaction [Aasberg-Petersen et al. 2003, Kugai et al. 2006, Cai et al. 2007, Pereira et al. 2008]. The addition of O_2 in oxidative steam reforming enhances the chances to prevent coke formation, but thermal sintering of active compounds and their supports provides many challenges [Cavallaro et al. 2003, Frusteri et al. 2006, Pojanavaraphan et al. 2012]. The general reaction of oxidative steam reforming or autothermal reforming is given below.

$$C_xH_yO_z + k\,H_2O + (x - 0.5k - 0.5z)\,O_2 \rightarrow xCO_2 + (k + 0.5y)\,H_2 \quad (1.1)$$

1.2.5 Aqueous phase reforming (APR)

Aqueous phase reforming, also known as liquid phase reforming, operates at low temperature and high pressure conditions. Due to liquid phase, this reforming is capable to suppress the unwanted decomposition reactions. Moreover, aqueous phase reforming exists at the operating conditions of temperature and pressure where the water gas shift reaction is favourable thermodynamically. Therefore, single stage reactor is enough to obtain desirable hydrogen gas with negligible quantity of carbon monoxide gas which is the essential requirement of fuel cell [Seretis and Tsiakaras, 2015].

1.2.6 Supercritical water reforming (SCWR)

The term 'Supercritical' refers to a state in which both gas and liquid phase do not lie at the temperature and pressure conditions above its critical point (T_C=647 K, P_C=220 bar) as shown in Figure 1.4.Supercritical water behaves as a non-polar solvent and possesses several properties like high solubility, low dielectric constant, high diffusivity, and low viscosity (Xu et al. 2009, Guo et al. 2012, Pairojpiriyakul et al. 2013). In this process, the reduction of mass transfer coefficient and enhancement of space time yield are possible. One of the advantages of this process is that it provides high conversion of reacting species with negligible coke formation over the surface of catalyst.

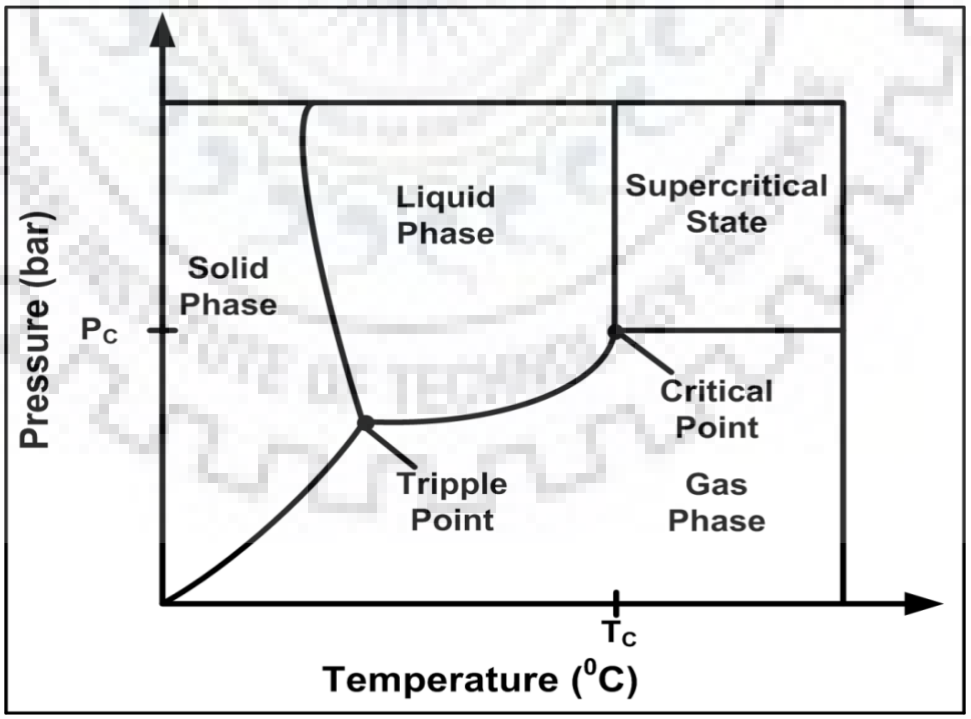

Figure 1.4 Phase diagram and critical point. Reprinted with permission from Anger et al. 2011. Copyright Elsevier.

Our prime concern is to produce maximum hydrogen and minimum amount of carbon monoxide. The spectrum of operating conditions of a reformer for the production of hydrogen fuel based on heat requirement has been presented in Figure 1.5.

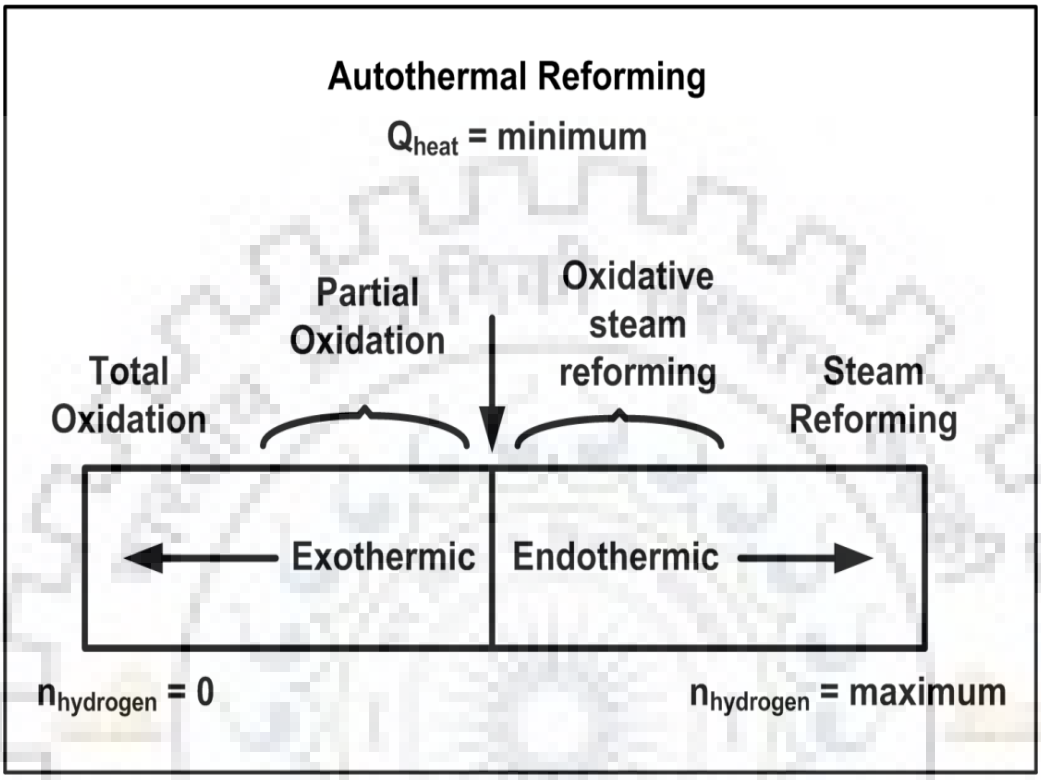

Figure 1.5 Operational regimes for SR, ATR, OSR and POX. Reprinted with permission from Rabenstein et al. 2008. Copyright Elsevier.

1.3 SELECTION OF REFORMING PROCESSES FOR PRESENT WORK

The concluding remarks on various reforming processes can be recapitulated as below:

- Dry reforming is thermodynamically unfavorable that's why less experimental studies have been performed on dry reforming so far. Thermodynamic study shows that the concentration of carbon monoxide is higher than that of hydrogen and methane in dry reforming of butanol. Due to environmental issues, dry reforming is not suitable on an industrial scale. Dry reforming is highly endothermic in nature in comparison to other reforming processes and produces more char which causes the deactivation of the catalyst. Only one advantage of dry reforming is the use of CO_2 as an oxidizing agent in the global reaction. However, it can be considered as an alternative for utilization of carbon dioxide gas only.
- Nowadays, aqueous phase reforming and supercritical water reforming are most attractive and prevailing technologies but require high pressure and high molar feed

ratio to operate a reformer which causes the increase of material costs as well as process cost in the operation.

- The oxidative steam reforming/autothermal reforming and partial oxidation can also be used due to atmospheric pressure, but it requires high temperature and supply of oxygen to process resulting in higher cost. One of the advantages of this process is that it minimizes the requirement of energy used in the process.
- On the basis of facts given in numerous literature studies, steam reforming is the most accessible and popular reforming process for the production of H_2 by using oxygenated fuels as a raw materials. This process is beneficial because of its ease of adapting instruments which are already in use in various chemical industries. It is noteworthy that the steam reforming produces more hydrogen than any other reforming processes.
- Catalytic reforming encounters many technical and scientific challenges containing feed quality and its conversion, hydrogen purification, and finding a way for continuous reaction-regeneration of the catalyst. Therefore, research should be focused on preparation and development of new catalysts to maximize desired products and suppress the formation of undesired compounds. Normally, Ni, Pt, and Ru supported by Al_2O_3, MgO, CeO_2, etc. are used to facilitate the reforming reactions for the production of hydrogen. Catalysts should have some attributes such as ease of availability, cost effective, higher stability, reusability, resistance to deactivation due to sintering, solid carbon deposition over the surface of the catalyst, and impurity fouling. It concludes mainly that the reforming reaction should be conducted in the carbon-free zone, which enhances the performance of a reformer.
- Moreover, the formation of carbon is unwanted in any kind of reforming due to catalyst breakage and deactivation. It leads to overheating problem in the reformer. The primary requirements of a reformer catalyst are given below:
  - High and stable activity
  - Low pressure drop
  - Better heat transfer
  - High resistance to carbon
  - Robust formulation or simple operation

The performance of steam reforming system is measured by three evaluation parameters; the effect of operating conditions (temperature, pressure, and steam/fuel molar feed ratio) on product composition, thermal efficiency through energy analysis, and exergy efficiency. The thermodynamic equilibrium analysis of the process provides the equilibrium composition of

desired and undesired products at given operating conditions to ensure whether or not an experimental investigation of the process would be worthwhile [Katiyar et al., 2013]. The performance of the system by energetic analysis is based upon the first law of thermodynamics. It gives the information about the thermal efficiency. This information does not provide details about the degradation of energy resources (quality) that occurs in the process, and generate thermodynamic inefficiencies associated with irreversible processes in the energy conversion system. It indicates that the meaningful information of the process operation cannot be assessed by an energy analysis alone. Therefore, an exergy analysis which is based on the first and second law of thermodynamics has been considered in the present study. The exergy efficiency provides the usefulness and quality of the various energy streams flowing through the system as products and wastes. The exergy efficiency provides a true measure of how nearly actual performance approaches the ideal condition. In the present study, a complete thermodynamic analysis of steam reforming of acetone, steam reforming of butanol, steam reforming of ethanol, and steam reforming of butanol-ethanol mixture, steam reforming of acetone-butanol-ethanol mixture, oxidative steam reforming of butanol-ethanol mixture has been carried out by Gibbs free energy minimization method. The effects of temperature, pressure, and steam/fuel molar feed ratio have been studied on the production of desired product H_2 and undesired products CH_4, CO, CO_2, and carbon. The operating conditions have been identified to minimize the production of methane and carbon, and maximize the production of h_2 in all three reforming processes. Additionally, the energy requirement for the endothermic steam reforming and oxidative steam reforming processes has been evaluated. It is followed by the thermal efficiency evaluation associated with SRA, SRB, SRE, SRB-E, SR-ABE, and OSRB–E processes. For the sake of the completeness in the end, the exergy analysis has been carried out for all aforementioned reforming processes.

1.4 OBJECTIVES OF THIS RESEARCH WORK

Objectives of present research work are formulated as given below.

Thermodynamic and Exergy Analysis of following biomass fermentation based Biofuels for efficient, environmental friendly and economic production of H_2 by steam reforming:

(i) Acetone, butanol, and ethanol as individual fuels,

(ii) Butanol-ethanol (B–E) mixture as a fuel

For this biofuel, oxidative steam reforming has also been studied.

(iii) Acetone-butanol-ethanol-water mixture as a fuel

Lastly, the comparative evaluation of these fuels has been done with respect to several parameters namely, yield of H_2 , process conditions, carbon formation, steam to fuel molar ratio, thermal and exergy efficiencies, etc.

1.5 ORGANIZATION OF THESIS

The thesis has been organized in seven chapters and their descriptions are given below:

Chapter I: This chapter presents information about energy crisis, alternatives to conventional sources of energy, fuel cell and its applications, various hydrogen production techniques, brief description of various reforming processes, and objectives of the thesis.

Chapter II: This chapter provides the relevant background information from available literature on various reforming processes of acetone, butanol, ethanol, and different mixtures for the production of valuable fuels by using renewable feedstocks.

Chapter III: This chapter presents the methodology of Gibbs free energy minimization as non-stoichiometric approach for conducting thermodynamic analysis of reforming systems supported by performance evaluation parameters namely, thermal efficiency through energy analysis and exergy analysis. The solution procedure for conducting the simulations and computations for reforming systems is also described in this chapter.

Chapter IV: This chapter deals with simulation results and their discussions in detail for various reforming processes involved in present research work such as steam reforming of acetone, steam reforming of butanol, steam reforming of ethanol, steam reforming of butanol-ethanol mixture. It involves thermodynamic analysis, thermal efficiency of reformer, analysis of energy used in the process, and exergy analysis.

Chapter V: This chapter describes the effects of addition of oxygen in feed which is commonly referred to as oxidative steam reforming, of butanol-ethanol mixture. The effects of process parameters such as temperature, pressure, molar feed ratio of steam/fuel, and molar feed ratio of oxygen/fuel have been discussed and compared with the steam reforming of butanol-ethanol mixture.

Chapter VI: This chapter investigates the optimum operating conditions of temperature, pressure, molar feed ratio of steam/fuel for the production of hydrogen by using steam reforming of ABE mixture. For this purpose, thermodynamic analysis via non-stoichiometric approach, energy and exergy analyses have been performed.

Chapter VII: This chapter highlights the main conclusions of the present research work, and suggests recommendations for future research work.

CHAPTER II

LITERATURE REVIEW

2.1 INTRODUCTION

A literature contains valuable information regarding any topic to pursue a reasonable research with novelty in right direction. It offers elaborated knowledge about any subject in terms of perceptions, opinions, interpretations, and conclusions. It also provides a platform for understanding and development of the particular research area based on available information. An emerging area of research has been found towards the production of hydrogen fuel through various reforming processes of oxygenated hydrocarbons as renewable sources of energy. This chapter compiles experiment work as well as thermodynamic analyses over different reforming technologies of acetone, butanol, ethanol, and mixtureof other compounds. Thermodynamic analyses are potentially viable tool to obtain theoretically possible results for evaluating experimental results.

2.2 ACETONE REFORMING

2.2.1 Steam reforming of acetone

Acetone has mainly been used in steam reforming process to produce clean energy carrier hydrogen using mostly nickel based catalysts with supports of Mg, Al, Ce, Pt, Cu, La, etc. Hu et al. (2012) investigated the catalytic activity of Ni/Al_2O_3 for the production of H_2 in steam reforming of acetone and acetic acid. The various species of nickel on alumina showed different behavior for the generation of acetone and acetic acid reforming reactions, precursors of coke via gasification, and other types of reactions, i.e., water gas shift reaction, decomposition of methane, disproportion of carbon monoxide, and methanation reactions. Mildly interaction of nickel with alumina was found efficient and effective for the reforming of acetic acid, acetone, and other by products.

Navarro et al. (2014) conducted experiments for the steam reforming (SR) of acetone as model compound of bio-oil to see the influences of bimetallic PtNi and CuNi catalysts supported on La-modified alumina with respect to structural and morphological characteristics of diffused Ni metallic phases. Various characterization tests such as XRD, TPR, and XPS were done to check the stability of different proportions of prepared catalysts. Bimetallic PtNi catalyst performed well in terms of enhancement of gasification and coke

resistant qualities in comparison to CuNi catalyst. Later, Navarro et al. (2015) also investigated the Ni- and PtNi- catalysts supported on Al_2O_3 with Ce, La, and Mg oxides in acetone steam reforming for the production of hydrogen. In terms of gasification capacity, Ni/LaAl combination showed best activity than other Ni/MgAl and Ni/CeAl catalysts. The NiLaAl sample with addition of Pt enhanced the stability of metallic nickel particles on catalyst surface and the mobility of H-atoms formed in the reforming reaction of acetone. In another study, Ni-Mg-Al oxides with different nickel atmosphere such as Ni-supported, Ni-mixed oxides, and Ni like spinel structure were tested to obtain high catalytic activity in steam reforming of acetone to produce hydrogen [Guil-Lopez et al., 2015]. Nickel interaction with Mg and Al oxides supports increases the stability of Ni-Mg-Al structures.

Acetone and ethanol as the fractions of bio-oil were used to produce hydrogen by using steam reforming route over nickel based catalysts [González-Gil et al., 2015]. They presented experimental as well as simulation results for Ni/Al_2O_3 and $Ni-Rh/Al_2O_3$. The maximum mole fraction of hydrogen within range of 0.6-0.7 was achieved in both acetone and ethanol reforming processes. The metal size of nickel and the deposition of coke on the surface of prepared catalyst were also observed through addition of Rh and Al_2O_3. Rh played an important role in both the reforming processes in terms of complete conversion of ethanol and acetone, maximum production of hydrogen, minimal carbon deposition over catalyst surface. Rh also supports the suppression of intermediates formed in the reforming reactions. A program in Matlab was written to obtain the favourable operating regime for both the components as acetone and ethanol. The steam/acetone and steam/ethanol ratios on molar basis were also studied to see the effects on the formation of products, conversion of reactants, and H_2/CO ratios. The simulation results were found identical to the data of experimental investigations as obtained in SR of acetone and ethanol. Braga et al. (2016)carried outexperiments regarding steam reforming of acetone over nickel and cobalt based catalysts. To obtain the information regarding stability of prepared catalysts, various characterizations such as X-ray diffraction, temperature programmed reduction, transmission electron microscopy, nitrogen physisorption, temperature programmed desorption, and X-ray absorption spectroscopy were performed. The results showed that the nickel based catalyst provided better stability than cobalt based catalysts at high temperature conditions. Moreover, the reaction pathways of steam reforming were completely dependent on temperature, nature of metals used, and the redox potential of the reactants.

Few studies are found in literature on thermodynamic analysis for the production of hydrogen. Esteban-Díez et al. (2016) investigated the influences of operating parameters such as temperature (748-948K), and various steam/carbon molar ratio with weight hourly space velocity on the production of hydrogen in sorption enhanced steam reforming (SESR) of bio-oil. The blends of acetic acid and acetone have been used as model compounds of bio-oil for the analysis under atmospheric pressure conditions over a Pd/Ni-Co hydrotalcite-like material catalyst using calcined dolomite CO_2 sorbent. The concentration of hydrogen first increases with increase in temperature, goes maximum and thereafter decreases. Higher temperature favours the high production of CO and CO_2, while reduces the concentration of methane. The purity value of hydrogen and selectivity are 99.2-99.4% and 99.7-99.9%, respectively at 848 K temperature and atmospheric pressure. Although hydrogen production in SESR process of blends of acetic acid and acetone (83.3-86.6%) is found lower as compared to individual model compounds (90.2-95.9%) under same operating conditions. In another study, thermodynamic study has also been done to obtain the optimum operating parameters on the production of hydrogen by using bio-oil compounds including acetone through sorption enhanced steam reforming (SESR) which is compared with conventional steam reforming (CSR) [Xie et al., 2017]. They evaluated equilibrium compositions of products such as hydrogen and energy consumption during whole process. SESR process performed well than CSR process in terms of higher hydrogen yield (more than 90%) at low temperature and steam/carbon ratios. The energy consumption in sorption enhanced steam reforming process was 30% lower than conventional steam reforming. The optimum conditions for highest hydrogen production are the temperatures of 773-873 K and steam/carbon ratio =3.

Table 2.1summarizes selective information about experimental as well as simulation studies on reforming technologies investigated by various researchers for the production of valuable fuels by using acetone with brief details of used catalysts, reactor, conversion of acetone, and operating process parameters.

Table 2.1 Acetone reforming (Experimental and thermodynamic modeling studies)

S. No.	Reforming Process	Authors	Operating conditions	Results	Reactor	Catalysts	Stability	Experimental/ Thermodynamic Modeling Study
1.	Steam Reforming	Hu et al. (2012)	Temperature = 873 K Pressure = 1 atm SAR = 6	Conversion = 100% H_2 = 80% (S_1) CO = 6% (S_2) CO_2 = 90% (S_2)	Fixed bed reactor	Ni/Al_2O_3	Stable	Experimental
		Navarro et al. (2014)	Temperature = 873K Pressure = 1 atm SAR= 6	Conversion= 100% H_2 = 60-65% (S_2) CO = 10-15% (S_2) CO_2 =20-22% (S_2) CH_4 =10-13% (S_2)	Fixed bed reactor	Ni/A-La PtNi/A-La CuNi/A-La	Stable (10 hr)	Experimental
		Guil-Lopez et al. (2015)	Temperature = 873 K Pressure = 1 atm SAR = 6	Conversion = 100 % H_2= 61% (S_2) CO = 10% (S_2) CO_2= 17% (S_2) CH_4 = 12% (S_2) Coke= 23 % (S_2)	Fixed bed reactor	Ni-Mg-Al	Stable (10 hr)	Experimental
		Navarro et al. (2015)	Temperature = 873 K Pressure = 1 atm SAR = 6	Conversion = 100 % H_2= 67% (S_2) CO = 5% (S_2) CO_2= 16% (S_2) CH_4 = 12% (S_2)	Fixed bed reactor	Ni/A Ni/LaA Ni/CeA Ni/MgA PtNi/LaA PtNi/CeA PtNi/MgA	Stable (10 hr)	Experimental
		González-Gil et al. (2015)	Temperature=473-973 K Pressure = 1 atm SAR= 3	Conversion = 82 % H_2 =69 (mol%)		Ni/Al_2O_3 $Ni/Rh-Al_2O_3$	Stable	Experimental

Table 2.1 Acetone reforming (Experimental and thermodynamic modeling studies) *contd.*

S. No.	Reforming Process	Authors	Operating conditions	Results	Reactor	Catalysts	Stability	Experimental/ Thermodynamic Modeling Study
		Xie et al. (2017)	Temperature=973-1073 K Pressure = 1 atm SAR ≤ 4	Conversion = 100 % H_2 = 29-32% (Y_1)	Fixed bed reactor	---	---	Thermodynamic Modeling
2.	Sorption enhanced steam reforming	Esteban-Díez et al. (2016)	Temperature = 800 K Pressure = 1 atm SAR = 10	Conversion = 100% H_2 = 70-72 (mol%) CO = 3 (mol%) CO_2 =25 (mol%) CH_4 = 2 (mol%)	Fluidized bed reactor	Pd/Ni–Co hydrotalcite	Stable	Experimental and Thermodynamic Modeling

$$\text{Acetone Conversion} = \left(\frac{\text{Initial moles - final moles remained}}{\text{Initial moles}} \right) \times 100$$

$$Y_1 = \frac{\text{moles of product formed}}{\text{stoichiometric coefficient} \times \text{moles of reactant fed}} \times 100$$

$$S_1 = \left(\frac{\text{Moles of } H_2 \text{ formed}}{\text{Maximum moles of } H_2 \text{ which can be formed}} \right) \times 100$$

$$S_2 = \left(\frac{\text{Moles of C or } H_2 \text{ in product gas}}{\text{Total moles of C in output gas product}} \right) \times 100$$

2.3 BUTANOL REFORMING TECHNOLOGIES

2.3.1 Steam reforming (SR) of butanol

The global reaction for steam reforming of butanol followed by water gas shift reaction which enhances hydrogen formation is given below:

$$C_4H_{10}O + 3\,H_2O \leftrightarrow 4\,CO + 8\,H_2 \quad (2.1)$$

$$CO + H_2O \leftrightarrow CO_2 + H_2 \quad (2.2)$$

The butanol steam reforming reaction is highly endothermic (Eq. 2.1); while water-gas shift reaction (Eq. 2.2) is exothermic which releases a small amount of energy. The appropriate selection of the molar feed ratio of steam to butanol and catalyst is necessary to obtain higher amounts of hydrogen under specified optimum operating conditions of temperature and pressure. The studies related with steam reforming so far exhibit the importance of supports over catalysts to obtain the stability of active phase of reaction with a strong bond between the support and the metal, which enhances the yield of desired products [Silva et al., 2015]. The support plays an important role to preserve the specific area of active component participating in the system to achieve higher thermal stability with prevention of sintering and formation of solid carbon over the surface of the catalyst. The selection criterion of support is based on various aspects such as structure, metal-support interaction, electronic modification, neutrality, and specific surface area [Cheng et al., 2010].

Bimbela et al.(2009) reported non-catalytic and catalytic SR processes of $C_3H_6O_2$ and $C_4H_{10}O$ as selected components of bio-oil operated at 823-1023 K with an increment of 100 K. In non-catalytic SR process, the effects of nature of model compounds and reaction temperature have been considered. Increasing reaction temperature results in an increase of total carbon conversion and gas yield. The highest conversions of $C_4H_{10}O$ and $C_3H_6O_2$are achieved as 50% and 86%, respectively at 1023 K. C_2 products came into existence at 823 K, higher at 923 K and significantly highest at 1023 K than the amount of other gaseous products such as H_2, CO_2, and CH_4. The production of H_2 and CO_2 decreases and the formation of CO, CH_4, and C_2 increase as the temperature rise. These results do not show similar trends as compared to other alcohols like ethanol in view of change in residence time during the experiment. In catalytic SR, various aspects such as the ratio of catalyst to feed flow rate, temperature, and nature of model compounds have been studied. Ni-Al coprecipitated catalyst with different weight ratios (23, 28, and 33%) was examined for yield of gaseous products

with respect to time. The nickel catalyst has a great effect on steam reforming of $C_4H_{10}O$ as well as $C_3H_6O_2$. When the ratio of catalyst weight to feed flow rate increases, then carbon conversion increases along with H_2 and CO_2 yield, but with the decrease in CO, CH_4, and C_2-products. SEM figures of utilized catalysts with different composition of nickel engaged in steam reforming of $C_4H_{10}O$ for two hours reaction time at 923 K ensure the possibility of filamentous type carbon formation on the catalyst surface.

Nahar et al. (2010) presented a simulation study on thermodynamic analysis of steam reforming of $C_4H_{10}O$ for the formation of H_2 via the method of Gibbs free minimization. The authors applied a range of operating conditions in temperature (573-1173 K), pressure (1-50 bar), and water to butanol molar feed ratio (1-18). The computed results reported optimal conditions (temperature of 873-1073 K, 1 atm pressure, and WBR of 9 to 12) for the maximum yield of hydrogen with minimum methane selectivity. The maximum hydrogen yield was 75.13-81.27 % on wet basis with 46.20-54.96% selectivity at the temperature of 1073 K and water to butanol feed ratios from 9 to 12. These operating conditions favoured the inhibition of carbon formation completely. Then, the simulations were divided into two sets of products such as H_2, CO, CO_2, and carbon as solid (with and without methane) to evaluate the influence of CH_4 over carbon formation at lower temperatures. The effect of higher pressure on hydrogen and carbon monoxide yield was found negative.

Wang et al. (2011) used Gibbs energy minimization formulation to carry out thermodynamic study for the sorption enhanced butanol steam reforming to examine the effects of temperatures (500-1500 K), pressure (1-100 atm), steam to butanol molar feed ratio (0-15) and calcium oxide to butanol molar feed ratio (0-15) on the concentration of H_2, CO, CO_2, CH_4 and coke. They found the optimum conditions for SESR of butanol process as the temperature of 800 K, atmospheric pressure, SBR of 10 and calcium oxide to butanol molar feed ratio of 8 under which 100% conversion of butanol, and 97.07% hydrogen, 2.84% methane, 0.05% carbon dioxide, 0.04% carbon monoxide, with an efficiency of 86.6% could be obtained. Under the same prevailing optimum conditions without calcium oxide to butanol molar feed ratio in steam reforming of butanol, 58.18% of H_2, 4.52% of CO, 15.67% of CO_2 and 21.62% of CH_4 and energy efficiency of 81.51% could be obtained. One of the advantages of butanol steam reforming with CO_2 adsorption using CaO for a proton exchange membrane fuel cell is higher hydrogen generation with better efficiency. This process also obviates the need for water gas shift reactor. Moreover, the operating conditions for carbon-formed and carbon-free regions in SR of butanol and SESRB are also analyzed. Hence, this

analysis helps us to find major components in the complex SESRB system without considering any kinetic constraints used in a real process.

Li et al. (2011) carried out the thermodynamic study of steam reforming of oxygenated fuels produced during biomass fermentation, hydrolysis, and pyrolysis like CH_3OH, C_2H_5OH, $C_6H_{12}O_6$, C_3H_7OH, C_4H_9OH, $C_2H_6O_2$, $C_6H_{14}O$, $C_3H_8O_3$, CH_3COOH, and C_3H_6O using the methodology of minimization of Gibbs free energy. They investigated operational conditions, energy efficiency, and reformate composition for reforming of various oxygenated fuels as mentioned above. They found that critical steam to carbon ratio with free carbon formation in the steam reforming process decreases as oxygen to carbon ratio increases in the given oxygenated fuels. The fuels having high hydrogen to carbon ratio have wider steam to carbon windows. The optimum temperature range for carrying out the steam reforming process is 873 to 973 K. Among the given fuels, methanol volunteers widest operational regime and the highest energy efficiency while glucose and acetic acid offer low energy efficiencies. The fuels like $C_2H_6O_2$ and $C_3H_8O_3$ termed as polyols also provide high energy efficiencies. In general, heavy fuels with a high oxygenation degree are not suitable for the production of H_2 in SR.

Thermodynamic study of steam reforming of several hydrocarbons enriched with O_2, such as CH_3OH, C_2H_5OH, C_3H_7OH, and $C_3H_8O_3$ with or without CaO as carbon dioxide sorbent has been accomplished to elucidate the optimum conditions for the production of high purity H_2 gas by using the formulation of Gibbs free energy minimization [Silva and Müller, 2011]. To fulfill this purpose, the effects of temperature, and molar feed ratio of steam to fuel on the concentration of desired products (H_2O, CO, CO_2, CH_4, and Carbon as solid) through steam reforming and sorption enhanced steam reforming have been considered. In SR technology, the highest concentration of H_2 (70-73, 70-72, 68-71, and 65-66 mol%, for methanol, ethanol, n-butanol and glycerol, respectively) with steam to carbon ratio of 2:1-4:1 for methanol and 2:1-3:1 for other oxygenated hydrocarbons (n-butanol, glycerol, and ethanol) at 973 K have been achieved with higher concentration of CO (greater than 5%). On the other hand, while using SESR technology, high-quality hydrogen (greater than 97%) with less concentration of CO, CH_4, and CO_2 at the temperature ranging 723-823 K can be achieved. Moreover, the removal of CO_2 from gaseous phase reduces the formation of solid carbon at low and moderate temperatures. Except this, SESR technology provides higher thermal efficiency (80-87% for methanol, and 79-83% for other compounds) between 723-873 K than SR with 67-70% for all compounds in the temperature range of 900-1000 K. The

computed results of Silva and Müller (2011) suggest a single step sorption enhanced steam reforming technology at the pressure of 3-5 atm and temperature ranging 723-773 K for the production of high-quality hydrogen with permissible CO content (less than 20 mg/L) which is the essential requirement for operating PEMFC. Therefore, WGS and COPROX reactors can be eliminated from further processing steps. The optimum steam to fuel ratios are 4:1, 6:1, 12:1, and 9:1 for methanol, ethanol, butanol, and glycerol respectively. In addition, the sorption enhanced steam reforming technology explores the better way to produce H_2 with minimum deposition of solid carbon as compared to SR process. This study also approbates the sorption enhanced steam reforming process over SR due to low temperature which can favour the activity of the catalyst and other constructional materials of the reformer. Another benefit of sorption enhanced steam reforming technology process is easy sequestration of CO_2.

The research work of Cai et al. (2012) demonstrates the production of H_2 gas from steam reforming of a bioresource-derived $C_4H_{10}O$ mixture processed by fermentation known as 'ABE mixture' (Acetone-Butanol-Ethanol = 3:6:1 expressed in terms of mass ratio) over supported Co-based bimetallic type catalysts. This support participates in catalytic performance actively and provides the better selection of catalyst to carry out steam reforming of biobutanol to produce a valuable fuel such as hydrogen with fewer amounts of undesirable products. For this purpose, various catalysts are tested successively and results depict that the Co/ZnO catalyst possesses the best catalytic properties as compared to Co/TiO_2 and Co/CeO_2. Besides, bimetallic Co-Ir/ZnO catalyst exhibits higher yield of hydrogen than only Co/ZnO. The amalgamation of Ir to Co/ZnO favours higher selectivity of hydrogen and minimizes CH_4 selectivity including prevention of carbon deposition under specified operating conditions of steam reforming of bio-butanol.

Medrano et al. (2014) investigated the catalytic steam reforming of butanol as a model compound of bio-oil at 923 K, and steam to carbon molar feed ratio of 14.7 to produce hydrogen gas in a quartz fluidized bed system at atmospheric pressure. Ni/Al catalyst with 28.5 weight% nickel content provides the thermodynamic equilibrium values obtained with catalyst weight to butanol ratio of 6.2 $g_{catalyst}.min/g_{butanol}$, without nitrogen and steam at 873 K, and a GHSV of around 11000 hr^{-1}. For the purpose of maximum production of hydrogen, various catalysts such as NiAl, NiAlMg0.26, NiAlCa0.12, and ImpNiAlCa0.03 are tested and results depict that the nickel catalyst modified with the magnesium is the appropriate catalyst because of its better performance and higher mechanical strength. The characterization

(FESEM and TPO) of magnesium modified catalyst shows high stability over alcohols with respect to time rather than other oxygenated compounds. Moreover, this combination of catalyst exhibits less carbon as solid on the surface of the catalyst when using the butanol and ethanol as compared to other compounds such as acetol and acetic acid.

Roy et al. (2014) prepared nickel catalysts on various supports (CeO_2 and Al_2O_3) using solution combustion route for the production of H_2 by butanol steam reforming at a pressure of 1034 kPa and in the temperature range of 458-488 K. The product gas was analyzed by a GC with a TCD and the liquid product was examined by GC with a FID. H_2, CO, CO_2, and alkanes (CH_4, C_2H_6, and C_3H_8) were considered as desired products while the liquid product was only butyraldehyde (C_4H_8O) with the negligible quantity of butyric acid ($C_4H_8O_2$) as the undesired product. The performance of these catalysts has been expressed in terms of butanol conversion, yield, and selectivity of gaseous and liquid products. In the case of both catalysts, the increase in pressure adversely affected the conversion of butanol but favoured the production of H_2 and CO_2. But from the selectivity point of view, the bubble point pressure was suggested as preferred operating condition for the reactor. The CeO_2 permits the higher O_2 mobility through the lattice and nickel doping which increases O_2 vacancy in the CeO_2 lattice. These two aspects greatly influenced oxygen capability of the Ni/CeO_2 in comparison to Ni/Al_2O_3 catalyst. The Ni/CeO_2 catalyst performed as a superior catalyst rather than Ni/Al_2O_3 and provided higher selectivity of H_2 and CO_2 with lower CO.

The catalytic steam reforming of butanol as a model compound of bio-oil for the production of H_2 gas as fuel over alumina and modified alumina supported nickel catalyst has been investigated [Bizkarra et al., 2015]. The catalysts were prepared by using wet impregnation method with the content of 13, 10, 6, and 3 wt% of Ni, CeO_2, La_2O_3, and MgO, respectively according to Sánchez- Sánchez et al. (2007). The prepared catalysts were tested at various temperatures and atmospheric pressure. After that, fresh and utilized catalysts were characterized to obtain their activity results. The higher amounts of hydrocarbons were achieved because WGS reaction did not participate actively at the operating condition in this experiment. At steam to carbon ratio of 5, complete conversion of butanol was acquired as well as higher hydrogen yield in a fixed bed reactor. The activity of Ni/CeO_2-Al_2O_3 catalyst was far better than other combinations of catalyst supports at 1073 K; maximum hydrogen yield was obtained due to the action of Ni/CeO_2-Al_2O_3.

Rh/ZrO_2 performed as a promising catalyst in catalytic reforming of butanol for the production of H_2 gas per weight of catalyst and per weight of active metals, in spite of internal diffusion limitation. The reaction scheme for butanol steam reforming is first direct reforming and then dehydration followed by reforming of butenes and WGS reaction.Rh/ZrO_2 catalyst performance was better at 1023 K with 100% conversion of butanol andhydrogen yield of 70%. The deactivation of Rh/ZrO_2 catalyst occurred due to the deposition of carbon over the surface of Rh nanoparticles during reforming [Harju et al., 2015]. They also described the role of C_4H_8 and C_4H_8O in Steam reforming of n-butanol over Rh/ZrO_2 catalyst [Harju et al., 2016]. Various characterization techniques such as BET surface area, XRF, TPO, CHNS+O elemental analysis, and FTIR were also utilized to study the fresh and spent catalyst surfaces. The catalyst activity was measured in term of stability, conversion, and product distribution, and coke deposition.

2.3.2 Dry reforming (DR) of butanol

Very little information is found in the literature on dry reforming of butanol, which concerns about the conversion of butanol, and the production of H_2 and CO in carbon free or carbon formed zones. The main reaction is depicted below in equation (2.3):

$$C_4H_{10}O + 3CO_2 \leftrightarrow 7CO + 5H_2 \quad (2.3)$$

Wang (2011) studied dry reforming of butanol using the method of Gibbs free energy minimization and assessed the effect of pressure, CO_2 to butanol ratio (CBR) and temperature. He analyzed that nearly complete butanol conversion (34.91-37.98% H_2 and 57.34-57.87% CO expressed in terms of concentration) could be accomplished if we provide optimum conditions (i.e. temperature range 1150-1200 K, a pressure of 1 atm and CBRs of 3.5-4.0); these are also the suitable conditions for in situ dry reforming of butanol to supply fuel for solid oxide fuel cell. At CBR (0 to 5) and temperature (500-1500 K), only carbon exists along with H_2, CO, CH_4 and H_2O while other compounds were found negligible. He found that higher pressure reduces H_2concentration, and hence maximum efficiency can be attained at atmospheric pressure only. He also showed that low temperature and low CBRs result in the coke formation. Hence, it was suggested to carry out the reaction in coke free region or otherwise in the presence of an appropriate catalyst.

2.3.3 Partial oxidation (POX) of butanol

Wang et al.(2010) reported thermodynamic analysis using Gibbs free energy minimization of partial oxidation of butanol. They studied the effects of temperature,

pressure, oxygen-butanol molar ratio, and nitrogen-butanol molar ratio and found 100% conversion of butanol with 93.07-96.56% yield of H_2 and 94.02-97.55% yield of CO under optimal conditions, i.e. reaction temperatures between 1115 and 1200 K, and OBR between 1.6 and 1.7 at a pressure of 1 atm. These conditions are favorable for in situ partial oxidation of butanol to supply fuels for a solid oxide fuel cell. With oxygen-butanol molar ratio (0 to 5) and temperature (500-1500 K) and pressure (1-20 atm), only carbon (graphite) exists along with H_2, CO, CO_2, CH_4 and H_2O while other compounds like C_2H_2, C_2H_4, C_3H_8, C_4H_8, and C_4H_8O were found negligible. Higher pressure tends to reduce H_2 efficiency while the presence of inert gases found to have the favorable effect. They also showed that low temperature and low oxygen-butanol molar ratio result in the carbon formation. Hence, it was suggested to carry out the reaction in coke free region or otherwise in the presence of an appropriate catalyst. Lastly, at optimized conditions, the energy efficiency was found between 88.78% and 91.13%.

CPOX of butanol for the production of hydrogen over LDH derived nickel-based and precious metal-promoted Ni-Mg-Al-Fe-O catalyst, prepared by co-precipitation and impregnation methods, have been done [Huang et al., 2013 and 2015]. The characterization tests such as XRD, XPS, and TPR were carried out to obtain activity results of above-mentioned catalysts for maximization of desired products and minimization of undesired products.

The formation of solid carbon over the surface of catalysts for the reactions of SR, POX, and DR of butanol is responsible for less activity, low durability, and deactivation of catalyst. Figure 2.1 describes the elegant information about carbon-free and carbon-formed zones for SR, POX, and DR of butanol as a function of SBR, POX, and CBR, respectively at different pressures [Wang et al., 2010 and 2011, Wang 2011].

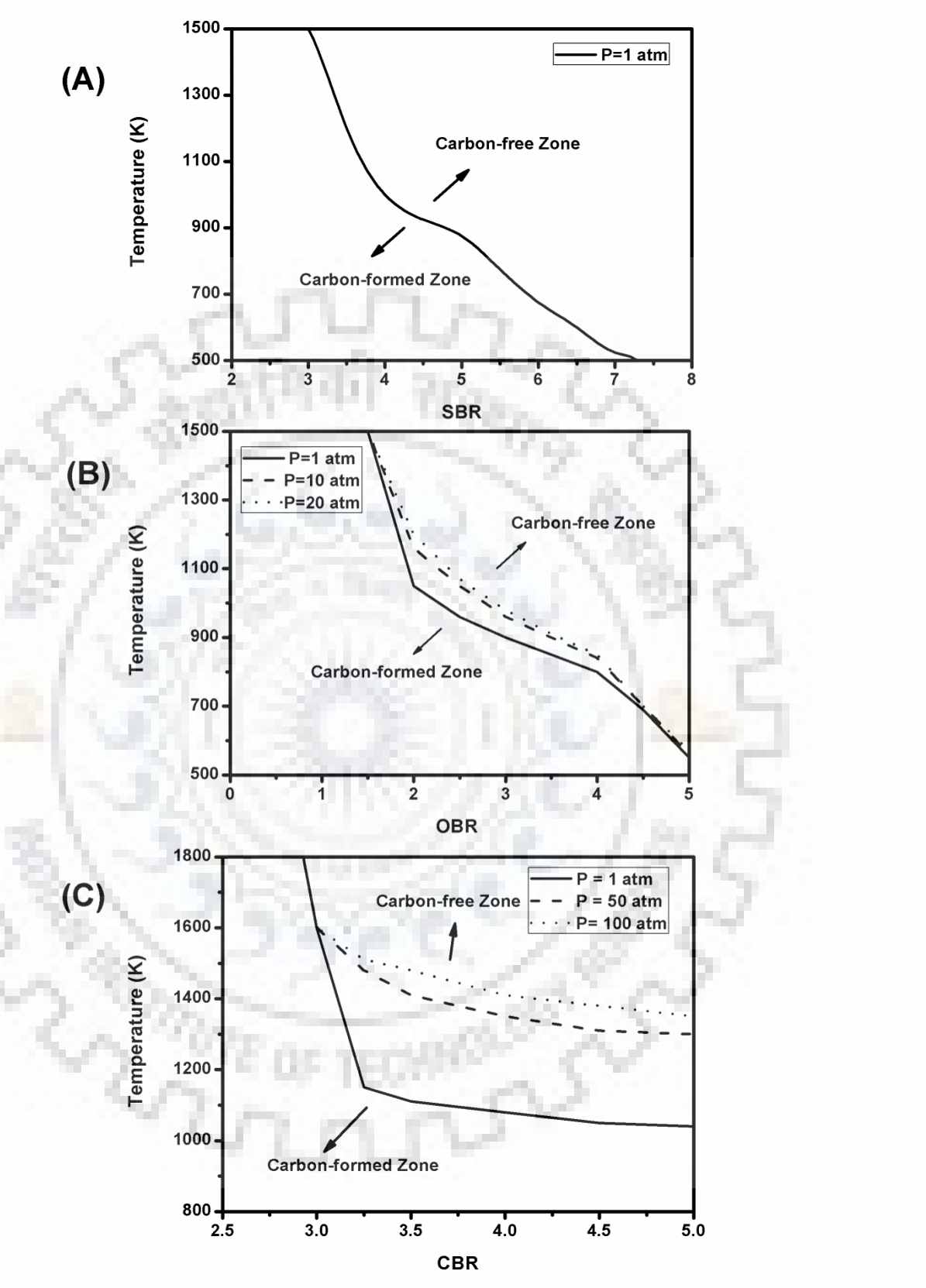

Figure 2.1 Coke formed and coke free zones in (A) SR, (B) POX, and (C) DR of butanol at different pressures. Reprinted with permission from Wang et al. 2010, 2011 and Wang 2011. Copyright Elsevier.

The thermodynamic evaluation of carbon formation has been done via stoichiometric approach method. Four equations of carbon formation are considered which are given below:

$$2CO \leftrightarrow CO_2 + C \tag{2.4}$$

$$CH_4 \leftrightarrow 2H_2 + C \tag{2.5}$$

$$CO + H_2 \leftrightarrow H_2O + C \tag{2.6}$$

$$CO_2 + 2H_2 \leftrightarrow 2H_2O + C \tag{2.7}$$

The carbon activities of Eqns. (2.4) to (2.7) are calculated by the expressions given below:

$$a_{C_{11}} = K_{11} \frac{Py_{CO}^2}{y_{CO_2}} \tag{2.8}$$

$$a_{C_{12}} = K_{12} \frac{y_{CH_4}}{Py_{H_2}^2} \tag{2.9}$$

$$a_{C_{13}} = K_{13} \frac{Py_{CO}y_{H2}}{y_{H_2O}} \tag{2.10}$$

$$a_{C_{14}} = K_{14} \frac{Py_{CO_2}y_{H_2}^2}{y_{H_2O}^2} \tag{2.11}$$

Where, K_{11}, K_{12}, K_{13}, *and* $K_{14}$are the equilibrium constants for reactions (2.4) to (2.7), respectively. Likewise, y_{CO}, y_{CO_2}, y_{CH_4}, and y_{H_2O} are the mole fractions of CO, CO_2, CH_4, and H_2O, respectively. For SR, POX, DR of butanol, the formation of carbon is possible when the maximum value of carbon activity a_C among four is greater than unity.

$$a_C = \max(a_{C_{11}}, a_{C_{12}}, a_{C_{13}}, a_{C_{14}}) > 1 \tag{2.12}$$

If, $a_C < 1$, then the region is carbon-free; and $a_C = 1$, which depicts the boundary of carbon formation [Chen et al., 2009].

2.3.4 Autothermal reforming (ATR) of butanol or Oxidative steam reforming (OSR)of butanol

Sun et al. (2012) conducted an autothermal reforming of isomers of butanol in a short contact-time reactor consisting of two stages, first was upstage stream incorporating 1% by weight of Pt on α-Al_2O_3 followed by downstream stage consisting of either HFER, HZSM-5 or γ-Al_2O_3 catalysts in which butanol can be converted into butenes with 95% yield. The effect of a certain temperature range over the conversion of butanol and its isomers was also investigated. The performance of catalysts was compared on the basis of the yield of butene. Higher butenes yields were obtained over γ- Al_2O_3 (90-95% at 593 K and 623 K) and HFER (90-95% at temperature range of 553-623 K) rather than HZSM-5 (75% at 503 K), which was at least 20% higher in view of small pore structure in HFER and the absence of large Bronsted acid sites in γ-Al_2O_3. To study the influence of hydrocarbon structure on product formation, a heated tube reactor at temperatures between 473-673 K was used in which the reactivity of the t-butanol was found higher. *trans*-2-butene and *cis*-2-butene were formed from isomers of linear structured $C_4H_{10}O$ while isobutene formed from isomers of branched structure type $C_4H_{10}O$. The selectivity of desired components with HZSM-5 in the staged autothermal reactor was compared with the heated tube type reactor with a margin of less than 10% at similar operating conditions. Hence, this method provides an alternate way to dehydrate butanol to butene instead of conventional methods for exploitation of biomass applications. One of the main advantages of the combination of exothermic and endothermic chemistry was as it provided a process technology to maintain the bed temperature in reaction atmosphere.

Oxidative steam reforming of bio-butanol (Acetone-Butanol-Ethanol = 3-6-1 expressed in terms of mass ratio) has been carried out to produce hydrogen over CoIr-based catalysts. This research work describes the influences of support on the activity of bimetallic CoIr catalyst which incorporated 6.5 wt% Co and 0.4 wt% Ir. Different tests of several supports for catalysts (CoIr/18$CeZrO_2$, CoIr/ZnO, and CoIr/TiO_2) were done at 773 K for 60 hours with raw material/water/air/Ar = 1/10/7.5/12 molar ratio and GHSV of 7500 hr^{-1}. CoIr/18$CeZrO_2$ was found best catalyst rather than CoIr/ZnO and CoIr/TiO_2. CoIr/18$CeZrO_2$ catalyst reported maximum conversion (86%) of bio-butanol raw material at 773 K with 68.5 mol% hydrogen. Characterization of post-experiment catalysts exhibited that CoIr/18$CeZrO_2$ had active cobalt sintering and capability to prevent the carbon formation on the surface of catalyst [Cai et al., 2013].

The effect of the addition of various noble metals (M=Ru, Rh, Ir, Pd) on bimetallic CoM/ZnO catalyst [Cai et al., 2014a] has been investigated for the production of H_2 via OSR of the bio-butanol raw mixture obtained from ABE fermentation. The addition of metal M improved the activity of monometallic Co/ZnO catalyst and reduced cobalt sintering and deposition of carbon under specified optimum operating conditions. CoRh/ZnO catalyst performed best among selected combinations and exhibited 84% conversion of bio-butanol with a higher amount of hydrogen (65.1 mol%) and less coke deposition on the surface of the catalyst.

Another research work of Cai et al. (2014b) presented detailed description about catalytic behavior and catalytic structure prepared by urea as precipitation agent and then treated with calcination at different temperatures (773, 973, and 1173 K). Various characterization tests such as BET surface area, basicity, reduction properties, crystallite size, and OSC were done to obtain the characteristics of the catalyst. Moreover, many other characterization techniques of the fresh and used catalyst such as XRD, TPR, CO_2 TPD, CAC, RS, DRIFTS, TEM, XPS, and OSC were performed to determine the stability and deactivation process of catalyst.

Moreover on autothermal reforming of *iso*-butanol for hydrogen production on low-cost materials like Ru-prompted nickel xerogel catalysts under optimum conditions to achieve less carbon formation was done by Sharma et al. (2015). The Sol-gel method was employed to prepare all the catalysts which were characterized (by XRD, BET surface area, TPR, pore size, TPD of H_2, TEM, SEM, and TPO) as having mesoporous pores, higher surface area, and type-IV N_2 adsorption and desorption isotherms. No clear crystallinity/phase identification was detected as active Ni and promoter Ru which were well dispersed in the support. Ru and Ce-Zr reduced the reaction temperature (termed as reduction temperature in this work) and consequently a higher availability of nickel was available on the catalyst surface. Autothermal reforming of butanol was processed in a fixed bed reactor under operating conditions of the temperature range from 873 to 1023 K, space velocity range of 130,000-650,000 h^{-1}, water to carbon molar feed ratio in the feed between 0 to 4, and oxygen/carbon molar ratio of 0 to 1. The 0.3wt% Ru/10 wt% Ni/Ce (3 wt%) $O_2/ZrO_2/Al_2O_3$ catalyst exhibited high catalytic activity for *iso*-butanol, less carbon deposition on the catalyst surface, good resistance to sintering and prolonged stability of the catalyst. Catalytic ATR reactions were done in a fixed bed reactor with optimum conditions as 973 K temperature, atmospheric pressure, H_2O to carbon molar ratio = 2, and O_2 to carbon molar ratio = 0.35 and space velocity = 217,000 h^{-1}.

Along with improving hydrogen production, Ru promotion also prevented the coke formations under these specified conditions.

Thermodynamic analysis and experimental studies have been carried out for the formation of H_2 from OSR of $C_4H_{10}O$ over several catalysts [Hartley et al., 2015, Dhanala et al., 2015]. For thermodynamic equilibrium computations, the method of minimization of Gibbs free energy was used. Hartley et al. (2015) suggested the operating conditions (temperature range of 573-1373 K, 1 atm, SBR ranging from 0-12, and OBR of 0 to 6) for oxidative steam reforming (OSR) of $C_4H_{10}O$ over Ni/Al_2O_3 and Rh/Al_2O_3 catalysts. The maximum yield of hydrogen (5.56 $mol/mol_{butanol}$)was achieved at the temperature of 973 K under atmospheric conditions with SBR of 12 whereas formation of carbon as solid and methane found low. They also determined thermoneutral conditions at OBR of 2.71-2.80 at 973 K and 2.65-2.75 at 1073 K, respectively. Rh/Al_2O_3 catalysts showed close results to the thermodynamic conditions at 973 K with SBR of 9 and OBR of 2.70 under atmospheric conditions. On the other hand, Dhanala et al. (2015) investigated the OSR and compared it with SR of isobutanol over alumina supported Ni catalysts ($Ni/\gamma\text{-}Al_2O_3$). The characterization of the catalyst has been done with several techniques such as XRD, TPR, BET surface area, and SEM. The experimental data were very close to thermodynamic equilibrium calculations. Increase in OBR from 0 to 2.5 at 923 K, and SBR of 2.5 described a decrease in hydrogen yield (68% from 80%) and methane selectivity (1.7% from 4.8%). It means that the rise of OBR led to a drop in H_2 yield and selectivity of methane as well as CO but the increase in SBR favoured high H_2 yield and minimize the selectivity of CO with CH_4 in both SR and OSR. The H_2/CO molar ratio was found 7-8 at 923 K and SBR of 2.5.

Horng et al. (2016) reported chemical equilibrium analysis of OSR of $C_4H_{10}O$ for the production of syngas and formation of carbon thermodynamically. At SBR of 3 and OBR of 1.5, the thermal neutral temperature was 873 K which generated 59.3% yield of H_2, 39.5% yield of CO, and 65.1% efficiency of the reformer. Moreover, a significant amount of O_2 was added during reforming reactions in the temperature range of 673-1073 K to prevent coke formation.

2.3.5 Aqueous phase reforming (APR) of butanol

Roy et al. (2011 and 2014) published two research articles on experimental analysis of aqueous phase reforming of butanol over nickel catalyst with supports of Al_2O_3 and CeO_2. These catalysts were prepared with both supports for nickel (20 wt%) by using solution

combustion process. This is a simple, fast, and highly efficient process for generation of porous and small size materials known as a catalyst [Shuk et al., 1996; Bosze et al., 2003; Jocobsohn et al., 2008]. A possible reaction network to understand the system in aqueous phase reforming of butanol has also been provided as shown in Figure 2.2.

This reaction scheme incorporated primarily dehydrogenation of butanol to form butyraldehyde and water followed by decarbonylation to propane which breaks C-C bond to obtain H_2 and CO through steam reforming reaction. This CO can be converted into CO_2 due to WGS reaction and CO_2 may be converted into methane or ethane via Fischer-Tropsch synthesis reaction. When this scheme is operated at high pressure and low temperature then aqueous phase reforming (APR) occurs. Roy et al. (2014) compared the results of APR with steam reforming and concluded as follows:

- An aqueous phase reformer can be utilized for the steam reforming of butanol at different operating conditions.
- As system pressure increases, the conversion of butanol decreases in aqueous phase reforming as in steam reforming.
- Increasing pressure reduces the production of H_2 as well as CO_2 and alkanes expressed in terms of selectivity.
- Aqueous phase reforming of butanol was responsible for high-pressure water in the liquid phase which helped in water gas shift reaction.
- The SR and APR of butanol over nickel catalysts with supports of CeO_2 and Al_2O_3 have been investigated where alkane's selectivity was found higher for Ni/CeO_2 catalyst in SR than APR.
- Ni/CeO_2 was more efficient than Ni/Al_2O_3 catalyst in both SR and APR processes to produce higher hydrogen and CO_2 with lower CO.

The demerit of APR as compared to SR is its lower hydrogen selectivity because it operates at a low temperature which results in the formation of alkanes, and depends on the catalyst for obtaining the higher yield of the products [Hirai et al., 2005; Ciftci et al., 2014].

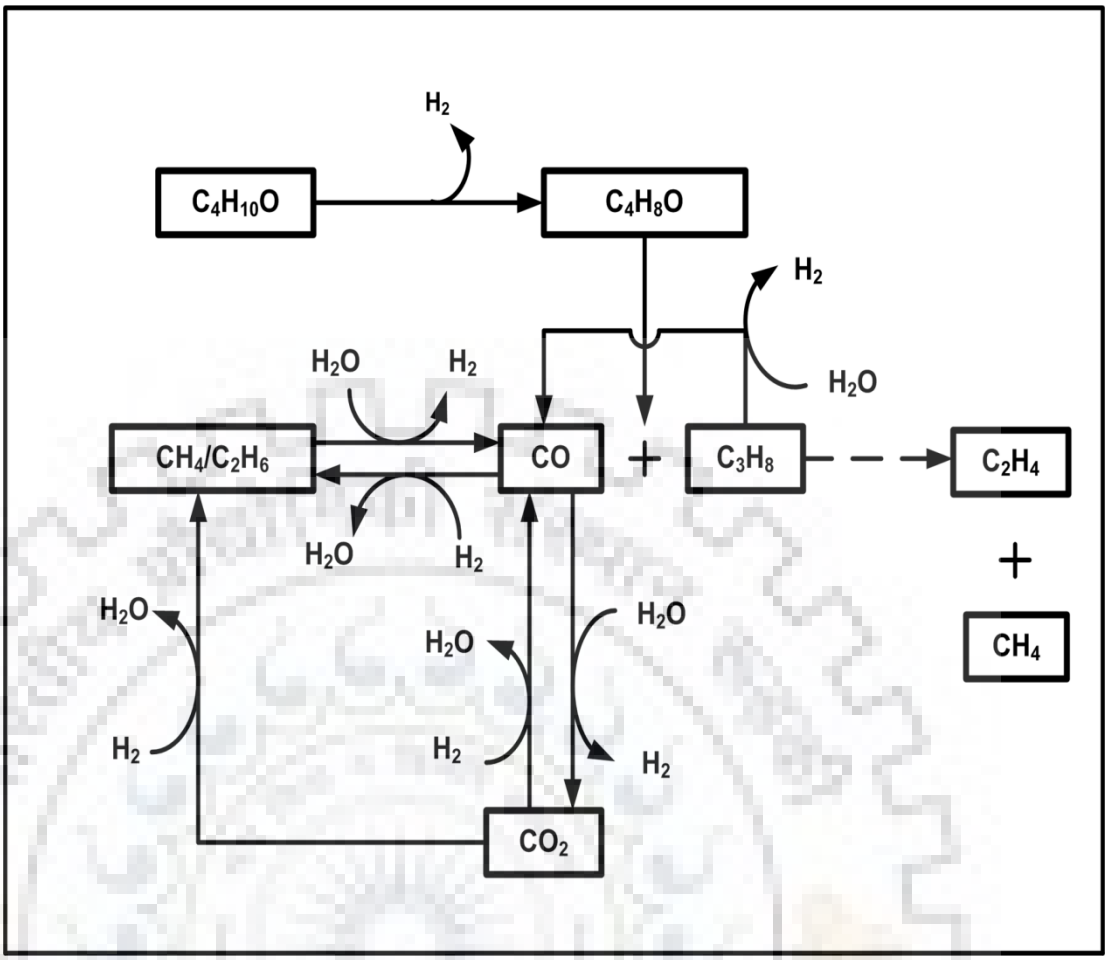

Figure 2.2 Possible reaction pathways for aqueous phase reforming of butanol. Reprinted with permission from Roy et al. 2011 and 2014. Copyright Elsevier.

2.3.6 Supercritical water reforming (SCWR) of butanol

SCWR is also an alternative process for the production of H_2 from $C_4H_{10}O$. This process has several unique properties such as it provides higher space time yields and reduces mass transfer coefficients. Besides, H_2 is generated in SCWR at high pressure and can be stored in a cylinder which requires less energy consumption for its compression [Pairojpiriyakul et al., 2014].

The disadvantage of this process is that high hydrogen production can be achieved above 873 K, while lower temperature less than 673 K favours CH_4 production. Moreover, the supercritical water provides some challenges to deal with such as high pressure, solid handling, and corrosion [Mitton et al., 2000]. Some catalysts which participate in the reaction system are difficult to recover from the reactor effluent during supercritical water reforming

process. This creates corrosion issue and can also plug the reactor due to the low solubility of salts in supercritical water reforming [Markočič et al., 2013]. Also from an economic point of view, high pressure costs more than low pressure in operating processes such as steam reforming and oxidative steam reforming. Ortiz et al. (2016) conducted an experiment on SCWR of some model compounds (CH_3COOH, $C_3H_6O_2$, $C_4H_{10}O$, and $C_6H_{12}O_6$), performed in a tubular reactor in the absence of a catalyst to obtain higher yield of hydrogen. Additionally, non-stoichiometric approach via Aspen Plus and stoichiometric approach via Matlab software have been carried out to obtain favourable thermodynamic conditions for supercritical reforming to maximize hydrogen concentration. Thermodynamic results were compared with the experimental data and found close to each other.

Table 2.2 depicts necessary information regarding experimental as well as simulation studies on various reforming technologies investigated by various researchers for the production of valuable fuels via butanol with brief description of used catalysts, reactor, conversion of butanol, and operating parameters.

Table 2.2 Butanol reforming (Experimental and thermodynamic modeling studies)

S. No.	Reforming Process	Authors	Operating conditions	Results	Reactor	Catalysts	Stability	Experiment/ Thermodynamic Modeling Study
1.	Steam Reforming	Bimbela et al. (2009)	Temperature = 923 K Pressure = 1 atm SBR = 14.71	Conversion = 97.50% H_2 = 74.60 (mol%) CO =2.81(mol%) CO_2 =22.56 (mol%)	Fixed bed reactor	Ni/(Ni + Al)	Stable	Experimental
		Nahar et al. (2010)	Temperature = 1073 K Pressure = 1 atm SBR = 12	Conversion = 100% H_2 = 81.16 (Y_1) CO = 52.38 (Y_1)	---	---	---	Thermodynamic Modeling
		Wang et al. (2011)	Temperature = 800 K Pressure = 1 atm SBR = 10	Conversion = 100% H_2 = 58.18 (mol%) CO = 4.52 (mol%) CH_4 = 15.67 (mol%) CO_2 = 21.62 (mol%)	---	---	---	Thermodynamic Modeling
		Li et al. (2011)	Temperature = 873-973 K Pressure = 1 atm SBR > 2.5	---	---	---	---	Thermodynamic Modeling
		Cai et al. (2012)	Temperature = 873 K Pressure = 1 atm SBR= 4	Conversion= 97% H_2 = 65.5 (mol%) CO =14.2 (mol %) CO_2 =7.4(mol %) CH_4 =12.6 (mol%)	Fixed bed reactor	Co/ZnO Co/CeO_2 Co/TiO_2 Co-Ir/ZnO	Stable (90 hr)	Experimental
		Medrano et al. (2014)	Temperature = 923 K Pressure = 1 atm SBR=14.7	Conversion= 97.41% H_2= 75.33 (mol%) CO= 3.55(mol%) CO_2= 20.59 (mol%) CH_4= 0.47 (mol%)	Fluidized bed reactor	NiAl NiAlMg0.26 NiAlCa0.12 ImpNiAlCa0.03	Stable	Experimental

Table 2.2 Butanol reforming (Experimental and thermodynamic modeling studies) *contd.*

S. No.	Reforming Process	Authors	Operating conditions	Results	Reactor	Catalysts	Stability	Experiment/ Thermodynamic Modeling Study
		Roy et al. (2014)	Temperature = 488 K Pressure = 10.20 atm SBR = 78.10	Conversion =5-6% H_2= 48% (S_1) CO = 34% (S_2) CO_2=63 % (S_2) Alkanes = 64% (S_2)	Fixed bed reactor	Ni/CeO_2 Ni/Al_2O_3	Stable	Experimental
		Bizkarra et al. (2015)	Temperature = 1073 K Pressure = 1 atm SBR= 5	Conversion =100% $H_2 \geq$ 80% (Y_1)	Fixed bed reactor	Ni/CeO_2-Al_2O_3	Stable	Experimental
2.	Sorption Enhanced Steam Reforming	Silva et al. (2011)	Temperature= 848 K Pressure = 1 atm SBR= 12	H_2 = 99.06 (mol%) CO = 0.12 (mol%) CO_2 = 0.17 (mol%) CH_4 = 0.65 (mol%)	---	---	---	Thermodynamic Modeling
3.	Dry Reforming	Wang et al. (2011)	Temperature = 1150-1200 K Pressure = 1 atm CBR = 3.5-4.0	Conversion =100% H_2 = 34.91-37.98 (mol%) CO = 57.34-57. 87 (mol%) CH_4 = 0.01-0.20 (mol%)	---	---	---	Thermodynamic Modeling
4.	Steam- and Autothermal - Reforming	Harju et al. (2015)	Temperature = 973 K Pressure = 1 atm SBR = 4 OBR = 0.1	Conversion =100% H_2 = 70% (Y_1)	Fixed bed reactor	Rh/ZrO_2	Stable (21 hr)	Experimental
5.	Aqueous Phase Reforming	Roy et al. (2011)	Temperature = 488 K Pressure = 27.22 atm WBR = 78.10	Conversion = 5.77% H_2=67 % (S_1) CO= 25% (S_2) CO_2= 76% (S_2) Alkanes= 66% (S_2)	Fixed bed reactor	Ni/Al_2O_3 Ni/CeO_2	Stable	Experimental

Table 2.2 Butanol reforming (Experimental and thermodynamic modeling studies) *contd.*

S. No.	Reforming Process	Authors	Operating conditions	Results	Reactor	Catalysts	Stability	Experiment/ Thermodynamic Modeling Study
6.	Autothermal Reforming or Oxidative Steam Reforming	Sun et al. (2012)	Temperature = 563K Pressure = 1 atm OBR = 0.83	Conversion = 95% Butene = 95% (Y_1) H_2 = NR	Autothermal stage reactor	Pt/α-Al_2O_3 γ- Al_2O_3 HFER HZSM-5	Stable (20 hrs)	Experimental
		Cai et al. (2013)	Temperature = 773 K Pressure = 1 atm SBR= 3 OBR = 1.5	Conversion = 86% H_2 = 68.5 (mol%) CO =2.5 (mol%)	Fixed bed reactor	CoIr/ZnO CoIr/TiO_2 CoIr/18$CeZrO_2$	Stable (60 hrs)	Experimental
		Cai et al. (2014 a)	Temperature = 773 K Pressure = 1 atm SBR= 3 OBR = 1.5	Conversion = 84 % H_2 = 65.1 (mol%) CO $\leq$ 2 (mol%)	Fixed bed reactor	Co/ ZnO CoIr/ZnO CoRh/ZnO CoRu/ZnO CoPd/ZnO	Stable (100 hrs)	Experimental
		Cai et al. (2014 b)	Temperature = 773 K Pressure = 1 atm SBR= 3 OBR = 1.5	Conversion = 70 % H_2 = 70 (mol%)	Fixed bed reactor	CoIr/$Ce_{0.82}Zr_{0.18}$ 500 CoIr/$Ce_{0.82}Zr_{0.18}$ 700 CoIr/$Ce_{0.82}Zr_{0.18}$ 900	Stable (100 hrs)	Experimental
		Hartley et al. (2015)	Temperature = 973-1073 K Pressure = 1 atm SBR= 9-12 OBR=1.5-3	Conversion =100 % H_2= 46.33% (Y_1)	Fixed bed reactor	Rh/Al_2O_3 Ni/Al_2O_3	Stable	Experimental
		Sharma et al. (2015)	Temperature = 973 K Pressure = 1 atm OBR =0.35	Conversion =100 % H_2 = 32 % (Y_1) CO = 10% (Y_1) CO_2= 12.5 % (Y_1)	Fixed bed reactor	Ru-Ni-CeO_2-ZrO_2-Al_2O_3	Stable (25 hrs)	Experimental

Table 2.2 Butanol reforming (Experimental and thermodynamic modeling studies) *contd.*

S. No.	Reforming Process	Authors	Operating conditions	Results	Reactor	Catalysts	Stability	Experiment/ Thermodynamic Modeling Study
		Horng et al. (2016)	Temperature = 773-923 K Pressure = NR OBR=1.5-3.2	Conversion =100 % H_2= 80% (Y_1) CH_4=4.8 (S_2)	Fixed bed reactor	γ-Al_2O_3 20NiOAl 30NiOAl 20NiAl 30NiAl	Stable	Experimental
		Horng et al. (2016)	Temperature = 1073 K Pressure = NR SBR = 3 OBR =1.5	Conversion =100 % H_2 =75.1 % (Y_1) CO = 74% (Y_1)	---	---	---	Thermodynamic Modeling
7.	Partial Oxidation	Huang et al. (2013)	Temperature = 973 K Pressure = 1 atm OBR = 2.0	Conversion =100 % H_2 = 80.6 % (S_1)	Fixed bed reactor	$Ni_{0.35}Mg_{2.65}Al_{0.5}Fe_{4.5\pm\delta}$	Stable (31 hr)	Experimental
		Wang et al. (2010)	Temperature = 1115-1200 K Pressure = 1 atm OBR = 1.6-1.7	Conversion =100 % H_2 = 93.07-96.56 (Y_1)	---	---	---	Thermodynamic Modeling
		Huang et al. (2015)	Temperature = 973 K Pressure = 1 atm OBR=2	Conversion =100% H_2 =34.17% (Y_1)	Fixed bed reactor	Ni-Mg-Al-Fe-O with or without precious metals of Rh, Ir, Ru, and Pt	Stable (8 hr)	Experimental

$$\text{Butanol Conversion} = \left(\frac{\text{Initial moles - final moles remained}}{\text{Initial moles}}\right)\times 100 \qquad Y_1 = \frac{\text{moles of product formed}}{\text{stoichiometric coefficient} \times \text{moles of reactant fed}}\times 100$$

$$S_1 = \left(\frac{\text{Moles of } H_2 \text{ formed}}{\text{Maximum moles of } H_2 \text{ which can be formed}}\right)\times 100 \qquad S_2 = \left(\frac{\text{Moles of C or } H_2 \text{ in product gas}}{\text{Total moles of C in output gas product}}\right)\times 100$$

2.4 ETHANOL REFORMING

2.4.1 Steam reforming of ethanol

Most of the research is found on steam reforming of ethanol for the production of hydrogen by using various types of catalysts. The experiments for steam reforming of ethanol have been carried out in a fixed bed reactor under atmospheric pressure to produce hydrogen as clean energy fuel which is expressed in terms of selectivity [Deng et al., 2008]. The results show that the catalysts with 31 wt% ZrO_2 performed well in comparison to other type of catalysts involved in the steam reforming of ethanol at 650ºC, steam to ethanol molar feed ratio=13, and LHSV= 4.8 h^{-1}. Under these operating conditions, the selectivity of hydrogen was 74.3 mol% with negligible methane formation. The activity of NiO/ZnO/ZrO_2catalyst provides high hydrogen production which can be used as fuel in molten carbonate fuel cells. The stability of this catalyst is approximately 60 hours without deactivation. Profeti et al. (2009) investigated the activity of Ni/CeO_2-Al_2O_3 catalysts promoted by noble catalysts such as Pt, Ir, Pd, and Ru for the production of hydrogen by using steam reforming of ethanol and glycerol as biofuels. Several characterization tests, e.g., energy dispersive X-ray (EDXR), BET surface area, X-ray diffraction (XRD), temperature-programmed reduction (TPR), UV-*vis* diffuse reflectance spectroscopy (UV-DRS) and X-ray absorption near edge structure (XANES) were used to determine physical and chemical properties of catalysts along with its activity and selectivity. Promoted catalyst provided higher yield of hydrogen than unpromoted catalysts as mentionedabove. Among all the combinations, NiPd/CeO_2-Al_2O_3 for ethanol steam reforming at 873 K, andNiPt/CeO_2-Al_2O_3 for glycerol steam reforming at 973 K is found feasible for the higher production of H_2. The addition of noble metals to the catalyst increases the stability and activity of Ni/CeO_2-Al_2O_3 catalyst which also improves the performance of reforming system.

Ni/Mg/Al hydrotalcite-like precursors prepared by co-precipitation method have been used for the production of H_2 in steam reforming of ethanol [Li et al., 2010]. Various characterization techniques such as XRD, TEM, TPR, and TGA have been used to identify the physico-chemical properties of the prepared catalyst. The composition Ni-Mg-O solid solution phase in the catalyst enhances its activity and stability for the steam reforming of ethanol. The complete conversion (100%) of ethanol over the NiMg6 catalyst in the reforming process was found at 400ºC. The equilibrium concentration of hydrogen increases with the increase in temperature, GHSV, and Ni/Mg ratio. At low Ni/Mg ratio, the coke formation occurs which reduces the activity and stability of catalyst. High reduction pretreatment

temperature greater than 650ºC improves the performance of catalyst. For complete elimination of coke in ethanol steam reforming system, the suggested optimum value of reduction temperature is 800ºC. Arslan et al. (2014) performed experiments for the production of high purity hydrogen via steam reforming of ethanol by using nickel based zirconia incorporated mesoporous silicate supported catalysts such as Zr-SBA-15 and Zr-MCM-41.The effects of operating variables, such as temperature (823-923 K) and steam/ethanol molar feed ratio (3.2, 4, and 5) are investigated on the formation of H_2 and other products (CO, CO_2, and CH_4) with carbon deposition on the surface of catalysts. Ni/Mg-Zr-SBA-15 provided high hydrogen yield (74.3%) at 873 K and steam/ethanol molar feed ratio = 4 after 5 hours of reaction. Both types of carbon (filamentous and graphite) were found over the surface of nickel based Zr-SBA-15 supported catalysts and this deposition can be minimized or avoided by increasing the temperature above 873 K. Dan et al. (2015) studied the steam reforming of ethanol at low temperature and high steam to ethanol feed ratio conditions for the production of H_2 fuel on nickel (8 wt%) based catalysts supported by CeO_2 (6 wt%) and La_2O_3 (6 wt%), and promoted by alumina and zirconia. The catalysts were prepared by the method of wet impregnation and characterized by some tests such as XRD, TPR, H_2-TPD, and H_2 chemisorption. The addition of alumina and zirconia with CeO_2 and La_2O_3 enhanced the activity of nickel based catalyst in terms of dispersion and stabilization. At the temperature of 573 K, the conversion of ethanol was 100% in case of addition of CeO_2 to Al_2O_3 supported catalytic material. For the sake of comparison, thermodynamic analysis has also been carried out by using CHEMCAD simulation software on the basis of GFE method in order to attain compositions of products at equilibrium. The maximum hydrogen yield was obtained at 623 K for Ni/La_2O_3-ZrO_2. Except Ni/ZrO_2 catalysts, other combinations were found stable in 24 hours of run time.

H_2 has been produced from steam reforming of ethanol by using Rh/CeO2 catalyst with a stoichiometric composition of feed material [Hou et al., 2015]. The conversion of ethanol was 100% at 673 K. The desired product hydrogen was achieved maximum at this temperature with other products such as CO, CO_2, and CH_4 due to the C-C bond cleavage capacity of Rh particles. The stability of Rh/CeO_2 catalyst was approximately 70 hours with no coke formation over its surface. In another study, the performance of Rh/Al_2O_3 and Rh/$CeZrO_2$ catalysts were compared for the production of H_2 by steam reforming of ethanol [Sharma et al., 2016]. The influences of operating parameters like temperature (723-873K), and feed flow rate (0.1, 0.2, and 0.3 mL/min) were studied with constant steam to ethanol molar feed ratio of 6 on the production of hydrogen. The higher hydrogen selectivity was

achieved for $Rh/CeZrO_2$ catalysts (62.9%) in comparison to Rh/Al_2O_3 (59.3%). The average flow rate at the exit was also higher for $Rh/CeZrO_2$ catalysts (263mL/min) than Rh/Al_2O_3 (236 mL/min). Moreover, the amount of carbon deposition was also lower in case of $Rh/CeZrO_2$ catalysts (6.75 $mmol/g_{catalyst}$) as compared to Rh/Al_2O_3 (10.57$mmol/g_{catalyst}$). The stability for both the catalysts were found upto 20 hours for steam reforming of ethanol to produce hydrogen.

Carvalho at al. (2016) performed experiments for the production of hydrogen by using steam reforming process of bio-ethanol over Co_3O_4/CeO_2 catalysts (5, 10, and 20% Co wt%) which were synthesized by one-step polymerization method. Several tests such as XRD, SEM, and TPR analyses were conducted to examine the activity of prepared catalyst. Co_3O_4/CeO_2 mixture with 20wt% cobalt (20 CoCe catalyst) was found promising among other combinations for steam reforming of bio-ethanol at 773 K in terms of high hydrogen selectivity, high surface area, high metallic dispersion, and less carbon deposition rate with good stability. González-Gil et al. 2016 prepared $RhCeNi/Al_2O_3$ as multimetallic catalyst with Rh:Ce:Ni = 0.0009:5:9 for the production of hydrogen in steam reforming of ethanol at laboratory and pilot plant scale. The interaction between Ce-Ni was found benefical where Ce was available in the forms of Ce^{4+} and Ce^{3+}, and addition of nickel into ceria fluorite-type structure also modified the average size of catalyst particles. The combination of Ni and Ce with Rh provided good activity and stability for the conversion of ethanol, and higher hydrogen selectivity with minimum production of other by-products at laboratory as well as pilot plant scale. Greluk et al. (2016) presented the results of steam reforming of ethanol (SRE) and oxidative steam reforming of ethanol (OSRE) over $PtKCo/CeO_2$ catalyst prepared by impregnation of high-surface CeO_2 (S_{BET}=42.5 m^2/g) with the citrate complex of cobalt and highly promoted potassium and platinum. The operating steam:ethanol ratio and steam:ethanol:oxygen ratio were 9:1 and 9:1:0.7, respectively. Addition of platinum in KCo/CeO_2 enhanced the cobalt dispersion and reduction of cobalt oxide. The complete conversion was achieved with high selectivity of hydrogen at 813 K. The presence of oxygen in the feed prevented coke deposition over the surface of $PtKCo/CeO_2$ catalyst. The activity of this catalyst was higher in OSRE than SRE. However, the selectivity of hydrogen was lower in OSRE than SRE.

Few research studies are found on theoretical evaluation of steam reforming of ethanol for the production of H_2. Li et al. (2011) investigated operating conditions, energy efficiency of reformer and H_2/CO ratio for steam reforming of various oxygenated fuels such as CH_4O,

C_2H_6O, $C_4H_{10}O$, $C_6H_{14}O$, $C_2H_6O_2$, $C_3H_8O_3$, $C_6H_{12}O_6$, $C_2H_4O_2$, and C_3H_6O, obtained from biomass fermentation, fast pyrolysis, and hydrolysis processes for the production of hydrogen via GFEM method. The three main conclusions were drawn out from the above study as (i) the operating temperature range for each fuel was 873-973K, (ii) the fuels with higher hydrogen/carbon ratio provided wide steam/carbon windows, (iii) the critical steam/carbon ratio with negligible carbon formation decreased with the increase in oxygen/carbon ratio of above mentioned oxygenated fuels. Likewise, Xie at al. (2013) presented thermodynamic equilibrium study on steam reforming of various components as ethanol, acetic acid, acetone, and phenol as model compounds of bio-oil to produce hydrogen with or without CaO as CO_2 sorbent. During thermal decomposition of ethanol the yield of hydrogen increased with the increase in temperature. At this stage, the maximum yield of hydrogen (49.28%) with complete conversion of ethanol was found at 1027 ºC with respect to maximum stoichiometric value. Pressure caused detrimental effect on H_2 production for each compound. In case of steam reforming of ethanol, the maximum hydrogen yields are73.27% at 577 ºC (without CaO) and 97.97% at 477ºC (with CaO) on dry basis. In another research article, the equilibrium compositions of products via steam reforming of bio-oil, ethanol, and mixture of bio-oil and ethanol were obtained thermodynamically [Montero et al., 2015]. The coke formation is higher for bio-oil steam reforming than ethanol steam reforming but it can be eliminated above 973 K and molar ratio of steam to fuel greater than 2. The yield of hydrogen was similar in the reforming of aforementioned compounds with minor differences. Increasing temperature and molar feed ratios of steam to carbon support higher hydrogen production. The energy requirement is higher in case of ethanol as compared to bio-oil. The hydrogen yield was approximately 0.94 with low carbon monoxide value of 0.14at 873 K and steam/ fuel molar ratio =8 in both type of reforming process. Under these conditions, the amounts of carbon and methane were negligible.

2.4.2 Dry reforming of ethanol

Dry reforming commonly referred to as CO_2 reforming of ethanol has also been studied by some researchers. The experiments were conducted for the production of H_2 by ethanol dry reforming using a recyclable and stable SS316 catalyst by which maximum hydrogen yield was 98% of the theoretical value [Oliveira-Vigier et al., 2005]. In another study, Blanchard et al. (2008) investigated CO_2 reforming of ethanol for the production of syngas and nanocarbon materials by using a carbon steel catalyst. Bellido et al. (2009) have studied the dry reforming of ethanol experimentally by using nickel based Y_2O_3-ZrO_2 catalysts. The maximum conversion of carbon dioxide (61%) was at high temperature of 1073 K.

Jankhah et al. (2008) have reported thermodynamic equilibrium analysis as well as experimental study on CO_2 reforming of ethanol with thermal and catalytic ethanol cracking by using carbon steel catalyst at different CO_2/C_2H_5OH ratios. The yields of H_2 and carbon as nanofilament were achieved maximum at 823 K. In another study, Wang and Wang (2009) have presented the thermodynamic analysis of ethanol dry reforming to produce H_2. The results indicated more than 94% yield of syngas with complete conversion of C_2H_5OH without coke formation at suitable operating conditions. Recently, Ortiz et al. (2015) reported the thermodynamic study for the production of H_2 by CO_2 reforming of C_2H_5OH with $CaCO_3$ as CO_2 source for the reforming reaction system. The maximum hydrogen production was obtained at 1063K. Moreover, with the temperature above 1073 K and $CaCO_3$ to ethanol ratio greater than 2.2, syngas can also be produced without carbon formation.

2.4.3 Aqueous phase reforming of ethanol

Cruz et al. (2008) reported H_2 production by using aqueous phase reforming of ethanol over Ni catalysts with different loadings which were prepared from hydrotalcite precursors. The reforming reaction was carried out in a batch reactor to test the activity of catalyst with 1wt% aqueous solution of ethanol at various temperatures of 473, 503, and 523 K. The hydrotalcite catalysts provided high activity than alumina supported nickel catalyst in terms of ethanol conversion (65%) at 523 K, high selectivity of H_2 and less formation of CH_4. Tokarev et al. (2010) prepared Pt/Al_2O_3 catalyst at 498 K for aqueous phase reforming of bio-ethanol to produce clean fuel H_2. This catalyst was found stable, and highly selective for above purpose. For the comparison, two components namely bio-ethanol and sorbitol were taken into consideration in which sorbitol performed well in terms of energy utilization for the particular process. But, the catalyst deactivation was less for bio-ethanol than sorbitol. Moreover, the mixture of bio-ethanol and sorbitol was suggested as an effective alternative for higher yield of H_2. Davidson et al. (2014) compared aqueous phase and vapour phase reforming of ethanol to see the effect of ZnO on Co/C catalyst. The presence of ZnO in the catalyst prevented the reduction of cobalt oxides by H_2 and provided the sites on its surface for H_2O activation. At 523 K, the reduction of cobalt was minimum and *insitu*XANES characterization technique showed that the addition of ZnO favoured oxidation of Co^0 in vapour phase reforming with lower yields of C_1 type products. The available sites due to presence of ZnO enhanced the CO_x selectivity at 523 K. Both types of Co/C and Co-ZnO/C catalysts continuously oxidized in aqueous phase reforming at 523 K with negligible activity. It was evident from the above study that ZnO addition affected the activation of H_2O for Co catalysts in aqueous and vapour phase reforming processes.

The study of Nozawa et al. (2014) on aqueous phase reforming of ethanol and acetic acid showed the effects of Ru particle size on the activity of Ru/TiO_2 catalyst at 200ºC. In case of ethanol, the complete elimination of methane was achieved due to small addition of Ru particles. The stability of prepared catalyst was found atleast 10 hours. In another study, Nozawa et al. (2015) investigated the effects of Re addition over TiO_2 supported Rh and It catalysts for aqueous phase reforming of ethanol. The experimental results revealed that the activity of Rh was high as compared to other substances such as IR, Ru, and Pt. Due to Re addition in Rh/TiO_2, H_2 production was increased two times in quantity. Moreover, Roy et al. (2015) reported the effects of oxidation or reduction on the activity of nickel-cerium oxide catalyst in aqueous phase reforming of ethanol. The O_2 mobility via reduction in CeO_xfavoured less CO generation. Furthermore, the efficiency of catalyst was affected by the difference present in the metal particle size. A sol-gel (SG) method with smaller nickel particles was found better than solution combustion synthesis (SCS) method for aqueous phase reforming of C_2H_5OH.

2.4.4 Oxidative steam reforming of ethanol

Rh/CeO_2 coated cordierite monoliths as catalytic material was used to perform OSR of ethanol [Baruah et al., 2017]. Detailed characterization was done in the form of various tests such as XRD, TPR, SEM, and TPD analysis. The experiments were conducted to obtain optimal operating conditions for the OSR of ethanol. A micro-kinetic model was also adapted from the literature and validated from these experiments in good agreement. Additionally, CFD analysis was also carried out for above purpose. Muñoz et al. (2017) reported experimental study on oxidative steam reforming of ethanol over NiCo-MgAl mixed oxides prepared from hydrotalcite precursors by using microwave radiation or sonication assisted coprecipitation. These preparation techniques lower down the preparation time and increase the basicity and redox properties of prepared material as compared to conventional method such as coprecipiation. The stability of catalyst was found approximately 10 hours in which 1Ni1Co mixed oxide performed better than other combinations of catalyst involved in the oxidative steam reforming of ethanol.

A thermodynamic analysis on oxidative steam reforming of ethanol has been done by using the formulation of GFE minimization technique [Graschinsky et al., 2012]. The addition of O_2 in feed, minimizes the energy requirement of process and also favours the recycling of heat. Thermal neutral points are also discovered at which there is no requirement of heat for the process from external source. The production of H_2, CO, CO_2, CH_4, and carbon as solid

are considered at equilibrium for the analysis. The ranges for temperature, steam/ethanol and oxygen/ethanol molar feed ratios are 700-1100K, 1-10, 0-0.9, respectively. Low oxygen/ethanol and high steam/ethanol molar feed ratios favour the H_2 production at 900K. High temperature suppresses the methane formation and favours the CO production. Carbon formation can also be eliminated at high temperature in OSR of ethanol. In another study, thermodynamic study for OSR of ethanol has carried out for the production of H_2 [Liu et al., 2008]. The effects of temperature (900-1200K), H_2O/C_2H_5OH (0-9), and O_2/C_2H_5OH (0-1.25) were investigated on the composition of product species involved in the system at equilibrium by using non-stoichiometric approach namely, GFE minimization method. The amount of O_2 in the feed lowers down the heat requirement in the OSR process but at the cost of low yields of H_2 and COas compared to steam reforming due to oxidation reactions. No carbon formation occurs by increasing the oxygen in the feed.

2.4.5 Partial oxidation of ethanol

CoAlZn and NiAlZn mixed oxide catalysts were prepared by sol gel methodology to perform bio-ethanol partial oxidation for the production of hydrogen [Kraleva et al., 2014].CoAlZn provided highest conversion of ethanol as well as selectivity of hydrogen and carbon monoxide as compared to NiAlZn catalyst at low temperature. But at higher temperature, NiAlZn provided complete conversion of ethanol with higher selectivity values of 95% for H_2, and 90% for CO at 1073 K as compared to CoAlZn (90% and 83% selectivities for H_2 and CO, respectively). Less carbon formation was found in the case of NiAlZn catalyst than CoAlZn catalyst. In another study, the nature of effect of oxide support on Rh based catalyst for ethanol partial oxidation was studied by diffuse reflectance infrared and X-ray photoelectron spectroscopy [Tóth et al., 2015]. Gas chromatography was used to analyse the conversion of ethanol and distribution of products. Rh/CeO_2 catalyst was responsible for achieving highest conversion of ethanol at 493 K as compared to other prepared catalysts such as Rh/Al_2O_3 and Rh/TiO_2.

2.4.6 Supercritical water reforming of ethanol

Supercritical water reforming of ethanol with or without oxidant was reported for the production of hydrogen [Therdthianwong et al., 2011]. The operating variables were temperature (773-873 K), pressure (25 MPa), and water/ethanol ratio (0-0.156). At T=873 K and water/ethanol ratio = 30, the conversion of ethanol was approximately 99.6%. The H_2/CO ratio was observed within range of 1.33-3.01 at specified reforming reaction conditions. By increasing water/ethanol ratio, the yield of H_2 and H_2/CO ratio also increased. High

temperature (greater than or equal to 823 K) and water to ethanol ratio (greater than or equal to 3) were responsible for the carbon elimination. Thee addition of O_2 minimized or eliminated carbon formation and also improved conversion of ethanol. Wongsakulphasatch et al. (2013) investigated the comparative theoretical study to produce fuel gas for SOFC application between steam and supercritical water reforming processes of bioethanol. The yield of H_2 was maximum at 850 K, 1 atm and H_2O/C_2H_5OH molar feed ratio of 20 in steam reforming process while in case of supercritical water reforming, the temperature, pressure, and H_2O/C_2H_5OH molar feed ratio were 1300 K, 22.1 MPa, and 20, respectively. After comparison, supercritical water reforming was found favorable process for SOFC applications. For energy recovery purpose, a gas turbine was used.

Table 2.3 shows the selective information about various ethanol reforming processes (experiment and thermodynamic modeling studies) including ethanol conversion, used catalyst, and operating process parameters with production of valuable fuels.

Table 2.3 Ethanol reforming (Experimental and thermodynamic modeling studies)

S. No.	Reforming Process	Authors	Operating conditions	Results	Reactor	Catalysts	Stability	Experiment/ Thermodynamic Modeling Study
1.	Steam Reforming	Deng et al. (2008)	Temperature = 923 K Pressure = 1 atm SER = 13	Conversion = 100% H_2 = 74.3 (mol %)	Fixed bed reactor	$NiO/ZnO/ZrO_2$	Stable (60 hr)	Experimental
		Profeti et al. (2009)	Temperature = 873K Pressure = 1 atm	Conversion= 99 % H_2 = 73.83 % (Y_1)	Fixed bed reactor	$Ni/CeO_2–Al_2O_3$	Stable	Experimental
		Li et al. (2010)	Temperature = 923 K Pressure = 1 atm SER = 6	Conversion = 100% H_2 = 66.7 (mol%) CO = 11.8 (mol%) CO_2 = 20.2 (mol%) CH_4 = 1.3 (mol%)	Fixed bed reactor	Ni/Mg/Al hydrotalcite	Stable	Experimental
		Montero et al. (2015)	Temperature = 1173 K Pressure = 1 atm SER= 1	Conversion =100% H_2= 71% (Y_1) CO =88% (S_2) CO_2=12 % (S_2)	---	---	---	Thermodynamic Modeling
		Hou et al. (2015)	Temperature = 923 K Pressure = 1 atm SER=3	Conversion= 100% H_2= 72 (mol%) CO= 14 (mol%) CO_2= 10 (mol%) CH_4= 4 (mol%)	Fixed bed reactor	Rh/CeO_2	Stable (70 hr)	Experimental
		Bilal et al. (2016)	Temperature = 773 K Pressure = 20 bar SER = 78.10	Conversion = 100% H_2= 44 % (S_2) CO =5 % (S_2) CO_2=19% (S_2) CH_4= 27% (S_2)	Fixed bed reactor	Pt/Al_2O_3 Rh/Al_2O_3	Stable (100 hr)	Experimental
		González-Gil et al. (2016)	Temperature = 873 K Pressure = 1 atm SER= 4	Conversion =100% H_2= 70% (mol%) CO =12 % (mol%) CO_2=197-10 (mol%) CH_4= 0-2 (mol%)	Fixed bed reactor	$RhCeNi/Al_2O_3$	Stable	Experimental

Table 2.3 Ethanol reforming (Experimental and thermodynamic modeling studies) *contd.*

S. No.	Reforming Process	Authors	Operating conditions	Results	Reactor	Catalysts	Stability	Experiment/ Thermodynamic Modeling Study
		Sharma et al. (2016)	Temperature = 873 K Pressure = 1 atm SER= 6	Conversion= 99.99 % H_2 = 62.9% (S_2) CO = 6.55% (S_2) CO_2 = 24 % (S_2) CH_4 = 7.4% (S_2)	Fixed bed reactor	Rh/Al_2O_3 Rh/ZrO_2	Stable (20 hr)	Experimental
		Greluk et al. (2016)	Temperature = 973 K Pressure = 1 atm SER= 9	Conversion =100% H_2= 76 (mol%) CO =2-2.5 (mol%) CO_2=20-22 (mol%) CH_4 = 3-3.5 (mol%)	Fixed bed reactor	$PtKCo/CeO_2$	Stable (25 hr)	Experimental
2.	Dry Reforming	Jankhah et al. (2008)	Temperature = 1073 K Pressure = 1 atm CER = 1	Conversion = 100% H_2 = 50.9(mol%) CO = 28.5 (mol%) CO_2 = 15 (mol%) CH_4 = 2.9 (mol%)	Fixed bed reactor	Stainless steal	Stable	Experimental
		Wang and Wang (2009)	Temperature = 1200-1300 K Pressure = 9.8 atm CER = 1.2-1.3	Conversion = 100% H_2 = 94.8-94.9% (Y_1)	---	---	---	Thermodynamic Modeling
		Bellido et al. (2009)	Temperature = 1073 K Pressure = 1 atm CER = 1	Conversion = 100%	Fixed bed reactor	$Ni/Y_2O_3–ZrO_2$	Stable (6 hr)	Experimental
		Ortiz et al. (2015)	Temperature = 1063 K Pressure = 1 atm CER ≥ 2.2	Conversion = 99.9% H_2 = 49.16 % (Y_1)	---	---	---	Thermodynamic Modeling
3.	Aqueous Phase Reforming	Cruz et al. (2008)	Temperature = 503 K Pressure = 28 atm	Conversion = 70% H_2 = 78 (mol%) CO = 1 (mol%)	Batch reactor	20NiHTC	Stable	Experimental

Table 2.3 Ethanol reforming (Experimental and thermodynamic modeling studies) *contd.*

S. No.	Reforming Process	Authors	Operating conditions	Results	Reactor	Catalysts	Stability	Experiment/ Thermodynamic Modeling Study
		Tokarev et al. (2010)	Temperature = 498 K Pressure = 28.92 atm	Conversion = 70% H_2 = 78 (mol%) CO = 1 (mol%)	Fixed bed reactor	Pt/Al_2O_3	Stable	Experimental
		Nozawa et al. (2015)	Temperature = 473 K Pressure = 19.74 atm SER = 10	Conversion = 36.4 % H_2 = 85.2/ $mmolg_{cat}^{-1}$	Fixed bed reactor	Ru/TiO_2 Ir/ TiO_2	Stable (10 hr)	Experimental
4.	Autothermal reforming Or Oxidative Steam Reforming	Graschinsky et al. (2012)	Temperature = 600-1200 K Pressure = 1 atm SER =0-9 OBR = 0-1.25	Conversion = 100% H_2 = 80-85% (Y_1)	---	---	---	Thermodynamic Modeling
		Greluk et al. (2016)	Temperature = 973 K Pressure = 1 atm SER= 9 OER =0.7	Conversion =100% H_2= 68-70 (mol%) CO =1.8-2 (mol%) CO_2=26-27 (mol%)	Fixed bed reactor	$PtKCo/CeO_2$	Stable (25 hr)	Experimental
		Muñoz et al. (2017)	Temperature = 973 K Pressure = 1 atm SER= 3 OER =0.5	Conversion =100% H_2= 55% (Y_1)	Fixed bed reactor	NiCo-MgAl	Stable (100 hr)	Experimental
5.	Partial Oxidation	Kraleva et al. (2014)	Temperature = 1023 K Pressure = 1 atm OBR = 1.6-1.7	Conversion =100 % H_2 = 95% (Y_1) CO= 90% (Y_1)	Fixed bed reactor	CoAlZn NiAlZn	Stable (50 hr)	Experimental
		Tóth et al. (2016)	Temperature = 493 K Pressure = 1 atm OBR = 2.0	Conversion =97 % CO = 6.4 % (S_2) CO_2= 77.9% (S_2) CH_4 =1.9 % (S_2)	Fixed bed reactor	Rh/CeO_2 Rh/Al_2O_3 Rh/TiO_2	Stable (2.3 hr)	Experimental

Table 2.3 Ethanol reforming (Experimental and thermodynamic modeling studies) *contd.*

S. No.	Reforming Process	Authors	Operating conditions	Results	Reactor	Catalysts	Stability	Experiment/ Thermodynamic Modeling Study
6.	Supercritical water reforming	Therdthianwong et al. (2011)	Temperature = 873 K Pressure = 246.73 atm SER=30	Conversion =99.6% H_2 = 60.1 % (S_2) CO = 16.3% (S_2) CO_2= 11.5 % (S_2) CH_4= 11.8% (S_2)	---	Ni/Al_2O_3 $Ni/CeZrO_2/Al_2O_3$	---	Experimental
		Wongsakulphasatch et al. (2013)	Temperature = 1300 K Pressure = 218.11 atm SER=20	Conversion =99.6% H_2>80 (Y_1) CO > 12% (Y_1) CO_2>30 % (Y_1) CH_4< 5% (Y_1)	---	---	---	Thermodynamic Modeling

$$\text{Ethanol Conversion} = \left(\frac{\text{Initial moles - final moles remained}}{\text{Initial moles}} \right) \times 100$$

$$Y_1 = \frac{\text{moles of product formed}}{\text{stoichiometric coefficient} \times \text{moles of reactant fed}} \times 100$$

$$S_2 = \left(\frac{\text{Moles of C or } H_2 \text{ in product gas}}{\text{Total moles of C in output gas product}} \right) \times 100$$

2.5 REFORMING OF MIXTURES

Few research papers have been found in literature on reforming of fuel mixture to produce hydrogen and syngas as fuels for fuel cell applications. Sadooghi and Rauch (2015) presented experimental as well as modeling investigations for the production of H_2 by using catalytic steam reforming of methane and H_2S mixture. They developed a 2D model of CH_4 steam reforming in a packed bed reactor for the simulation purpose. The various parameters such as steam/carbon ratio, temperature, space velocity, and quantity of sulphur on conversion of methane, and temperature distribution within the reactor have been investigated. The simulation results were also compared with the experimental data so that the design and optimization of real reactor can be done. In another study, the thermodynamic evaluation of hydrogen production from mixed-acid fermentations via 2 feedstocks such as bagasse and paper has been done in terms of energy selectivity. Batch fermentation has been used to analyze the hydrogen production, acid production, and sugar digestion [Forrest et al., 2011]. The results showed that the paper fermentation was more productive than bagasse fermentation. Ong et al. (2016) depicted the effect of carbon monoxide in syngas mixture over SOFC efficiency by using internal reforming and direct oxidation. The results depict that the important part of SOFC performance is CO electro-oxidation via WGS reforming and direct oxidation in presence of hydrogen. Moreover, Thermodynamic analysis on bio-oil and ethanol mixtures for the production of H_2 has been carried out via steam reforming process using a non-stoichiometric method by Montero et al. (2015). They provided compositions of products at equilibrium in the steam reforming of bio-oil, ethanol and bio-oil+ethanol mixture, respectively. The results showed significant H_2 production in steam reforming of bio-oil+ethanol mixture. The optimum operating conditions (i.e., temperature, pressure, and molar feed ratio of steam to fuel) to maximize the hydrogen production with total energy requirement for the processes have been identified in non-dimensional way. Many types of bioreactors are also used to treat biorenewable reactors [Maiti et al., 2005 and 2006; Katuri et al., 2011].

2.6 REFORMING OF OTHER OXYGENATED COMPONENTS TO PRODUCE HYDROGEN

Ding et al. (2014) conducted experiments for the conversion of glucose in solid, liquid, and gas phases by using supercritical water gasification at 673 K and 773 K with or without catalysts. In non-catalytic system, the glucose was converted into 21-24 wt% solid, 8-17 wt% gas, 8-10 wt% water and 9-16 wt% acetone. By increasing the temperature, the yield of solid decreased and the yields of gas increased. In catalytic gasification, NaOH showed best results

in terms of increasedgas. NaOH also showed best results in terms of activity to produce higher yield of hydrogen at 773 K. Ding et al. (2014) also studied catalytic gasification of cellulose and pinewood to produce hydrogen in supercritical water at specified operating conditions with or without using catalysts.Barati et al. (2014) studied hydrogen production via both catalytic and noncatalytic approaches in supercritical water gasification by using bagasse. In another study, Kang et al. (2015) investigated the production of hydrogen by using non catalytic gasification process of lignin as biomass in a batch reactor. For this purpose, they conducted an experimental as well as modeling study. The effects of operating variables were studied on the production of hydrogen such as temperature (672-924 K), pressure (226.99-286.21 atm), and water to biomass ratio (3-8). The highest hydrogen yield (1.60 mmol/g) was achieved at 924 K, 246.73 atm, and water to biomass ratio of 3.9.

Azadi et al. (2010) performed catalytic near-critical water gasification to produce hydrogen by using steam reforming of glucose as model compound in fixed bed reactor.Ruthenium/carbon and nickel/yttria stabilized zirconia catalysts were used to test their activity on hydrogen production. High temperature and atmospheric pressure were used as operating variables for reforming reactions to achieve carbon and methane free conditions. Moreover, Azadi et al. (2013) investigated supercritical water reforming of glucose, glycine, glycerol, lauric acid and humic acid as model compounds of activated sludge at 653 K using Raney nickel, Ni/α-Al_2O_3, Ru/C, and Ru/γ-Al_2O_3 catalysts. The catalysts loading enhanced the carbon conversion in which the conversion of glycerol was found more than glucose, glycine, lauric acid, and humic acid. In another study, Azadi et al. (2014) reported an integrated hydrolysis-reforming process to produce H_2 and syngas by using wet biomass as feedstocks namely, cellulose and hemicellulose. For above purpose, several experiments were performed at a steam to carbon ratio of 32, a WHSV of 30 (gfeed/gcatalyst.h) supported by Ni catalyst containing 5 wt% active metal. Some supports such as MgO, α-Al_2O_3, hydrotalcite, H-ZSM5, YSZ, TiO_2, and SiO_2 were applied. The same method can be used for the conversion of other wet biomass feedstocks such as algae and activated sludge into useful products.

Byrd et al. (2007) prepared Ru/Al_2O_3 catalyst for the production of hydrogen by using supercritical water reforming of glucose as model compound of biomassin a continuous tubular reactor with and without catalyst. The presence of catalyst enhanced hydrogen yield with conversion of glucose, and suppressed the methane production with minimal carbon formation.Byrd et al. (2008) also used same catalyst for glycerol supercritical water reforming

for the production of hydrogen under high pressure and high temperature conditions. All experiments were conducted in a fixed bed reactor at 973-1073 K in which glycerol was completely converted into hydrogen, carbon monoxide and methane with minimal amount of carbon monoxide. Nahreen and Gupta (2013) also conducted experiments to convert Acetone−Butanol−Ethanol mixture into hydrocarbons to produce valuable fuels such as hydrogen by using catalytic dehydration process.

2.7 MOTIVATION FOR THE PRESENT STUDY

In this chapter, the literature on experimental and theoretical studies for various reforming processes of acetone, butanol, ethanol, and various available mixtures to produce hydrogen by using different renewable fuels has been reviewed. From this, following observations have been made:

- In the literature, thermodynamic studies for steam reforming of acetone, butanol, and ethanol are presented based on non-stoichiometric method such as Gibbs free energy minimization method.
- There is no study available on thermodynamic analysis of steam reforming of butanol-ethanol mixture, and acetone-butanol-ethanol mixture obtained from cellulosic biomass fermentation.
- There is no study conducted on the thermodynamic analysis for butanol-ethanol mixture by using oxidative steam reforming.
- For the reforming processes, thermal efficiency and exergy efficiency are also presented in the literature but in a limited way.
- Only very few studies are available for the comparison of various renewable fuels.

In view of the above, the research work for the thesis has been planned with the objectives mentioned in the chapter I for the thermodynamic and exergetic analyses of acetone, butanol, and, ethanol (for validation purpose only), and butanol-ethanol, and acetone-butanol-ethanol mixtures. The results of the analyses have been presented in the chapters IV, V, and VI with the computational methodology in chapter III.

CHAPTER III

METHODOLOGY

3.1 INTRODUCTION

This chapter describes the formulations of Gibbs free energy minimization method, thermal efficiency of reformer through energy analysis, and exergy efficiency. The solution procedure for above purposes has also been provided in detail to perform simulations and other necessary computations.

3.2THERMODYNAMIC EQUILIBRIUM ANALYSIS

Thermodynamic analysis is used to determine the equilibrium composition of chemical reaction species at given conditions of temperature, pressure and feed composition. In a reacting system, when independent chemical reactions are known, the equilibrium constant for each of the independent chemical reaction must be satisfied for the system to reach a state of equilibrium at specified temperature and pressure conditions. The equilibrium composition of the reaction components is then found by using equilibrium constant which is evaluated for each reaction as a function of temperature and can be written in terms of fugacities of chemical reaction components involved in that reaction. For gaseous reactions, if equilibrium mixture behaves as an ideal gas, fugacity can be replaced by partial pressure or mole fraction of the reaction components. Thus, a set of equations is developed where each equation is corresponding to one independent chemical reaction relating equilibrium constant and mole fraction of the components. These equations are non-linear in nature and are solved simultaneously to compute mole fraction of each reaction component at equilibrium. If a large number of independent reactions are occurring in the system, it is computationally difficult to simultaneously solve the set of non-linear equations corresponding to the complex reacting system. More often, this type of solution requires numerical technique. For the simple reaction scheme, analytical solution may be possible.

An alternative criterion of equilibrium relies on the fact that the total Gibbs free energy of the reaction system decreases at constant temperature and pressure conditions with progress of reaction and has its minimum value at the state of equilibrium. For the multiple reaction system, this criterion is the basis for the determination of equilibrium composition of reaction components. This method is known as Gibbs free energy (GFE) minimization technique. This method has the advantage that the knowledge of independent chemical reactions occurring in

the system and value of corresponding equilibrium constants is not necessary to determine the equilibrium composition of the reaction components. In this method, the problem is stated as to find out the set of moles of the gaseous reaction components which minimize GFE of the system at specified conditions of temperature and pressure subject to the constraints of the material balances.

In the reaction system, the change in GFE of the system can be written as

$$\Delta G_T = -SdT + VdP + \sum_i^N \mu_i dn_i \qquad (3.1)$$

At constant T and P conditions, the total GFE of the system can be represented by Eq. (3.2) as the sum of chemical potential of all the components [Perry et al., 1999; Lwin et al., 2000; Smith et al., 2010].

$$G_T = \sum_i^N \mu_i n_i \qquad (3.2)$$

The minimization of total GFE (G_T) of the system is subjected to the elemental mass balance constraints as given below.

$$\sum_i^N n_i a_{ik} = A_k; \qquad k = 1, 2, 3, ...M \qquad (3.3)$$

The minimization of G_T (Eq. (3.2)) with Eq. (3.3) constitutes the constrained minimization problem. Two procedures could be used to solve this problem. In the most commonly used procedure, the problem is transformed into unconstrained minimization problem by using method of Lagrange multipliers. Alternatively, it may also be solved as a constrained problem by suitable optimization method. For this purpose, G_T (Eq. (3.2)) is directly minimized by using constrained minimization tool *'fmincon'* in MATLAB software. In Lagrange multiplier method [Perry et al., 1999; Lwin et al., 2000], Lagrange multiplier λ_k which is one for each element, is introduced by multiplying each element balance by its λ_k.

$$\lambda_k \left(\sum_{i=1}^{N} n_i a_{ik} - A_k\right) = 0; \qquad k = 1, 2, ..., M \qquad (3.4)$$

These equations are summed up over *k* as given below.

$$\sum_{k=1}^{M} \lambda_k \left(\sum_{i=1}^{N} n_i a_{ik} - A_k \right) = 0 \tag{3.5}$$

The objective function G_T is modified by incorporating equality constraint (Eq. (3.5)) into it to form a new function *F*.

$$F = G_T + \sum_{k=1}^{M} \lambda_k \left(\sum_{i=1}^{N} n_i a_{ik} - A_k \right) \tag{3.6}$$

On making an observation of Eq. (3.3) and (3.6), it is clear that the second term in the right hand side of Eq. (3.6) is null. Hence, new function *F* is identical to G_T. However, the partial derivatives of *F* and G_T with respect to n_i are different because function *F* incorporates the elemental mass balance constraints. At equilibrium, the minimum value of *F* is obtained by setting partial derivative of *F* with respect to n_i and λ_k equal to zero.

The Eq. (3.6) is rewritten by using Eq. (3.2) as

$$F = \sum_{i=1}^{N} \mu_i n_i + \sum_{k=1}^{M} \lambda_k \left(\sum_{i=1}^{N} n_i a_{ik} - A_k \right) \tag{3.7}$$

During experimental studies of steam reforming of hydrocarbons, the existence of solid carbon has been found on surface of catalysts [Medrano et al., 2014; Guil-Lopez et al., 2015; Zhu et al., 2015; Cifuentes et al., 2016; Anjaneyulu et al., 2016]. Since the vapour pressure of carbon is negligible at operating *T* and *P* conditions, only solid carbon is considered here. On considering the GFE of solid carbon component (C_s), the Eq. (3.7) is notified as,

$$F = \sum_{i=1}^{N} \mu_i n_i + \left(\sum_{k=1}^{M} \lambda_k \left(\sum_{i=1}^{N} n_i a_{ik} - A_k \right) \right) + n_C G^0_{fC(s)} \tag{3.8}$$

where, $G^0_{fC(s)}$ is standard GFE of formation of solid carbon which is zero. Therefore, carbon is only calculated in the elemental constraints. On differentiating Eq. (3.7) and on equating the resultant derivative to zero, one gets

$$\frac{\partial F}{\partial n_i} = \mu_i + \sum_{k=1}^{M} \lambda_k a_{ik} = 0; \qquad k = 1, 2, ..., M \tag{3.9}$$

$$\frac{\partial F}{\partial \lambda_k} = \sum_{i=1}^{N} n_i a_{ik} - A_k = 0\,; \qquad i = 1, 2, ..., N \tag{3.10}$$

The chemical potential μ_i for the gaseous components is given by

$$\mu_i = G_i^0 + RT \ln(\overline{f_i} / f_i^0) \tag{3.11a}$$

If G_i^0 is arbitrarily set equal to zero for all elements in their standard states, then for components, $G_i^0 = \Delta G_{fi}^0$ [Smith et al., 2010].

$$\mu_i = \Delta G_{fi}^0 + RT \ln(\overline{f_i} / f_i^0) \tag{3.11b}$$

For gas phase reaction, fugacity can be defined as [Smith et al., 2010]

$$\overline{f_i} = y_i \phi_i P \tag{3.12}$$

$$f_i^0 = P_0 \tag{3.13}$$

Combination of Eq. (3.9), Eq. (3.11b), Eq. (3.12), and Eq. (3.13) gives,

$$\Delta G_{fi}^0 + RT \ln(y_i \phi_i P / P_0) + \sum_{k=1}^{M} \lambda_k a_{ik} = 0\,; \qquad i=1, 2,\ldots\ldots, N \tag{3.14}$$

n_T refers to the total number of moles of all components and can be written as

$$n_T = \sum_{i=1}^{N} n_i\,; \tag{3.15}$$

By using Eq. (3.15), Eq. (3.14) is modified as

$$\Delta G_{fi}^0 + RT \ln\left(\frac{n_i}{n_T} \phi_i \frac{P}{P_0}\right) + \sum_{k=1}^{M} \lambda_k a_{ik} = 0\,; \qquad i=1, 2,\ldots\ldots, N \tag{3.16}$$

If the gaseous mixture of reaction system behaves as an ideal gas, then for each component; ϕ_i=1. For real gases; ϕ_i is a function of y_i and can be calculated using any equation of state applicable to the system being considered for computation. ΔG_{fi}^0 for each component, is only a function of temperature and its value is available in the data handbooks [Perry et al., 1999; Yaws, 1999]. According to Eq. (3.16), one equation can be written for one component and thus results in *N* nonlinear equations. Eq. (3.10) represents *M* material balance equations, one

for each element. The unknowns are n_i and λ_k . Thus, the Eq. (3.10), Eq. (3.15), and Eq. (3.16) represent a set of (N+ M) non-linear algebraic equations in which (N+M) unknowns can be easily solved by suitable numerical method. The advantage of method of Lagrange multiplier is that it transforms a constrained minimization problem into unconstrained minimization problem. This transformed problem results into the solution of a set of nonlinear equations. Whenever number of components in the reacting system is large, then this method results into a large number of nonlinear equations. Under these, circumstances, it is always advisable to solve the problem directly as a constrained minimization problem by resorting to suitable optimization method [Rao, 2009].

3.3 THERMAL EFFICIENCY

Thermal efficiency is a measure of the performance of the system in terms of energy utilization. It is defined on the basis of first law of thermodynamics and, therefore, it is also referred to as first law efficiency [Cengel and Boles, 2008]. In the present study, the system is fuel-steam reformer and is viewed a fuel processor which converts the feeding fuel to the clean fuel hydrogen. In this case, the thermal efficiency indicates how efficiently the fuel processor converts the input energy of the fuel into useful work. In other words, thermal efficiency is defined as the fraction of energy input to fuel processor which is converted to net work output. The thermal efficiency of reformer is written as

$$\eta_{th} = \frac{\text{net work output}}{\text{total energy input}} \tag{3.17}$$

In every system, there always exists some amount of input energy which is wasted in order to complete the process. Therefore, net work output is always less than the total energy input which in turn makes η_{th} less than unity. In reforming system, the net work output is termed as the desired output which is energy associated with produced hydrogen at prevailing operating conditions, and total energy input is the total energy supplied to the reformer associated with the feed consisting of fuel as well as system. Mathematically, thermal efficiency is expressed as [Cengel and Boles, 2008; Silva and Müller, 2011; Katiyar et al., 2013]

$$\eta_{th}(\%) = \frac{n_{H_2}^{out} LHV_{H_2}}{n_{fuel}^{in} LHV_{fuel} + \text{Energy used for reforming process}} \times 100 \tag{3.18}$$

In Eq. (3.18), the energy used for reforming process is represented as the sum of heat of reactions at the given reforming temperature and heat required to produce steam. On incorporating this term, Eq. (3.18) can be restated as

$$\eta_{th}(\%) = \frac{n_{H_2}^{out} LHV_{H_2}}{n_{fuel}^{in} LHV_{fuel} + Q_T + n_{steam}^{in} \Delta H_L} \times 100 \tag{3.19}$$

In Eq. (3.19) LHV_{H_2} and LHV_{fuel} are the low heating values of H_2 and fuel feed respectively.*LHV* is the amount of heat released when a unit amount of fuel at environmental temperature (298 K) is completely burnt and the combustion products are cooled to the same environmental temperature. ΔH_L is the latent heat of steam in the feed which represents the internal energy of steam associated with its vapour phase at system temperature and pressure conditions. The *LHV* values of hydrogen, butanol, and ethanol are 241.82 kJ/mol, 2444.6 kJ/mol, and 1240 kJ/mol, respectively. The ΔH_L value of steam is 40.69 kJ/mol [Cengel and Boles, 2008]. n_{fuel}^{in} and n_{steam}^{in} are the number of moles of fuel and steam in the inlet (feed) stream and $n_{H_2}^{out}$ is the number of moles of hydrogen in the outlet stream at equilibrium conditions.

In Eq. (3.19), Q_T is the net change in total enthalpies of inlet and outlet streams due to conversion of fuel at reaction temperature and pressure conditions. Thus,

$$Q_T = H_T^{out} - H_T^{in} \tag{3.20}$$

where, H_T^{out} and H_T^{in} are the total enthalpies of inlet and outlet streams at temperature *T*. These enthalpies are expressed as

$$H_T^{out} = \sum_{i=1}^{N_2} H_{T,i}^{out} \tag{3.21a}$$

$$H_T^{in} = \sum_{i=1}^{N_1} H_{T,i}^{in} \tag{3.21b}$$

where,

$$H_{T,i}^{in} = n_i^{in} \left[H_{298,i} + \int_{298}^{T} c_{p_i} dT \right] \tag{3.22a}$$

$$H_{T,i}^{out} = n_i^{out}\left[H_{298,i} + \int_{298}^{T} c_{p_i} dT \right] \quad (3.22b)$$

In Eq. (3.22a), *i* refers to the components present in the inlet (feed) stream and in Eq. (3.22b), *i* refers to the components present in the outlet stream. $H_{298,i}$ is the molar enthalpy of component *i* at a temperature of 298 K. c_{p_i} is the heat capacity of component *i* expressed as a function of temperature in the form of a polynomial [Perry et al., 1999; Cengel and Boles, 2008].

3.4 EXERGY EFFICIENCY

The first law of thermodynamics deals with the quantity of energy, and therefore, it is not a realistic measure of performance of fuel processor. The second law of thermodynamics deals with the quality of energy and is concerned with the degradation of energy during the process, the entropy generation, and the lost opportunity to do work [Cengel and Boles, 2008; Smith et al., 2010]. Therefore, a process does not occur unless it satisfies both the first and second law of thermodynamics. The information regarding the amount of energy contained in the fuel alone is of little value. It is really required to know work potential of the fuel. Exergy is the measure of work potential of the energy contained in the fuel processing system. It is associated with the state of the system and the environmental conditions. Exergy is defined on the basis of second law of thermodynamics. Unlike energy, the exergy is not conserved. Once the exergy is wasted, it can never be recovered [Cengel and Boles, 2008] whereas the energy is not destroyed; rather it is converted to less useful form. The exergy destroyed or destruction represents the lost or wasted work potential during the process as a result of irreversibility associated with the process. It should be noted that no actual process is reversible. More irreversible a process is, more generation of entropy is, the larger will be the exergy destruction during that process [Ji et al., 2003; Ishihara et al., 2004; Chen et al., 2012; Kumar et al., 2013].

For a multicomponent gaseous stream flowing through the reformer, the total exergy comprises three components, namely physical exergy (Ex_{phy}), chemical exergy (Ex_{chem}), and exergy of mixing (Ex_{mix}) [Tzanetis et al., 2012; Kumar et al., 2013]. Thus, the total exergy of the flowing stream (Ex_T) can be written as

$$Ex_T = Ex_{phy} + Ex_{chem} + Ex_{mix} \quad (3.23)$$

The physical exergy is the maximum amount of work obtainable when the stream is brought from its operating state (*T, P*) to the environmental state (T_0, P_0) by physical process where thermal and mechanical equilibrium exist. The environmental condition of T_0 is 298 K and P_0 is 1 atm. The physical exergy of stream is associated with changes in enthalpy (ΔH), and entropy (ΔS) of the stream as given below [Kumar et al., 2013; Tippawan and Arpornwichanop, 2014].

$$Ex_{phy} = \Delta H - T_0 \Delta S \tag{3.24}$$

where,

$$\Delta H = \sum_{i=1}^{N_s} y_i \left(\int_{T_0}^{T} c_{p_i} dT \right) \tag{3.25}$$

$$\Delta S = \sum_{i=1}^{N_s} y_i \left(\int_{T_0}^{T} \frac{c_{p_i}}{T} dT - R \ln \frac{P}{P_0} \right) \tag{3.26}$$

where, N_s represents the number of chemical reaction components present in the stream. For inlet stream N_s=N_1 and for outlet stream N_s=N_2. $N_1$and N_2 represent the number of components present in inlet and outlet streams respectively.

The chemical exergy is defined as the maximum work that can be obtained from the system when the substance is brought to chemical equilibrium with reference environment at constant *T* and *P* conditions by reversible process involving only heat transfer and exchange of substance with the environment [Yan et al., 2016, Hedayati et al., 2016]. The standard chemical exergy values of components can be taken from Kumar et al. (2013). The chemical exergy of a flowing gaseous stream is estimated by Eq. (3.27)

$$Ex_{chem} = \left[\sum_{i=1}^{N_s} y_i Ex_{chem,i} \right] \tag{3.27}$$

where, y_i is mole fraction of component *i* in the gaseous stream, and $Ex_{chem,i}$ denotes the standard molar chemical exergy of pure component *i* in gas phase.

Ex_{mix} can be calculated by Eq. (3.28)

$$Ex_{mix} = RT_0 \sum_{i=1}^{N_s} y_i \ln y_i \tag{3.28}$$

For a steady state process, the overall exergy balance can be written as

$$(Ex_T)_{in} = (Ex_T)_{out} + Ex_{dest} \tag{3.29}$$

In Eq. (3.29), Ex_{dest} indicates the exergy destruction. This destruction in exergy is a positive quantity and can be expressed as

$$Ex_{dest} = T_0 S_{gen} \tag{3.30}$$

The exergy efficiency is a realistic measure of performance of a device relative to the performance under reversible conditions for the same end state. Since, exergy is defined on the basis of second law of thermodynamics; the exergy efficiency is also referred to as second law efficiency. The exergy efficiency is the ratio of useful work output and the maximum possible work output. In terms of exergy, it is defined as the ratio between useful exergy output from the process and the necessary exergy input to this process. The overall exergy efficiency of the process is defined on the basis of overall exergy of inlet and outlet streams as given by

$$\eta_{Ex}(\%) = \frac{(Ex_T)_{out}}{(Ex_T)_{in}} \times 100 \tag{3.31}$$

Exergy efficiency indicates that $\eta_{Ex}(\%)$ of available work potential is converted to useful work.

3.5 SOLUTION PROCEDURE

Although in the GFE minimization method, a set of chemical reactions involved are not required in the formulation of nonlinear equations and in the estimation of equilibrium composition, yet the set of gaseous components must be first defined. Different set of components not only provides different equilibrium composition but also sometimes misleading results. Therefore, the selection of the components is very critical to the entire calculations and it should be made on the basis of experimental reforming data.

In the present work, thermodynamic analyses of reforming of acetone, butanol, ethanol and butanol-ethanol mixture, acetone-butanol-ethanol mixture have been carried out. The reaction components in these reforming systems are resulted from the atomic combination of elements *C*, *H*, and *O*. In order to carry out the simulation, components are decided on the basis of experimental studies [Profeti et al., 2009; Bimbela et al., 2009; Li et al., 2010;

Bizkarra et al., 2015; Navarro et al., 2015; Braga et al., 2016]. The reforming processes consist of gaseous components as acetone (C_3H_6O), butanol ($C_4H_{10}O$), ethanol (C_2H_6O), steam (H_2O), carbon monoxide (CO), carbon dioxide (CO_2), hydrogen (H_2), methane (CH_4), ethane (C_2H_6), propane (C_3H_8), Isopropyl alcohol (C_3H_8O), 1-butene (C_4H_8), butyraldehyde (C_4H_8O), acetylene (C_2H_2), ethylene (C_2H_4), and solid component Carbon (graphite). The operating parameters chosen for the simulation are temperature (*T*), pressure (*P*), molar ratio of reactants in the feed, and mole fractions of butanol and ethanol in the butanol-ethanol (B–E) mixture, mole fraction of acetone, butanol, and ethanol in the acetone-butanol-ethanol (ABE) mixture. The ranges for these operating parameters are decided on the basis of reforming process in subsequent chapters.

At high temperature and low pressure, the gaseous reforming reaction mixture behaves ideally. The non-ideality arises at high *T* and *P* conditions due to difference in physicochemical properties of gaseous components. Challiwala et al. (2017) demonstrates that gaseous mixture significantly deviates from the ideality at high *T* and *P* and the non-ideality is one of the critical factors which affect the equilibrium state of the reforming mixture. In this regard, the associated non-ideality with the system is accounted for the estimation of fugacity coefficient ϕ_i of the component and then accordingly, is incorporated in GFE minimization equation at given *T* and *P* conditions. Fugacity coefficient can be calculated by using Redlich–Kwong (RK), Soave modification of Redlich-Kwong (SRK), Peng–Robinson (PR), and Virial equations of state (EOS) [Rao, 1997; Smith et al., 2010]. Out of various EOS, Peng–Robinson (PR) is generally found suitable for hydrocarbon and light gases in estimating the properties of gaseous components existed in the reforming reaction system [Tippawan and Arpornwichanop, 2014; Louw et al., 2014; Seretis et al., 2015; Ortiz et al., 2015; Hartley et al., 2015].

As stated earlier, for constrained GFE minimization method, appropriate simulation tools are available in mathematical softwares such as Chemcad, ProII-Simsci, HYSYS, Aspen Plus, etc. [Nahar and Madhani, 2010; Özkara-Aydinoğlu, 2010;Wang and Cao, 2011;Tippawan and Arpornwichanop, 2014; Montero et al., 2015;Louw et al., 2016]. These softwares include an extensive thermodynamic database for all components participating in the reacting system. Here, in the present work, the equilibrium composition computations are performed using the Aspen Plus 8.4 engineering process simulator. The module of Aspen Plus that is used to evaluate reaction system is R–Gibbs (Gibbs Reactor) which is based on the GFE minimization technique for multiple reactions and material balances. R–Gibbs reactor is

operated non-adiabatically in order to provide constant P and T conditions in the reactor [Hajjaji et al., 2014]. The physical and thermodynamic properties are calculated by Peng–Robinson equation of state. For the convergence, the mass balance tolerance limit is set to 10^{-10}. This minimization in R–Gibbs yields unknown molar amounts of components (n_i) for a specified conditions of T, P and molar feed ratios.

3.6 CONCLUDING REMARKS

In this chapter, the detailed description of methodologies for Gibbs free energy minimization, thermal efficiency, and exergy efficiency have been given, which have been used for computations of equilibrium compositions of reacting components involved in the reforming processes at a given temperature and pressure.

CHAPTER IV

STEAM REFORMING OF BUTANOL-ETHANOL MIXTURE

4.1 INTRODUCTION

This chapter describes the steam reforming of individual components of mixtures namely, acetone, butanol, and ethanol. First, steam reforming of acetone has been done. Thereafter, steam reforming of butanol-ethanol mixture (B-E mixture) has been performed in which molar composition of butanol varies from 0-100%. It is mentioned that 0% butanol in the mixture simply represents 100% pure ethanol while 100% butanol in the mixture is pure butanol. Thus, steam reforming of butanol and ethanol has been implicitly performed with the steam reforming of butanol-ethanol mixture. There are several studies available in the literature on thermodynamic analysis and experimental work of steam reforming of acetone, butanol and ethanol. Still, these studies have been done to validate our computational procedure and algorithm. To the best of our knowledge, no experimental or thermodynamic study is available in the literature on steam reforming process of butanol-ethanol mixture. Analyses of steam reforming of these fuels have been carried out by varying the pressure of the system from 1-10 atm, molar feed ratio from 0-12, temperature from 573-1473 K with different compositions of B-E mixture and other individual fuels. Besides, energetic analysis and exergetic analysis have also been performed to assess the likely requirement of energy for the process. Lastly, the results of both the analyses have been discussed in detail and the comparison of the performance of various fuels have also been carried out.

4.2 METHODOLGY

Although, the detailed procedure has already been described in Chapter III but the procedure in brief has also been given in this section so that the chapter can be complete in itself. First, the products of reforming are chosen on the basis of experimental studies available in the literature on SRA, SRB and SRE. The products with trace amounts are ignored and the products with significant quantity are included for further study. Prior to the computations for the performance evaluation of the reformer, the thermodynamically feasible chemical components are screened out amongst them. For this purpose, the simulations are carried out for steam reforming of acetone (SRA), steam reforming of butanol (SRB), and steam reforming of ethanol (SRE) separately at the desired conditions of temperature,

pressure, and molar feed ratio of steam/fuel. The results indicate that chemical components present at equilibrium over the whole range of operating conditions are hydrogen, carbon monoxide, carbon dioxide, methane, steam, and carbon (graphite). The fuels, acetone, butanol and ethanol are completely converted. Other hydrocarbons are found to be present in trace amounts. Therefore, all these above components are not considered in further computations. Negligible molar amounts of these components lead to the conclusion that these components are present as intermediates in reaction mixture when the fuel is not completely converted to products, and the reforming reactions are in progress, and are incomplete. The components are not stable products thermodynamically. These results also indicate that the existence of these components in experimental work is attributed to the fact that the reforming reactions are under kinetic control. It implies that suitable catalyst may be manufactured which are able to convert the fuel completely into desired products and are able to convert the intermediate components too quickly to avoid their detection experimentally.

In order to determine the composition of components present in fuel reforming system at equilibrium, R–Gibbs reactor has been used which directly minimizes the Gibbs free energy of the system. In different thermodynamic studies reported in the literature, the authors have programmed their models in different softwares as discussed in section 3.5. Therefore, before proceeding further, sufficient attempts are made to verify the accuracy of R-Gibbs reactor tool against available experimental studies as well as theoretical model predictions. Due to unavailability of reported experimental and theoretical studies on SRB-E process, the accessible experimental and theoretical results only on steam reforming of acetone,steam reforming of butanol and steam reforming of ethanol have been used to validate the thermodynamic results in the present study. The comparison of these results in terms of percent conversion of acetone, butanol and ethanol is compiled in Table 4.1. It is clear from this table that the simulation results from the present study are in good agreement with the experimental as well as theoretical predictions. This table comprises the optimum operating values of process variables namely, temperature, pressure and molar feed ratio of steam/ fuel considered for steam reforming of acetone (SRA), steam reforming of butanol (SRB), steam reforming of ethanol (SRE) processes (experimental as well as theoretical studies) by various researchers.

Table 4.1 Validation of simulation results with reported experimental and computational results

Acetone Steam Reforming					
Operating Conditions	**Experimental Studies**				**Computational Study**
	Hu et al. (2012)	**Navarro et al. (2014)**	**Guil-Lopez et al. (2015)**	**González-Gil et al. (2015)**	**Xie et al. (2017)**
Temperature (K)	873	873	873	473-973	973-1073
Pressure (atm)	1	1	1	1	1
SAR	6	6	6	3	≤ 4
% A-Conversion	100	100	100	82	100
Present Study (% A-Conversion)	100	100	100	100	100

Butanol Steam Reforming						
Operating Conditions	**Experimental Studies**			**Computational Study**		
	Bimbela et al. (2009)	**Cai et al. (2012)**	**Medrano et al. (2014)**	**Nahar et al. (2010)**	**Wang et al. (2011)**	**Silva et al. (2011)**
Temperature (K)	923	873	923	873	800	848
Pressure (atm)	1	1	1	1	1	1
SBR	14.71	4	14.7	12	10	12
% E-Conversion	97.50	97	97.41	100	100	100
Present Study (% E-Conversion)	100	100	100	100	100	100

Ethanol Steam Reforming						
Operating Conditions	**Experimental Studies**					**Computational Study**
	Profeti et al. (2009)	**Hou et al. (2015)**	**Cifuentes et al. (2016)**	**Arslan et al. (2014)**	**Dan et al. (2015)**	**Silva et al. (2011)**
Temperature (K)	873	923	953	873	623	848
Pressure (atm)	1	1	1	1	1	1
SER	3	3	3	4	30	6
% E-Conversion	100	100	100	100	100	100
Present Study (% E-Conversion)	100	100	100	100	100	100

4.3 STEAM REFORMING OF ACETONE

4.3.1 Thermodynamic analysis

After separation from ABE mixture, acetone can also be used as feed for steam reforming of acetone. The simulations were carried out to analyze the effects of operating variables such as pressure (1-10 atm), temperature (573-1473 K), and steam to acetone molar feed ratio (F_A) between 0–12 for steam reforming of acetone. There is no significant change found by varying pressure on molar formation of products. Therefore, atmospheric pressure is used for further simulations. Table 4.2 includes all possible reactions which can participate in the acetone steam reforming process.

Table 4.2 Reactions network for steam reforming of acetone

Reaction No.	**Reactions**	**Reaction types**	**ΔH_R (kJ/mol) at 298 K, 1atm**
R1	$C_3H_6O + 2H_2O \leftrightarrow 3CO + 5H_2$	Steam reforming of acetone	127.87
R2	$C_3H_6O + \leftrightarrow CO + CH_4 + H_2 + C$	Decomposition of acetone	32.22
R3	$CO + H_2O \leftrightarrow CO_2 + H_2$	Water-Gas Shift Reaction	-41.17
R4	$CO_2 + 4H_2 \leftrightarrow CH_4 + 2H_2O$	Methanation Reactions (R4 and R5)	-164.94
R5	$CO + 3H_2 \leftrightarrow CH_4 + H_2O$		-206.11
R6	$CO_2 + 2H_2 \leftrightarrow C + 2H_2O$	Carbon dioxide Reduction Reaction	-90.09
R7	$CO + H_2 \leftrightarrow C + H_2O$	Carbon monoxide Reduction Reaction	-131.26
R8	$2CO \leftrightarrow CO_2 + C$	Boudouard Reaction	-172.43
R9	$CH_4 \leftrightarrow 2H_2 + C$	Methane Decomposition	74.85

Figure 4.1 depicts the molar production of hydrogen, carbon monoxide, carbon dioxide, methane at optimum operating condition of F_A=12 by varying temperature from 573 to 1473 K. It is clear from the figure that hydrogen production increases upto 900 K and then slightly decreases. This is possible due to R1 to R3 reactions. Likewise, the formation of carbon dioxide also follows same trend as hydrogen production which increases upto 873 K and then decreases. This trend can be explained by R3 and R8 reactions. But, CO production increases

with respect to temperature at any value of F_A whereas the methane formation can be suppressed by increasing temperature and molar feed ratio of steam to acetone. Above F_A = 5, carbon formation can be completely eliminated at any temperature. The corresponding results of optimum conditions can be found in Table 4.3. The maximum hydrogen (6.93 mol) is achieved at F_A=5, 1 atm and temperature of 973 K. Under these operating conditions, the amounts of CO, CO_2, and CH_4 with respect to maximum production of H_2 are 1.03, 1.96, and 0.01 moles, respectively.

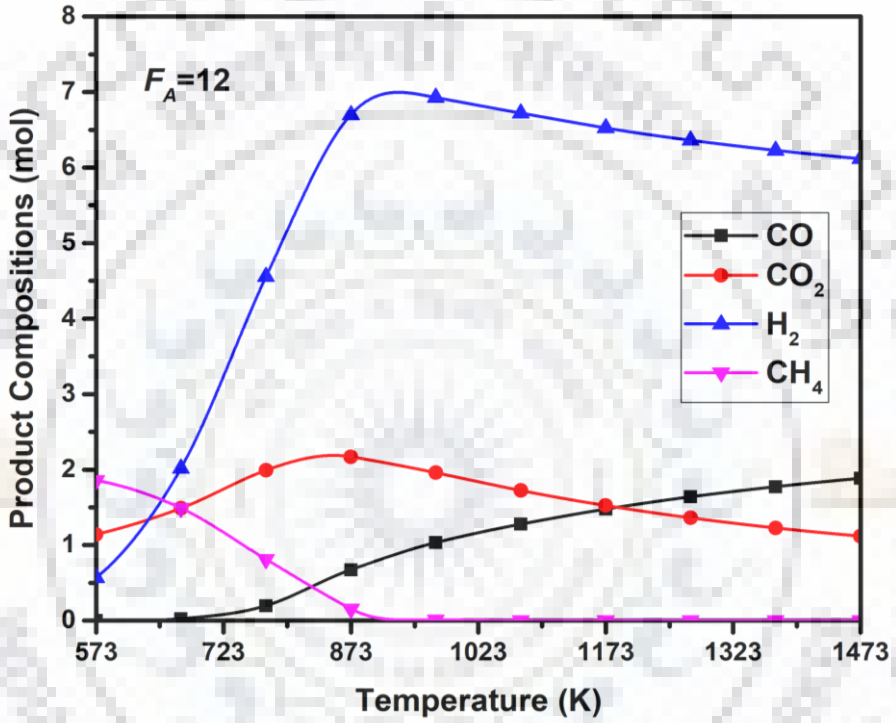

Figure 4.1 Molar production of products in steam reforming of acetone at F_A=12 with respect to temperature

4.3.2 Thermal efficiency and exergy efficiency

Thermal efficiency of acetone steam reformer is dependent on the hydrogen production and amount of steam in the feed. Thermal efficiency, energy required for the process, and exergy efficiency can be computed by using Eqs. (3.19), (3.20) and (3.31). In short, thermal efficiency increases with respect to temperature and molar feed ratios of steam to acetone. Likewise, exergy efficiency also increases with the progress of temperature and molar feed ratios of steam to acetone.Table 4.3 provides the maximum values of molar production of H_2, thermal efficiency, total energy requirement, and exergy efficiency of steam reforming of acetone process at highest H_2 production conditions on the basis of 1 mole fuel in feed at

different molar feed ratio of steam to acetone. It is clear from the table that the values of exergy efficiency are always less than thermal efficiency.

Table 4.3 Molar production of H_2, thermal efficiency, and exergy efficiency of SRA process at maximum H_2 production conditions on the basis of 1 mol fuel in the feed

Molar Feed Ratio (F_A)	**Temperature**	**Maximum H_2 moles**	**Thermal efficiency**	**Total energy requirement**	**Exergy efficiency**
0	1473 K	2.99	40.24 %	79.50 kJ	08.31%
2	1473 K	4.98	54.96%	394.19 kJ	26.61%
4	1073 K	5.58	59.96%	372.65 kJ	35.47%
5	1073 K	5.83	61.67%	366.75 kJ	39.73%
6	973 K	6.04	63.56%	336.95 kJ	40.69%
8	973 K	6.47	65.77%	334.91 kJ	46.00%
10	973 K	6.74	66.40%	330.76 kJ	48.34%
12	973 K	6.93	66.16%	326.68 kJ	48.72%

4.4 STEAM REFORMING OF BUTANOL-ETHANOL MIXTURE

The butanol–ethanol water mixture (B-E mixture) contains 8.66 moles of butanol, 2.32 moles of ethanol and 89.02 moles of water. If butanol and ethanol mixture is considered as a renewable biofuel, then it consists of 78.87 mol% butanol and 21.13 mol% ethanol or in this renewable fuel butanol and ethanol are approximately in 80:20 ratio on molar basis. Likewise, water is about 8 times this renewable fuel on molar basis. The operating parameters are temperature, pressure and steam/fuel molar feed ratio. The simulations have been carried out in terms of molar amounts of components (n_i) as H_2, CO, CO_2, CH_4, and carbon. All the equilibrium calculations are carried out on the basis of 1 mol/s of fuel in the feed to the reformer. For three fuels in feed namely, butanol (100% B), ethanol (0% B), and butanol-ethanol mixtures (50-90% B). $n_{fuel}^{in} LHV_{fuel}$ and n_{steam}^{in} can be calculated as follows:

For butanol

$$n_{fuel}^{in} LHV_{fuel} = n_{butanol}^{in} LHV_{butanol} \quad (4.1)$$

$$n_{steam}^{in} = f_1 . n_{butanol}^{in} \quad (4.2)$$

For ethanol

$$n_{fuel}^{in} LHV_{fuel} = n_{ethanol}^{in} LHV_{ethanol} \quad (4.3)$$

$$n_{steam}^{in} = f_2 . n_{ethanol}^{in} \quad (4.4)$$

For butanol-ethanol mixture

$$n_{fuel}^{in} LHV_{fuel} = n_{butanol}^{in} LHV_{butanol} + n_{ethanol}^{in} LHV_{ethanol} \quad (4.5)$$

$$n_{steam}^{in} = f_3 . (n_{butanol}^{in} + n_{ethanol}^{in}) \quad (4.6)$$

In order to analyze the effect of pressure, the computations are carried out at various pressures between 1–10 atm keeping temperature constant at 973 K for SRB, and 873 K for SRE, and varying f_1 and f_2 between 0–12 for both the systems (SRB and SRE). Figures 4.2 (a) and (b) depict the molar production of hydrogen in SRB and SRE respectively at various values of pressure, f_1 *or* f_2. In Figure 4.2 (a), the production of H_2 is favoured by f_1 and is suppressed by the pressure. The maximum H_2 production is achieved at pressure of 1 atm and f_1 of 12. At 10 atm pressure, the reduction in moles of H_2 is pronounced. Similar trends are found in case of SRE process as shown in Figure 4.2 (b). These trends can be explained on the basis of reactions occurring in reforming system as listed in Table 4.4. The reactions (R1–R4) are gaseous endothermic reactions where moles in the system increase with the progress of reactions. According to Le Chatelier's principle, in this case, high pressure will favour the reactions to proceed in backward direction. As a result, high pressure shows detrimental effect on the thermodynamic equilibrium and thereby on hydrogen production. Therefore, the total pressure of 1 atm has been selected for all equilibrium calculations. The detailed discussions regarding the effects of remaining 2 variables (temperature and molar feed ratios f_1 *or* f_2 *or* f_3) in all the processes which show significant influence on the formation of desired product (H_2) and the undesired products (CO, CO_2, CH_4, and carbon) are presented in the following sections.

Table 4.4 Chemical reactions involved in SRB, SRE, and SRB-E processes

Reaction No.	Reactions	Reaction Types	ΔH_R (kJ/mol) at 298 K, 1atm
R1	$C_4H_{10}O + 3H_2O \leftrightarrow 4CO + 8H_2$	Steam reforming of Butanol	557.67
R2	$C_4H_{10}O \leftrightarrow CO + 2CH_4 + H_2 + C$	Decomposition of Butanol	14.19
R3	$C_2H_6O + H_2O \leftrightarrow 2CO + 4H_2$	Steam reforming of Ethanol	255.53
R4	$C_2H_6O \leftrightarrow CO + CH_4 + H_2$	Decomposition of Ethanol	49.42
R5	$CO + H_2O \leftrightarrow CO_2 + H_2$	Water-Gas Shift Reaction	-41.17
R6	$CO_2 + 4H_2 \leftrightarrow CH_4 + 2H_2O$	Methanation Reactions (R6 and R7)	-164.94
R7	$CO + 3H_2 \leftrightarrow CH_4 + H_2O$		-206.11
R8	$CO_2 + 2H_2 \leftrightarrow C + 2H_2O$	Carbon dioxide Reduction Reaction	-90.09
R9	$2CO \leftrightarrow CO_2 + C$	Boudouard Reaction	-172.43
R10	$CO + H_2 \leftrightarrow C + H_2O$	Carbon monoxide Reduction Reaction	-131.26
R11	$CH_4 \leftrightarrow 2H_2 + C$	Methane Decomposition	74.85

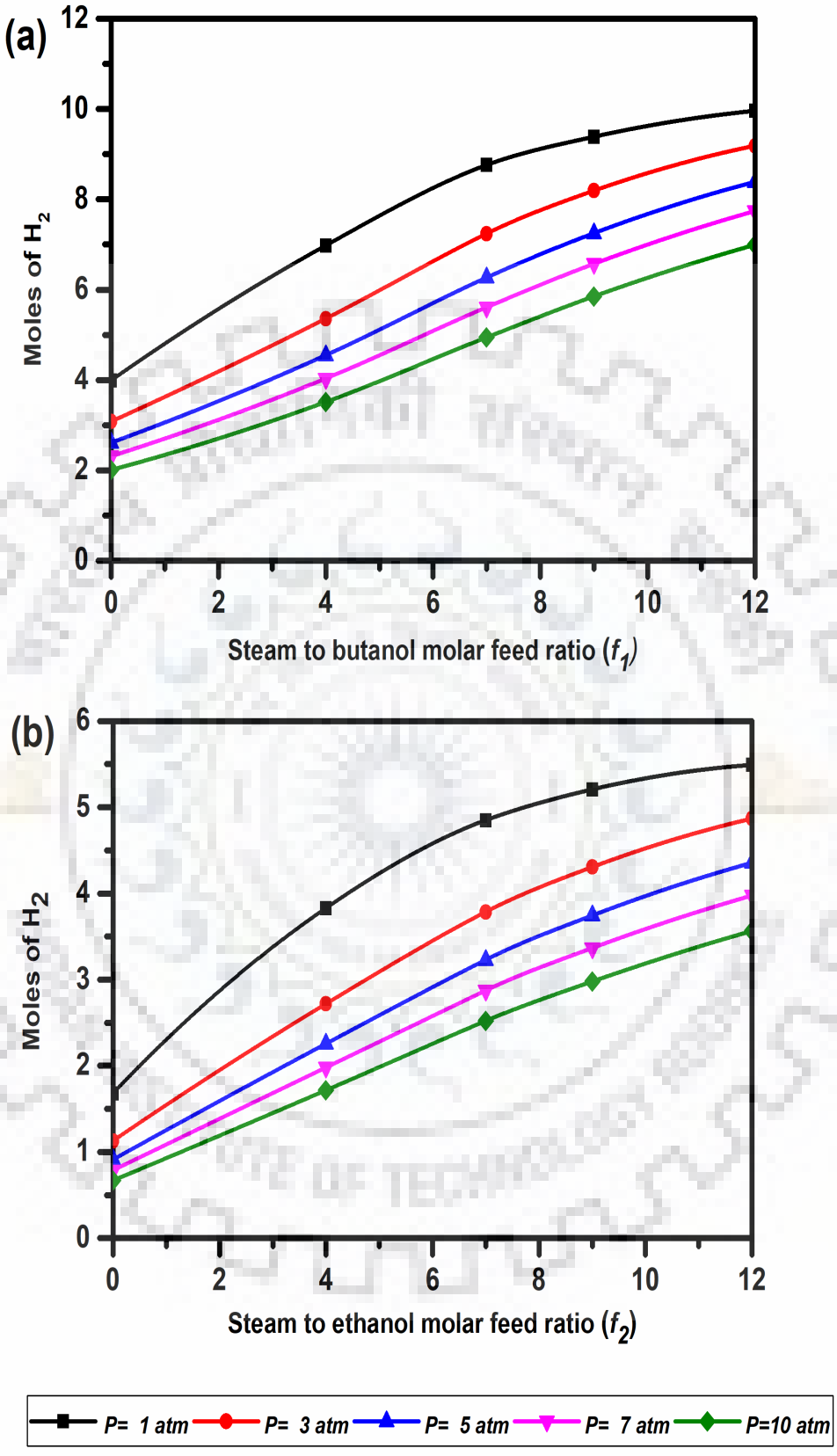

Figure 4.2 Effect of pressure on production of H_2 with (a) $f_1$in SRB process at 973 K (b) f_2 in SRE process at 873 K

4.4.1 Production of H_2

Figure 4.3 illustrates various performance evaluation trends for H_2 production at equilibrium as a function of temperature (T) and steam/fuel molar feed ratio (f_1 *or* f_2 *or* f_3) in SRB, SRE, and SRB–E processes with complete conversion of fuel. Figure 4.3 (a) depicts that in absence of steam (f_1=0), the decomposition of butanol (R2) dominates completely over steam reforming of butanol (R1). At low temperature, methanation reactions (R6, R7) are thermodynamically more feasible. This causes the small production of H_2 at low temperature of 573 K. Temperature greater than 573 K favours the reaction R2 due to its endothermicity and disfavours exothermic reaction R7. As a result, H_2 production increases with temperature. In this case, the maximum amount of H_2 (4.979 moles) is achieved at T=1473 K. On increasing the amount of steam in the feed ($f_1 > 0$), steam reforming reaction (R1) and water gas shift reaction (R5) become more prominent resulting in higher production of H_2 according to the stoichiometry of reactions R1 and R5 with f_1 values at one temperature. High temperature suppresses the methanation reaction (R7), enhances CH_4 consumption reaction (reverse R7), and reaction R1 causing increase in H_2 production. High endothermicity of reaction R1 indicates that more amount of steam in the feed not only increases the production of H_2 but maximum amount is achieved at relatively lower temperature. For instance, maximum amounts of H_2 are 8.23 moles (f_1=4, T =1173 K), 9.01 moles (f_1=7, T =1073 K), 9.38 moles (f_1=9, T =973 K), and 9.96 moles (f_1=12, T =973 K). After attaining the maximum value, the moles of H_2 are reduced with temperature but the reduction is insignificant. This trend mainly occurs due to existence of more feasible reverse water gas shift reaction (reverse of R5) at high temperatures. Similar variational trend for H_2 production are observed by SRE (Figure 4.3 (b)). In this case, steam reforming of ethanol (R3) and decomposition of ethanol (R4) reactions occur along with other remaining side reactions (R5 to R11) depending upon the operating conditions. High temperature and high molar feed ratio of steam to ethanol (f_2) favour the H_2 production due to endothermicity of reactions R3 and R4. Out of specified range of conditions of T and f_2, the maximum values of H_2 are achieved as 2.99 moles (f_2=0, T=1473 K), 4.69 moles (f_2=4, T=973 K), 5.16 moles (f_2=7, T=973 K), 5.32 moles (f_2=9, T=973 K), and 5.49 moles (f_2=12, T=873 K). The comparison between maximum H_2 production by SRB and SRE reveals that the production is more in SRB than SRE due to stoichiometry of reactions R1 and R3.

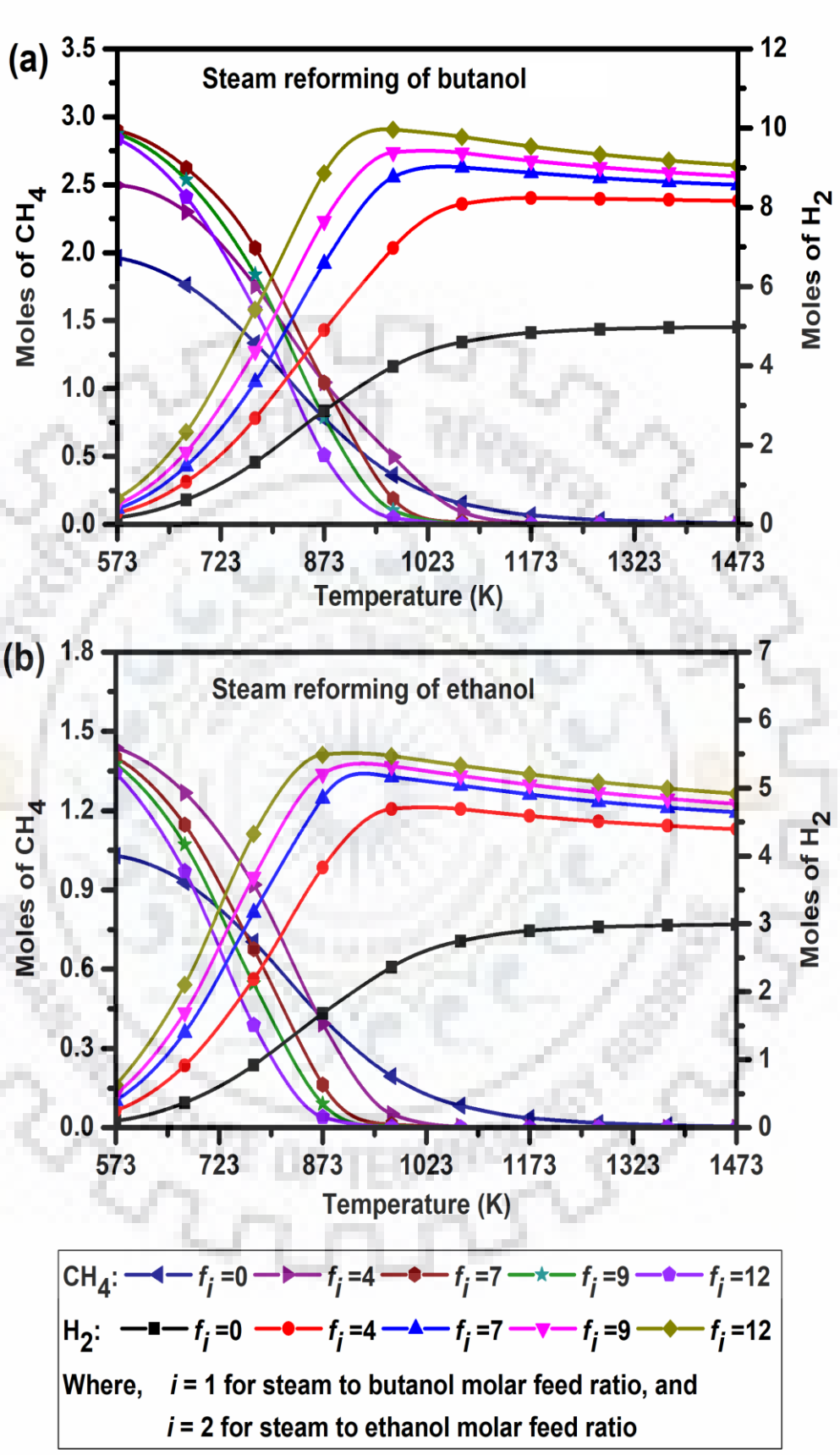

Figure 4.3 (a) and (b): Molar Production of H_2 and CH_4 as a function of temperature at molar feed ratio (a) f_1 (0-12) in SRB (b) f_2 (0-12) in SRE

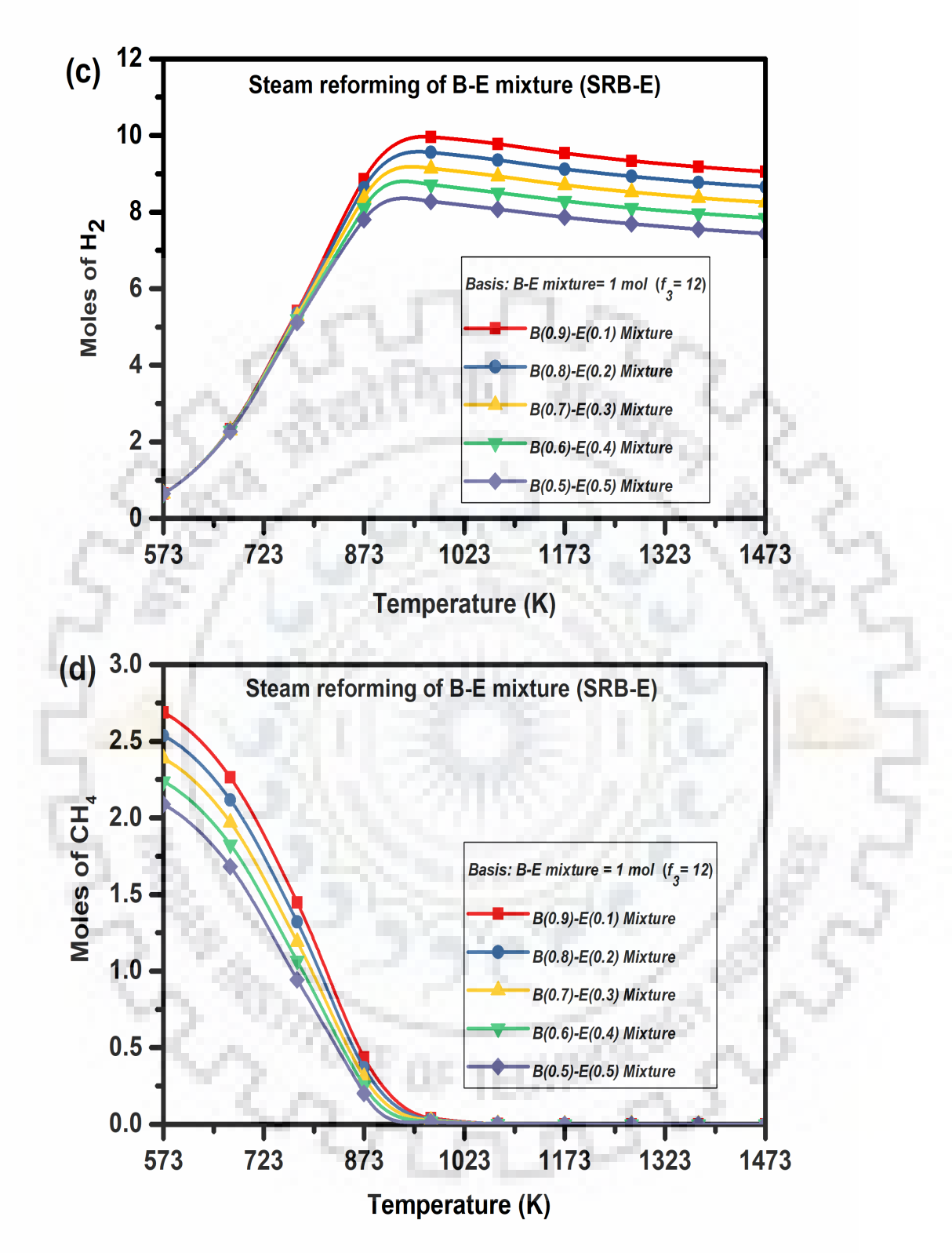

Figure 4.3 (c) and (d): Molar Production of H_2 and CH_4 as a function of temperature at molar feed ratio (c) f_3=12 in SRB-E for H_2, (d) f_3=12 in SRB-E for CH_4

In the next part of study, the mixture of butanol and ethanol is taken in different molar compositions as mentioned in the Figure 4.3 (c), and SRB-E process is thermodynamically analyzed. From the aforementioned studies on SRB and SRE processes, it is clear that maximum production of H_2 is achieved at high temperature and steam/fuel molar feed ratio f_1=f_2=12. Therefore, the molar production of H_2 at equilibrium in SRB-E process has been analyzed at temperature range of 573-1473 K keeping molar steam to B-E ratio in feed constant at f_3=12. It can be clearly seen in Figure 4.3 (c) that variational trends for H_2 production with temperature for all mixture compositions are similar to the trends shown in Figures 4.3 (a) and (b) except different mixture compositions, the maximum production of H_2 (9.96 moles) has been achieved in SRB while minimum (5.49 moles) in SRE processes. The amounts of H_2 at different compositions of B and E in B–E mixture vary between these two extremes. For instance, the moles of H_2 are 9.56 (90% B), 9.14 (80% B), 8.71 (70% B), 8.28 (60% B), and 7.84 (50% B).

4.4.2 Production of CH_4

The molar production of CH_4 at equilibrium is shown in Figures 4.3 (a), 4.3(b) and 4.3(d) in case of SRB, SRE and SRB-E processes respectively at specified operating conditions of *T*, f_1, f_2, *and* f_3. The molar content of CH_4 is very high at low temperature of 573 K (Figure 4.3 (a)) in case of SRB. At this temperature, methane amount increases as $f_1$is increased and varies between 1.96 to 2.90 moles. On increasing the temperature, the CH_4 production decreases sharply and becomes zero in the temperature range of 1073 to 1473 K depending upon $f_1$values as is shown clearly in Figure 4.3 (a). This trend evidences that CH_4 formation through methanation reaction of CO (R7) is thermodynamically more feasible at lower temperature. Initially, in the absence of steam (f_1=0), butanol decomposition (R2) and methanation (R7) reactions are responsible to form methane at low temperatures of 573 K. As the amount of steam in feed increases (f_1 > 0), reaction R1 occurs with reaction R2 and enhances reaction R7 resulting in more production of CH_4 with f_1 at temperature of 573 K. Further, the methanation reaction (R7) is thermodynamically disfavoured while CH_4 decomposition (R11) is thermodynamically favoured by the increase in temperature above 573 K which explains the sharp decrease in moles of CH_4 with temperature at all $f_1$values.

Regarding the CH_4 production in SRE process, Figure 4.3 (b) depicts the effect of temperature and steam to ethanol molar feed ratio (f_2) on production of methane at equilibrium. In this case, the observed variational trends are similar to SRB process as shown in Figure 4.3 (a). The reactions responsible for the production/consumption of CH_4 are

decomposition of ethanol (R4) along with methanation reactions (R6 and R7) and methane decomposition reaction (R11). The high value of moles of CH_4 at equilibrium lies between 1.03 to1.50 moles at temperature of 573 K depending upon f_2 values. The high temperature reduces the amount of CH_4 and finally becomes almost zero for all f_2 values in the temperature range of 1173 to 1473 K. From Figures 4.3 (a) and (b), it is observed that a lower amount of CH_4 is predicted in SRE process than in SRB process due to stoichiometry of reactions (R1 to R4) and corresponding feasibility of side reactions such as methanation reaction (R7) at the prevailing operating conditions of T, $f_1$and f_2. The variation in the amount of methane with T and f_2 values can be reasoned and explained on the same lines as discussed in case of SRB process. Further, Figure 4.3 (d) presents the CH_4 production at equilibrium as a function of temperature in SRB–E process. Here, the molar steam to B–E ratio in feed (f_3) is kept constant at 12. From the Figure 4.3 (d), it can be seen that CH_4 amount at temperature of 573 K is high and varies between two extremes 2.09 (B=50%) to 2.69 (B=90%) moles obtained in case of SRB–E at f_3=12. Once the temperature increases to the values between (973 to1473 K), CH_4 moles becomes almost zero through reverse methanation reaction (reverse R7) and methane decomposition (R11) for all B–E compositions.

The aforementioned discussion of results clearly indicates that CH_4 is highly undesirable product because its production adversely affects production of hydrogen quantitavely and qualitatively. Although, the CH_4 production can be reduced by increasing the temperature above 800 K to enhance the feasibility of CH_4 steam reforming reactions (reverse of R6 and R7) to occur, these reactions result in high production of CO and CO_2. In the presence of steam, WGS reaction (R5) being thermodynamically less feasible than methanation reaction, is not able to produce sufficient amount of H_2 in comparison to its consumption in methanation reaction. For the catalytic fuel reforming reaction, if the reformer is catalytically inert towards methanation and temperature is high, the formation of CH_4 can be reduced. Thus, the search of stable and active catalyst is needed which can produce H_2 rich gas with negligible amount of CH_4 at prescribed operating conditions of temperature, pressure and steam/fuel molar feed ratios (f_1, f_2, and f_3).

4.4.3 Production of CO and CO_2

The molar production of CO and CO_2 at equilibrium is computed for SRB, SRE, SRB-E processes. The influence of T, f_1, f_2, and f_3 on their production is illustrated in Figures 4.4 (a)-(d). For SRB and SRE processes (Figures 4.4 (a) and (b)), the moles of CO_2 increase noticeably with temperature in the 573–800K range for all $f_1$and f_2 values between 0 and 12.

This evidences that the reforming reactions R1 and R3 accompanied by water gas shift reaction (R5), CO methanation reaction (R7), and Boudouard reaction (R9) which are thermodynamically favoured in this temperature range. Consequently, very low amount of CO is observed in low temperature range. In the absence of steam in the feed ($f_1 = f_2 = 0$), very small amount of CO_2 is produced through reverse CO_2 reduction reaction (R8) and Boudouard reaction (R9). At high temperature (T > 800 K), the exothermic reactions namely water gas shift reaction (R5), CO_2 and CO methanation reactions (R6, R7), CO_2 and CO reduction reactions (R8, R10), and Boudouard reaction (R9), are not thermodynamically favoured. As a result, these reactions proceed in reverse direction. This fact justifies the decrease in the production of CO_2 and the increase in the production of CO above 800 K for all f_1 and f_2 greater than zero (4–12). However, CO content is reduced in SRB with f_1 and in SRE with f_2 at one temperature. The minimum value at T=1473 K is achieved at f_1=12 (1.85 moles) in SRB and at f_2=12 (0.35 moles) in SRE. This trend is attributed to suppression of RWGS reaction (reverse of R5) on increasing the amount of steam in feed and temperature. It can be seen from the Figures 4.4 (a) and 4.4 (b) that there is lower production of CO and CO_2 in SRE process than in SRB process. This result can be explained by the stoichiometry of reforming reactions (R1-R4). In SRB-E process, CO and CO_2 production profiles with temperature are shown in Figures 4.4 (c) and 4.4 (d) respectively at fixed value of molar ratio of steam to B-E mixture in feed f_3=12. It is evident from the Figure 4.4 (c) that high temperature favours the production of CO. The molar value of CO decreases as the amount of butanol in the mixture decreases and it lies between two extremes (1.85-0.35 moles). Further, the production of CO_2 is also favoured by lower temperature lying in the range of (573-800 K). Above 800 K, CO_2 production is reduced with temperature. This trend is similar to the trends received in SRB and SRE processes (Figures 4.4 (a) and 4.4 (b)), and is true for all B–E compositions in the mixture. Finally, the molar production of CO_2 lies between two extremes (2.10-1.61 moles). These observations lead to the following conclusions. In reforming of fuels butanol and ethanol, CO and CO_2 are undesired products. The concept of mixing of butanol and ethanol provides lower production of CO and CO_2 during reforming process with sufficient production of desirable product hydrogen.

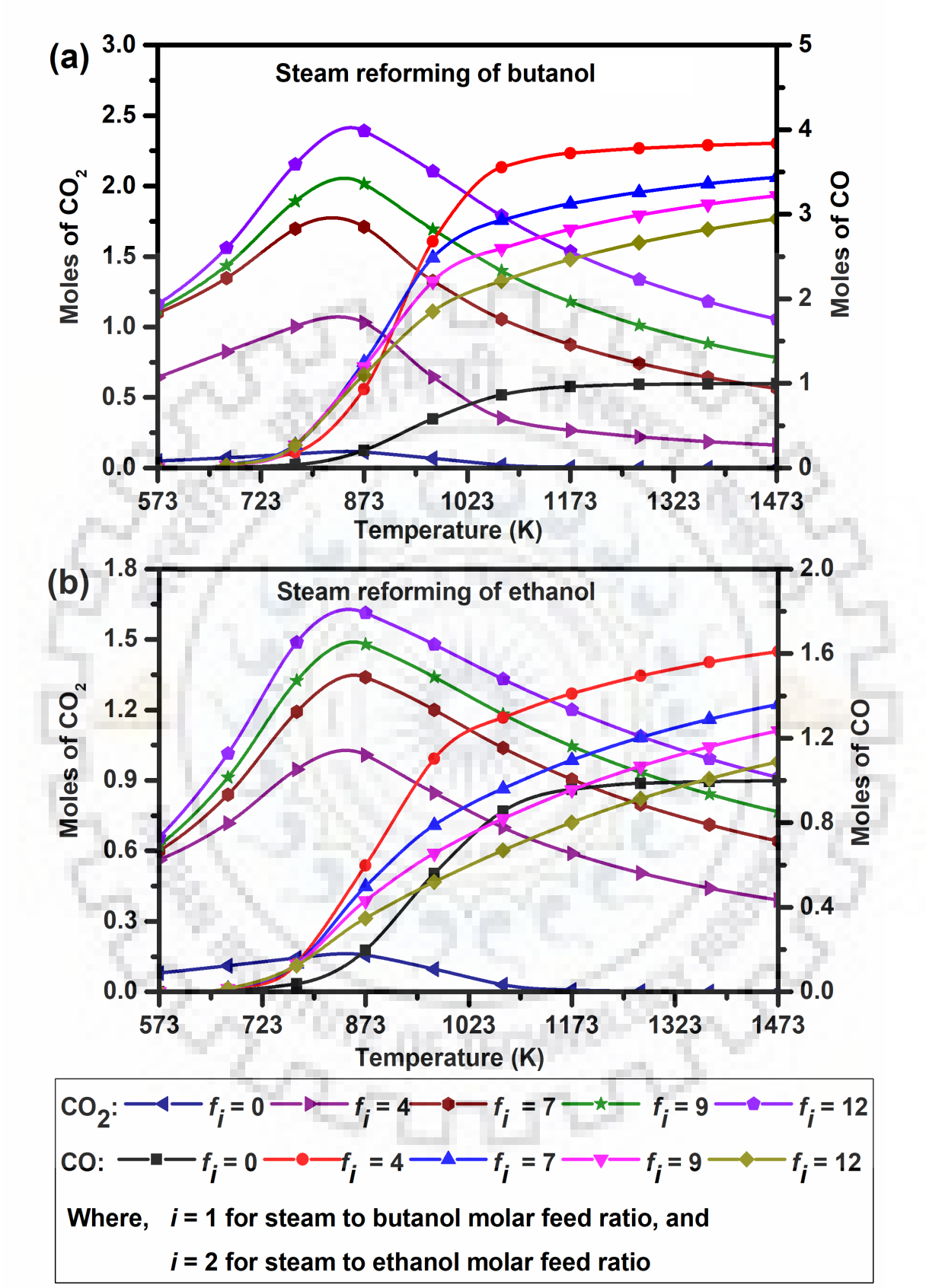

Figure 4.4 (a) and (b): Molar production of CO and CO_2 as a function of temperature at molar feed ratio (a) f_1 (0-12) in SRB (b) f_2 (0-12) in SRE

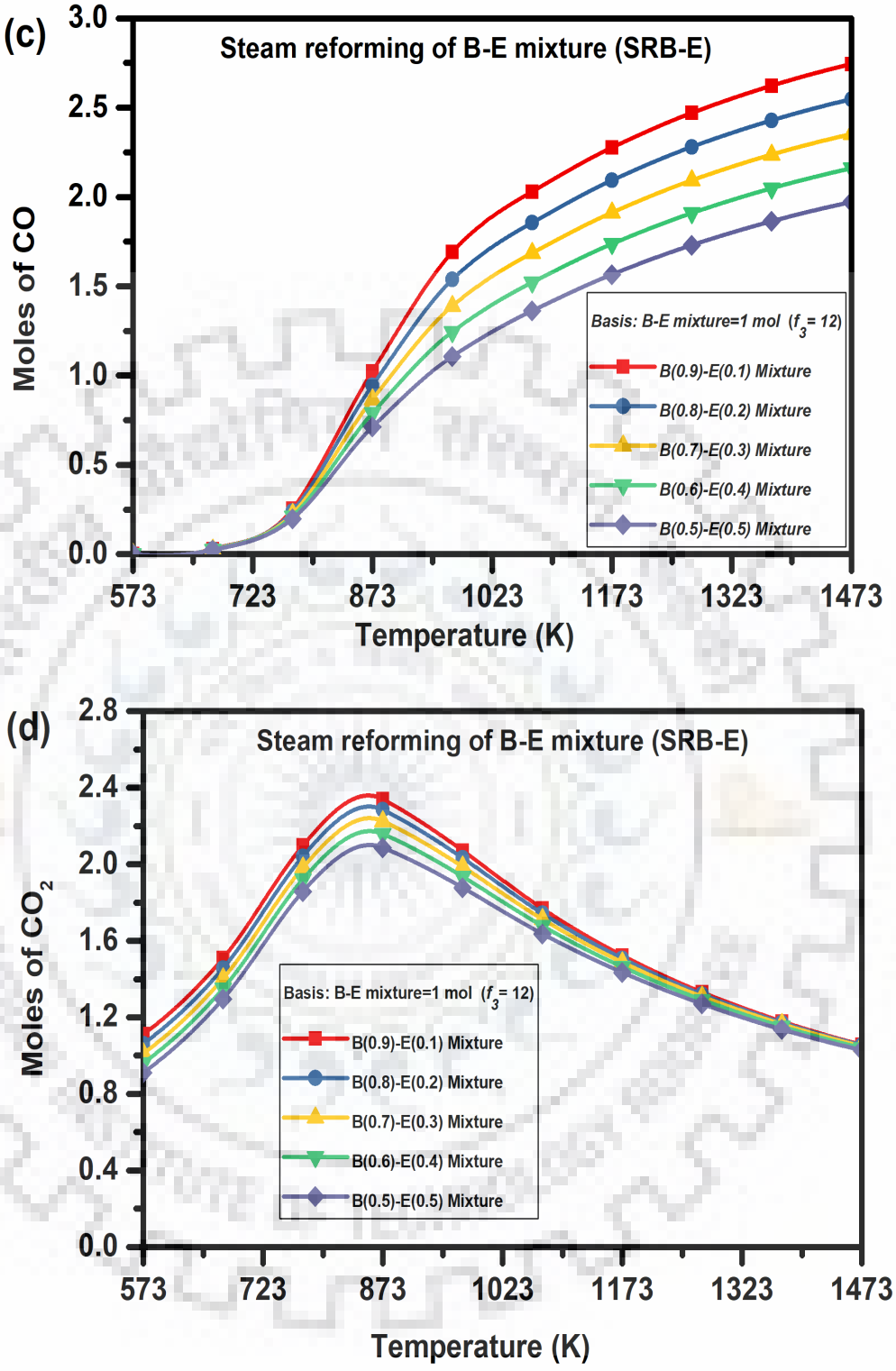

Figure 4.4 (c) and (d): Molar production of CO and CO_2 as a function of temperature at molar feed ratio (c) f_3=12 in SRB-E for CO, (d) f_3=12 in SRB-E for CO_2

4.4.4 Carbon formation

The carbon is considered to be an undesired product during fuel reforming process as its formation and deposition on the surface of the catalyst cause the deactivation of reforming catalysts. Therefore, it is necessary to analyse the fuel reforming process thermodynamically to identify the operating conditions which can minimize the carbon formation and can be implemented in industrial plant. In the equilibrium simulation, the formation of solid carbon of graphite type is considered during fuel reforming reactions. The molar amount of carbon produced during SRB and SRE processes is shown in Figures 4.5 (a) and 4.5 (b) respectively as a function of temperature and molar feed ratios f_1 and f_2. In case of SRB process, decomposition reaction (R2), CO_2 and CO reduction reactions (R8, R10), Boudouard reaction (R9), and methane decomposition reaction (R11) are considered to form carbon. Whereas, in case of SRE process only reactions (R8-R11) are considered to form carbon. Low temperature (T=573–873 K) promotes the carbon formation through exothermic CO_2 and CO reduction reactions, and Boudouard reaction (R8, R9, and R10) as CO_2 production also increases (Figures 4.4 (a) and 4.4 (b)). However, the consumption of carbon occurs due to reverse of methane decomposition reaction (R11). High temperature (T > 800 K) disfavours the exothermic reactions (R8, R9, and R10) resulting in the suppression of carbon formation. Complete reduction of CH_4 at high temperatures (Figures 4.3 (a) and 4.3 (b)) also justifies no formation of carbon through methane decomposition reaction (R11) at high temperature and for all f_1 and f_2 values. In absence of steam in feed (f_1= f_2 =0), carbon is produced through reactions R2, R8, R9, and R10 (Table 4.3) in SRB. In SRE, the reactions R8, R9, R10 are responsible for carbon formation. It implies that maximum production of carbon is achieved at f_1= f_2 =0 (Figures 4.5 (a) and 4.5 (b)) at full temperature range in comparison to at other f_1 and f_2 values. In SRE process, the decomposition of ethanol (R4) does not produce carbon whereas in SRB, the additional production of carbon is observed through butanol decomposition reaction (R2). This fact is clearly seen in Figures 4.5 (a) and 4.5 (b) when the amount of steam in feed is increased (f_1 and f_2> 0), carbon formation is not favoured and carbon gasification is promoted due to the occurrence of CO_2 and CO reduction reactions (R8, R10) in reverse direction. Thus, large reduction in carbon formation is observed at higher temperature and higher feed ratios f_1 and f_2 as illustrated in Figures 4.5 (a) and 4.5 (b). However, in comparison to temperature, the influence of feed ratios f_1 and f_2 on carbon formation is more pronounced.

In case of SRB-E process, Figures 4.6 (a)-(e) represent the moles of carbon formed at various temperatures; molar feed ratio f_3 values, and specified compositions of B–E mixtures.

Five figures (Figures 4.6 (a) – 4.6 (e)) depict the carbon formation for 90% B, 80% B, 70% B, 60% B, and 50% B in B-E mixture respectively. The variational trends with both operating variables (T and f_3) are similar to trends found in 100% B (Figure 4.5 (a)) and 100% E (Figure 4.5 (b)) cases. The maximum production, 2.99 moles of carbon has been with 100% B and 1.23 moles of carbon with 100% E. The maximum carbon production in all B–E compositions lies between two extremes of 2.99 and 1.23 moles. The formation of carbon decreases with decrease in percentage of B in the B-E mixtures. The negligible amount of carbon is observed at comparatively lower f_3 value as percent ethanol in B-E mixture increases. Thus regarding the carbon formation, the aforementioned results may lead to the conclusion that carbon formation is avoided at those operating conditions of temperature and feed ratios which maximize the H_2 production in all concerned SRB, SRE, and SRB–E processes.

4.4.5 Analysis of energy requirement

The energy requirement associated with SRB, SRE, and SRB–E processes is an important parameter for the performance evaluation of reforming processes as the energy cost associated with reforming process directly influences the product cost. A precise energy analysis of reforming processes is presented here. The energy requirement for the reforming processes (SRB, SRE, and SRB-E) at various temperatures and feed ratios is computed by using Eq. (3.20).

Table 4.5 compiles the amount of energy required to provide maximum production of hydrogen at $f_1=f_2=f_3=12$ and at corresponding temperature in SRB, SRE, and SRB-E processes. The percent decrease in the value of energy required and hydrogen production in SRB, SRE, and SRB-E processes with respect to the values in SRB process are mentioned. Table 4.5 provides the information regarding energy required and the equilibrium molar amounts of undesired products (CO, CO_2, CH_4) per mole of H_2 produced in all three SRB, SRE, and SRB–E processes. It is known that the presence of ethanol in butanol-ethanol mixture causes the suppression of carbon formation. Also, high temperature and feed ratios provide complete elimination of carbon from equilibrium compositions (Figures 4.5 and 4.6) in SRB, SRE, and SRB-E processes. Therefore, the undesired products do not include carbon formation in Table 4.5. It is clear from this table that energy demand in case of SRB is the highest (513.99 kJ/mol) whereas in SRE, it is the lowest (210.35 kJ/mol). In all B–E mixture, the energy requirement lies between these two extremes depending upon the composition of the mixture. It implies that the presence of ethanol and butanol in the mixture reduces the energy requirement as compared to SRB process. However, SRE and SRB-E process suffer

from a reduced hydrogen production. The percent reductions in H_2 and energy requirement are uniform in SRB-E process at all compositions. The energy required per mole of H_2 produced decreases with the increase in ethanol content in the B-E mixture. The increased ethanol content in the mixture negatively affects the CO and CH_4 production per mole of H_2 produced by decreasing them more significantly. On the contrary, CO_2 production per mole of H_2 produced increases with ethanol content in the mixture but this increase is not appreciable.

Further, regarding the influence of temperature and feed ratio, the energy requirement is observed to decrease with the addition of ethanol to butanol at all temperatures and feed ratios f_1, f_2 and f_3. However, the overall process of SRB, SRE, and SRB-E remains slightly exothermic in lower temperature range and thereafter endothermicity increases steadily with an increase in temperature and feed ratio. Figure 4.7 shows the variational trends of energy demand with temperature at feed ratio f_1 range (0-12) for SRB process. Similar trends are obtained in case of SRE and SRB-E processes. Low temperature range is favourable for exothermic reactions R5-R10 which in turn makes the overall reforming system exothermic. High temperature is favourable for endothermic reactions and shifts the exothermic forward reactions towards endothermic backward reactions. As a result, overall reforming system behaves as endothermic. In between exothermicity and endothermicity conditions, overall system attains thermal neutral condition at one temperature where no amount of energy is consumed or produced. This temperature varies with feed ratios. For instance, in SRB (Figure 4.7), the temperatures corresponding to thermal neutral condition are 839 K ($f_1=0$), 741 K ($f_1=4$), 701 K ($f_1=7$), 684 K ($f_1=9$), and 665 K (f_1=12). This indicates low temperature range for thermal neutral point achievement. It is noteworthy here that the low temperature range in all three reforming processes (SRB, SRE, and SRB-E) provides very low production of desired product H_2 and high production of undesired products CH_4, CO_2, and carbon (Figures 4.3 to 4.6). In order to enhance the production of H_2 and to suppress the production of CH_4, CO_2, and carbon, the high temperature and high feed ratio are recommended. Thus, the reforming process is operated at the condition of higher energy requirement. However, Table 4.5 clearly shows that energy requirement per mole of H_2 produced reduces with the increase of ethanol in the mixture. This mixture of butanol and ethanol as found during fermentation process seems to be one of the suitable fuel propositions to produce hydrogen. This energy analysis leads to inference that mixture of butanol and ethanol, high temperature and high feed ratio result in considerable incentive in terms of quality of H_2 (with negligible carbon deposition and CH_4 formation) but at the same time requires lower energy cost in comparison to SRB process.

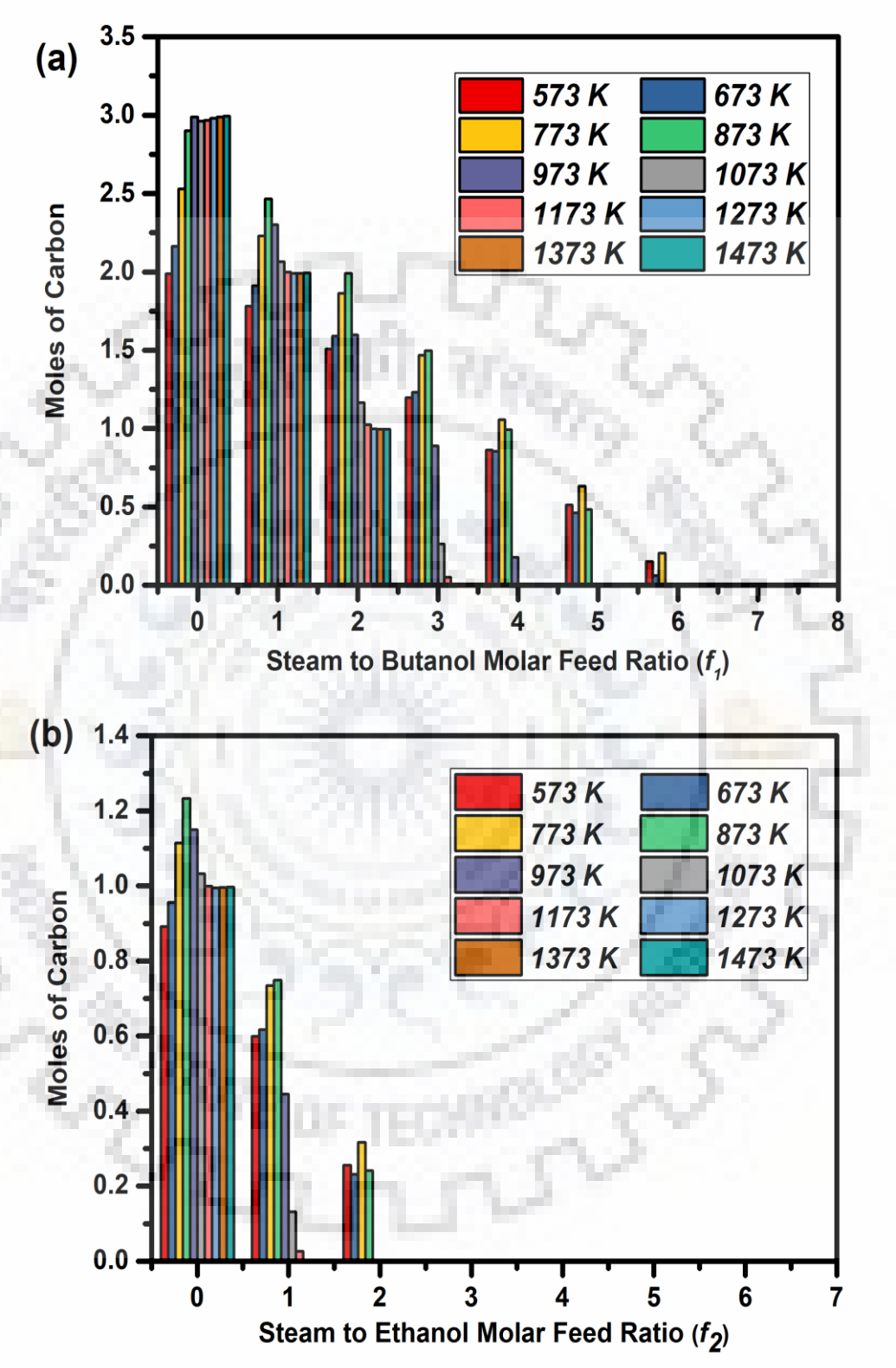

Figure 4.5 Molar production of carbon as a function of temperature at molar feed ratio (a) f_1(0-12) in SRB (b) f_2(0-12) in SRE

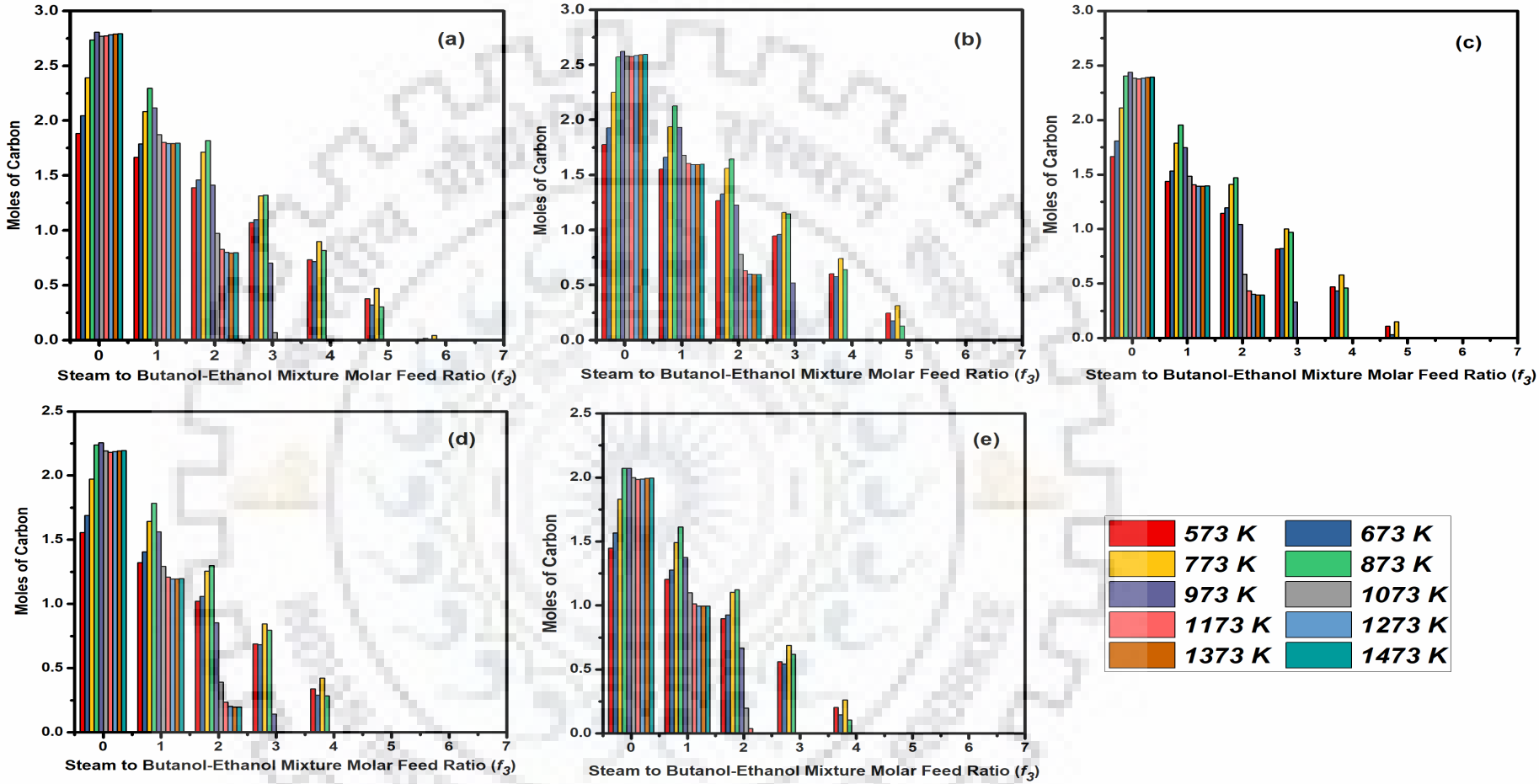

Figure 4.6 Molar production of carbon as a function of temperature at molar feed ratio f_3 (0-12) in SRB-E with (a) 90% B (b) 80% B (c) 70% B (d) 60% B (e) 50% B

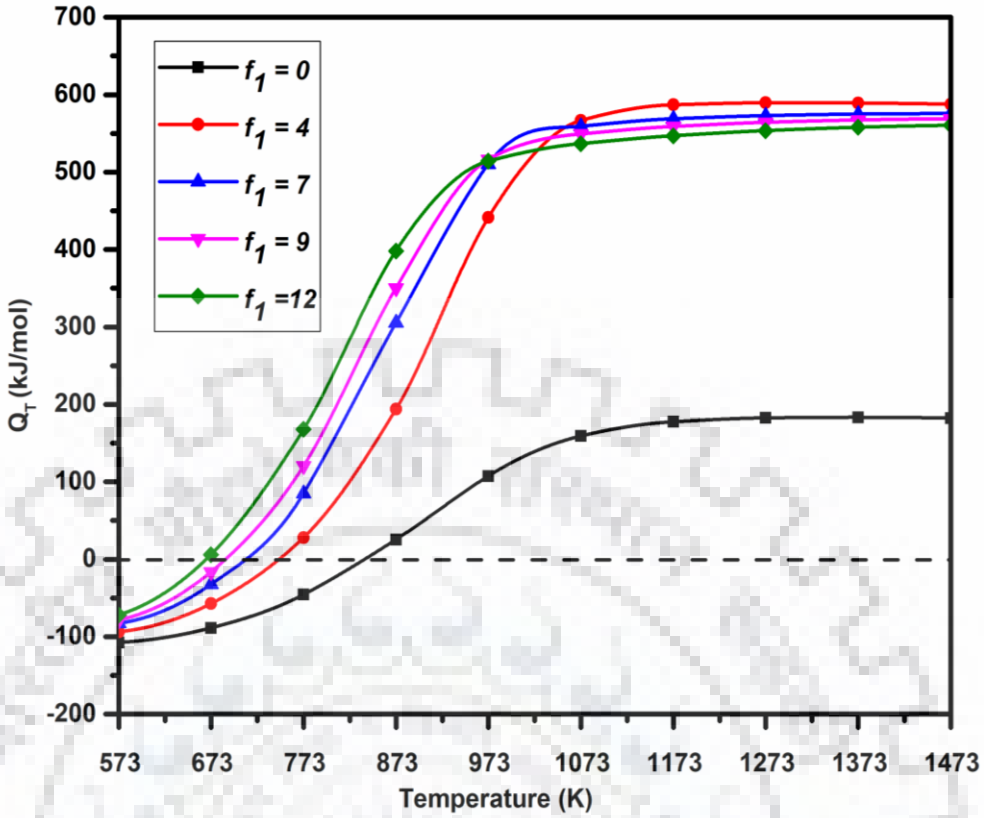

Figure 4.7 Energy requirement as a function of temperature at different f_1 values for SRB process

Table 4.5 Energy and component analysis in SRB, SRE, and SRB-E processes at molar feed ratio of 12

Parameters	**B-E =100-0%**	**B-E =90-10%**	**B-E =80-20%**	**B-E =70-30%**	**B-E =60-40%**	**B-E =50-50%**	**B-E =0-100%**
Temperature (K)	973	973	973	973	973	973	873
H_2 (moles)	9.96	9.56	9.139	8.72	8.28	7.84	5.49
% Decrease in H_2	---	4.08	8.252	12.52	16.89	21.43	44.88
Total energy requirement (kJ/mol) of fuel	513.99	485.13	456.181	427.19	398.19	369.12	210.54
% Decrease in energy	---	5.62	11.247	16.89	22.53	28.17	59.04
Energy requirement (kJ/mol) per mol of H_2	51.60	50.77	49.916	49.02	48.10	47.12	38.34
CO/H_2	0.19	0.18	0.168	0.16	0.17	0.14	0.06
CO_2/H_2	0.21	0.22	0.222	0.23	0.23	0.24	0.29
CH_4/H_2	4.82×10^{-3}	4.08×10^{-3}	3.392×10^{-3}	2.75×10^{-3}	2.30×10^{-3}	1.79×10^{-3}	7.29×10^{-3}

4.4.6 Thermal efficiency

Thermal efficiency is computed at different molar feed ratios (0-12), and temperature at which H_2 production is maximum for SRB, SRE, and SRB-E processes. Table 4.6 summarizes the thermal efficiency data at different feed ratios for all three reforming processes. It is clear from this table that molar feed ratio positively affects the thermal efficiency in SRB, SRE, and SRB-E processes. It is worth noting that the thermal efficiency of reforming process (Eq. (3.19)) is directly proportional to H_2 production and is adversely affected by the increase in the amount of steam in the feed, *LHV* of fuel and overall heat of reaction. In the absence of the steam in the feed, small increment in H_2 production cannot compensate the energy required to initiate the reforming resulting in lower thermal efficiency. At higher feed ratio, further increase in thermal efficiency occurs due to much higher H_2 production in comparison to heat energy requirement to vaporize the water in the feed. This trend is observed in all SRB, SRE, and SRB-E processes. This implies that the reduction or increase in thermal efficiency in any of the reforming process with molar feed ratio is trade-off between H_2 production and the energy required to vaporize the steam in the feed. At one molar feed ratio, the thermal efficiency of SRB process is less than SRE process. This may be probably due to higher *LHV* of butanol as compared to ethanol. In case of B-E mixture, the thermal efficiency increases with the increase in amount of ethanol in mixture. Increased amount of ethanol in the mixture reduces the H_2 production and total *LHV* of fuel (B-E) as well. Thus, the reduction or increase in thermal efficiency in case of SRB-E process is trade-off between the H_2 production and *LHV* of fuel plus heat required to produce steam. For instance, thermal efficiency of 80:20 B-E mixture is 46.60 % (f_3 = 0) and 70.20 % (f_3 =12). It indicates that at f_3 =12, 70.20 % of energy fed to the reforming process is recovered in the form of useful product H_2 and the remaining 29.80 % is exhausted with other gaseous products.

4.4.7 Exergy efficiency

The exergy efficiency is calculated (Eq. (3.31)) for SRB, SRE and SRB-E processes at different molar feed ratios (0-12) and temperature corresponding to maximum production of H_2. The inlet stream contains two components (steam and fuel) and outlet stream contains five components (H_2, CO, CO_2, CH_4, H_2O) with complete conversion of fuel for all three reforming processes under study. The exergy efficiency for any reforming system is affected by the reforming temperature and molar feed ratios. The exergy efficiency results are presented in Table 4.6. It is clear from this table that the exergy efficiency is favoured by

high value of molar feed ratios f_1, f_2 and f_3 in case of SRB, SRE and SRB-E processes respectively. For SRB-E process, the exergy efficiency increases with the increase in amount of ethanol in B-E mixture at fixed value of molar feed ratio f_3. But the incremental difference is not significant at high f_3 values say f_3=9 and 12. Further, Table 4.6 also indicates that exergy efficiency is less than the thermal efficiency in the reforming process. This difference occurs due to exergy that is exhausted in outgoing off-gases and the exergy that is destroyed as discussed earlier in section 3.4. The exergy destruction is not taken into account by the first law of thermodynamics to calculate thermal efficiency. The exergy destruction is due to the combination of high irreversibities of the chemical reactions and large difference in temperature between the reactants and the products of the reformer [Tippawan and Arpornwichanop, 2014]. When temperature of reactants and products are taken same in the analysis, then chemical reactions affect the overall process irreversibility. The valid reason is that the chemical reactions are related to the motion of electrons during forming and breaking of chemical bonds between atoms [Tippawan and Arpornwichanop, 2014]. Also, the high frequency of collisions causes an increase in entropy within the system resulting in high exergy destruction. Thus, the exergy destruction in case of butanol is more than ethanol and thereby the exergy efficiency of SRB is less than that of SRE. Similar conceptual basis regarding exergy destruction has been justified by Leo et al. (2011) in their study on exergy destruction using different fuels stating that ethanol (C_2 compound) reforming shows comparatively lower exergy destruction than other oxygenated hydrocarbons (> C_2 compounds). In addition to this, the exothermic or combustion processes lose more energy [Tippawan and Arpornwichanop, 2014]. Conversely, endothermic reactions show lower exergy destruction. Thus, high value of the energy demand turns into an excellent exergetic performance. Therefore, total exergy destruction is lower in case of endothermic steam reforming of fuels. For one reforming process, the high value of molar feed ratio increases the endothermicity resulting in lower exergy destruction and thereby high exergy efficiency. In another way, it can be stated that the high molar amount of steam in feed, and high temperature cause high H_2 production which in turn allows to increase the exergy efficiency. Thus, in order to minimize the exergy destruction, the suitable reforming temperature and molar feed ratios should be selected accordingly. However, the exergy efficiency is trade-off between H_2 production and overall endothermicity of the reforming process. This can be clearly seen in few exergy efficiency data presented in Table 4.6 specifically at higher molar feed ratios of 9 and 12.

Table 4.6 Thermal efficiency and exergy efficiency of SRB, SRE, and SRB-E processes at highest H_2 production conditions on the basis of 1 mol fuel in the feed

Molar Feed Ratio	Parameters	B-E= 100-0%	B-E= 90-10%	B-E= 80-20%	B-E= 70-30%	B-E= 60-40%	B-E= 50-50%	B-E= 0-100%
0	**T (K)**	**1473**	**1473**	**1473**	**1473**	**1473**	**1473**	**1473**
	Thermal Efficiency (%)	45.84	46.20	46.60	47.05	47.54	48.10	52.12
	Exergy Efficiency (%)	8.31	8.61	8.94	9.30	9.72	10.19	29.87
4	**T (K)**	**1173**	**1173**	**1173**	**1173**	**1073**	**1073**	**973**
	Thermal Efficiency (%)	62.33	62.73	63.14	63.56	64.44	65.11	69.18
	Exergy Efficiency (%)	36.88	37.59	38.31	39.05	39.36	40.39	46.25
7	**T(K)**	**1073**	**1073**	**1073**	**1073**	**973**	**973**	**973**
	Thermal Efficiency (%)	66.22	66.60	66.98	67.35	68.44	69.09	70.99
	Exergy Efficiency (%)	44.87	45.36	45.84	46.28	47.17	47.93	50.12
9	**T(K)**	**973**	**973**	**973**	**973**	**973**	**973**	**973**
	Thermal Efficiency (%)	68.20	68.71	69.19	69.61	69.98	70.28	70.08
	Exergy Efficiency (%)	47.476	47.97	48.41	48.79	49.09	49.31	48.13
12	**T (K)**	**973**	**973**	**973**	**973**	**973**	**973**	**873**
	Thermal Efficiency (%)	69.89	70.07	70.20	70.27	70.27	70.18	68.49
	Exergy Efficiency (%)	48.72	48.69	48.58	48.38	48.08	47.67	46.15

4.4.8 Comparison of steam reforming of acetone, butanol, and ethanol

Table 4.7 summarizes necessary results regarding steam reforming of acetone, butanol, and ethanol individually in terms of maximum hydrogen production and thermal efficiency of steam reformer. It is clear from the table that butanol provides higher hydrogen production namely, 1.44 times more than acetone, and 1.81 times more than ethanol. Moreover, thermal efficiency of steam reformer is higher for butanol than acetone and ethanol.

Table 4.7 Comparison of SRA, SRB, and SRE

Operating parameters	**SRA**	**SRB**	**SRE**
Temperature	973 K	973 K	873 K
Pressure	1 atm	1 atm	1 atm
Steam/fuel molar feed ratio	12	12	12
Conversion	100%	100%	100%
H_2 (mol)	6.93	9.96	5.49
η_{th}(%)	66.17	69.89	68.49

4.5 CONCLUDING REMARKS

Table 4.7 shows that the performance of butanol as renewable fuel is higher than that of acetone and ethanol fuels. The activity of fuels are found on the basis of highest hydrogen production as butanol > ethanol > acetone. The butanol-ethanol mixture has performed well in terms of thermal efficiency (more than 70% for 50-90% B compositions) of steam reformer at a molar ratio of 12, temperature of 973 K, and 1 atm pressure. Therefore, it is concluded that the butanol-ethanol mixture as obtained after separation of acetone from ABE mixture can be used as a fuel for steam reformer.

CHAPTER V

OXIDATIVE STEAM REFORMING OF BUTANOL-ETHANOL MIXTURE

5.1 INTRODUCTION

In this chapter, the effect of addition of oxygen in the feed for steam reforming of butanol-ethanol mixture has been investigated for the production of hydrogen which is commonly referred to as oxidative steam reforming of butanol-ethanol mixture. To the best of our knowledge, no experimental or thermodynamic study is available in the literature on oxidative steam reforming process of butanol-ethanol mixture. This mixture has been investigated by thermodynamic analysis via Gibbs free energy minimization method, for thermal efficiency of reformer through energy analysis, and exergy efficiency.

5.2 METHODOLOGY

The methodology described in section 4.2 has also been used for the thermodynamic and energy analysis of OSRB-E process. The operating parameters for the simulation are temperature (573-1473 K), pressure (1-10 atm), and molar feed ratios of steam/B-E mixture (f_{O1}=9 and 12) and O_2/B-E mixture (f_{O2} =0-3). The chemical reactions concerned with OSR of butanol and ethanol are summarized in Table 5.1. It is evident from the Table 5.1 that in main reforming reactions, the total moles of products increase with the progress of reactions resulting in the shift of equilibrium in favour of product formation at lower pressure. Therefore, the simulations are carried out at 1 atm pressure in the present study [Liu et al., 2008; Horng et al, 2016]. The B-E mixture from fermentation broth contains water in the molar ratio of 9:1 (water: B-E mixture) [Zheng et al., 2015; Yang et al., 2017]. Therefore, the simulation is carried out at molar ratio of steam/B-E mixture (f_{O1}) of 9 and 12 in the feed. The value of f_{O1}=12 is considered because water content in B-E mixture from fermentation broth may vary and secondly the higher production of H_2 is reported at f_{O1} =12 in the available literature on oxidative steam reforming of pure butanol and ethanol [Hartley et al., 2015, Dhanala et al., 2015]. The amount of liberated heat depends upon quantity of O_2 mixed with steam in the feed. Insufficient amount of O_2 is not able to supply the required heat energy to endothermic steam reforming process, whereas large amount of O_2 may result in oxidation of H_2 to H_2O and CO to CO_2. Therefore, O_2 to B-E mixture molar feed ratio (f_{O2}) has been

varied in the range of 0-3 as reported in the literature on OSR of butanol and ethanol separately [Hartley et al., 2015; Dhanala et al., 2015; Horng et al, 2016]. In butanol-ethanol mixture, the mole fraction of butanol (*f*) is varied from 0.5-0.9 where rest is ethanol. During the simulation, the molar amount of B-E mixture is kept constant at 1 mol. The molar amounts of steam and oxygen in the feed are calculated accordingly. For the convergence, the mass balance tolerance limit is set to 10^{-10}. The simulation provides the molar amount of components (n_i) in the outlet stream of the reformer at specified conditions of *T* and molar feed ratios (f_{O1} and f_{O2}).

For butanol-ethanol mixture, the following equations are used for the calculation of f_{O1} and f_{O2}:

$$f_{O1} = \frac{n_{steam}^{in}}{n_{butanol}^{in} + n_{ethanol}^{in}} \tag{5.1}$$

$$f_{O2} = \frac{n_{O_2}^{in}}{n_{butanol}^{in} + n_{ethanol}^{in}} \tag{5.2}$$

The performance of OSRB-E process has been analyzed in terms of yields of product components as defined below [Montero et al., 2015; Özkara-Aydınoğlu, 2010].

$$Yield_{H_2}(\%) = \frac{Moles\ of\ H_2\ at\ outlet \times 2}{f_{O1} \times 2 + f \times 10 + (1-f) \times 6} \times 100 \tag{5.3a}$$

Eq. (5.3a) provides percent yield of hydrogen on the basis of reactants consumed.

$$Yield_{H_2}(\%) = \frac{Moles\ of\ H_2}{Mole\ of\ all\ products} \times 100 \tag{5.3b}$$

In Eq. (5.3b), percent yield of hydrogen is defined on the basis of product composition alone.

$$Yield_{i(CO,CO_2,CH_4)}(\%) = \frac{Moles\ of\ i\ (CO, CO_2, CH_4)\ at\ outlet}{f \times 4 + (1-f) \times 2} \times 100 \tag{5.4}$$

where, *f*= mole fraction of butanol in feed, and (*1-f*) = mole fraction of ethanol in feed.

Table 5.1 Chemical reactions involved in OSRB-E process

Reaction No.	**Reactions**	**Reaction Types**	**ΔH_R (kJ/mol) at 298 K, 1atm**
R1	$C_4H_{10}O + 3H_2O \leftrightarrow 4CO + 8H_2$	Steam reforming of butanol	557.67
R2	$C_4H_{10}O \leftrightarrow CO + 2CH_4 + H_2 + C$	Decomposition of butanol	14.19
R3	$C_2H_6O + H_2O \leftrightarrow 2CO + 4H_2$	Steam reforming of ethanol	255.53
R4	$C_2H_6O \leftrightarrow CO + CH_4 + H_2$	Decomposition of ethanol	49.42
R5	$CO + H_2O \leftrightarrow CO_2 + H_2$	Water-gas shift reaction	-41.17
R6	$CO_2 + 4H_2 \leftrightarrow CH_4 + 2H_2O$	Methanation reactions (R6 and R7)	-164.94
R7	$CO + 3H_2 \leftrightarrow CH_4 + H_2O$		-206.11
R8	$C_4H_{10}O + 1.5O_2 \leftrightarrow 4CO + 5H_2$	Partial oxidation of butanol	-167.73
R9	$C_4H_{10}O + 6O_2 \leftrightarrow 4CO_2 + 5H_2O$	Oxidation of butanol	-2508.61
R10	$C_2H_6O + 0.5O_2 \leftrightarrow 2CO + 3H_2$	Partial oxidation of ethanol	13.73
R11	$C_2H_6O + 1.5O_2 \leftrightarrow 2CO_2 + 3H_2$	Oxidation of ethanol	-552.21
R12	$CH_4 + 0.5O_2 \leftrightarrow CO + 2H_2$	Partial oxidation of methane	-35.69
R13	$CH_4 + 2O_2 \leftrightarrow CO_2 + 2H_2O$	Oxidation of methane	-802.26

It is worth noting here that the selection of components in the outlet stream is very critical to the entire thermodynamic simulation and it should be made on the basis of experimental reforming data. Different sets of components not only provide different equilibrium compositions but also provides sometimes misleading results. In the present study, the set of gaseous components in the outlet stream is selected on the basis of experimental studies of pure butanol and ethanol on oxidative steam reforming [Cai et al., 2013;Dhanala et al., 2015; Greluk et al., 2016; Baruah et al., 2017]. After simulations, the outlet stream is found to contain few components in trace amounts. The conversions of

butanol and ethanol in B-E mixture are found to be 100% for all operating conditions simulated at equilibrium. In view of these findings, the most dominant feasible reforming products are H_2, CO, CO_2, CH_4 and water. The detailed discussion regarding the effects of pressure, temperature and molar feed ratios (f_{O1} and f_{O2}) on the equilibrium yields of products, energy and exergy are presented in the subsequent sections.

5.3 OXIDATIVE STEAM REFORMING OF BUTANOL-ETHANOL MIXTURE

5.3.1 Effect of pressure

The calculations for analyzing the effect of pressure on H_2 production have been carried out at 973 K for OSRB-E process. Figures 5.1 (a) and (b) show the molar production of H_2 in OSRB-E process at f_{O1} values of 9 and 12, f_{O2}=0-3, and pressure in the range of 1-10 atm. It is clear from the figures that H_2 production is suppressed by increasing pressure above 1 atm. Moreover, f_{O2} values more than zero also provide detrimental effect on H_2 formation. These trends can be justified on the basis of reforming reactions listed in Table 5.1.

The endothermic gaseous reactions are responsible for increasing the production of hydrogen in the system with the progress of reaction. In this case, Le Chatelier's principle is applicable as high pressure will favour the reactions to proceed in backward direction. Due to this reason high pressure shows negative effect on the production of hydrogen at equilibrium. Therefore, the total pressure of 1 atm has been chosen further for all thermodynamic equilibrium calculations.

5.3.2 Carbon formation

The analysis of carbon formation during reforming process is essential as its deposition on the surface of the catalyst deactivates the catalyst and thereby adversely affects the performance of reforming process. Therefore, the simulations are carried out on SR of pure butanol and pure ethanol separately under wide range of temperature and steam/fuel molar feed ratios. Figures 5.2 (a) and (b) clearly indicate that at prescribed values of steam/fuel molar feed ratios of 9 and 12, there is no possibility of carbon formation at any temperature. The available literature also reports negligible carbon formation at all temperature conditions and molar feed ratios of 9 and 12 [Hartley et al., 2015; Dhanala et al., 2015; Ortiz et al., 2015; Horng et al., 2016]. Therefore, carbon has been excluded from the product list for further result and discussions.

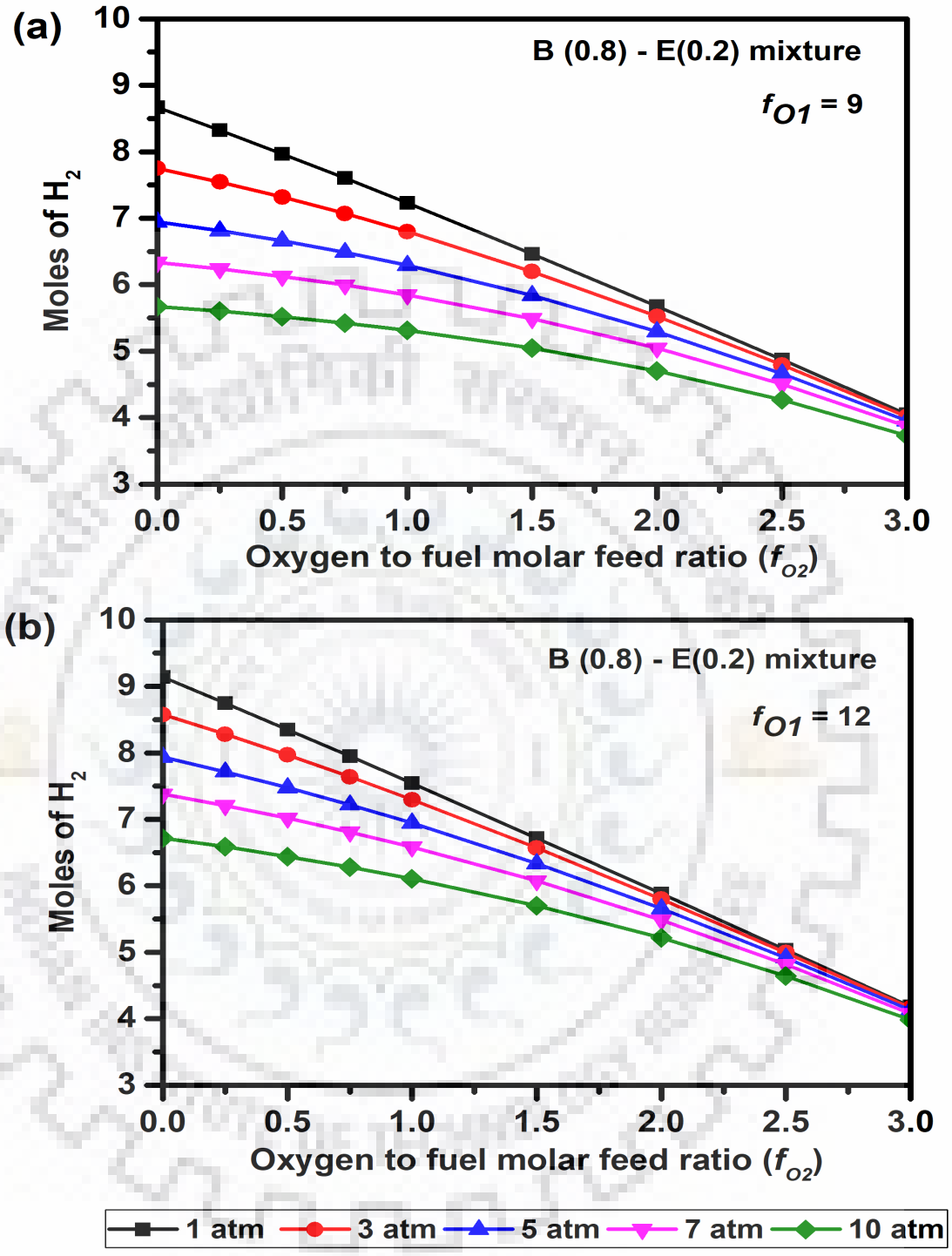

Figure 5.1 Effect of pressure on production of H_2 with (a) f_{O1}=9 and (b) f_{O1}=12 in OSRB-E process at 973K

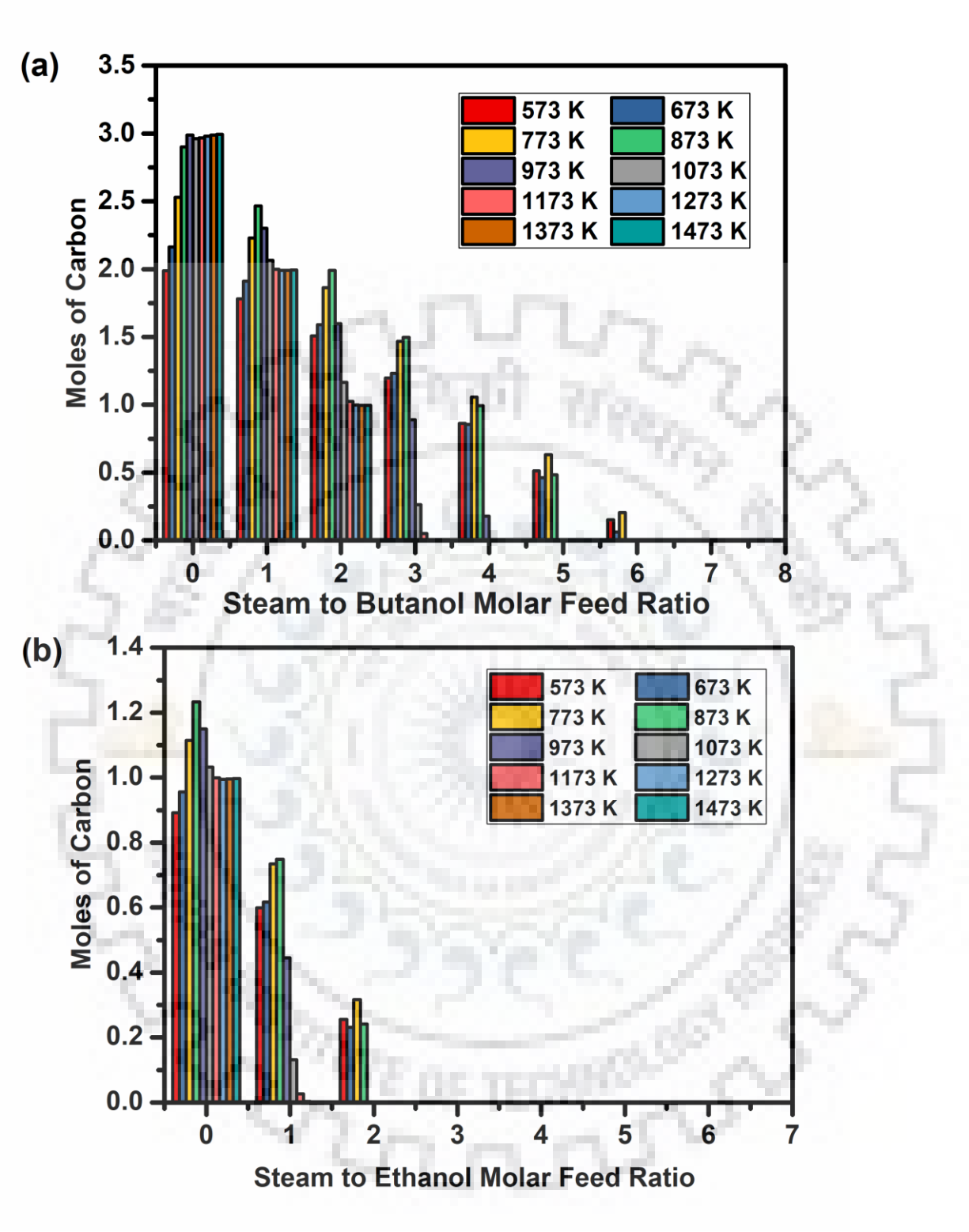

Figure 5.2 Molar production of carbon as a function of temperature and steam to fuel molar feed ratio in (a) steam reforming of butanol and, (b) steam reforming of ethanol

5.3.3 Yield of H_2

Figures 5.3 (a) and (b) illustrate the effects of reaction temperature and O_2/B-E mixture molar feed ratio (f_{O2}) on the yield of H_2 for B-E mixture (0.8 B) under f_{O1}=9 and 12, respectively. In SR process (f_{O2}=0), the low temperature favours exothermic methanation reactions (R6 and R7) and WGS reaction (R5). Methanation reaction largely consume H_2 resulting in low H_2 yield at low temperature. At high f_{O1} values (≥ 9), SR and WGS reactions are more prominent for H_2 production. The yield of H_2 continuously increases with temperature due to suppression of methanation reaction and attains highest yield (63.75%) at temperature of 973 K. On further increasing temperature, endothermic RWGS slightly reduces the H_2 yield. Table 5.2 shows the highest H_2 yields for all compositions of B-E mixture (0.5B-0.9B). The variational trends in all these compositions are similar to Figures 5.3 (a) and (b). The highest H_2 yields are 65.46% (0.9B) and 57.75% (0.5B). It is clear that H_2 yield decreases with decrease in B in B-E mixture. This is mainly attributed to the stoichiometry of SR reactions (R1 and R3). According to Figure 5.3 (b), in case of f_{O1}=12, the H_2 yield is lower than that as achieved at f_{O1}=9 at all temperatures. The highest H_2 yield (56.88%) is achieved at 973 K (Table 5.2). Though, the molar production of H_2 at f_{O1}=12 is higher than at f_{O1}=9, but this molar increase in H_2 production is not significant in comparison to increase in steam amount in feed for f_{O1}=12 causing reduction in H_2 yield. In presence of O_2 in feed (f_{O2}>0), the oxidation reactions (R8 to R11) and SR reactions (R1 and R3) occur simultaneously. Figures 5.3 (a) and (b) depict the variational trends of H_2 yields at various f_{O2} values. The upper limit of f_{O2} for simulation is fixed at 0.75 as above 0.75 (approximately 1), the overall reforming system starts behaving as exothermic. On addition of O_2 in steam, a fraction of butanol and ethanol get oxidized through oxidation reactions (R8 to R11). According to the stoichiometry of these reactions, the yield of H_2 is reduced in presence of O_2 than at without O_2. In addition to this, small amount of H_2 also gets oxidized to H_2O causing reduction in H_2 yield (Figures 5.3 (a) and (b)). Tables 5.2 and 5.3 compile the highest H_2 yield data under f_{O2}=0.75 for all compositions of B-E mixture. The highest yields at f_{O2}=0.75 are 58.00% (0.9B), 55.92% (0.8B), and 48.80% (0.5B) at f_{O1}=9 and are 49.92% (0.9B), 47.88% (0.8B), and 41.12% (0.5B) at f_{O1}=12.

Further for the sake of the comparison, percent yields of H_2 at various temperatures, molar O_2/fuel ratio (f_{O2}) and molar steam/fuel ratio (a) f_{O1}=9 (b) f_{O1}=12 have also been done, and are shown in Figures 5.4 (a) and (b). It is noted that the trends of variation of H_2 yield are similar as discussed above. The corresponding data of H_2 yield for Eq. (5.3a) and Eq. (5.3b) are presented in Tables 5.2and 5.3. In all the above operating conditions of f_{O1} and f_{O2}, the

highest H_2 yield has been achieved at the same temperature of 973 K. The above results indicate that addition of O_2 to steam in OSRB-E process reduces the energy requirement in endothermic SR process as discussed in later sections but at the expense of H_2 yield.

Table 5.2 Equilibrium yields (%) of products and energy evaluation for various B-E mixtures at f_{O1} =9, f_{O2}= 0 and 0.75, and temperature corresponding to maximum H_2 yield

Parameters	**Fraction of B in B-E mixture**						
		0.9	**0.8**	**0.7**	**0.6**	**0.5**	
Temperature (K)		973	973	973	973	973	
H_2 (%)	f_{O2}=0	65.46	63.75	61.90	59.90	57.75	Eq.(5.3a)
		51.82	50.81	49.70	48.47	47.12	Eq.(5.3b)
	f_{O2}=0.75	58.00	55.92	53.70	51.33	48.80	Eq.(5.3a)
		45.69	44.38	42.95	41.40	39.71	Eq.(5.3b)
CH_4 (%)	f_{O2}=0	2.23	1.90	1.61	1.34	1.10	Eq.(5.4)
	f_{O2}=0.75	1.05	0.87	0.71	0.56	0.44	Eq.(5.4)
CO (%)	f_{O2}=0	53.39	51.55	49.60	47.54	45.36	Eq.(5.4)
	f_{O2}=0.75	45.68	43.60	41.42	39.15	36.79	Eq.(5.4)
CO_2(%)	f_{O2}=0	44.38	46.54	48.79	51.12	53.54	Eq.(5.4)
	f_{O2}=0.75	53.27	55.53	57.87	60.29	62.78	Eq.(5.4)
Q_T(kJ)	f_{O2}=0	488.53	460.46	432.09	403.48	374.69	Eq.(3.20)
	f_{O2}=0.75	114.98	102.11	72.82	43.48	14.15	Eq.(3.20)
% η_{th}	f_{O2}=0	68.71	69.19	69.61	69.98	70.28	Eq.(3.19)
	f_{O2}=0.75	68.99	68.83	68.99	69.06	69.01	Eq.(3.19)
% η_{Ex}	f_{O2}=0	47.97	48.41	48.78	49.09	49.31	Eq.(3.31)
	f_{O2}=0.75	43.13	43.02	42.88	42.50	42.03	Eq.(3.31)
Ex_{dest} (kJ/mol)	f_{O2}=0	224.68	214.55	204.82	195.50	186.61	Eq.(3.30)
	f_{O2}=0.75	241.14	232.98	225.22	217.88	210.99	Eq.(3.30)

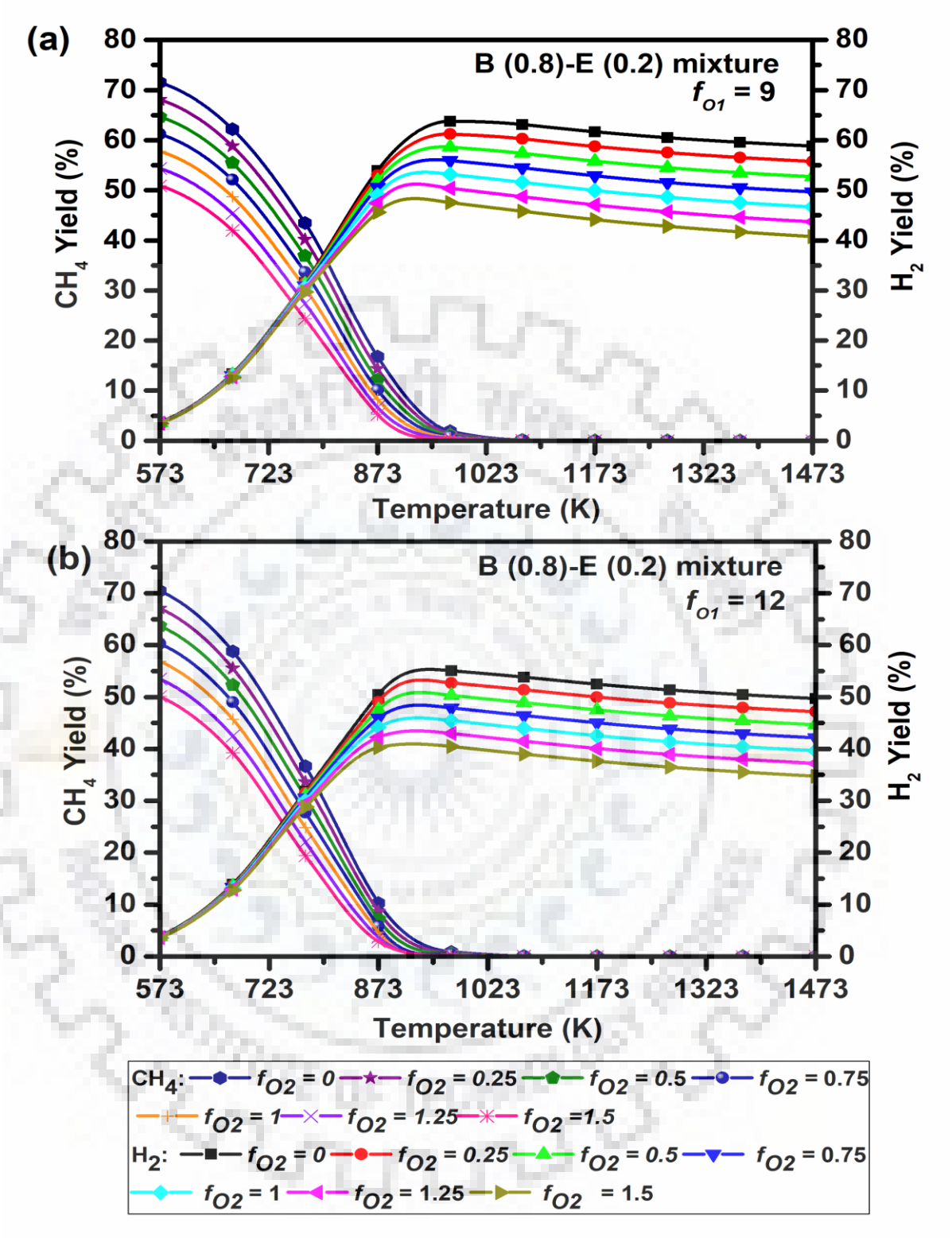

Figure 5.3 Percent yields of $H_2$and CH_4 at various temperatures, molar O_2/fuel ratio (f_{O2}) and molar steam/fuel ratio (a) f_{O1}=9 (b) f_{O1}=12 (by using Eq. 5.3a)

Table 5.3 Equilibrium yields (%) of products and energy evaluation for various B-E mixtures at f_{O1} =12, f_{O2}= 0 and 0.75, and temperature corresponding to maximum H_2 yield

Parameters	**Fraction of B in B-E mixture**						
		0.9	**0.8**	**0.7**	**0.6**	**0.5**	
Temperature (K)		973	973	973	973	973	
H_2 (%)	f_{O2}=0	56.88	55.06	53.13	51.11	48.970	Eq.(5.3a)
		46.56	45.38	44.12	42.76	41.30	Eq.(5.3b)
	f_{O2}=0.75	49.92	47.88	45.73	43.48	41.12	Eq.(5.3a)
		40.79	39.40	37.92	36.34	34.65	Eq.(5.3b)
CH_4 (%)	f_{O2}=0	1.02	0.86	0.72	0.59	0.48	Eq.(5.4)
	f_{O2}=0.75	0.50	0.41	0.33	0.26	0.20	Eq.(5.4)
CO (%)	f_{O2}=0	44.49	42.70	40.84	38.91	36.92	Eq.(5.4)
	f_{O2}=0.75	37.82	35.93	34.00	31.98	29.92	Eq.(5.4)
CO_2 (%)	f_{O2}=0	54.50	56.45	58.45	60.50	62.60	Eq.(5.4)
	f_{O2}=0.75	61.68	63.66	65.69	67.76	69.88	Eq.(5.4)
Q_T(kJ)	f_{O2}=0	485.13	456.18	427.19	398.19	369.21	Eq.(3.20)
	f_{O2}=0.75	108.37	95.46	66.28	37.19	8.21	Eq.(3.20)
% η_{th}	f_{O2}=0	70.07	70.20	70.27	70.27	70.18	Eq.(3.19)
	f_{O2}=0.75	69.44	68.95	68.76	68.45	68.02	Eq.(3.19)
% η_{Ex}	f_{O2}=0	48.69	48.58	48.38	48.08	47.67	Eq.(3.31)
	f_{O2}=0.75	42.73	42.14	41.52	40.78	39.80	Eq.(3.31)
Ex_{dest} (kJ/mol)	f_{O2}=0	210.39	204.20	198.34	192.81	187.62	Eq.(3.30)
	f_{O2}=0.75	234.48	229.95	224.97	220.22	216.82	Eq.(3.30)

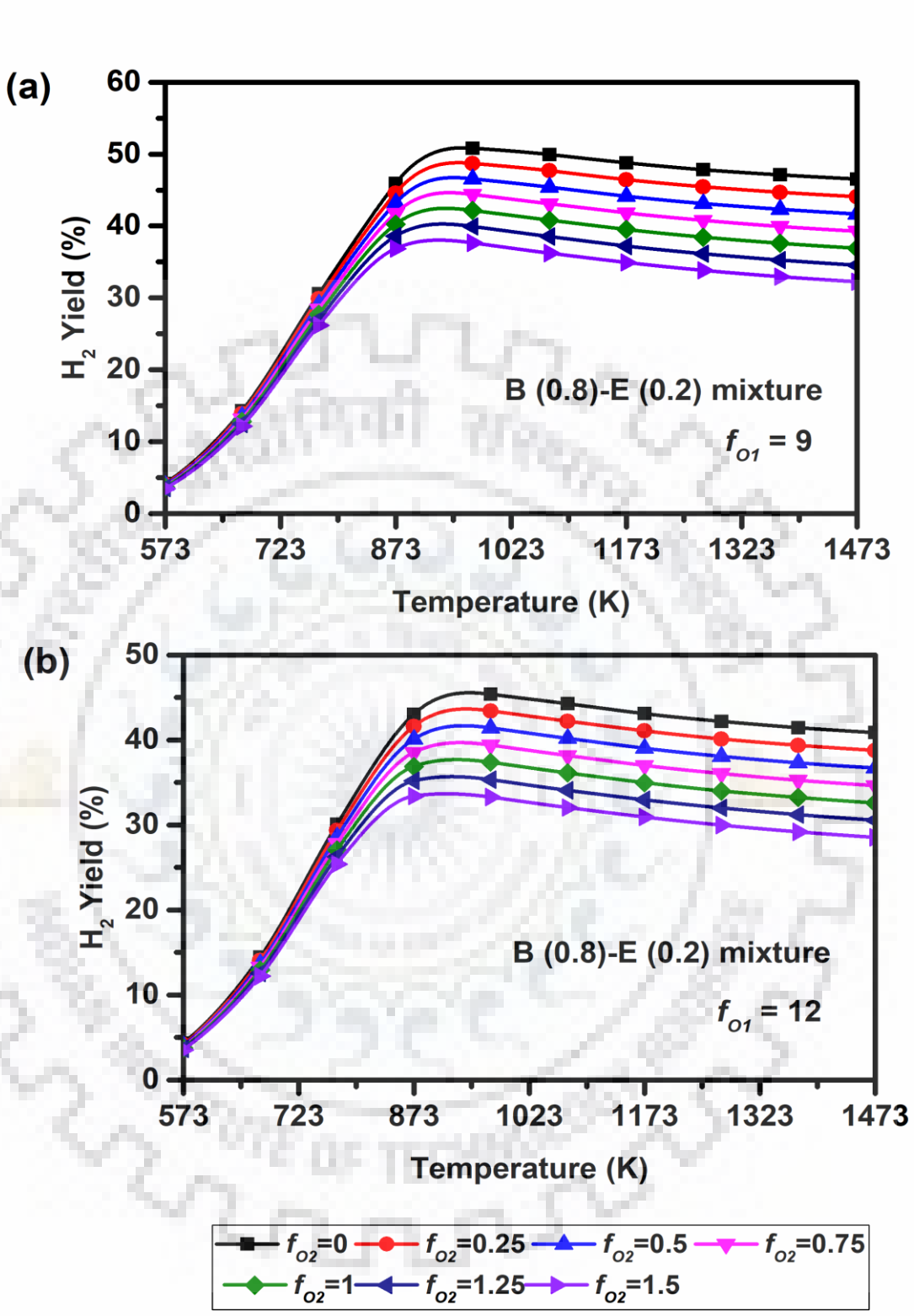

Figure 5.4 Percent yields of H_2 at various temperatures, molar O_2/fuel ratio (f_{O2}) and molar steam/fuel ratio (a) f_{O1}=9 (b) f_{O1}=12 (by using Eq.5.3b).

5.3.4 Yield of CH_4

The variation of CH_4 yield with temperature and f_{O2} is shown in Figures 5.3 (a) and (b) under f_{O1} of 9 and 12, respectively for OSRB-E process (0.8 B). At high f_{O1} values (9 and 12), the decomposition reactions (R2 and R4) are not prominent than SR reactions (R1 and R3). Therefore, CH_4 production is mainly due to methanation reactions (R6 and R7). Low temperature favours exothermic methanation reactions, resulting in high yield of CH_4 at low temperature of 573 K. As temperature increases, methanation reactions are suppressed leading to sharp decrease in CH_4 yield. Finally, it becomes negligibly small as is clear from Figures 5.3 (a) and (b). For SR process (f_{O2}=0), the highest yields of CH_4 are 71.41% (f_{O1}=9) and 70.47% (f_{O1}=12) at temperature 573 K. In case of other B-E compositions of OSRB-E, the CH_4 amount at temperature of 573 K decreases with fraction of B in B-E mixture. This trend can be understood on the basis of stoichiometry of SR reactions (R1 and R3) for the production of H_2, and thereby CH_4 (R6 and R7), the highest and the lowest yields of CH_4 depend upon fraction of B in B-E mixture. Under f_{O1}=9, these are 71.68% (573 K) and 0.0001% (1473 K) for 0.9 B and 70.81% (573 K) and 0.00008% (1473 K) for 0.5 B in B-E mixture. At f_{O1}=12 value, the yield of CH_4 increases due to more molar production of H_2. However, the variation trends remain similar to that of f_{O1}=9. In OSR process, the small addition of O_2 to feed initiates oxidation reactions (R12 and R13). The OSR process produces lower molar amount of H_2 which in turn reduces the CH_4 production through methanation reactions. Additionally, a small fraction of CH_4 also gets oxidized to H_2O and CO_2 (R13). Higher f_{O2} values further reduce CH_4 yield. Tables 5.2 and 5.3 give CH_4 yield corresponding to highest H_2 yield under f_{O1}=0 and f_{O1}=0.75 for all B compositions in B-E mixture. CH_4 yields under f_{O1}=9 are 2.22% (f_{O2}=0), 1.05% (f_{O2}=0.75) for 0.9 B and 1.90% (f_{O2}=0), 0.87% (f_{O2}=0.75) for 0.8 B and 1.10% (f_{O2}=0), 0.44% (f_{O2}=0.75) for 0.5 B in B-E mixture. The same CH_4yield under f_{O1}=12 are 1.02% (f_{O2}=0), 0.50% (f_{O2}=0.75) for 0.9 B and 0.86% (f_{O2}=0), 0.41% (f_{O2}=0.75) for 0.8 B and 0.48% (f_{O2}=0), 0.20% (f_{O2}=0.75) for 0.5 B in B-E mixture. In view of above discussion on CH_4 production, it can be clearly concluded that CH_4 production adversely affects H_2 production and is therefore considered as a highly undesirable product in reforming processes. Although, CH_4 production can be reduced thermodynamically by increasing the temperature above approximately 973K, yet it can also be reduced for commercial purposes by manufacturing suitable reforming catalyst which can behave as inert towards methanation reactions at prevailing operating conditions for reforming process.

5.3.5 Yields of CO and CO_2

The yields of CO and CO_2 at equilibrium as a function of temperature and O_2/fuel molar feed ratio (f_{O2}) are illustrated in Figures 5.5 (a) and (b) under f_{O1}=9 and 12, respectively for OSRB-E process (0.8 B). The yield of CO_2 increases remarkably with temperature in the range of 573 to 873 K. This trend is attributed to the thermodynamic feasibility of WGS reaction in lower temperature range. As a result, very low yield of CO is observed in low temperature range. At high temperature T > 873 K, the endothermic reactions R1 and R3 are more favoured whereas WGS reactions and methanation reactions are suppressed. These facts justified the decrease in yield of CO_2 and increase in yield of CO above 873K for f_{O1}=9in Figure 5.5 (a) and f_{O1}=12 in Figure 5.5 (b). However, CO yield is lower in case of f_{O1}=12. This is attributed to suppression of RWGS reaction (reverse of R5) on increasing the amount of steam in feed. Additionally, the reduction in CH_4 yield also results in increase of yield of CO and CO_2 in that particular range of temperature. In case of OSR process (f_{O2} > 0), O_2 in feed causes the oxidation reactions (R8 and R11). The oxidation reactions result in lower production of CO and higher production of CO_2 as fraction of CO is converted to CO_2. Increase in f_{O2} value (more O_2 in feed), further reduces the yield of CO and consequently enhances the yield of CO_2. Similar trends are observed in case of OSRB-E process of all B-E compositions in the mixture. In comparison, the yield of CO decreases and the yield of CO_2 increases as the fraction of B in the B-E mixture decreases. This trend can be explained by the stoichiometry of reforming reactions (R1 and R3). Tables 5.2 and 5.3 compile the yields of CO and CO_2 corresponding to maximum production of H_2 for f_{O2}=0 and f_{O2}=0.75 under f_{O1}=9 and 12, respectively. The yields of CO are 53.39% (f_{O1}=0), 45.68% (f_{O1}=0.75) at 0.9 B, 51.55% (f_{O1}=0), 43.60% (f_{O1}=0.75) at 0.8 B, and 45.36% (f_{O1}=0), 36.79% (f_{O1}=0.75) at 0.5B under f_{O1}=9. Similarly, under f_{O1}=12, the yields of CO are 44.49% (f_{O1}=0), 37.82% (f_{O1}=0.75) at 0.9 B, 42.70% (f_{O1}=0), 35.93% (f_{O1}=0.75) at 0.8 B, and 36.92% (f_{O1}=0), 29.92% (f_{O1}=0.75) at 0.5 B.

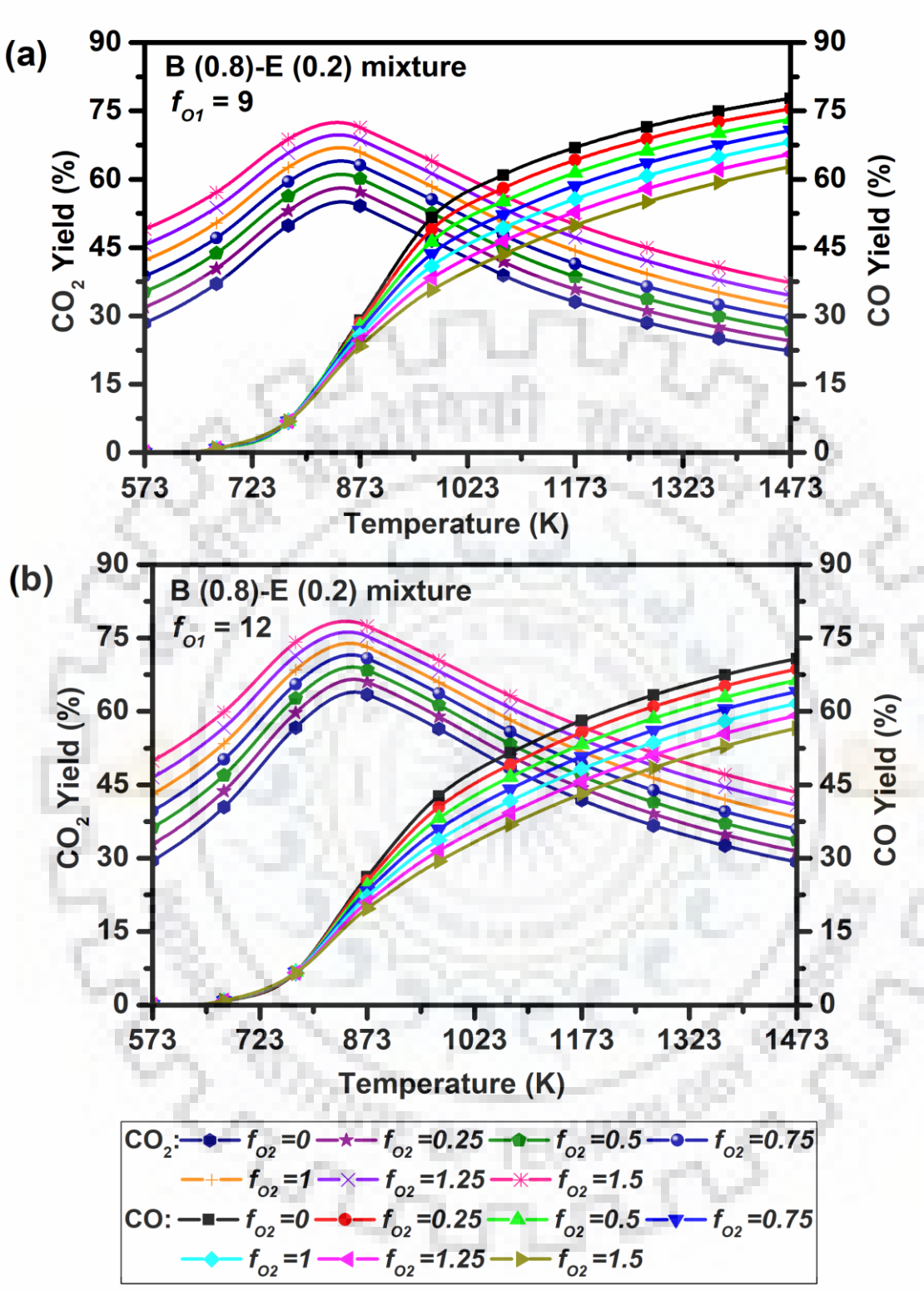

Figure 5.5 Percent yields of CO and CO_2 at various temperatures, molar O_2/fuel ratio (f_{O2}) and molar steam/fuel ratio (a) f_{O1}=9 (b) f_{O1}=12

5.3.6 Energy requirement

Energy requirement is a key parameter for every reforming process. The energy requirement trends for SRB-E (f_{O2}=0) and OSRB-E (0.8B) as a function of temperature corresponding to the various O_2/fuel molar feed ratio under f_{O1}=9 are shown in Figure 5.6. Tables 5.2 and 5.3 compile the energy requirements by SRB-E and OSRB-E processes to provide maximum H_2 yield at f_{O1}=9 and 12 respectively for all compositions of B-E mixture for f_{O2} equals to 0 and 0.75. SRB-E process (f_{O2}=0), is endothermic in nature. It requires heat energy in increasing quantity as the reaction progresses at low temperature of 573 K. The exothermic reactions (R5 to R7) are more pronounced making overall process slightly exothermic. The increase in temperature results in more production of H_2 through endothermic reforming reactions which in turn increases the overall endothermicity of the process and thereby increases the energy requirement. In between endothermicity and exothermicity conditions, the overall system attains thermal neutral condition at one temperature where no amount of energy is either consumed or produced. The thermal neutral point lies between temperatures of 676.18-1055.16 K (Figure 5.6) and the energy requirements corresponding to maximum hydrogen yield are 488.53 kJ/mol (f_{O1}=9, f_{O2}=0), 485.13 kJ/mol (f_{O1}=12, f_{O2}=0) at 0.9 B, and 374.69 kJ/mol (f_{O1}=9, f_{O2}=0) and 369.21 kJ/mol (f_{O1}=12, f_{O2}=0) at 0.5 B (Tables 5.2 and 5.3). The addition of B to E causes the reduction in overall endothermicity of the reforming process. Therefore, the energy requirement is reduced as % B in B-E mixture decreases.

In OSRB-E process, the addition of O_2 in feed initiates the exothermic oxidation reaction (R8-R11). Consequently, the overall endothermicity of OSRB-E process gets reduced. Thus, the penalty requirement for OSRB-E process is dropped down. On increasing the temperature at fixed value of f_{O2} more yield of H_2 by endothermic reforming reaction is achieved, which increases the endothermicity. On further increasing the f_{O2} value, the temperature range increases, where OSRB-E process remains in overall in exothermic zone (Figure5.6). Therefore, the thermal neutral points are achieved accordingly at higher temperatures. For instance, under f_{O1}= 9 for 0.8 B the temperatures corresponding to thermal neutral points are 751.73 K (f_{O2} =0.25), 807.40 K(f_{O2}=0.5),and 863.07 K (f_{O2}=0.75). At f_{O2}=1, the process does not proceed in endothermic zone, and remains in either exothermic zone or thermal neutral zone (Figure 5.6). Since, in OSRB-E process, the increase in O_2 in feed drops down the H_2 yield, therefore f_{O2} values above 0.75 are not considered in the present study. The Tables 5.2 and 5.3 clearly indicate the reduction in heat requirement at f_{O2}=0.75 corresponding to maximum yield, which is smaller than as achieved at f_{O2}=0 for all B-E compositions under

f_{O1}=9. For instance, the energy requirements at f_{O2}=0.75 are 114.98 kJ/mol (0.9 B) and 14.15 kJ/mol (0.5 B). Here, again the energy requirement gets reduced as % B in B-E mixture decreases. This can be explained on the same lines discussed before. This energy analysis leads to the inference that the mixture of B-E as found during ABE fermentation seems to be one of the suitable fuel proportion to produce H_2.

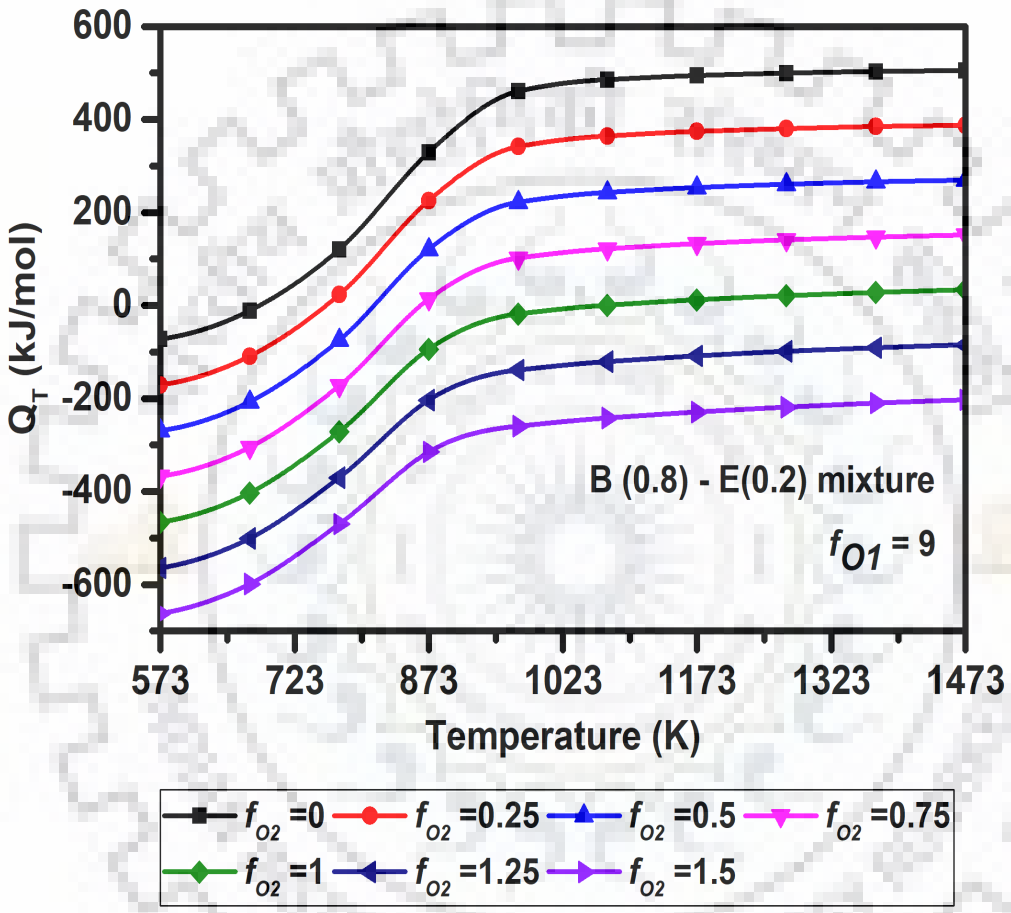

Figure 5.6 Energy requirement as a function of temperature at f_{O1} = 9 for SRB-E process

5.3.7 Thermal efficiency

Thermal efficiency is computed by using Eq. (3.19) as a function of temperature and f_{O2}values under f_{O1}=9 and 12 for SBR-E and OSRB-E processes. Figure 5.7 illustrates the computed results for f_{O1}=9 and 0.8 B in B-E mixture. Further, the thermal efficiency corresponding to the maximum H_2 yield are mentioned in Tables 5.2 and 5.3 for f_{O1}=9 and 12, respectively. For all B-E mixture composition in SRB-E (f_{O2}=0) and OSRB-E (f_{O2}=0.75) processes. It is noteworthy that the efficiency of reforming processes (Eq. (3.19)) is directly proportional to the H_2 production and is adversely affected by the increase in the amount of steam in the feed, *LHV* of fuel, and overall heat of reaction. In SRB-E processes ((f_{O2}=0), H_2 production increases with temperature. At fixed value of f_{O1} (9 or 12) and % B in B- mixture (fixed *LHV* of fuel), the increment in H_2 production results increment in the overall endothermic heat of reaction but in lower proportion, indicating the rise in thermal efficiency (Figure 5.7). The maximum thermal efficiency 70.28% is achieved at 973 K (0.5 B). The addition of O_2 to feed ($f_{O2} > 0$) reduces the H_2 production as well as overall endothermic heat of reaction. At all f_{O2} values, no significant change in thermal efficiency is observed. The maximum thermal efficiency is achieved at 973 K for all f_{O2} values (Figure 5.7). From Tables 5.2 and 5.3, it can be seen that thermal efficiency corresponding to maximum H_2 production for all B-E compositions in fuel does not reveal significant difference. For instance, under f_{O1}=9, the thermal efficiencies are 68.71% (0.9 B) and 70.28% (0.5 B) for SRB-E (f_{O2}=0), whereas for OSRB-E (f_{O2}=0.75), the thermal efficiencies are 68.99% (0.9 B) and 69.02% (0.5 B). In case of variable compositions of B in fuel, the *LHV* of fuel in Eq. (3.19) decreases with decrease in % B in fuel as *LHV* of B is higher than *LHV* of E. On the other hand, H_2 production and thereby overall endothermic heat of reaction also decrease with decrease in % B in the fuel. The aforementioned results imply that the change in thermal efficiency with f_{O2} values and fuel compositions is tradeoff between H_2 production and LHV of fuel + overall heat of reaction. At higher f_{O1} =12 value (Table 5.3), the thermal efficiency is slightly higher than as achieved at f_{O1}= 9 (Table 5.2). This occurs due to much higher H_2 production in comparison to heat requirement to vaporize the water in feed. The thermal efficiency under f_{O1}=12 are 70.07 (0.9 B) and 69.44% (0.5 B) for SRB-E (f_{O2}=0) and 70.18% (0.9 B) and 68.02% (0.5 B) for OSRB-E (f_{O2}=0.75). These results reveal that in all SRB-E and OSRB-E process around 70% of energy fed to the reforming process is recovered in the form of useful products H_2 and remaining 30% is exhausted with other gaseous products. Further, it can be concluded that H_2 production by reforming of B-E mixture obtained from ABE fermentation broth can be efficiently performed.

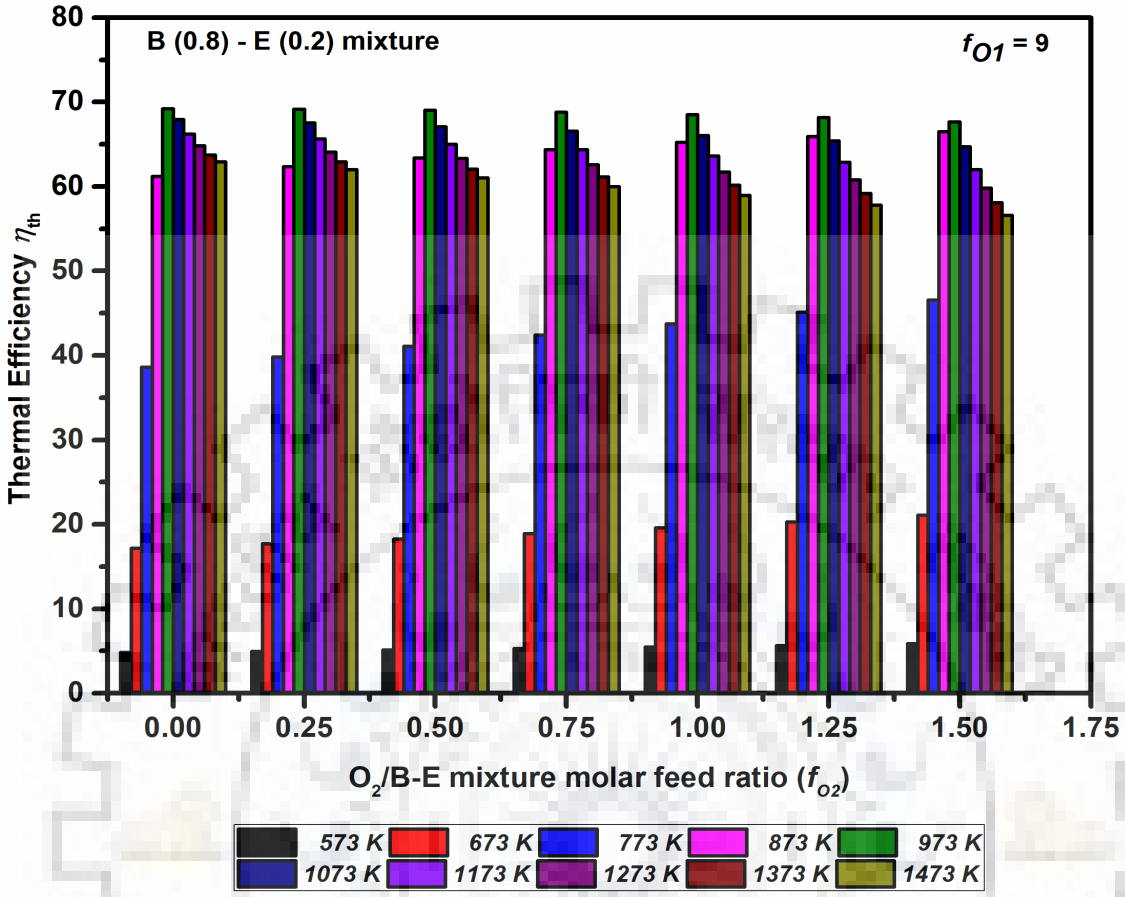

Figure 5.7 Thermal efficiency of SRB-E process with respect to temperature and O_2/ B-E mixture molar feed ratio (f_{O2})

5.3.8 Exergy efficiency

The exergy efficiency is evaluated by applying Eq. (3.31) for SRB-E and OSRB-E processes at different f_{O2} values and temperatures. The exergy efficiency and exergy destruction results are presented in Figures 5.8 and 5.9, respectively for B-E mixture (0.8 B) at f_{O1}=9. Tables 5.2 and 5.3 present the exergy efficiency and exergy destruction data corresponding to maximum H_2 yield under f_{O1}= 9 and 12 respectively for all B-E mixture compositions at f_{O2}= 0 and 0.75. Before discussing the results, it is necessary to provide the conceptual information regarding exergy of the system. It is known that exergy is destroyed due to combination of high irreversibilities occurring during chemical reactions and heat transfer between reactants and products [Kumar et al., 2013]. The chemical reactions are related to the motion of electrons during formation and breaking of bonds between atoms. The high frequency of collisions causes an increase in entropy within the system resulting in high exergy destruction on the basis of this concept; exergy destruction of ethanol is lower than that of butanol. In addition to this, the exothermic and combustion processes loose more energy. Therefore, low endothermicity of reaction system shows high exergy destruction. Figure 5.8 clearly show the exergy efficiency increases with temperature and attains a maximum value and then decreases due to high exergy destruction (Figure 5.9). In case of SRB-E process, exergy efficiency is maximum as f_{O2} value in feed increases and in OSRB-E process, the exergy efficiency decreases due to low endothermicity of the processes. The values according to the Tables 5.2 and 5.3, that the exergy efficiencies are 47.97% (0.9 B) and 49.31% (0.5 B) for SRB-E (f_{O2}=0, f_{O1}=9), whereas for OSRB-E (f_{O2}=0.75, f_{O1}=9), the exergy efficiencies are 43.13% (0.9B) and 42.03% (0.5B). Likewise, for SRB-E (f_{O2}=0, f_{O1}=12), the values of exergy efficiencies are 48.69% (0.9 B) and 47.67% (0.5 B) whereas for OSRB-E (f_{O2}=0.75, f_{O1}=12), the exergy efficiencies are 42.73% (0.9B) and 39.80% (0.5B). It is clear from the Tables 5.2 and 5.3, that the exergy efficiency although is higher in case of SRB-E process but there is no significant change with B-E compositions in feed. Similarly, the exergy efficiency in case of OSRB-E is lower than as achieved in SRB-E process but low significant change is observed with variable composition of B in feed. According to Eq. (3.31), this can be concluded that the exergy efficiency for the system is actually the tradeoff between H_2 production and overall endothermicity of the reacting system. Exergy destruction is higher in case of OSRB-E (f_{O2}=0.75) than that of SRB-E (f_{O2}=0) for f_{O1}=9 and 12 but decreases with decrease in the % B in the feed. For instance, under f_{O1}=9 and f_{O2}= 0, the exergy destruction values are 224.68 kJ/mol (0.9 B) and 186.61 kJ/mol (0.5 B). Likewise, under f_{O1}=9 and f_{O2}=0.75, the exergy destruction values are 241.14 kJ/mol (0.9 B) and 210.99

kJ/mol (0.5 B). Whereas, under f_{O1}=12 and f_{O2}=0, the destruction values of exergy are 210.39 kJ/mol (0.9 B) and 187.62 kJ/mol (0.5 B). Similarly, under f_{O1}=12 and f_{O2}=0.75, the destruction values of exergy are 234.48 kJ/mol (0.9 B) and 216.82 kJ/mol (0.5 B).

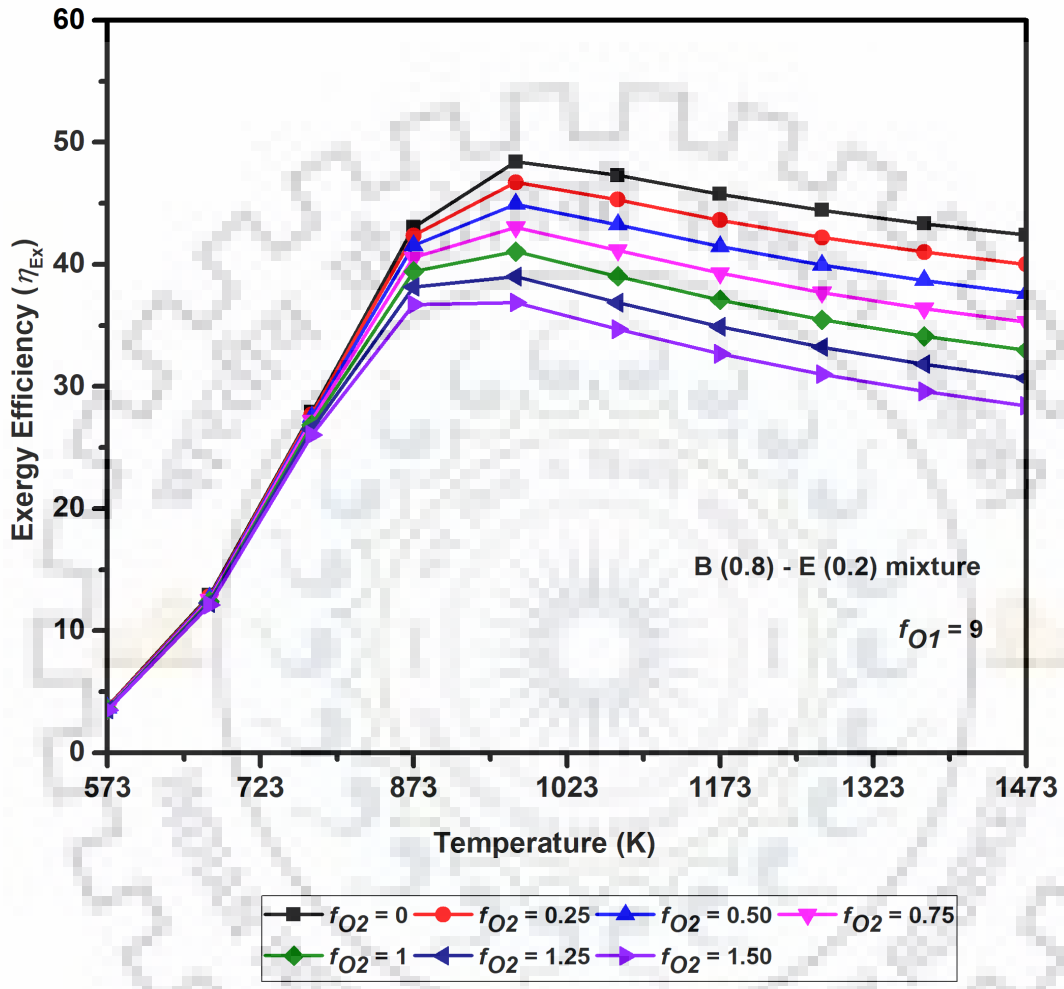

Figure 5.8 Exergy efficiency of SRB-E process with respect to temperature and O_2/ B-E mixture molar feed ratio (f_{O2})

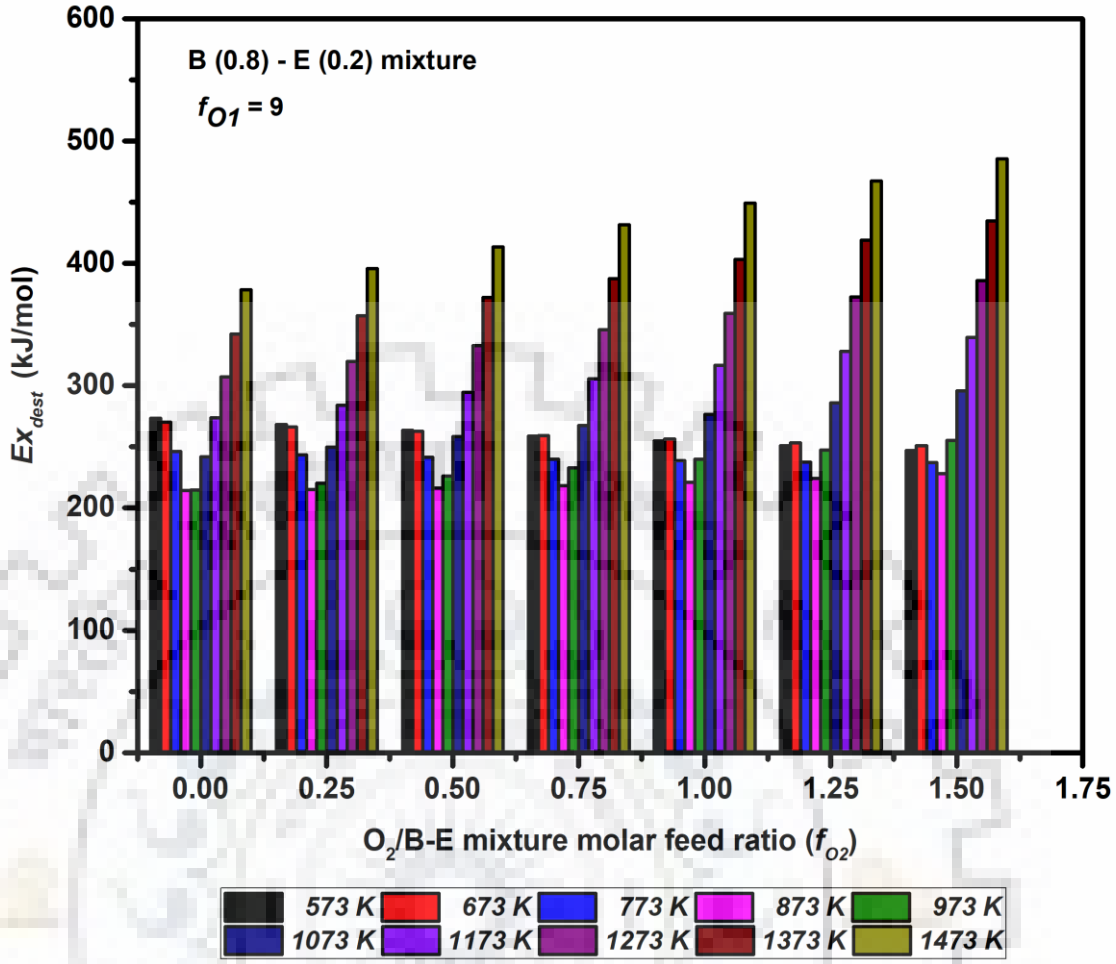

Figure 5.9 Effect of O_2/B-E mixture molar feed ratio (f_{O2}) and temperature on exergy destruction

5.4 CONCLUDING REMARKS

Tables 5.2 and 5.3 compare steam reforming and oxidative steam reforming of butanol-ethanol mixture in terms of maximum hydrogen production at f_{O1} =9 and 12, f_{O2}= 0 and 0.75. It is clear from the tables that the performance of oxidative steam reforming is less than that of steam reforming of butanol-ethanol mixture in which f_{O2}= 0 is simply known as steam reforming while f_{O2}= 0.75 shows oxidative steam reforming results. The production of hydrogen and thermal efficiency of reformer are found less in oxidative steam reforming of B-E mixture (OSRB-E) as compared to steam reforming of butanol-ethanol mixture (SRB-E). Therefore, steam reforming of ABE mixture (SR-ABE) has only been investigated and is discussed in next chapter.

CHAPTER VI

STEAM REFORMING OF ACETONE-BUTANOL-ETHANOL MIXTURE

6.1 INTRODUCTION

In this chapter, acetone-butanol-ethanol mixture (ABE) as obtained from fermentation of a large variety of substrates (glucose, sucrose, xylose, lactose, and starch) and ligno-cellulosic biomass materials is used as biorenewable fuel to produce hydrogen by using steam reforming process. To the best of our knowledge, no experimental or thermodynamic study is available in the literature on steam reforming process of acetone-butanol-ethanol mixture. The effects of process parameters such as temperature, pressure, and molar feed ratio of steam to fuel have been investigated. Thermal efficiency of reformer and exergy efficiency have also been computed to evaluate the performance of steam reforming of ABE mixture.

6.2 METHODOLOGY

The stepwise procedure for performing thermodynamic analysis is as follows:

Step I: Specify the reactants of the reforming process.

For this system, reactants are:

Acetone (C_3H_6O), Butanol ($C_4H_{10}O$), Ethanol (C_2H_6O), and Steam (H_2O).

Step II: Identify the possible products of reforming process on the basis of available experimental studies in the literature.

For this system, products are:

Acetone (C_3H_6O), Butanol ($C_4H_{10}O$), Ethanol (C_2H_6O), Steam (H_2O), Carbon monoxide (CO), Carbon dioxide (CO_2), Hydrogen (H_2), Methane (CH_4), Ethane (C_2H_6), Propane (C_3H_8), Isopropyl alcohol (C_3H_8O), 1-Butene (C_4H_8), Butyraldehyde (C_4H_8O), Acetylene (C_2H_2), Ethylene (C_2H_4), and solid component Carbon (graphite).

As a thumb rule, the products with very small or trace amounts are ignored/neglected and the products with appreciable quantities are considered for further computations.

Step III: Perform trial simulations runs for reforming process at desired operating conditions namely, feed compositions, temperature, and pressure.

Operating conditions for the simulation of this system are:

Temperature (T) =573-1473 K,

Pressure (P) =1-10 atm,

Steam/fuel molar feed ratio (F_{ABE})= 5.5-12.

Step IV: Now, on the basis of results of simulation, retain the compounds with significant quantities and ignored those with negligible or trace amounts.

For this system, finally chosen compounds in products are:

Hydrogen (H_2), Carbon monoxide (CO), Carbon dioxide (CO_2), Methane (CH_4), and Carbon.

Step V: Perform simulations by using R-Gibbs reactor tool of Aspen Plus for the reforming system. These simulations will provide the equilibrium compositions of input (reactants) and output (products).

In this step, simulation runs are made for those operating conditions of feed compositions, temperature and pressure for which either some experimental or theoretical /computational results of reforming system are available in literature. This would enable us to validate our computational procedure.

Since no results are available on steam reforming of ABE mixture or B-E mixture. Therefore, the validation has been done with the steam reforming of individual components namely, acetone, butanol, and ethanol, for which some results are available in the literature. The validation results have already been given in Table 4.1.

Step VI: After validation of procedure, perform simulation by using R-Gibbs reactor tool at desired operating conditions namely, feed compositions, temperature, and pressure.

Results of simulations at desired operating conditions have been obtained and discussed in the following sections.

Step VII: Organize the simulation results in the required format and print them.

6.3 STEAM REFORMING OF ACETONE-BUTANOL-ETHANOL MIXTURE

The mixture of acetone-butanol-ethanol-water contains 5.24 mol of acetone, 8.21 mol of butanol, 2.20 mol of ethanol, and 84.35 mol of water, respectively. In this biorenewable fuel; acetone, butanol, and ethanol are present approximately in terms of molar ratio of 33:52:15. Moreover, quantity of water is about 5.5 times of this biorenewable fuel on molar basis. Therefore, this existing water can also be used in steam reforming to reduce excess water requirement. Although, it seems that the steam to fuel (ABE) molar feed ratio (F_{ABE}) should be greater than 5.5 in the reforming system, but for showing its effect on the performance, a wide range of 5.5-12 has been considered here. The molar quantity of feeding fuel (acetone (0.33) + butanol (0.52) + ethanol (0.15)) is kept constant at 1 mol and molar amount of steam is computed accordingly. The complete conversion (100%) of acetone, butanol, and ethanol has been achieved at all specified ranges of temperatures, pressures, and steam/fuel molar feed ratio.

6.3.1 Effect of pressure

The simulations have been carried out to analyze the effect of change in pressure on the production of hydrogen in steam reforming process of ABE mixture at fixed temperature of 973 K. Steam to fuel (F_{ABE}) varies from 5.5 to 12 and the pressure ranges between 1 and 10 atm. Figure 6.1 (a) clearly shows that H_2 production decreases with the increase in pressure above 1 atm. The negative effect on the production of hydrogen due to increasing pressure can be justified on the basis of reforming gaseous reactions (R1, R3, and R5) given in Table 6.1. The reforming reactions are endothermic in nature which affects the production of hydrogen in the system with the progress of reactions. Le Chatelier's principle also supports the behavior of reactions in the backward direction due to high pressure. It means that the high pressure shows the detrimental effects on the formation of hydrogen at thermodynamic equilibrium. Therefore, atmospheric pressure (1 atm) has been selected for all further thermodynamic computations at equilibrium.

The detailed discussion regarding the effects of remaining two variables (temperature and molar feed ratios) for maximization of desired product H_2, minimization of CO, formation of CO_2, solid carbon formation, and suppression of CH_4 production are presented in the following sections. The possible reaction network for steam reforming of Acetone-Butanol-Ethanol (SR-ABE) is provided in Table 6.1.

6.3.2 Carbon formation

Further, Figure 6.1 (b) depicts the carbon formation and carbon free zones at all temperature and steam/fuel molar feed ratio conditions. It can also be concluded from the figure that no carbon formation occurs for $F_{ABE} > 6$ at all temperature conditions which are in good agreement with above discussed results. This concept of carbon formation and carbon free zones (Figure 6.1 (b)) can be estimated by using following carbon activity expressions as given in Eqns. (6.1)-(6.4) [Chen et al., 2009] by using R10-R13 reactions (Table 6.1).

$$a_{C10} = K_{10} \frac{P y_{CO_2} y_{H_2}^2}{y_{H_2O}^2} \tag{6.1}$$

$$a_{C_{11}} = K_{11} \frac{P y_{CO} y_{H_2}}{y_{H_2O}} \tag{6.2}$$

$$a_{C_{12}} = K_{12} \frac{P y_{CO}^2}{y_{CO_2}} \tag{6.3}$$

$$a_{C_{13}} = K_{13} \frac{y_{CH_4}}{P y_{H_2}^2} \tag{6.4}$$

Where, K_{10}, K_{11}, K_{12}, and K_{13} are the equilibrium constants for reactions (R10) to (R13) respectively. Likewise, y_{CO} , y_{CO_2} , y_{CH_4} , and y_{H_2O} are the mole fractions of CO, CO_2, CH_4, and H_2O, respectively. For SR-ABE, the formation of carbon is possible when the maximum value of carbon activity a_C among four is greater than unity.

$$a_C = \max (a_{C_{11}} , a_{C_{12}} , a_{C_{13}} , a_{C_{14}}) > 1 \tag{6.5}$$

If, $a_C < 1$, then the region is carbon-free; and $a_C = 1$, which depicts the boundary of carbon formation [Chen et al., 2009]. The forthcoming sections are focused on the operating conditions which maximize the H_2 production and inhibition of solid carbon formation in SR-ABE process.

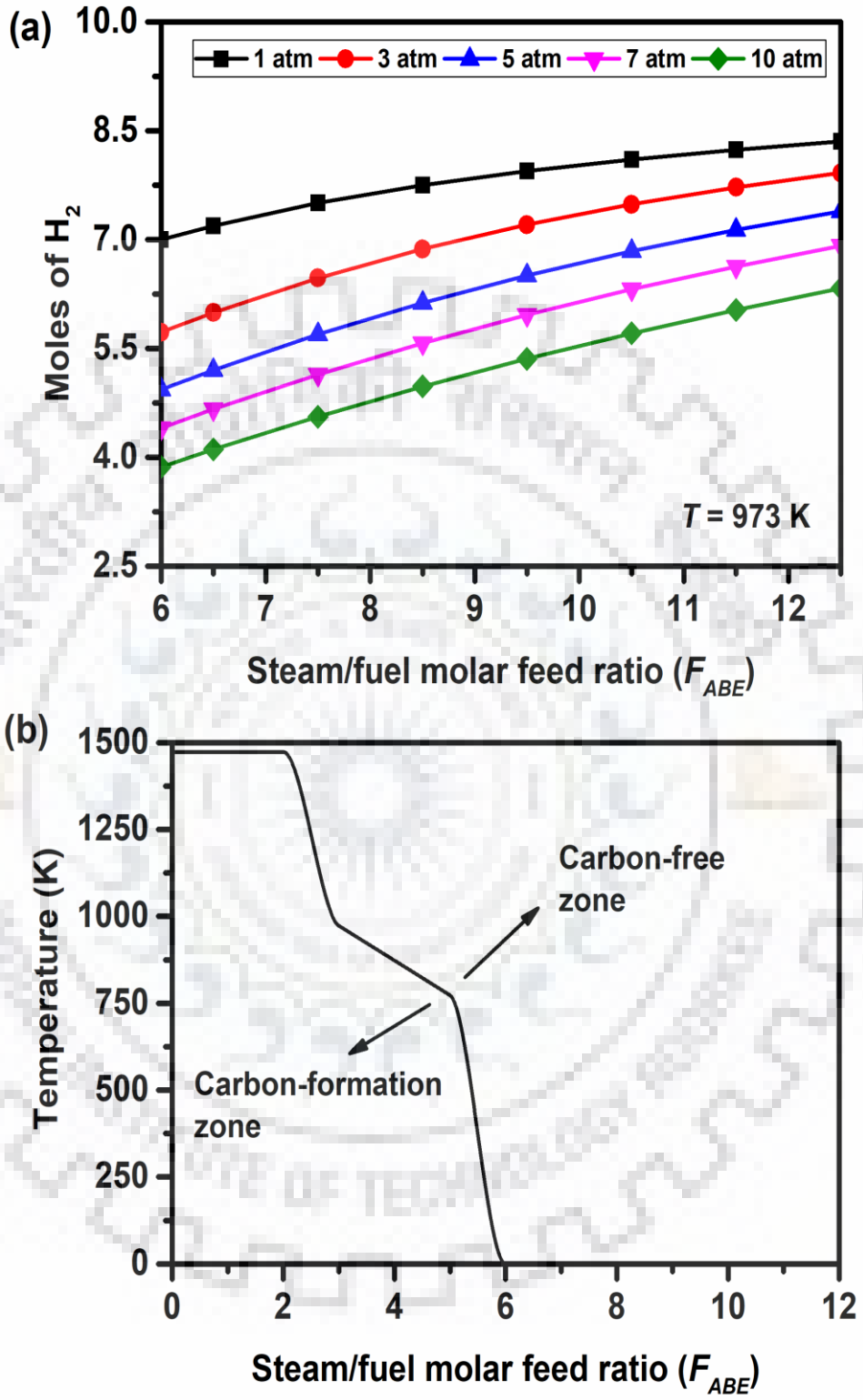

Figure 6.1 (a) Molar production of H_2 as a function of steam/fuel molar feed ratio (F_{ABE}) at different pressures; (b) Carbon formation and carbon-free zones at various temperatures and molar feed ratios of steam/fuel (F_{ABE}), 1 atm

Table 6.1 Chemical reactions network for SR-ABE process

Reaction No.	**Reactions**	**Reaction types**	**ΔH_R (kJ/mol) at 298 K, 1atm**
R1	$C_3H_6O + 2H_2O \leftrightarrow 3CO + 5H_2$	Steam reforming of acetone	127.87
R2	$C_3H_6O+ \leftrightarrow CO + CH_4 + H_2 + C$	Decomposition of acetone	32.22
R3	$C_4H_{10}O + 3H_2O \leftrightarrow 4CO + 8H_2$	Steam reforming of Butanol	557.67
R4	$C_4H_{10}O \leftrightarrow CO + 2CH_4 + H_2 + C$	Decomposition of Butanol	14.19
R5	$C_2H_6O + H_2O \leftrightarrow 2CO + 4H_2$	Steam reforming of Ethanol	255.53
R6	$C_2H_6O \leftrightarrow CO + CH_4 + H_2$	Decomposition of Ethanol	49.42
R7	$CO + H_2O \leftrightarrow CO_2 + H_2$	Water-Gas Shift Reaction	-41.17
R8	$CO_2 + 4H_2 \leftrightarrow CH_4 + 2H_2O$	Methanation Reactions (R8 and R9)	-164.94
R9	$CO + 3H_2 \leftrightarrow CH_4 + H_2O$		-206.11
R10	$CO_2 + 2H_2 \leftrightarrow C + 2H_2O$	Carbon dioxide Reduction Reaction	-90.09
R11	$CO + H_2 \leftrightarrow C + H_2O$	Carbon monoxide Reduction Reaction	-131.26
R12	$2CO \leftrightarrow CO_2 + C$	Boudouard Reaction	-172.43
R13	$CH_4 \leftrightarrow 2H_2 + C$	Methane Decomposition	74.85

6.3.3 Hydrogen production

The most desired product of reforming processes is hydrogen. Figure 6.2 depicts the variational trends for the molar production of hydrogen with respect to temperature (T) and steam/fuel molar feed ratio (F_{ABE}) at equilibrium. Table 6.1 describes the fact that R1-R6 and R7 (endothermic reactions), and R13 (exothermic reactions) are responsible for the generation of hydrogen while R8-R11 (exothermic reactions) consume hydrogen. It is important to obtain operating conditions which maximize H_2 formation, decrease CH_4 generation and eliminate the carbon formation.

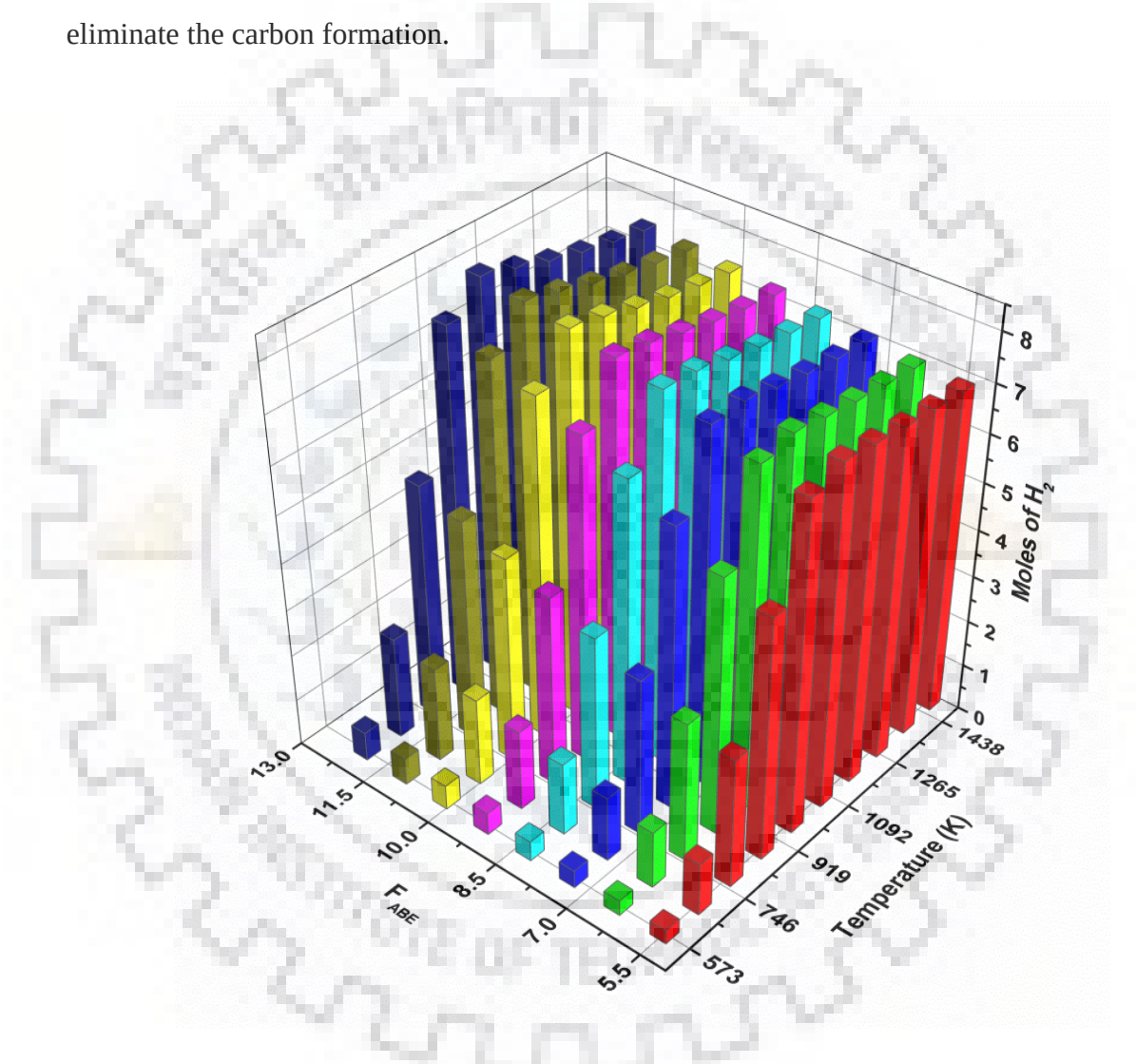

Figure 6.2 Molar production of hydrogen with variation in temperature and molar feed ratio of steam/fuel (F_{ABE})

Table 6.2 Operating conditions and corresponding results with respect to maximum hydrogen production for SRA, SRB, SRE, SRB-E, and SR-ABE processes and comparison with other oxygenated compounds reported in the literature

	Present Study						Katiyar et al., 2013	Silva and Müller, 2011
Operating parameters	**SRA**	**SRB**	**SRE**	**SRB-E (90%B-10%E)**	**SRB-E (50%B-50%E)**	**SR-ABE**	**SRM**	**SRG**
Fuel	Acetone	Butanol	Ethanol	Butanol+Ethanol mixture	Butanol+Ethanol mixture	Acetone+Butanol +Ethanol mixture	Methanol	Glycerol
Basis	1 mol	1 mol	1 mol	0.9+0.1= 1 mol	0.5+0.5= 1 mol	0.33+0.52+0.15=1 mol	1 mol	1 mol
Temperature	973 K	973 K	873 K	973 K	973 K	973 K	500 K	848 K
Pressure	1 atm	1 atm	1 atm	1 atm	1 atm	1 atm	1 atm	1 atm
Steam/fuel molar feed ratio	12	12	12	12	12	12	1	9
Conversion	100%	100%	100%	100%	100%	100%	100%	100%
H_2 (mol)	6.93	9.96	5.49	9.56	7.84	8.35	0.03	0.65*
CO (mol)	1.03	1.85	0.35	1.69	1.10	1.34	3.15×10^{-5}	0.06*
CO_2 (mol)	1.96	2.10	1.61	2.07	1.88	2.01	0.25	0.26*
CH_4 (mol)	0.01	0.05	0.04	0.04	0.01	0.02	0.74	0.03*
Carbon (mol)	Nil	Nil	Nil	Nil	Nil	Nil	0.02	Nil
Total energy requirement (kJ)	326.68	513.99	210.54	485.13	369.21	408.84	NR	NR
Energy requirement (kJ) per mol H_2	34.12	51.60	38.34	50.77	47.12	48.96	NR	NR
η_{th} (%)	66.17	69.89	68.49	70.07	70.18	69.13	NR	64.50*
η_{Ex} (%)	58.75	48.73	46.15	48.69	47.67	55.09	NR	NR
Ex_{Dest} (kJ/mol)	65.60	216.91	136.15	210.39	187.62	85.36	NR	NR
S_{gen} (kJ/mol.K)	0.22	0.73	0.46	0.71	0.63	0.29	NR	NR

NR: Not reported * Dry Basis (mole fraction)

As seen from the Figure 6.2, it is clear that the production of hydrogen initially increases with the increase in temperature from 573 K and reaches maximum at 1073 K for F_{ABE} = 5.5-7 (7.23-7.55mol of H_2) and 973 K for F_{ABE} = 8-12 (7.75-8.35 mol of H_2), and thereafter slightly decreases which is insignificant, at constant pressure (1 atm). Steam reforming of ABE is more feasible process for the production of hydrogen with progress in temperature upto a certain range from 573-1073 K for F_{ABE} =5.5-7, and for 573-973 K, by increasing the amount of steam in the feed, i.e. F_{ABE} =8-12. Low temperature favours the exothermic methanation reactions (R8 and R9) which results in less generation of hydrogen. Moles of hydrogen decrease together with that of carbon dioxide at T > 873-1073K with different steam/fuel molar feed ratios; but at the same conditions, the moles of H_2O and carbon monoxide increase. This fact can be explained due to the occurrence of water gas shift reaction (R7) in backward direction (R-WGS). On the other side at the similar conditions methanation reactions (R8 and R9) forms less methane which can be a favourable condition for the steam reformer. Moreover, the highest amount of hydrogen can be obtained due to the presence of excess water in the system at all temperature conditions. The maximum hydrogen production (8.35 mol) is achieved at T=973 K and F_{ABE}=12 in the present study (Table 6.2).

6.3.4 Methane production

Methane is considered as an inevitable but highly undesirable by-product of SR-ABE process because it adversely affects the production of hydrogen. Presence of methane in the reforming process prevents the hydrogen formation. Figure 6.3 shows the influence of change in temperature and steam/fuel molar feed ratio on the production of methane at equilibrium during steam reforming of ABE mixture. The methane production is mainly dependent on the existence of the methanation reactions (R8 and R9) in the reforming system. Moreover, in the absence of steam, decomposition reactions of acetone, butanol and ethanol (R2, R4, and R6) occur which can also lead to the methane formation. It is clear from the Figure 6.3 that the number of moles of methane decreases when the temperature and molar feed ratio of steam/fuel increase.

At higher temperatures (T > 1173 K), the production of methane is almost negligible at all above specified F_{ABE} values. Higher temperature favours the steam reforming of methane (backward reactions of R8 and R9) which can raise the hydrogen amount accompanied with more CO and CO_2. In addition to this, WGS reaction (R7) has less potential to produce substantial quantity of H_2 in comparison to its consumption by methanation reactions. For the higher production of hydrogen and reduction in methane amount in the reforming process,

stable and efficient catalysts working at high temperature are required. The maximum amount of methane (2.36 mol) is obtained at temperature of 573 K and F_{ABE} =5.5 at equilibrium.

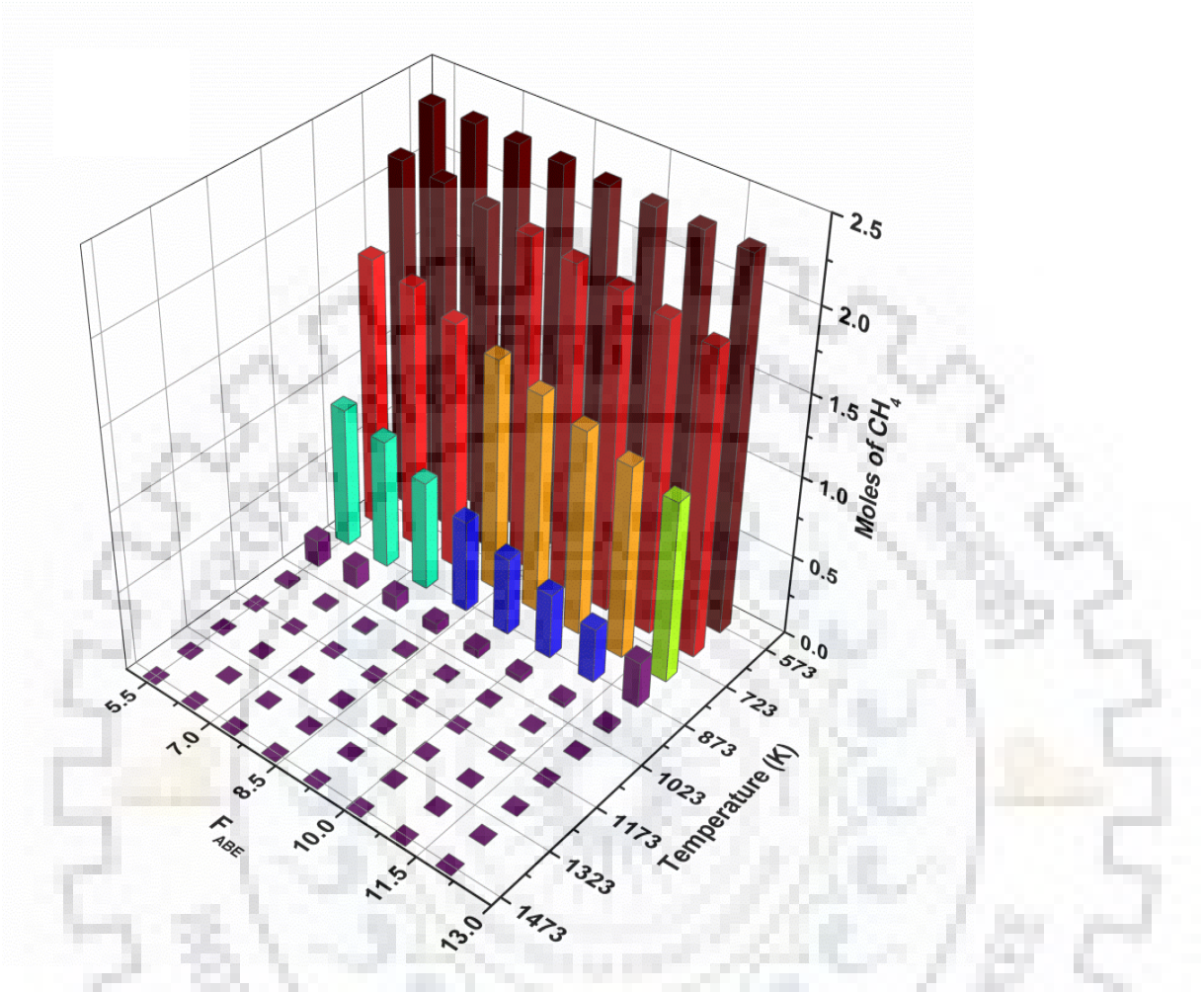

Figure 6.3 Molar production of methane with variation in temperature and molar feed ratio of steam/fuel (F_{ABE})

6.3.5 Carbon monoxide and carbon dioxide production

Figures 6.4 (a) and (b) illustrate the molar production of CO and CO_2 at equilibrium conditions as a function of temperature under specified range of steam/fuel molar feed ratio in SR-ABE process. Table 6.1 suggests that reactions R1-R6 are responsible for the formation of carbon monoxide whereas reactions R7, R9, R11, and R12 consume CO. Table 6.1 also clarifies that the reforming reactions R1, R3 and R5 provide higher molar production of CO than other decomposition reactions R2, R4, and R6. The production of CO increases with the increase in temperature but decreases with the rise in molar ratio of steam to fuel whereas the condition is somewhat different for the formation of CO_2 gas.

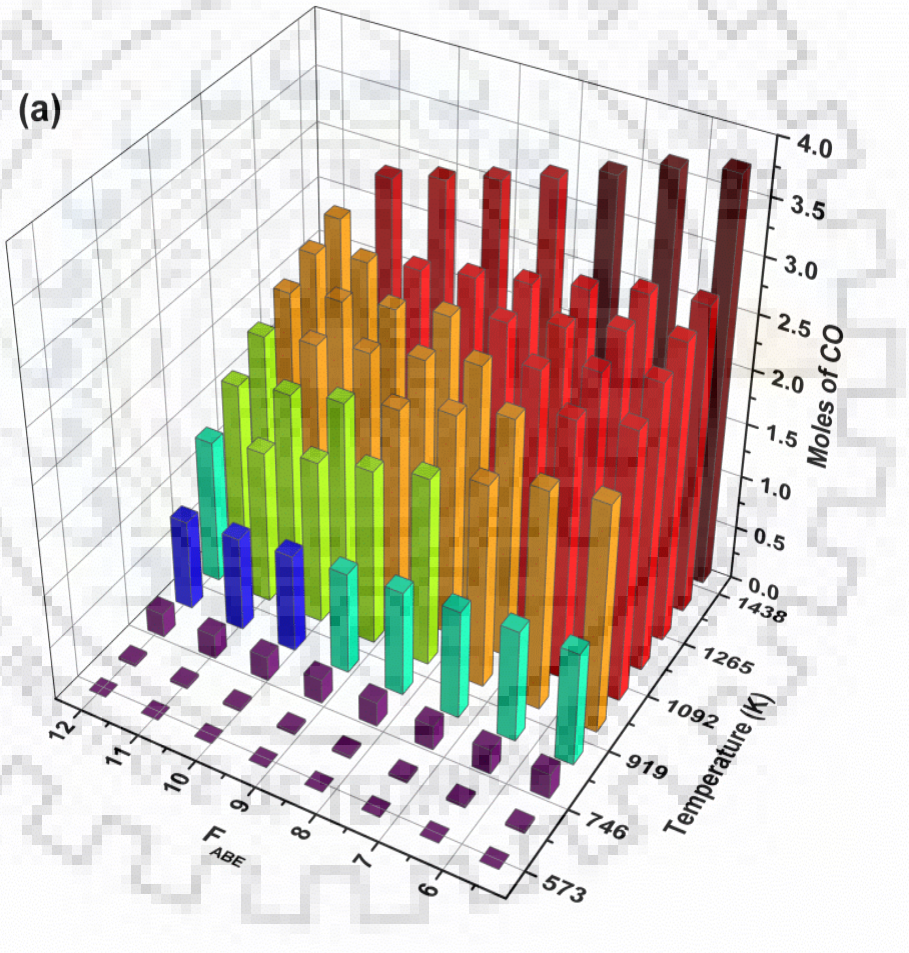

Figure 6.4 (a) Molar Production of carbon monoxide with variation in temperature and molar feed ratio of steam/fuel (F_{ABE})

For the production of carbon dioxide, the exothermic water gas shift (R7) and Boudouard reactions (R12) are mainly accountable. The number of moles of carbon dioxide increases with the increase in temperature, goes through maximum and then decreases continuously at higher temperatures. These decreasing trends can be explained on the basis of exothermic methanation reaction (R8) and carbon monoxide reduction reaction (R10) in which carbon dioxide is consumed. On the other side, the molar production of carbon dioxide increases with the increase in molar feed ratio of steam to fuel. Carbon monoxide and carbon dioxide, generally known as oxygenated compounds, are considered impurities in reforming system because these gases do not compete against hydrogen. The maximum production of CO (3.37 mol) can be achieved at 1473 K and F_{ABE} value of 5.5 while the highest production of CO_2 (2.24 mol) can be obtained at F_{ABE} of 12 and 873 K.

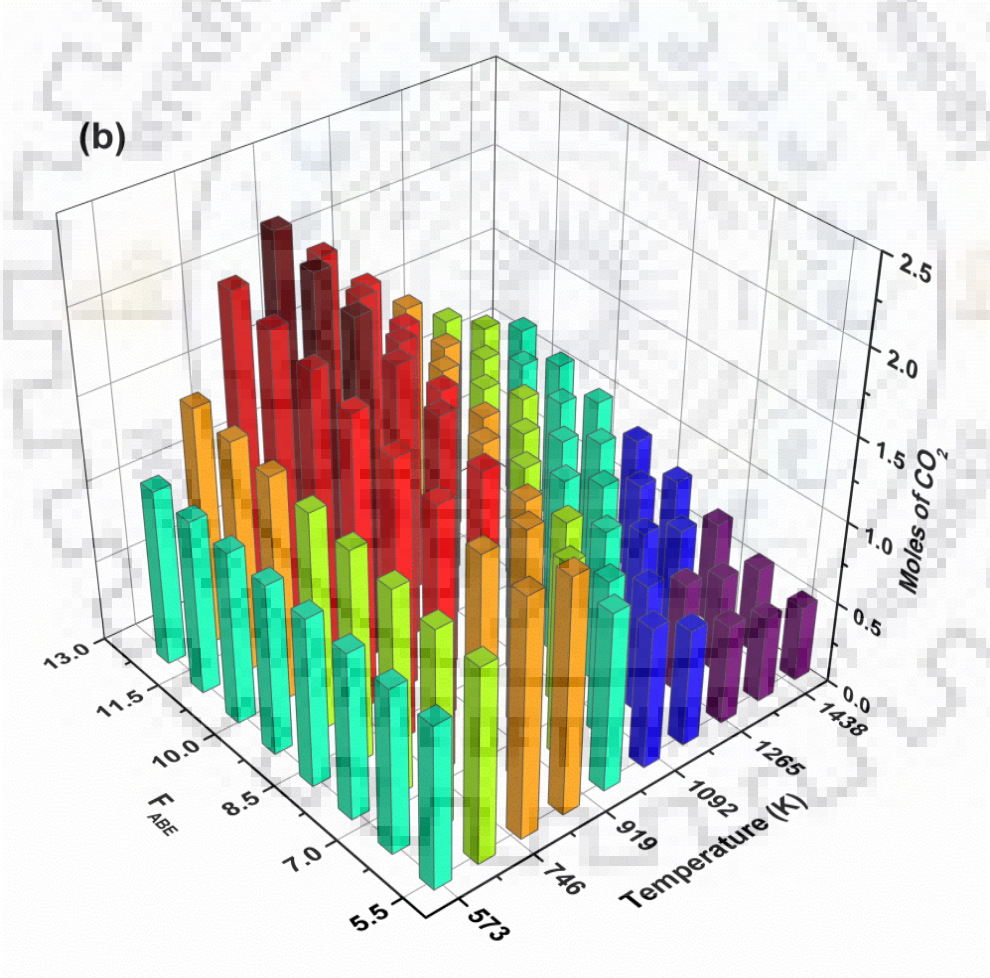

Figure 6.4 (b) Molar Production of carbon dioxide with variation in temperature and molar feed ratio of steam/fuel (F_{ABE})

6.3.6 Energy analysis and thermal efficiency of reformer

An energy analysis is essential requirement to evaluate the performance of reforming process as the energy cost directly affects the product cost. The energy requirement for SR-ABE process with change in temperature and feed ratios is calculated by using Eq. (3.20). Table 6.2 includes total energy required per mol of feeding fuel to produce maximum quantity of hydrogen at F_{ABE} =12 and temperature of 973 K. Figure 6.5 (a) shows the variational trends for the energy requirement at different temperatures with addition of steam to fuel being fed. Low temperature favours progress of exothermic reactions (R7-R12) which implies that the overall reforming process is exothermic. On the other side, high temperature deals with the endothermic nature of reactions (R1-R6, R13) which shift the exothermic forward reactions towards endothermic backward reactions. Therefore, the overall reforming system behaves as endothermic in nature. In between exothermic and endothermic conditions, the overall reforming process achieves thermal neutral point at which no quantity of energy is produced and destroyed. This temperature varies with different molar feed ratios of steam to fuel. The thermal neutral points with respect to specified feed ratios are 660 K (F_{ABE} =5.5), 668K (F_{ABE} =6), 673 K (F_{ABE} =7), 681 K (F_{ABE} =8), 692 K (F_{ABE} =9), 700 K (F_{ABE} =10), 714 K (F_{ABE} =11), and 724 K (F_{ABE} =12). These results show that the reforming process should be operated in the temperature range of 660-724 K. However, in this range H_2 production is not significant. Therefore, higher temperatures are normally chosen, and the overall process becomes endothermic.

Thermal efficiency is a measure of the performance evaluation of the system in terms of energy utilization. The thermal efficiency indicates how efficiently the fuel processor converts the input energy of the fuel into useful work. Figure 6.5 (b) shows the change in thermal efficiency of SR-ABE process as a function of temperature and feed ratio of steam to fuel. At any steam/fuel molar feed ratio (F_{ABE}), thermal efficiency increases with temperature, attains a maximum, and then decreases continuously. It is clear from the Figure 6.5 (b) that the addition of steam favours the thermal efficiency in steam reforming of acetone-butanol-ethanol mixture. It is noteworthy that the thermal efficiency is directly proportional to the hydrogen quantity and so it increases with the increase in hydrogen quantity. While thermal efficiency decreases with the increase in the amount of steam in the feed, *LHV* of feed, or the total change in enthalpies (energy used for the process). The increase or decrease in thermal efficiency of reforming process with temperature or feed ratio is trade-off between hydrogen production and amount of steam required to convert water into steam to complete the process.

Table 6.2 provides the thermal efficiency (69.13%) with respect to maximum hydrogen production at T=973 K and F_{ABE} =12; incidentally thermal efficiency is also maximum at these operating conditions in steam reforming of ABE mixture.

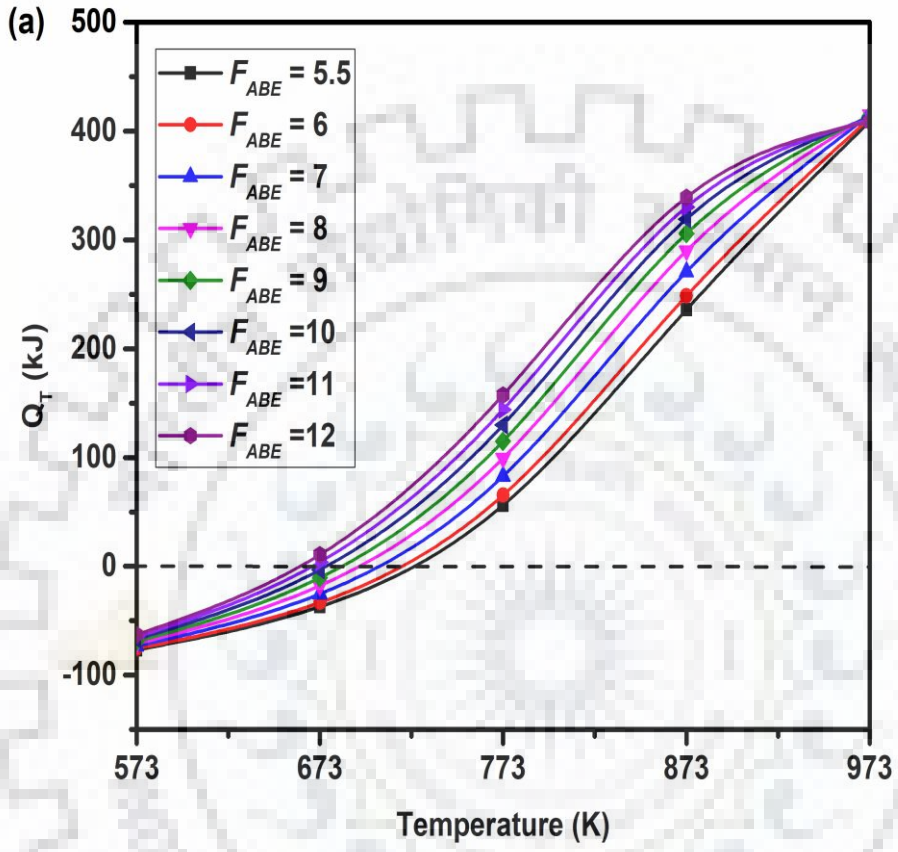

Figure 6.5(a) Energy requirement with variation in temperature at different molar feed ratio of steam/fuel (F_{ABE})

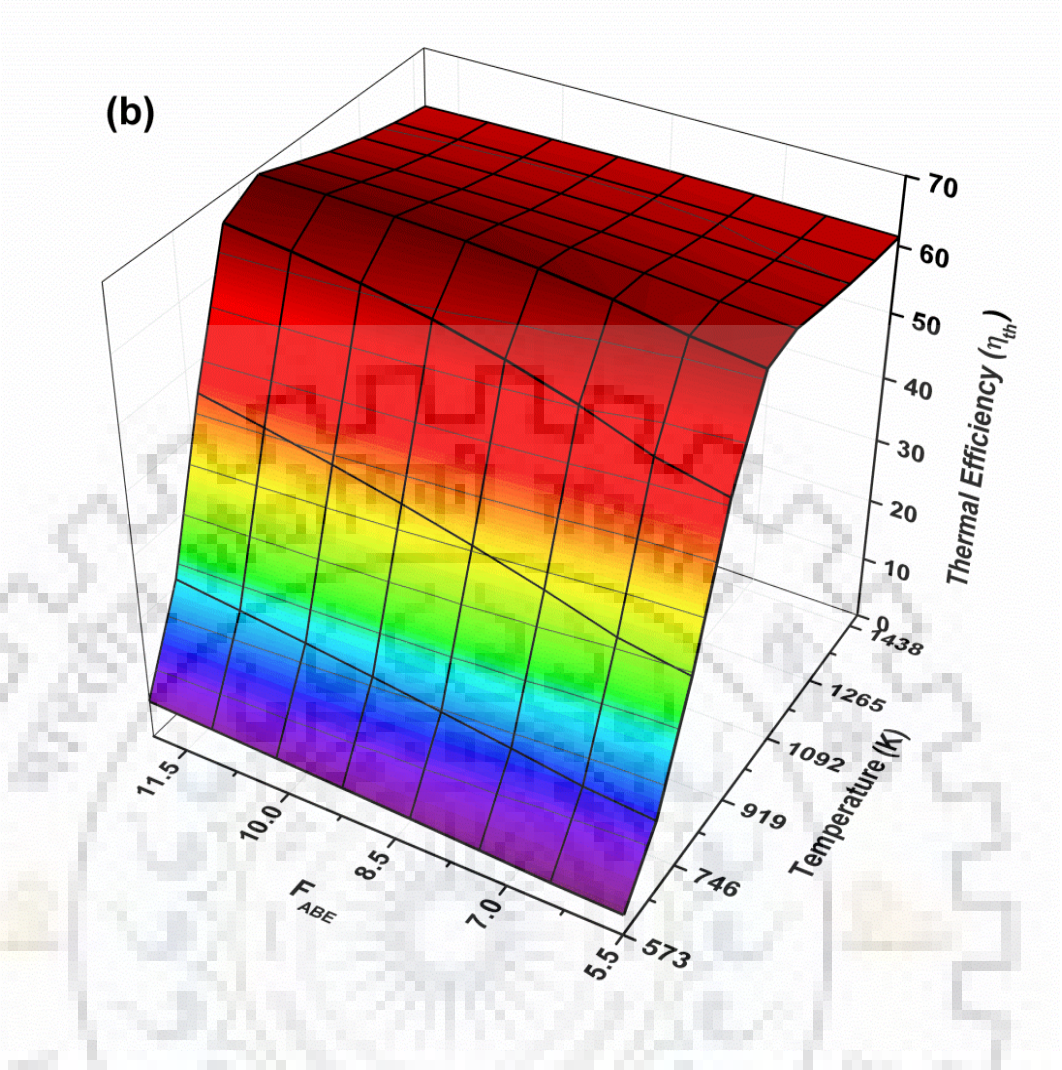

Figure 6.5(b) Thermal efficiency with variation in temperature at different molar feed ratio of steam/fuel (F_{ABE})

6.3.7 Exergy analysis

Figure 6.6 (a) shows the variational trends of exergy efficiency with change in process variables such as temperature and molar feed ratio of steam to fuel for SR-ABE process. Exergy efficiency first increases with increase in temperature upto certain limit and then decreases. It is clear from the Figure 6.6 (a) that the exergy efficiency is favoured by the increase in molar feed ratio. The addition of steam to feeding fuel enhances the exergy efficiency of reformer. In case of exergy destruction, the condition is reverse. At any F_{ABE}, the exergy destruction first decreases with temperature, attains a minimum value, and then starts increasing (Figure 6.6 (b)). Table 6.2 shows that the value of exergy efficiency is less than the thermal efficiency in the reforming process. This difference occurs due to the exergy being exhausted in outgoing off-gases and also the exergy, being destroyed in the system. The exergy destruction is not taken into account by the first law of thermodynamics to calculate thermal efficiency. The exergy destruction is due to the combination of high irreversibities of the chemical reactions and large differences in temperature between the reactants and the products of the reformer [Tippawan and Arpornwichanop, 2014]. When temperature of reactants and products are taken into account in the analysis, then chemical reactions affect the overall process irreversibility. The valid reason is that the chemical reactions are related to the motion of electrons during forming and breaking of chemical bonds between atoms [Tippawan and Arpornwichanop, 2014]. Also, the high frequency of collisions causes an increase in entropy within the system resulting in high exergy destruction. Thus, in order to minimize the exergy destruction, the suitable reforming temperature and molar feed ratios should be selected accordingly. However, the exergy efficiency is a trade-off between H_2 production and overall endothermicity of the reforming process. The highest exergy efficiency (55.09%) is found at 973 K and F_{ABE}=12 for SR-ABE process. Under these operating conditions, the exergy destruction and generated entropy are 85.36 kJ/mol and 0.29 kJ/mol.K, respectively.

The simulations were carried out for each fuel (acetone, butanol, and ethanol) separately and with mixture compositions (butanol-ethanol mixture and acetone-butanol-ethanol mixture). Table 6.2 summarizes the data with essential information for the comparison of SRA, SRB, SRE, SRB-E, and SR-ABE processes. The optimum operating conditions were investigated for each aforementioned reforming process with respect to maximum hydrogen production in which SR-ABE performed well. It is clear from the Table 6.2 that the complete conversion of each fuel, negligible carbon formation, very less amount of methane were

achieved for each reforming process at prescribed operating conditions which are necessary requirements to evaluate the feasibility of any type of reforming.

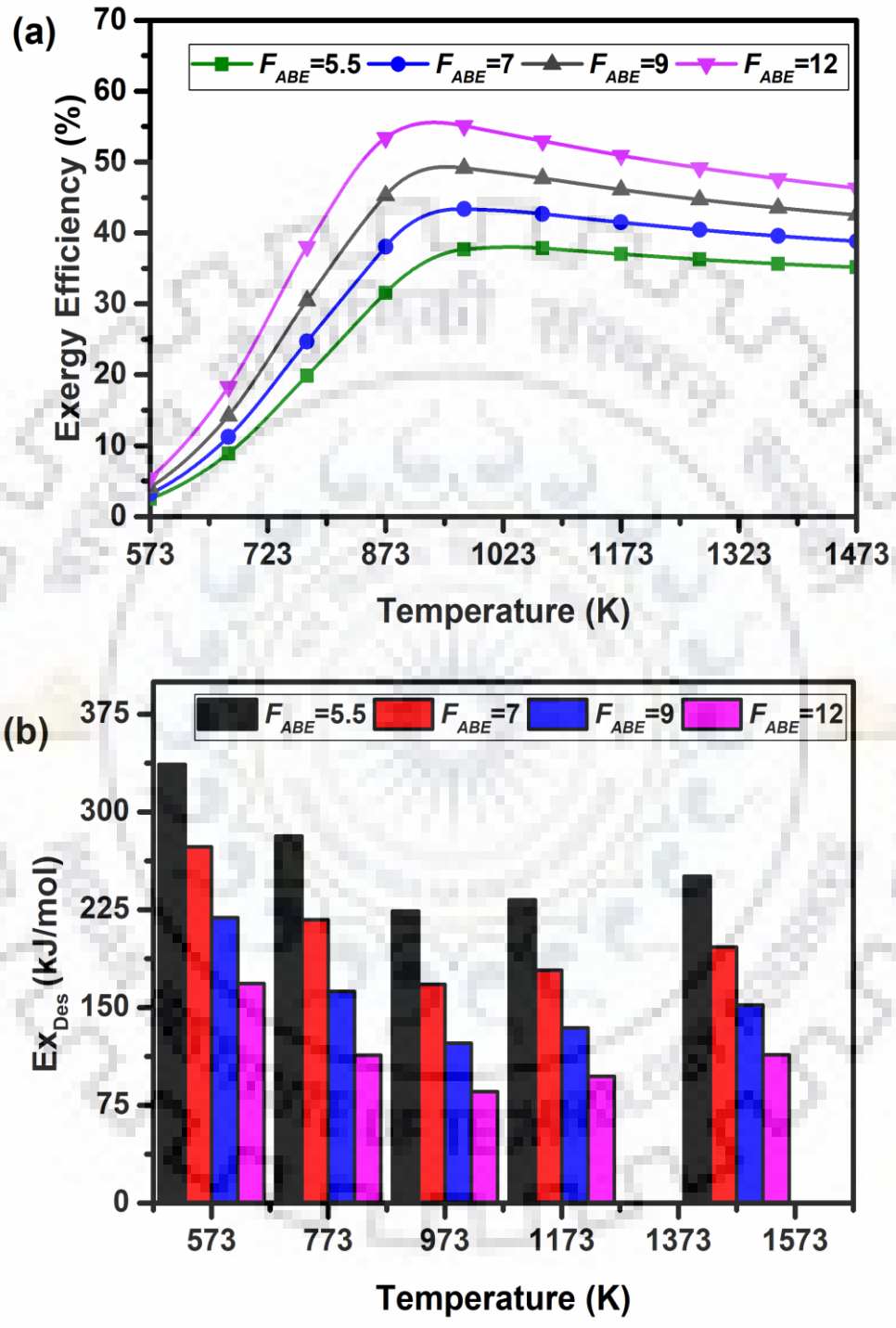

Figure 6.6 (a) Exergy efficiency and (b) exergy destruction with variation in temperature at different molar feed ratio of steam/fuel (F_{ABE})

6.4 CONCLUDING REMARKS

The thermodynamic evaluation for H_2 production via steam reforming of ABE mixture has been investigated. Operating conditions for higher production of H_2 by this process are high temperature = 973 K, low pressure = 1 atm and high steam/fuel molar feed ratio=12. Under these conditions, carbon formation is thermodynamically inhibited and the methane formation is minimized. Further, the evaluation of various fuels such as acetone, butanol, ethanol, methanol, and glycerol, butanol-ethanol mixture, acetone-butanol-ethanol mixture suggests that SR-ABE process is efficient, economical and environment friendly, and utilizes water rich ABE mixture as a renewable fuel for H_2 production without any requirement of separation units.

CHAPTER VII

CONCLUSIONS AND RECOMMENDATIONS

7.1 CONCLUSIONS

The conclusions of present research work on reforming of acetone, butanol, ethanol, butanol-ethanol mixture, and acetone-butanol-ethanol mixture are summarized below. It is mentioned that optimum pressure for all studies is 1 atm.

7.1.1 Steam reforming of acetone, butanol, and ethanol

The thermodynamic equilibrium analysis for fuel reforming processes namely steam reforming of acetone (SRA), steam reforming of butanol (SRB), and steam reforming of ethanol (SRE) have been investigated for individual fuels to validate our solution procedure. For this purpose, the simulations have been carried out at operating conditions on few studies of steam reforming of acetone, butanol, and ethanol available in the literature. The comparison of our results with thoseof previous studies in terms of percent conversion is summarized in Table 4.1. It is clear that the simulation results are in good agreement with previous experimental as well as thermodynamic studies.

Table 4.7 summarizes necessary results regarding steam reforming of acetone, butanol, and ethanol individually. It is clear from the table that

(i) Butanol provides higher hydrogen production namely, 1.44 times more than acetone, and 1.81 times more than ethanol.

(ii) The performance of butanol as renewable fuel is higher than that of acetone and ethanol fuels in terms of thermal efficiency.

(iii) The activity of fuels are found on the basis of highest hydrogen production asbutanol > ethanol> acetone.

(iv) For each reforming process (SRA, SRB, and SRE), high temperature and high steam/fuel molar feed ratio promote the H_2 production and suppress methane production.

(v) Moreover, steam reforming of acetone (SRA) is not a viable option.

7.1.2 Steam reforming of butanol-ethanol mixture

The simulation resultsof the thermodynamic equilibrium analysisfor steam reforming of butanol-ethanol mixture (composition varies from 50 to 90% butanol in the mixture of butanol-ethanol) are presented and compared with steam reforming of butanol and ethanol.

(i) High temperature and high steam/fuel molar feed ratio promote the H_2 production. The maximum amounts of H_2 were 9.96 moles (f_1=12, T=973 K) in SRB, 5.49 moles (f_2=12, T=873 K) in SRE, and 9.56 moles (f_3=12, T=973 K) in SRB-E (90% B) process.

(ii) At a lower temperature of 573 K, CH_4 production was very high at all f_1, f_2, and f_3 values for all three reforming systems and increased with the feed ratio at this temperature. CH_4 production was reduced to negligible amount at temperature above approximately 873 K in SRB, SRE, and SRB-E processes.

(iii) The carbon formation was disfavoured by high temperature and high steam/fuel molar feed ratio. In comparison to temperature, the influence of steam/fuel molar feed ratio on carbon formation was more pronounced. The complete elimination of carbon was observed at f_1>6 (SRB), f_2>2 (SRE) and f_3> 5 (SRB-E).

In view of (i), (ii), and (iii), therefore, high temperature greater than 873 K, and high steam/fuel molar feed ratio of 12 are recommended operating conditions for negligible production of highly undesired products methane and carbon and thereby maximum production of desired product H_2.

(iv) High temperature favours the production of CO and suppresses the production of CO_2. Very low amount of CO was observed in low temperature range (573-800 K). The amounts of CO were 1.85 moles (f_1=12) in SRB and 1.69 moles (f_3=12) in SRB-E (B=90%) at 973 K, and 0.35 moles (f_2=12) in SRE at 873 K.

(v) For maximum hydrogen production conditions, the energy requirements were 513.99 kJ/mol (SRB), 210.54 kJ/mol (SRE), and 485.13 kJ/mol (SRB-E, 90% B). Further, the energy required per mole of hydrogen produced decreased with the increase in ethanol content in B-E mixture. Thermal efficiency increases with the amount of steam in the feed for SRB, SRE, and SRB-E processes. On the basis of maximum production of H_2, the thermal efficiency was found to be 69.89 % (f_1=12, SRB), 68.49 % (f_2=12, SRE) and 70.07 % (f_3=12, SRB-E, 90% B).

(vi) Exergy efficiency was also favoured by steam/fuel molar feed ratio. The exergy destruction was higher in SRB than in SRE processes at f_1 and f_2 lower than 9. The

exergy efficiency values were found to be 48.72 % (f_1=12, SRB), 46.15 % (f_2=12, SRE), and 48.69 % (f_3=12, SRB-E, 90% B).

The present work proposes that although butanol and ethanol are suitable renewable fuels for the production of hydrogen, yet the mixture of butanol and ethanol produced during fermentation process is a good renewable fuel proposition which can be successively reformed for the production of H_2 by steam reforming process.

7.1.3 Oxidative steam reforming of butanol-ethanol mixture

Thermodynamic analysis combined with energetic and exergetic analyses are also presented for OSR of B-E mixture to produce H_2 to see the effect of addition of oxygen in feed. The conclusions are as follows:

(i) H_2 yield increases with the temperature up to 973 K and attains highest yield 65.46% at f_{O2}=0, and 58% at f_{O2}=0.75 for 90% B mixture composition and f_{O1}=9. On further increasing the temperature, the H_2 yield slightly reduces. Whereas, the yield of CH_4 continuously decreases with temperature and reaches negligible formation above approximately 973 K. The CH_4 yields of 2.23% for f_{O2}=0, and 1.05% for f_{O2}=0.75 with respect to maximum H_2 production have been obtained at 973 K and f_{O1}=9.

(ii) CO yield increases with increasing temperature but decreases with respect to f_{O2} values. On the other hand, CO_2 yield first increases up to approximately 873 K and then decreases continuously with the temperature rise but increases with the f_{O2} values. The CO yields of 53.39% for f_{O2}=0, and 45.68% for f_{O2}=0.75 whereas, the CO_2 yields of 44.38% for f_{O2}=0, and 53.27% for f_{O2}=0.75 at 973 K have been obtained with respect to maximum H_2 production.

(iii) OSRB-E process reduces the energy requirement per mol of H_2 as %B in B-E mixture decreases. Thermal efficiency in OSRB-E process first increases up to 973 K and then decreases, but no significant change is found with f_{O2} values. Moreover, the exergy efficiency increases with increasing temperature up to 1000K and then slightly decreases but decreases with increasing f_{O2} values.

The results of steam reforming and oxidative steam reforming of butanol-ethanol mixture in terms of maximum hydrogen production are compared in Table 5.2 and 5.3. It is clear from the tables that the overall performance of oxidative steam reforming is less than that of steam reforming of butanol-ethanol mixture. The production of hydrogen and thermal efficiency of reformer are found less in oxidative steam reforming of B-E mixture (OSRB-E) as compared to its steam reforming.

7.1.4 Steam reforming of acetone-butanol-ethanol mixture

The thermodynamic evaluation for hydrogen production via steam reforming of Acetone-Butanol-Ethanol mixture has been done. Operating conditions for the higher hydrogen production (8.35 mol) by this process are high temperature = 973 K, low pressure = 1 atm and high steam/fuel molar feed ratio=12. Under these conditions, carbon formation is thermodynamically inhibited and the methane formation is minimized.

Further, the evaluation of various fuels such as acetone, butanol, ethanol, methanol, and glycerol, butanol-ethanol mixture, acetone-butanol-ethanol mixturehave been done and compared in Table 6.2, which suggests that SR-ABE process is efficient, economical and environment friendly, and utilizes water rich ABE mixture as a renewable fuel for H_2 production without any requirement of separation units.

7.2 RECOMMENDATIONS FOR FUTURE WORK

In the present research work, optimum operating conditions are investigated for various fuel reforming processes for the mixtures of butanol-ethanol, and acetone-butanol-ethanolby thermodynamic analysis which is very helpful for conducting experiments for the production of hydrogen to save time and materials due to expensive hit and trial process.

Besides, catalytic reforming process encounters many technical and scientific challenges containing feed quality and its conversion, hydrogen purification, and finding a way for continuous reaction-regeneration of the catalyst. Therefore, research should be focused on preparation and development of new catalysts to maximize desired products and suppress the formation of undesired compounds.

Normally, Ni, Pt, and Ru supported by Al_2O_3, MgO, CeO_2, etc. are used to facilitate the reforming reactions for the production of hydrogen. Catalysts should have some attributes such as ease of availability, cost effective, higher stability, reusability, resistance to deactivation due to sintering, solid carbon deposition over the surface of the catalyst, and impurity fouling.

BIBLIOGRAPHY

1. **Aasberg-Petersen, K., Christensen, T.S., Nielsen, C.S. and Dybkjær, I., 2003.** Recent developments in autothermal reforming and pre-reforming for synthesis gas production in GTL applications. *Fuel Processing Technology*, *83*(1-3), pp.253-261.
2. **Adhikari, S., Fernando, S.D. and Haryanto, A., 2008.** Hydrogen production from glycerin by steam reforming over nickel catalysts. *Renewable Energy*, *33*(5), pp.1097-1100.
3. **Al Jibouri, A.K.H., Upreti, S.R. and Wu, J., 2018.** Optimal control of continuous ozonation of non-biodegradable pollutants. *Journal of Process Control*, *66*, pp.1-11.
4. **Anjaneyulu, C., da Costa, L.O., Ribeiro, M.C., Rabelo-Neto, R.C., Mattos, L.V., Venugopal, A. and Noronha, F.B., 2016.** Effect of Zn addition on the performance of Ni/Al_2O_3 catalyst for steam reforming of ethanol. *Applied Catalysis A: General*, *519*, pp.85-98.
5. **Arslan, A., Gunduz, S. and Dogu, T., 2014.** Steam reforming of ethanol with zirconia incorporated mesoporous silicate supported catalysts. *International Journal of Hydrogen Energy*, *39*(32), pp.18264-18272.
6. **Azadi, P., Afif, E., Foroughi, H., Dai, T., Azadi, F. and Farnood, R., 2013.** Catalytic reforming of activated sludge model compounds in supercritical water using nickel and ruthenium catalysts. *Applied Catalysis B: Environmental*, *134*, pp.265-273.
7. **Azadi, P., Foroughi, H., Dai, T., Azadi, F. and Farnood, R., 2014.** An integrated hydrolysis-reforming process for the production of hydrogen from wet biomass feedstocks. *Fuel*, *117*, pp.1223-1230.
8. **Azadi, P., Otomo, J., Hatano, H., Oshima, Y. and Farnood, R., 2010**. Hydrogen production by catalytic near-critical water gasification and steam reforming of glucose. *International Journal of Hydrogen Energy*, *35*(8), pp.3406-3414.
9. **Bakenne, A., Nuttall, W. and Kazantzis, N., 2016.** Sankey-Diagram-based insights into the hydrogen economy of today. *International Journal of Hydrogen Energy*, *41*(19), pp.7744-7753.
10. **Balat, M., Balat, H. and Öz, C., 2008.** Progress in bioethanol processing. *Progress in Energy and Combustion Science*, *34*(5), pp.551-573.

11. **Baruah, R., Dixit, M., Parejiya, A., Basarkar, P., Bhargav, A. and Sharma, S., 2017.** Oxidative steam reforming of ethanol on rhodium catalyst–I: Spatially resolved steady-state experiments and microkinetic modeling. *International Journal of Hydrogen Energy*, *42*(15), pp.10184-10198.

12. **Bellido, J.D., Tanabe, E.Y. and Assaf, E.M., 2009.** Carbon dioxide reforming of ethanol over $Ni/Y_2O_3–ZrO_2$ catalysts. *Applied Catalysis B: Environmental*, *90*(3-4), pp.485-488.

13. **Bimbela, F., Oliva, M., Ruiz, J., García, L. and Arauzo, J., 2009.** Catalytic steam reforming of model compounds of biomass pyrolysis liquids in fixed bed: acetol and n-butanol. *Journal of Analytical and Applied Pyrolysis*, *85*(1-2), pp.204-213.

14. **Bizkarra, K., Barrio, V.L., Yartu, A., Requies, J., Arias, P.L. and Cambra, J.F., 2015.** Hydrogen production from n-butanol over alumina and modified alumina nickel catalysts. *International Journal of Hydrogen Energy*, *40*(15), pp.5272-5280.

15. **Blanchard, J., Oudghiri-Hassani, H., Abatzoglou, N., Jankhah, S. and Gitzhofer, F., 2008.** Synthesis of nanocarbons via ethanol dry reforming over a carbon steel catalyst. *Chemical Engineering Journal*, *143*(1-3), pp.186-194.

16. **Borisov, I.L., Volkov, V.V., Kirsh, V.A. and Roldugin, V.I., 2011.** Simulation of the temperature-driven pervaporation of dilute 1-butanol aqueous mixtures through a PTMSP membrane in a cross-flow module. *Petroleum Chemistry*, *51*(7), pp.542-554.

17. **Bosze, E.J., McKittrick, J. and Hirata, G.A., 2003.** Investigation of the physical properties of a blue-emitting phosphor produced using a rapid exothermic reaction. *Materials Science and Engineering: B*, *97*(3), pp.265-274.

18. **Braga, A.H., Sodré, E.R., Santos, J.B.O., de Paula Marques, C.M. and Bueno, J.M.C., 2016.** Steam reforming of acetone over Ni-and Co-based catalysts: effect of the composition of reactants and catalysts on reaction pathways. *Applied Catalysis B: Environmental*, *195*, pp.16-28.

19. **Byrd, A.J., Pant, K.K. and Gupta, R.B., 2007.** Hydrogen production from glucose using Ru/Al2O3 catalyst in supercritical water. *Industrial & Engineering Chemistry Research*, *46*(11), pp.3574-3579.

20. **Byrd, A.J., Pant, K.K. and Gupta, R.B., 2008.** Hydrogen production from glycerol by reforming in supercritical water over Ru/Al2O3 catalyst. *Fuel*, *87*(13-14), pp.2956-2960.

21. **Cai, W., de la Piscina, P.R. and Homs, N., 2014b.** Oxidative steam reforming of bio-butanol for hydrogen production: effects of noble metals on bimetallic CoM/ZnO catalysts (M= Ru, Rh, Ir, Pd). *Applied Catalysis B: Environmental*, *145*, pp.56-62.

22. **Cai, W., de la Piscina, P.R., & Homs, N., 2012.** Hydrogen production from the steam reforming of bio-butanol over novel supported Co-based bimetallic catalysts. *Bioresource Technology*, *107*, pp.482-486.

23. **Cai, W., de la Piscina, P.R., Gabrowska, K. and Homs, N., 2013.** Hydrogen production from oxidative steam reforming of bio-butanol over CoIr-based catalysts: effect of the support. *Bioresource Technology*, *128*, pp.467-471.

24. **Cai, W., Homs, N. and de la Piscina, P.R., 2014a.** Renewable hydrogen production from oxidative steam reforming of bio-butanol over CoIr/$CeZrO_2$ catalysts: Relationship between catalytic behaviour and catalyst structure. *Applied Catalysis B: Environmental*, *150*, pp.47-56.

25. **Cai, W., Zhang, B., Li, Y., Xu, Y. and Shen, W., 2007.** Hydrogen production by oxidative steam reforming of ethanol over an Ir/CeO_2 catalyst. *Catalysis Communications*, *8*(11), pp.1588-1594.

26. **Cao, W., Chen, G., Li, S. and Yuan, Q., 2006.** Methanol-steam reforming over a ZnO–Cr_2O_3/CeO_2–ZrO_2/Al_2O_3 catalyst. *Chemical Engineering Journal*, *119*(2-3), pp.93-98.

27. **Carrette, L., Friedrich, K.A. and Stimming, U., 2001.** Fuel cells–fundamentals and applications. *Fuel cells*, *1*(1), pp.5-39.

28. **Carvalho, F.L., Asencios, Y.J., Bellido, J.D. and Assaf, E.M., 2016.** Bio-ethanol steam reforming for hydrogen production over Co_3O_4/CeO_2 catalysts synthesized by one-step polymerization method. *Fuel Processing Technology*, *142*, pp.182-191.

29. **Cavallaro, S., Chiodo, V., Freni, S., Mondello, N. and Frusteri, F., 2003.** Performance of Rh/Al_2O_3 catalyst in the steam reforming of ethanol: H_2 production for MCFC. *Applied Catalysis A: General*, *249*(1), pp.119-128.

30. **Cengel, Y.A., Boles, M.A., 2008.** *Thermodynamics: An engineering approach.* 6th edition, McGraw-Hill Inc., New York.

31. **Challiwala, M.S., Ghouri, M.M., Linke, P., El-Halwagi, M.M. and Elbashir, N.O., 2017.** A combined thermo-kinetic analysis of various methane reforming technologies: comparison with dry reforming. *Journal of CO_2 Utilization*, *17*, pp.99-111.

32. **Chen, B., Liao, Z., Wang, J., Yu, H. and Yang, Y., 2012.** Exergy analysis and CO_2 emission evaluation for steam methane reforming. *International Journal of Hydrogen Energy*, *37*(4), pp.3191-3200.

33. **Chen, H., Zhang, T., Dou, B., Dupont, V., Williams, P., Ghadiri, M. and Ding, Y., 2009.** Thermodynamic analyses of adsorption-enhanced steam reforming of glycerol for hydrogen production. *International Journal of Hydrogen Energy*, *34*(17), pp.7208-7222.

34. **Cheng, C.K., Foo, S.Y. and Adesina, A.A., 2010.** H_2-rich synthesis gas production over Co/Al_2O_3 catalyst via glycerol steam reforming. *Catalysis Communications*, *12*(4), pp.292-298.

35. **Ciftci, A., Ligthart, D.M., Sen, A.O., van Hoof, A.J., Friedrich, H. and Hensen, E.J., 2014.** Pt-Re synergy in aqueous-phase reforming of glycerol and the water–gas shift reaction. *Journal of Catalysis*, *311*, pp.88-101.

36. **Cifuentes, B., Hernández, M., Monsalve, S. and Cobo, M., 2016.** Hydrogen production by steam reforming of ethanol on a $RhPt/CeO_2/SiO_2$ catalyst: Synergistic effect of the Si:Ce ratio on the catalyst performance. *Applied Catalysis A: General*, *523*, pp.283-293.

37. **Cohce, M.K., Dincer, I. and Rosen, M.A., 2011.** Energy and exergy analyses of a biomass-based hydrogen production system. *Bioresource Technology*, *102*(18), pp.8466-8474.

38. **Cruz, I.O., Ribeiro, N.F., Aranda, D.A. and Souza, M.M., 2008.** Hydrogen production by aqueous-phase reforming of ethanol over nickel catalysts prepared from hydrotalcite precursors. *Catalysis Communications*, *9*(15), pp.2606-2611.

39. **Dan, M., Mihet, M., Tasnadi-Asztalos, Z., Imre-Lucaci, A., Katona, G. and Lazar, M.D., 2015.** Hydrogen production by ethanol steam reforming on nickel catalysts: effect of support modification by CeO_2 and La_2O_3. *Fuel*, *147*, pp.260-268.

40. **Davidson, S.D., Sun, J., Hong, Y., Karim, A.M., Datye, A.K. and Wang, Y., 2014.** The effect of ZnO addition on Co/C catalyst for vapor and aqueous phase reforming of ethanol. *Catalysis Today*, *233*, pp.38-45.

41. **Demirbas, A., 2008.** Hydrogen production from carbonaceous solid wastes by steam reforming. *Energy Sources, Part A*, *30*(10), pp.924-931.

42. **Deng, X., Sun, J., Yu, S., Xi, J., Zhu, W. and Qiu, X., 2008.** Steam reforming of ethanol for hydrogen production over NiO/ZnO/ZrO_2 catalysts. *International Journal of Hydrogen Energy*, *33*(3), pp.1008-1013.

43. **Deng, X., Wang, H., Huang, H. and Ouyang, M., 2010.** Hydrogen flow chart in China. *International Journal of Hydrogen Energy*, *35*(13), pp.6475-6481.

44. **Dhanala, V., Maity, S.K. and Shee, D., 2015.** Oxidative steam reforming of isobutanol over Ni/γ-Al_2O_3 catalysts: A comparison with thermodynamic equilibrium analysis. *Journal of Industrial and Engineering Chemistry*, *27*, pp.153-163.

45. **Ding, N., Azargohar, R., Dalai, A.K. and Kozinski, J.A., 2014a.** Catalytic gasification of cellulose and pinewood to H_2 in supercritical water. *Fuel*, *118*, pp.416-425.

46. **Ding, N., Azargohar, R., Dalai, A.K. and Kozinski, J.A., 2014b.** Catalytic gasification of glucose to H_2 in supercritical water. *Fuel Processing Technology*, *127*, pp.33-40.

47. **Eckert, G. and Schügerl, K., 1987**. Continuous acetone-butanol production with direct product removal. *Applied Microbiology and Biotechnology*, *27*(3), pp.221-228.

48. **Elfasakhany, A., 2016.** Performance and emissions analysis on using acetone–gasoline fuel blends in spark-ignition engine. *Engineering Science and Technology, An International Journal*, *19*(3), pp.1224-1232.

49. **Esteban-Díez, G., Gil, M.V., Pevida, C., Chen, D. and Rubiera, F., 2016.** Effect of operating conditions on the sorption enhanced steam reforming of blends of acetic acid and acetone as bio-oil model compounds. *Applied Energy*, *177*, pp.579-590.

50. **Evans, P.J. and Wang, H.Y., 1988.** Enhancement of butanol formation by Clostridium acetobutylicum in the presence of decanol-oleyl alcohol mixed extractants. *Applied and Environmental Microbiology*, *54*(7), pp.1662-1667.

51. **Forrest, A.K., Wales, M.E. and Holtzapple, M.T., 2011.** Thermodynamic prediction of hydrogen production from mixed-acid fermentations. *Bioresource Technology*, *102*(20), pp.9823-9826.

52. **Frusteri, F., Freni, S., Chiodo, V., Spadaro, L., Di Blasi, O., Bonura, G. and Cavallaro, S., 2004.** Steam reforming of bio-ethanol on alkali-doped Ni/MgO catalysts: hydrogen production for MC fuel cell. *Applied Catalysis A: General*, *270*(1-2), pp.1-7.

53. **Funk, J.E., 2001.** Thermochemical hydrogen production: past and present. *International Journal of Hydrogen Energy*, *26*(3), pp.185-190.

54. **Garcia, E.Y. and Laborde, M.A., 1991.** Hydrogen production by the steam reforming of ethanol: thermodynamic analysis. *International Journal of Hydrogen Energy*, *16*(5), pp.307-312.

55. **González-Gil, R., Chamorro-Burgos, I., Herrera, C., Larrubia, M.A., Laborde, M., Marino, F. and Alemany, L.J., 2015.** Production of hydrogen by catalytic steam reforming of oxygenated model compounds on Ni-modified supported catalysts. Simulation and experimental study. *International Journal of Hydrogen Energy*, *40*(34), pp.11217-11227.

56. **González-Gil, R., Herrera, C., Larrubia, M.A., Mariño, F., Laborde, M. and Alemany, L.J., 2016.** Hydrogen production by ethanol steam reforming over multimetallic RhCeNi/Al_2O_3 structured catalyst. Pilot-scale study. *International Journal of Hydrogen Energy*, *41*(38), pp.16786-16796.

57. **Graschinsky, C., Giunta, P., Amadeo, N. and Laborde, M., 2012.** Thermodynamic analysis of hydrogen production by autothermal reforming of ethanol. *International Journal of Hydrogen Energy*, *37*(13), pp.10118-10124.

58. **Greluk, M., Słowik, G., Rotko, M. and Machocki, A., 2016.** Steam reforming and oxidative steam reforming of ethanol over PtKCo/CeO_2 catalyst. *Fuel*, *183*, pp.518-530.

59. **Guil-Lopez, R., Navarro, R.M., Ismail, A.A., Al-Sayari, S.A. and Fierro, J.L.G., 2015.** Influence of Ni environment on the reactivity of Ni-Mg-Al catalysts for the acetone steam reforming reaction. *International Journal of Hydrogen Energy*, *40*(15), pp. 5289-5296.

60. **Guo, S., Guo, L., Cao, C., Yin, J., Lu, Y. and Zhang, X., 2012.** Hydrogen production from glycerol by supercritical water gasification in a continuous flow tubular reactor. *International Journal of Hydrogen Energy*, *37*(7), pp.5559-5568.

61. **Hajjaji, N., Baccar, I. and Pons, M.N., 2014.** Energy and exergy analysis as tools for optimization of hydrogen production by glycerol autothermal reforming. *Renewable Energy*, *71*, pp.368-380.

62. **Harju, H., Lehtonen, J. and Lefferts, L., 2015.** Steam-and autothermal-reforming of n-butanol over Rh/ZrO_2 catalyst. *Catalysis Today*, *244*, pp.47-57.

63. **Harju, H., Lehtonen, J. and Lefferts, L., 2016.** Steam reforming of n-butanol over Rh/ZrO_2 catalyst: role of 1-butene and butyraldehyde. *Applied Catalysis B: Environmental*, *182*, pp.33-46.

64. **Hartley, U.W., Amornraksa, S., Kim-Lohsoontorn, P. and Laosiripojana, N., 2015.** Thermodynamic analysis and experimental study of hydrogen production from oxidative reforming of n-butanol. *Chemical Engineering Journal*, *278*, pp.2-12.

65. **Hedayati, A., Le Corre, O., Lacarrière, B. and Llorca, J., 2016.** Experimental and exergy evaluation of ethanol catalytic steam reforming in a membrane reactor. *Catalysis Today*, *268*, pp.68-78.

66. **Hirai, T., Ikenaga, N.O., Miyake, T. and Suzuki, T., 2005.** Production of hydrogen by steam reforming of glycerin on ruthenium catalyst. *Energy & Fuels*, *19*(4), pp.1761-1762.

67. **Hohn, K.L. and Schmidt, L.D., 2001.** Partial oxidation of methane to syngas at high space velocities over Rh-coated spheres. *Applied Catalysis A: General*, *211*(1), pp.53-68.

68. **Holladay, J.D., Hu, J., King, D.L. and Wang, Y., 2009.** An overview of hydrogen production technologies. *Catalysis today*, *139*(4), pp.244-260.

69. **Horng, R.F., Lai, M.P., Chiu, W.C. and Huang, W.C., 2016.** Thermodynamic analysis of syngas production and carbon formation on oxidative steam reforming of butanol. *International Journal of Hydrogen Energy*, *41*(2), pp.889-896.

70. **Hou, T., Yu, B., Zhang, S., Xu, T., Wang, D. and Cai, W., 2015.** Hydrogen production from ethanol steam reforming over Rh/CeO_2 catalyst. *Catalysis Communications*, *58*, pp.137-140.

71. **Hu, X., Zhang, L. and Lu, G., 2012.** Pruning of the surface species on Ni/Al_2O_3 catalyst to selective production of hydrogen via acetone and acetic acid steam reforming. *Applied Catalysis A: General*, 427, pp. 49-57.

72. **Huang, L., Zhong, X., Duan, Y., Xie, W. and Chen, R., 2015.** Precious metal-promoted Ni–Mg–Al–Fe–O catalyst for hydrogen production with fast startup via catalytic partial oxidation of butanol. *International Journal of Hydrogen Energy*, *40*(4), pp.1717-1725.

73. **Huang, L., Zhou, J., Hsu, A.T. and Chen, R., 2013.** Catalytic partial oxidation of n-butanol for hydrogen production over LDH-derived Ni-based catalysts. *International Journal of Hydrogen Energy*, *38*(34), pp.14550-14558.

74. **Ishihara, A., Mitsushima, S., Kamiya, N. and Ota, K.I., 2004.** Exergy analysis of polymer electrolyte fuel cell systems using methanol. *Journal of Power Sources*, *126*(1-2), pp.34-40.

75. **Jacobsohn, L.G., Blair, M.W., Tornga, S.C., Brown, L.O., Bennett, B.L. and Muenchausen, R.E., 2008.** Y_2O_3: Bi nanophosphor: Solution combustion synthesis, structure, and luminescence. *Journal of Applied Physics*, *104*(12), pp.124303.

76. **Jankhah, S., Abatzoglou, N. and Gitzhofer, F., 2008.** Thermal and catalytic dry reforming and cracking of ethanol for hydrogen and carbon nanofilaments' production. *International Journal of Hydrogen Energy*, *33*(18), pp.4769-4779.

77. **Janssen, H., Bringmann, J.C., Emonts, B. and Schröder, V., 2004.** Safety-related studies on hydrogen production in high-pressure electrolysers. *International Journal of Hydrogen Energy*, *29*(7), pp.759-770.

78. **Ji, P., Van der Kooi, H.J. and de Swaan Arons, J., 2003.** Simulation and thermodynamic analysis of conventional and oxygen permeable CPO reactors. *Chemical Engineering Science*, *58*(13), pp.2921-2930.

79. **Jin, C., Yao, M., Liu, H., Chia-fon, F.L. and Ji, J., 2011.** Progress in the production and application of n-butanol as a biofuel. *Renewable and Sustainable Energy Reviews*, *15*(8), pp.4080-4106.

80. **Jurado, N., Somorin, T., Kolios, A.J., Wagland, S., Patchigolla, K., Fidalgo, B., Parker, A., McAdam, E., Williams, L. and Tyrrel, S., 2018.** Design and commissioning of a multi-mode prototype for thermochemical conversion of human faeces. *Energy Conversion and Management*, *163*, pp.507-524.

81. **Kalamaras, C.M. and Efstathiou, A.M., 2013.** Hydrogen Production Technologies: Current State and Future Developments. In: Conference Papers in Energy, 2013, Article ID 690627, 9 pages. http://dx.doi.org/10.1155/2013/690627.

82. **Kang, K., Azargohar, R., Dalai, A.K. and Wang, H., 2015.** Noncatalytic gasification of lignin in supercritical water using a batch reactor for hydrogen production: an experimental and modeling study. *Energy & Fuels*, *29*(3), pp.1776-1784.

83. Katiyar, N., Kumar, S. and Kumar, S., 2013. Thermodynamic analysis for quantifying fuel cell grade H_2 production by methanol steam reforming. *Chemical Engineering & Technology*, *36*(4), pp.581-590.

84. Katuri, S.R., Ranjan, R. and Khanna, R., 2011. Mathematical Modeling of Mist Bioreactor for the Growth of Hairy Roots. *National Workshop-Cum-Conference on Recent Trends in Mathematics and Computing (RTMC) Proceedings published in International Journal of Computer Applications® (IJCA).*

85. Kraleva, E., Sokolov, S., Nasillo, G., Bentrup, U. and Ehrich, H., 2014. Catalytic performance of CoAlZn and NiAlZn mixed oxides in hydrogen production by bio-ethanol partial oxidation. *International Journal of Hydrogen Energy*, *39*(1), pp.209-220.

86. Krummenacher, J.J., West, K.N. and Schmidt, L.D., 2003. Catalytic partial oxidation of higher hydrocarbons at millisecond contact times: decane, hexadecane, and diesel fuel. *Journal of Catalysis*, *215*(2), pp.332-343.

87. Kugai, J., Subramani, V., Song, C., Engelhard, M.H. and Chin, Y.H., 2006. Effects of nanocrystalline CeO_2 supports on the properties and performance of Ni–Rh bimetallic catalyst for oxidative steam reforming of ethanol. *Journal of Catalysis*, *238*(2), pp.430-440.

88. Kujawska, A., Kujawski, J., Bryjak, M. and Kujawski, W., 2015. ABE fermentation products recovery methods—a review. *Renewable and Sustainable Energy Reviews*, *48*, pp.648-661.

89. Kumar, S., Katiyar, N., Kumar, S. and Yadav, S., 2013. Exergy Analysis of Oxidative Steam Reforming of Methanol for Hydrogen Producton: Modeling Study. *International Journal of Chemical Reactor Engineering*, *11*(1), pp.489-500.

90. Leo, T.J., Raso, M.A., Navarro, E. and Sánchez-de-la-Blanca, E., 2011. Comparative exergy analysis of direct alcohol fuel cells using fuel mixtures. *Journal of Power sources*, *196*(3), pp.1178-1183.

91. Levario, T.J., Dai, M., Yuan, W., Vogt, B.D. and Nielsen, D.R., 2012. Rapid adsorption of alcohol biofuels by high surface area mesoporous carbons. *Microporous and Mesoporous Materials*, *148*(1), pp.107-114.

92. Li, J., Yu, H., Yang, G., Peng, F., Xie, D., Wang, H. and Yang, J., 2011. Steam reforming of oxygenate fuels for hydrogen production: a thermodynamic study. *Energy & Fuels*, *25*(6), pp.2643-2650.

93. **Li, M., Wang, X., Li, S., Wang, S. and Ma, X., 2010.** Hydrogen production from ethanol steam reforming over nickel based catalyst derived from Ni/Mg/Al hydrotalcite-like compounds. *International Journal of Hydrogen Energy*, *35*(13), pp.6699-6708.

94. **Licht, S., 2003.** Solar water splitting to generate hydrogen fuel: photothermal electrochemical analysis. *The Journal of Physical Chemistry B*, *107*(18), pp.4253-4260.

95. **Lin, X., Wu, J., Fan, J., Qian, W., Zhou, X., Qian, C., Jin, X., Wang, L., Bai, J. and Ying, H., 2012.** Adsorption of butanol from aqueous solution onto a new type of macroporous adsorption resin: studies of adsorption isotherms and kinetics simulation. *Journal of Chemical Technology and Biotechnology*, *87*(7), pp.924-931.

96. **Lin, Y.C., 2013.** Catalytic valorization of glycerol to hydrogen and syngas. *International Journal of Hydrogen Energy*, *38*(6), pp.2678-2700.

97. **Liu, S., Zhang, K., Fang, L. and Li, Y., 2008.** Thermodynamic analysis of hydrogen production from oxidative steam reforming of ethanol. *Energy & Fuels*, *22*(2), pp.1365-1370.

98. **Louw, J., Schwarz, C.E. and Burger, A.J., 2016.** Supercritical water gasification of Eucalyptus grandis and related pyrolysis char: Effect of feedstock composition. *Bioresource Technology*, *216*, pp.1030-1039.

99. **Louw, J., Schwarz, C.E., Knoetze, J.H. and Burger, A.J., 2014.** Thermodynamic modelling of supercritical water gasification: Investigating the effect of biomass composition to aid in the selection of appropriate feedstock material. *Bioresource Technology*, *174*, pp.11-23.

100. **Luo, N., Cao, F., Zhao, X., Xiao, T. and Fang, D., 2007**. Thermodynamic analysis of aqueous-reforming of polylols for hydrogen generation. *Fuel*, *86*(12-13), pp.1727-1736.

101. **Luyben, W.L., 2012.** Pressure-swing distillation for minimum-and maximum-boiling homogeneous azeotropes. *Industrial & Engineering Chemistry Research*, *51*(33), pp.10881-10886.

102. **Lwin, Y., Daud, W.R.W., Mohamad, A.B. and Yaakob, Z., 2000.** Hydrogen production from steam–methanol reforming: thermodynamic analysis. *International Journal of Hydrogen Energy*, *25*(1), pp.47-53.

103. Maiti, A., DasGupta, S, Basu, J.K. and De, S., 2007. Adsorption of arsenite using natural laterite as adsorbent. *Separation and Purification Technology*, *55*(3), pp.350-359.

104. Maiti, R., Khanna, R. and Nigam, K.D.P., 2005. Trickle-bed reactors: Porosity-induced hysteresis. *Industrial & Engineering Chemistry Research*, *44*(16), pp.6406-6413.

105. Maiti, R., Khanna, R. and Nigam, K.D.P., 2006. Hysteresis in trickle-bed reactors: a review. *Industrial & Engineering Chemistry Research*, *45*(15), pp.5185-5198.

106. Mariano, A.P., Keshtkar, M.J., Atala, D.I., Maugeri Filho, F., Wolf Maciel, M.R., Maciel Filho, R. and Stuart, P., 2011. Energy requirements for butanol recovery using the flash fermentation technology. *Energy & Fuels*, *25*(5), pp.2347-2355.

107. Markočič, E., Kramberger, B., van Bennekom, J.G., Heeres, H.J., Vos, J. and Knez, Ž., 2013. Glycerol reforming in supercritical water; a short review. *Renewable and Sustainable Energy Reviews*, *23*, pp.40-48.

108. Mathew, T., Yamada, Y., Ueda, A., Shioyama, H. and Kobayashi, T., 2005. Metal oxide catalysts for DME steam reforming: Ga_2O_3 and Ga_2O_3–Al_2O_3 catalysts. *Catalysis Letters*, *100*(3-4), pp.247-253.

109. Medrano, J.A., Oliva, M., Ruiz, J., García, L. and Arauzo, J., 2014. Catalytic steam reforming of butanol in a fluidized bed and comparison with other oxygenated compounds. *Fuel Processing Technology*, *124*, pp.123-133.

110. Methekar, R.N., Prasad, V. and Gudi, R.D., 2007a. Dynamic analysis and linear control strategies for proton exchange membrane fuel cell using a distributed parameter model. *Journal of Power Sources*, *165*(1), pp.152-170.

111. Methekar, R.N., Prasad, V., Patwardhan, S.C. and Gudi, R.D., 2007b. November. Control of PEMFC using empirical dynamic models in an IMC and LQG framework. In *AIChE Annual meeting, Salt lake city, Utah, USA*.

112. Miletić, N., Izquierdo, U., Obregon, I., Bizkarra, K., Agirrezabal-Telleria, I., Bario, L.V. and Arias, P.L., 2015. Oxidative steam reforming of methane over nickel catalysts supported on Al_2O_3–CeO_2–La_2O_3. *Catalysis Science & Technology*, *5*(3), pp.1704-1715.

113. Mitton, D.B., Yoon, J.H., Cline, J.A., Kim, H.S., Eliaz, N. and Latanision, R.M., 2000. Corrosion behavior of nickel-based alloys in supercritical water

oxidation systems. *Industrial & Engineering Chemistry Research*, *39*(12), pp.4689-4696.

114. Mohan, M., Goud, V.V. and Banerjee, T., 2015. Solubility of glucose, xylose, fructose and galactose in ionic liquids: Experimental and theoretical studies using a continuum solvation model. *Fluid Phase Equilibria*, *395*, pp.33-43.

115. Montero, C., Oar-Arteta, L., Remiro, A., Arandia, A., Bilbao, J. and Gayubo, A.G., 2015. Thermodynamic comparison between bio-oil and ethanol steam reforming. *International Journal of Hydrogen Energy*, *40*(46), pp.15963-15971.

116. Muñoz, M., Moreno, S. and Molina, R., 2017. Oxidative steam reforming of ethanol (OSRE) over stable NiCo–MgAl catalysts by microwave or sonication assisted coprecipitation. *International Journal of Hydrogen Energy*, *42*(17), pp.12284-12294.

117. Nahar, G.A. and Madhani, S.S., 2010. Thermodynamics of hydrogen production by the steam reforming of butanol: analysis of inorganic gases and light hydrocarbons. *International Journal of Hydrogen Energy*, *35*(1), pp.98-109.

118. Nahreen, S. and Gupta, R.B., 2013. Conversion of the Acetone–Butanol–Ethanol (ABE) Mixture to Hydrocarbons by Catalytic Dehydration. *Energy & Fuels*, *27*(4), pp.2116-2125.

119. Naterer, G.F., Fowler, M., Cotton, J. and Gabriel, K., 2008. Synergistic roles of off-peak electrolysis and thermochemical production of hydrogen from nuclear energy in Canada. *International journal of hydrogen energy*, *33*(23), pp.6849-6857.

120. Navarro, R.M., Guil-Lopez, R., Gonzalez-Carballo, J.M., Cubero, A., Ismail, A.A., Al-Sayari, S.A. and Fierro, J.L.G., 2014. Bimetallic MNi/Al_2O_3-La catalysts (M= Pt, Cu) for acetone steam reforming: Role of M on catalyst structure and activity. *Applied Catalysis A: General*, *474*, pp.168-177.

121. Navarro, R.M., Guil-Lopez, R., Ismail, A. A., Al-Sayari, S. A. and Fierro, J.L.G., 2015. Ni-and PtNi-catalysts supported on Al_2O_3 for acetone steam reforming: Effect of the modification of support with Ce, La and Mg. *Catalysis Today*, *242*, pp. 60-70.

122. Ni, M., Leung, D.Y. and Leung, M.K., 2007. A review on reforming bio-ethanol for hydrogen production. *International Journal of Hydrogen Energy*, *32*(15), pp.3238-3247.

123. Norbeck, J.M., Heffel, J.W., Durbin, T.D., Tabbara, B., Bowden, J.M. and Montano, M.C., 1996. *Hydrogen Fuel for Surface Transportation,160*, pp. 548.

124. Nozawa, T., Mizukoshi, Y., Yoshida, A. and Naito, S., 2014. Aqueous phase reforming of ethanol and acetic acid over TiO_2 supported Ru catalysts. *Applied Catalysis B: Environmental*, *146*, pp.221-226.

125. Nozawa, T., Yoshida, A., Hikichi, S. and Naito, S., 2015. Effects of Re addition upon aqueous phase reforming of ethanol over TiO_2 supported Rh and Ir catalysts. *International Journal of Hydrogen Energy*, *40*(11), pp.4129-4140.

126. Ogden, J.M., Steinbugler, M.M. and Kreutz, T.G., 1999. A comparison of hydrogen, methanol and gasoline as fuels for fuel cell vehicles: implications for vehicle design and infrastructure development. *Journal of Power Sources*, *79*(2), pp.143-168.

127. Oliveira-Vigier, D., Abatzoglou, N. and Gitzhofer, F., 2005. Dry-reforming of ethanol in the presence of a 316 stainless steel catalyst. *The Canadian Journal of Chemical Engineering*, *83*(6), pp.978-984.

128. Onabanjo, T., Kolios, A.J., Patchigolla, K., Wagland, S.T., Fidalgo, B., Jurado, N., Hanak, D.P., Manovic, V., Parker, A., McAdam, E. and Williams, L., 2016. An experimental investigation of the combustion performance of human faeces. *Fuel*, *184*, pp.780-791.

129. Onabanjo, T., Patchigolla, K., Wagland, S.T., Fidalgo, B., Kolios, A., McAdam, E., Parker, A., Williams, L., Tyrrel, S. and Cartmell, E., 2016. Energy recovery from human faeces via gasification: a thermodynamic equilibrium modelling approach. *Energy Conversion and Management*, *118*, pp.364-376.

130. Ong, K.M., Lee, W.Y., Hanna, J. and Ghoniem, A.F., 2016. Isolating the impact of CO concentration in syngas mixtures on SOFC performance via internal reforming and direct oxidation. *International Journal of Hydrogen Energy*, *41*(21), pp.9035-9047.

131. Onozaki, M., Watanabe, K., Hashimoto, T., Saegusa, H. and Katayama, Y., 2006. Hydrogen production by the partial oxidation and steam reforming of tar from hot coke oven gas. *Fuel*, *85*(2), pp.143-149.

132. Ortiz, A.L., Sámano, R.P., Zaragoza, M.M. and Collins-Martínez, V., 2015. Thermodynamic analysis and process simulation for the H_2 production by dry reforming of ethanol with $CaCO_3$. *International Journal of Hydrogen Energy*, *40*(48), pp.17172-17179.

133. Ortiz, F.G., Campanario, F.J. and Ollero, P., 2016. Supercritical water reforming of model compounds of bio-oil aqueous phase: Acetic acid, acetol, butanol and glucose. *Chemical Engineering Journal*, *298*, pp.243-258.

134. Ortiz, F.G., Ollero, P., Serrera, A. and Sanz, A., 2011. Thermodynamic study of the supercritical water reforming of glycerol. *International Journal of Hydrogen Energy*, *36*(15), pp.8994-9013.

135. Oudshoorn, A., Van Der Wielen, L.A. and Straathof, A.J., 2009. Assessment of options for selective 1-butanol recovery from aqueous solution. *Industrial & Engineering Chemistry Research*, *48*(15), pp.7325-7336.

136. Özkara-Aydınoğlu, Ş., 2010. Thermodynamic equilibrium analysis of combined carbon dioxide reforming with steam reforming of methane to synthesis gas. *International Journal of Hydrogen Energy*, *35*(23), pp.12821-12828.

137. Pairojpiriyakul, T., Croiset, E., Kiatkittipong, W., Kiatkittipong, K., Arpornwichanop, A. and Assabumrungrat, S., 2013. Hydrogen production from catalytic supercritical water reforming of glycerol with cobalt-based catalysts. *International Journal of Hydrogen Energy*, *38*(11), pp.4368-4379.

138. Pairojpiriyakul, T., Kiatkittipong, W., Assabumrungrat, S. and Croiset, E., 2014. Hydrogen production from supercritical water reforming of glycerol in an empty Inconel 625 reactor. *International Journal of Hydrogen Energy*, *39*(1), pp.159-170.

139. Patraşcu, I., Bîldea, C.S. and Kiss, A.A., 2017. Eco-efficient butanol separation in the ABE fermentation process. *Separation and Purification Technology*, *177*, pp.49-61.

140. Peela, N.R. and Kunzru, D., 2011. Oxidative steam reforming of ethanol over Rh based catalysts in a micro-channel reactor. *International Journal of Hydrogen Energy*, *36*(5), pp.3384-3396.

141. Pereira, E.B., Homs, N., Martí, S., Fierro, J.L.G. and de la Piscina, P.R., 2008. Oxidative steam-reforming of ethanol over Co/SiO_2, $Co–Rh/SiO_2$ and $Co–Ru/SiO_2$ catalysts: catalytic behavior and deactivation/regeneration processes. *Journal of Catalysis*, *257*(1), pp.206-214.

142. Perry R.H., Green, D.W., Maloney, J.O., 1999. Perry's chemical engineers' handbook. 7th edition, McGraw-Hill Inc., New York, USA.

143. Pettersson, J., Ramsey, B. and Harrison, D., 2006. A review of the latest developments in electrodes for unitised regenerative polymer electrolyte fuel cells. *Journal of Power Sources*, *157*(1), pp.28-34.

144. Pojanavaraphan, C., Luengnaruemitchai, A. and Gulari, E., 2012. Hydrogen production by oxidative steam reforming of methanol over Au/CeO_2 catalysts. *Chemical Engineering Journal*, *192*, pp.105-113.

145. Profeti, L.P., Ticianelli, E.A. and Assaf, E.M., 2009. Production of hydrogen via steam reforming of biofuels on $Ni/CeO_2–Al_2O_3$ catalysts promoted by noble metals. *International Journal of Hydrogen Energy*, *34*(12), pp.5049-5060.

146. Purkait, M.K., DasGupta, S. and De, S., 2005. Adsorption of eosin dye on activated carbon and its surfactant based desorption. *Journal of Environmental Management*, *76*(2), pp.135-142.

147. Purkait, M.K., Gusain, D.S., DasGupta, S. and De, S., 2005. Adsorption behavior of chrysoidine dye on activated charcoal and its regeneration characteristics by using different surfactants. *Separation Science and Technology*, *39*(10), pp.2419-2440.

148. Qureshi, N. and Blaschek, H.P., 2001. Recent advances in ABE fermentation: hyper-butanol producing Clostridium beijerinckii BA101. *Journal of Industrial Microbiology and Biotechnology*, *27*(5), pp.287-291.

149. Rao, S.S., 2009. Engineering Optimization: Theory and Practice. 4th edition, John Wiley & Sons, New Jersey, USA.

150. Rao, Y.V.C., 1997. Chemical Engineering Thermodynamics. 1st edition, University Press Pvt. Ltd., Hyderabad, India.

151. Roffler, S., Blanch, H.W. and Wilke, C.R., 1987. Extractive fermentation of acetone and butanol: process design and economic evaluation. *Biotechnology Progress*, *3*(3), pp.131-140.

152. Roy, B. and Leclerc, C.A., 2015. Study of preparation method and oxidization/reduction effect on the performance of nickel-cerium oxide catalysts for aqueous-phase reforming of ethanol. *Journal of Power Sources*, *299*, pp.114-124.

153. Roy, B., Sullivan, H. and Leclerc, C.A., 2011. Aqueous-phase reforming of n-BuOH over Ni/Al_2O_3 and Ni/CeO_2 catalysts. *Journal of Power Sources*, *196*(24), pp.10652-10657.

154. Roy, B., Sullivan, H. and Leclerc, C.A., 2011. Aqueous-phase reforming of n-BuOH over Ni/Al_2O_3 and Ni/CeO_2 catalysts. *Journal of Power Sources*, *196*(24), pp.10652-10657.

155. Roy, B., Sullivan, H. and Leclerc, C.A., 2014. Effect of variable conditions on steam reforming and aqueous phase reforming of n-butanol over Ni/CeO_2 and Ni/Al_2O_3 catalysts. *Journal of Power Sources*, *267*, pp.280-287.

156. Sadooghi, P. and Rauch, R., 2015. Experimental and modeling study of hydrogen production from catalytic steam reforming of methane mixture with hydrogen sulfide. *International Journal of Hydrogen Energy*, *40*(33), pp.10418-10426.

157. Sánchez-Sánchez, M.C., Navarro, R.M. and Fierro, J.L.G., 2007. Ethanol steam reforming over $Ni/M_xO_y–Al_2O_3$ (M= Ce, La, Zr and Mg) catalysts: influence of support on the hydrogen production. *International Journal of Hydrogen Energy*, *32*(10-11), pp.1462-1471.

158. Schwengber, C.A., Alves, H.J., Schaffner, R.A., da Silva, F.A., Sequinel, R., Bach, V.R. and Ferracin, R.J., 2016. Overview of glycerol reforming for hydrogen production. *Renewable and Sustainable Energy Reviews*, *58*, pp.259-266.

159. Serdaroglu, G., Khzouz, M., Gillott, M., Shields, A. and Walker, G.S., 2015. The effect of environmental conditions on the operation of a hydrogen refuelling station. *International Journal of Hydrogen Energy*, *40*(47), pp.17153-17162.

160. Seretis, A. and Tsiakaras, P., 2015. A thermodynamic analysis of hydrogen production via aqueous phase reforming of glycerol. *Fuel Processing Technology*, *134*, pp.107-115.

161. Setlhaku, M., Heitmann, S., Górak, A. and Wichmann, R., 2013. Investigation of gas stripping and pervaporation for improved feasibility of two-stage butanol production process. *Bioresource Technology*, *136*, pp.102-108.

162. Sharma, M.P., Akyurtlu, J.F. and Akyurtlu, A., 2015. Autothermal reforming of isobutanol over promoted nickel xerogel catalysts for hydrogen production. *International Journal of Hydrogen Energy*, *40*(39), pp.13368-13378.

163. Sharma, P.K., Saxena, N., Roy, P.K. and Bhatt, A., 2016. Hydrogen generation by ethanol steam reforming over Rh/Al_2O_3 and $Rh/CeZrO_2$ catalysts: a comparative study. *International Journal of Hydrogen Energy*, *41*(14), pp.6123-6133.

164. Shuk, P., Wiemhöfer, H.D., Guth, U., Göpel, W. and Greenblatt, M., 1996. Oxide ion conducting solid electrolytes based on Bi_2O_3. *Solid State Ionics*, *89*(3-4), pp.179-196.

165. Silva, A.L. and Müller, I.L., 2011. Hydrogen production by sorption enhanced steam reforming of oxygenated hydrocarbons (ethanol, glycerol, n-butanol and methanol): thermodynamic modelling. *International Journal of Hydrogen Energy*, *36*(3), pp.2057-2075.

166. Silva, J.M., Soria, M.A. and Madeira, L.M., 2015. Challenges and strategies for optimization of glycerol steam reforming process. *Renewable and Sustainable Energy Reviews*, *42*, pp.1187-1213.

167. Singh, A., Tiwari, A., Mahajani, S.M. and Gudi, R.D., 2006. Recovery of acetic acid from aqueous solutions by reactive distillation. *Industrial & Engineering Chemistry Research*, *45*(6), pp.2017-2025.

168. Smith, J.M., Ness, H.C.V., Abbott, M.M., 2010. Introduction to chemical engineering thermodynamics. 7th edition, McGraw-Hill Inc., New York, USA.

169. Song, C., 2002. Fuel processing for low-temperature and high-temperature fuel cells: Challenges, and opportunities for sustainable development in the 21st century. *Catalysis Today*, *77*(1-2), pp.17-49.

170. Specchia, S., Cutillo, A., Saracco, G. and Specchia, V., 2006. Concept study on ATR and SR fuel processors for liquid hydrocarbons. *Industrial & Engineering Chemistry Research*, *45*(15), pp.5298-5307.

171. Steinfeld, A., 2005. Solar thermochemical production of hydrogen—a review. *Solar Energy*, *78*(5), pp.603-615.

172. Sun, H., Blass, S., Michor, E. and Schmidt, L., 2012. Autothermal reforming of butanol to butenes in a staged millisecond reactor: Effect of catalysts and isomers. *Applied Catalysis A: General*, *445*, pp.35-41.

173. Takata, H., Mizuno, N., Nishikawa, M., Fukada, S. and Yoshitake, M., 2007. Adsorption properties of water vapor on sulfonated perfluoropolymer membranes. *International Journal of Hydrogen Energy*, *32*(3), pp.371-379.

174. Thakur, V.K., Thakur, M.K. and Gupta, R.K., 2013a. Graft copolymers from cellulose: synthesis, characterization and evaluation. *Carbohydrate Polymers*, *97*(1), pp.18-25.

175. Thakur, V.K., Thakur, M.K. and Gupta, R.K., 2013b. Synthesis of lignocellulosic polymer with improved chemical resistance through free radical polymerization. *International Journal of Biological Macromolecules*, *61*, pp.121-126.

176. Therdthianwong, S., Srisiriwat, N., Therdthianwong, A. and Croiset, E., 2011. Hydrogen production from bioethanol reforming in supercritical water. *The Journal of Supercritical Fluids*, *57*(1), pp.58-65.

177. Timung, R., Mohan, M., Chilukoti, B., Sasmal, S., Banerjee, T. and Goud, V.V., 2015. Optimization of dilute acid and hot water pretreatment of different lignocellulosic biomass: a comparative study. *Biomass and Bioenergy*, *81*, pp.9-18.

178. Tippawan, P. and Arpornwichanop, A., 2014. Energy and exergy analysis of an ethanol reforming process for solid oxide fuel cell applications. *Bioresource Technology*, *157*, pp.231-239.

179. Tokarev, A.V., Kirilin, A.V., Murzina, E.V., Eränen, K., Kustov, L.M., Murzin, D.Y. and Mikkola, J.P., 2010. The role of bio-ethanol in aqueous phase reforming to sustainable hydrogen. . *International Journal of Hydrogen Energy*, *35*(22), pp.12642-12649.

180. Tóth, M., Varga, E., Oszkó, A., Baán, K., Kiss, J. and Erdőhelyi, A., 2016. Partial oxidation of ethanol on supported Rh catalysts: Effect of the oxide support. *Journal of Molecular Catalysis A: Chemical*, *411*, pp.377-387.

181. Turco, M., Bagnasco, G., Costantino, U., Marmottini, F., Montanari, T. and Ramis, G., 2004. Production of hydrogen from oxidative steam reforming of methanol: I. Preparation and characterization of $Cu/ZnO/Al_2O_3$ catalysts from a hydrotalcite-like LDH precursor. *Journal of catalysis*, *228*(1), pp.43-55.

182. Tyagi, A., Tripathi, K.M. and Gupta, R.K., 2015. Recent progress in micro-scale energy storage devices and future aspects. *Journal of Materials Chemistry A*, *3*(45), pp.22507-22541.

183. Tzanetis, K.F., Martavaltzi, C.S. and Lemonidou, A.A., 2012. Comparative exergy analysis of sorption enhanced and conventional methane steam reforming. *International Journal of Hydrogen Energy*, *37*(21), pp.16308-16320.

184. Vaidya, P.D. and Rodrigues, A.E., 2009. Glycerol reforming for hydrogen production: a review. *Chemical Engineering & Technology*, *32*(10), pp.1463-1469.

185. Verma, V.K. and Banerjee, T., 2010. Ionic liquids as entrainers for water+ ethanol, water+ 2-propanol, and water+ THF systems: A quantum chemical approach. *The Journal of Chemical Thermodynamics*, *42*(7), pp.909-919.

186. Wanat, E.C., Venkataraman, K. and Schmidt, L.D., 2004. Steam reforming and water–gas shift of ethanol on Rh and Rh–Ce catalysts in a catalytic wall reactor. *Applied Catalysis A: General*, *276*(1-2), pp.155-162.

187. Wang, M., Wang, Z., Gong, X. and Guo, Z., 2014. The intensification technologies to water electrolysis for hydrogen production–A review. *Renewable and Sustainable Energy Reviews*, *29*, pp.573-588.

188. Wang, W. and Cao, Y., 2010. Hydrogen-rich gas production for solid oxide fuel cell (SOFC) via partial oxidation of butanol: thermodynamic analysis. *International Journal of Hydrogen Energy*, *35*(24), pp.13280-13289.

189. Wang, W. and Cao, Y., 2011. Hydrogen production via sorption enhanced steam reforming of butanol: thermodynamic analysis. *International Journal of Hydrogen Energy*, *36*(4), pp.2887-2895.

190. Wang, W. and Wang, Y., 2009. Dry reforming of ethanol for hydrogen production: thermodynamic investigation. *International Journal of Hydrogen Energy*, *34*(13), pp.5382-5389.

191. Wang, W., 2011. Hydrogen production via dry reforming of butanol: thermodynamic analysis. *Fuel*, *90*(4), pp.1681-1688.

192. Wen, G., Xu, Y., Ma, H., Xu, Z., Tian, Z., 2008. Production of hydrogen by aqueous-phase reforming of glycerol. *International Journal of Hydrogen Energy*, 33, pp.6657-6666.

193. Wongsakulphasatch, S., Kiatkittipong, W. and Assabumrungrat, S., 2013. Comparative study of fuel gas production for SOFC from steam and supercritical-water reforming of bioethanol. *International Journal of Hydrogen Energy*, *38*(14), pp.5555-5562.

194. Wu, J., Ein-Mozaffari, F. and Upreti, S., 2013a. Effect of ozone pretreatment on hydrogen production from barley straw. *Bioresource Technology*, *144*, pp.344-349.

195. Wu, J., Upreti, S. and Ein-Mozaffari, F., 2013b. Ozone pretreatment of wheat straw for enhanced biohydrogen production. *International Journal of Hydrogen Energy*, *38*(25), pp.10270-10276.

196. Xie, H., Yu, Q., Lu, H., Zhang, Y., Zhang, J. and Qin, Q., 2017. Thermodynamic study for hydrogen production from bio-oil via sorption-enhanced steam reforming: Comparison with conventional steam reforming. *International Journal of Hydrogen Energy*, *42*(48), pp.28718-28731.

197. Xie, H., Yu, Q., Wang, K., Shi, X. and Li, X., 2014. Thermodynamic analysis of hydrogen production from model compounds of bio-oil through steam reforming. *Environmental Progress & Sustainable Energy*, *33*(3), pp.1008-1016.

198. **Xu, D., Wang, S., Hu, X., Chen, C., Zhang, Q. and Gong, Y., 2009.** Catalytic gasification of glycine and glycerol in supercritical water. *International Journal of Hydrogen Energy*, *34*(13), pp.5357-5364.

199. **Yan, L., Yue, G. and He, B., 2016.** Thermodynamic analyses of a biomass–coal co-gasification power generation system. *Bioresource Technology*, *205*, pp.133-141.

200. **Yang, M., Kuittinen, S., Vepsäläinen, J., Zhang, J. and Pappinen, A., 2017.** Enhanced acetone-butanol-ethanol production from lignocellulosic hydrolysates by using starchy slurry as supplement. *Bioresource Technology*, *243*, pp.126-134.

201. **Yaws, C.L., 2013.** Chemical properties handbook. 1st edition, McGraw Hill Inc., New York, USA.

202. **Zhang, B., Cai, W., Li, Y., Xu, Y. and Shen, W., 2008.** Hydrogen production by steam reforming of ethanol over an Ir/CeO_2 catalyst: reaction mechanism and stability of the catalyst. *International Journal of Hydrogen Energy*, *33*(16), pp.4377-4386.

203. **Zheng, J., Tashiro, Y., Wang, Q., Sakai, K. and Sonomoto, K., 2015.** Feasibility of acetone–butanol–ethanol fermentation from eucalyptus hydrolysate without nutrients supplementation. *Applied Energy*, *140*, pp.113-119.

204. **Zhou, N., Huo, M., Wu, H., Nithyanandan, K., Chia-fon, F.L. and Wang, Q., 2014.** Low temperature spray combustion of acetone–butanol–ethanol (ABE) and diesel blends. *Applied Energy*, *117*, pp.104-115.

205. **Zhu, L., Li, L. and Fan, J., 2015.** A modified process for overcoming the drawbacks of conventional steam methane reforming for hydrogen production: Thermodynamic investigation. *Chemical Engineering Research and Design*, *104*, pp.792-806.

APPENDIX A1: HEAT CAPACITY CORRELATIONS

Following heat capacity correlations (polynomials) have been used in the present work.

$Cp_i = A_1 + A_2T + A_3T^2 + A_4T^3 + A_5T^4$ **(kJ/mol K)** **For Gases**

$Cp_i = A_1 + A_2T + A_3T^2$ **(kJ/mol K)** **For Solids**

$$\Delta G_T = \Delta G_{Products} - \Delta G_{Reactants}$$

$$\Delta G_T = -RT \ln K$$

$$\Delta G_{i,T} = \Delta H_{i,T} - T\Delta S_{i,T}$$

$$\Delta G_{i,T} = \Delta H_{i,T} - T\Delta S_{i,T}$$

$$\Delta H_{i,T} = H^f_{i,298} + \int_{298}^{T} c_{p_i}\, dT$$

$$\Delta S_{i,T} = S^f_{i,298} + \int_{298}^{T} \frac{c_{p_i}}{T}\, dT$$

For Gases,

$$\Delta H_{i,T} = H^f_{i,298} + \int_{298}^{T} \left(A_1 + A_2T + A_3T^2 + A_4T^3 + A_5T^4\right) dT$$

After integrating,

$$\Delta H_{i,T} = H^f_{i,298} + A_1(T - 298) + \frac{A_2}{2}(T^2 - 298^2) + \frac{A_3}{3}(T^3 - 298^3) + \frac{A_4}{4}(T^4 - 298^4) + \frac{A_5}{5}(T^5 - 298^5)$$

$$\Delta S_{i,T} = S^f_{i,298} + \int_{298}^{T} \frac{\left(A_1 + A_2T + A_3T^2 + A_4T^3 + A_5T^4\right)}{T} dT$$

After integrating,

$$\Delta S_{i,T} = S^f_{i,298} + A_1 \ln\left(\frac{T}{298}\right) + A_2(T - 298) + \frac{A_3}{2}(T^2 - 298^2) + \frac{A_4}{3}(T^3 - 298^3) + \frac{A_5}{4}(T^4 - 298^4)$$

For Solids,

$$\Delta H_{i,T} = H_{i,298}^{f} + \int_{298}^{T} \left(A_1 + A_2 T + A_3 T^2\right) dT$$

After integrating,

$$\Delta H_{i,T} = H_{i,298}^{f} + A_1 (T - 298) + \frac{A_2}{2} (T^2 - 298^2) + \frac{A_3}{3} (T^3 - 298^3)$$

$$\Delta S_{i,T} = S_{i,298}^{f} + \int_{298}^{T} \frac{\left(A_1 + A_2 T + A_3 T^2\right)}{T} dT$$

After integrating,

$$\Delta S_{i,T} = S_{i,298}^{f} + A_1 \ln\left(\frac{T}{298}\right) + A_2 (T - 298) + \frac{A_3}{2} (T^2 - 298^2)$$

The values of coefficients of polynomials are given in Table A1.

Table A1: Coefficients of heat capacity correlations (polynomials)

Components	**Coefficients of polynomials**					$H^f_{i,298}$ **(kJ/mol)**	$S^f_{i,298}$ **(kJ/mol/K)**
	A_1	**A_2**	**A_3**	**A_4**	**A_5**		
C_3H_6O (g) (Acetone)	35.92×10^{-3}	9.39×10^{-5}	1.87×10^{-7}	-2.16×10^{-10}	6.317×10^{-14}	-218.5	-0.216401
$C_4H_{10}O$ (g) (n-Butanol)	8.16×10^{-3}	41.03×10^{-5}	-2.26×10^{-7}	6.04×10^{-11}	-6.28×10^{-15}	-274.43	-0.415093
C_2H_6O (g) (Ethanol)	27.09×10^{-3}	1.11×10^{-4}	1.10×10^{-7}	-1.50×10^{-10}	4.66×10^{-14}	-235.3	-0.223143
H_2O (g) (Steam)	33.93×10^{-3}	-0.84×10^{-5}	0.29×10^{-7}	-1.78×10^{-11}	3.69×10^{-15}	-241.80	-0.04470
CO (g) (Carbon monoxide)	29.56×10^{-3}	-0.66×10^{-5}	0.20×10^{-7}	-1.22×10^{-11}	2.26×10^{-15}	-110.54	0.089686
CO_2 (g) (Carbon dioxide)	27.44×10^{-3}	4.23×10^{-5}	-0.19×10^{-7}	0.39×10^{-11}	-0.29×10^{-15}	-393.51	0.002918
H_2 (g) (Hydrogen)	25.40×10^{-3}	2.02×10^{-5}	-0.39×10^{-7}	3.19×10^{-11}	-8.76×10^{-15}	---	---
CH_4 (g) (Methane)	39.94×10^{-3}	-3.99×10^{-5}	1.92×10^{-7}	-15.30×10^{-11}	39.32×10^{-15}	-74.85	-0.080530
C_2H_6 (g) (Ethane)	28.146×10^{-3}	4.3447×10^{-5}	1.8946×10^{-7}	-1.9082×10^{-10}	5.3349×10^{-14}	-84.68	-0.173570
C_3H_8 (g) (Propane)	28.28×10^{-3}	11.60×10^{-5}	1.96×10^{-7}	-23.27×10^{-11}	68.67×10^{-15}	-103.85	-0.269596
C_4H_8 (g) (1-Butene)	24.92×10^{-3}	20.65×10^{-5}	0.59×10^{-7}	-14.17×10^{-11}	47.05×10^{-15}	-0.13	-0.239577
C_4H_8O (g) (n-Butyraldehyde)	64.37×10^{-3}	6.48×10^{-5}	3.51×10^{-7}	-35.37×10^{-11}	100.82×10^{-15}	-205.02	-0.302700
C_2H_2 (g) (Acetylene)	19.36×10^{-3}	11.52×10^{-5}	-1.24×10^{-7}	7.24×10^{-11}	-16.59×10^{-15}	226.73	0.05879
C_2H_4 (g) (Ethylene)	32.08×10^{-3}	-1.48×10^{-5}	2.48×10^{-7}	-23.77×10^{-11}	68.27×10^{-15}	52.30	-0.53061
C (s) (Carbon)	-0.83×10^{-3}	3.48×10^{-5}	-0.13×10^{-7}	---	---	---	---

APPENDIX A2: STANDARD CHEMICAL EXERGY

Table A2: Standard Chemical Exergy of substances [Kumar et al. 2013]

Substances	**Standard Chemical Exergy (kJ/mol)**
H_2 (g)	235.39
CO(g)	275.55
CO_2 (g)	20.11
C_3H_6O (g)	1784.70
$C_4H_{10}O$ (g)	2667.75
C_2H_6O (g)	1356.9
CH_4 (g)	831.2
C(s)	409.87
O_2 (g)	3.94